INFORMATION TO USERS

This manuscript has been reproduced from the microfilm master. UMI films the text directly from the original or copy submitted. Thus, some thesis and dissertation copies are in typewriter face, while others may be from any type of computer printer.

The quality of this reproduction is dependent upon the quality of the copy submitted. Broken or indistinct print, colored or poor quality illustrations and photographs, print bleedthrough, substandard margins, and improper alignment can adversely affect reproduction.

In the unlikely event that the author did not send UMI a complete manuscript and there are missing pages, these will be noted. Also, if unauthorized copyright material had to be removed, a note will indicate the deletion.

Oversize materials (e.g., maps, drawings, charts) are reproduced by sectioning the original, beginning at the upper left-hand corner and continuing from left to right in equal sections with small overlaps.

Photographs included in the original manuscript have been reproduced xerographically in this copy. Higher quality 6" x 9" black and white photographic prints are available for any photographs or illustrations appearing in this copy for an additional charge. Contact UMI directly to order.

ProQuest Information and Learning
300 North Zeeb Road, Ann Arbor, MI 48106-1346 USA
800-521-0600

CROSS-LINKING POLYMERIZATION OF HYDRATED LIPID BILAYERS

by

Sanchao Liu

A Dissertation Submitted to the Faculty of the

DEPARTMENT OF CHEMISTRY

In Partial Fulfillment of the Requirements
For the Degree of

DOCTOR OF PHILOSOPHY

In the Graduate College

THE UNIVERSITY OF ARIZONA

2001

UMI Number: 3026579

UMI Microform 3026579

Bell & Howell Information and Learning Company
300 North Zeeb Road
P.O. Box 1346
Ann Arbor, MI 48106-1346

THE UNIVERSITY OF ARIZONA ®
GRADUATE COLLEGE

As members of the Final Examination Committee, we certify that we have read the dissertation prepared by Sanchao Liu

entitled Cross-linking Polymerization of Hydrated Lipid Bilayers

and recommend that it be accepted as fulfilling the dissertation requirement for the Degree of Doctor of Philosophy

	8/13/01 Date
	8/13/01 Date
	8-13-01 Date
	8/13/01 Date
	Date

Final approval and acceptance of this dissertation is contingent upon the candidate's submission of the final copy of the dissertation to the Graduate College.

I hereby certify that I have read this dissertation prepared under my direction and recommend that it be accepted as fulfilling the dissertation requirement.

Dissertation Director — Date: Aug 17, 2001

STATEMENT BY AUTHOR

This dissertation has been submitted in partial fulfillment of requirements for an advanced degree at The University of Arizona and is deposited in the University Library to be made available to borrowers under rules of the Library.

Brief quotations from this dissertation are allowable without special permission, provided that accurate acknowledgment of source is made. Requests for permission for extended quotation from or reproduction of this manuscript in whole or in part may be granted by the head of the major department or the Dean of the Graduate College when in his or her judgment the proposed use of the material is in the interests of scholarship. In all other instances, however, permission must be obtained from the author.

SIGNED: Sandra Li

ACKNOWLEDGEMENTS

I would like to express my sincere gratitude to my research advisor, Dr. David F. O'Brien, for his marvelous understanding, patient guidance and unreserved support throughout my graduate study and research work in his group, as well as my writing of this dissertation. I would like to thank Drs. Bates, Barfield, and Mash for serving on my dissertation committee and offering very helpful comments and suggestion. In particular, Dr. Bates's sincere attitude to every student has touched me deeply.

My sincere appreciation goes to Dr. Anja Mueller for her friendship, encouragement and confidence in me in times of difficulty. She always made herself available whenever I needed help. I thank her for all the wonderful time we shared together.

I am also thankful for the former and present members of the O'Brien group: Warunee and Tom Sisson for their previous contribution on this project and their initial assistant in the starting of my research work, Bruce Bondurant for his help with trouble shooting for many instrument problems, especially HPLC, and other fellow graduate students in Dr. O'Brien's group for their assistance and friendship. I wish to acknowledge the special assistance from David Bentley with electron microscopy.

I am grateful to my family and friends for their moral support. My father, Zhenglun Liu, and my late mother, Yufang Li, in far away China have been very supportive and understanding during my graduate study. My brother, Qiang, and sister-in-law Mei have also been encouraging. I would also thank many of my friends in TCCF.

I am thankful for the Department of Chemistry, University of Arizona for the graduate assistantship granted to me for the first two years and the financial support from the Division of Materials Research of the National Science Foundation throughout my graduate study.

I extended my sincere gratitude to Joan and Bob Miller, the family I stayed with during the last period of my graduate study. Their love and support accompanying me go through the most lonely and intensive time.

Last but not least, I would like to express my deepest thanks to my wonderful husband Song. Words can never express my appreciation for all he has done for me within the past five more years of my graduate study. He has given me as much help as he could both as a husband and as a chemist. Without his love, support, encouragement and endurance I would have never succeeded in obtaining my Ph.D. I also like to thank my little son Lucas, who is so lovely, who brightens my live so much, and gave me so much comfort during my study.

DEDICATION

To my late mother, Yufang Li, a great Chinese mother, who loved and sacrificed for her children so much, from whom I learnt so much about life. It was always her greatest wish that I would go to graduate school and get an advanced degree. Even though she cannot be here to see it happen, I pray that she is smiling with comfort in heaven now.

TABLE OF CONTENTS

TABLE OF CONTENTS - *Continued*

TABLE OF CONTENTS - *Continued*

TABLE OF CONTENTS - *Continued*

TABLE OF CONTENTS - *Continued*

TABLE OF CONTENTS - *Continued*

LIST OF ILLUSTRATIONS

LIST OF ILLUSTRATIONS - *Continued*

LIST OF ILLUSTRATIONS – *Continued*

LIST OF ILLUSTRATIONS – *Continued*

LIST OF TABLES

ABBREVIATIONS

AAPD	2,2'- azobis-(2-amidinopropane)dihydrochloride
AIBN	2,2'- azobis-(isobutyronitrile)
CF	carboxyfluorescein
CMC	critical micellar concentration
CU	cooperative unit
DCC	1,3-dicyclohexylcarbodiimide
DenPC	dienoylphosphatidylcholine
DMAP	4-(N,N-dimethylamino)pyridine
DOPE	dioleoylphosphatidylethanolamide
DPPC	dipalmitoylphosphatidylcholine
DPX	α,α'-bispyridinium-*p*-xylene dibromide
DSC	differential scanning calorimetry
ΔH_{cal}	calorimetric enthalpy
ΔH_{vH}	van't Hoff enthalpy
HPLC	high pressure liquid chromatography
L_α	liquid-crystalline phase
L_β	gel phase
LUV	large unilamellar vesicles
MLV	multilamellar vesicles

NMR	nuclear magnetic resonance
P_β	ripple phase
PC	phosphatidylcholine
PEG	polyethylene glycol
PTSA	1,3,6.8-pyrenetetrasulfonic acid, tetrasodium salt
QELS	quasi-elastic light scattering
REV	reverse-phase evaporation
SEC	size exclusion chromatography
SUV	small unilamellar vesicles
TEM	transimison electron microscopy
T_m	gel to liquid crystalline phase transition temperature

ABSTRACT

The objective of this work was to investigate the cross-linking polymerization of lipids in supramolecular assemblies in order to stabilize the assembly structures.

One approach to obtain a cross-linked polymer is by addition of a cross-linking agent. Homobifunctional lipids with two polymerizable groups, one in each of the two hydrophobic chains, can serve as a cross-linking agent. The lipids chosen were dienoyl-substituted lipids, mono- and bis-DenPC, where the reactive diene group is located near the glycerol backbone of the lipids. MonoDenPC$_{16:18}$ and bisDenPC$_{18:18}$ were synthesized. Redox initiation was used to polymerize mixed mono/bisDenPC vesicles. To test the stability of the polymeric vesicles, Triton X-100 (TX-100) was added to the sample and the size determined by quasi-elastic light scattering (QELS). The stability of polymerized LUV to TX-100 depended on the initial composition of the LUV. It was found that 15 mol % bis-substituted lipids, bisDenPC, were needed for cross-linking polymerization. The capability of varying the cross-linking density in these poly(lipid) structures provides researchers with a means to further modify the physical properties of these polymers and membranes.

Another approach to achieve cross-linking utilizes heterobifunctional lipids, which have two different reactive groups in one of the lipid tails. These heterobifunctional lipids formed bilayer vesicles or lamellar structures. The properties of the vesicles could be varied by the polymerization of the reactive groups. The design of

heterobifunctional monomers allowed either simultaneous or selective polymerization of these groups. The difference in reactivity as well as the difference in polarity of each group also made possible selective polymerization of these reactive groups. Simultaneous polymerization of both reactive groups was achieved by either redox polymerization or direct photoirradiation. UV polymerization showed the formation of oligomers, which dissolved in organic solvents and TX-100. On the other hand, redox polymerization gave cross-linked polymers, which were insoluble in most organic solvents and stable towards addition of TX-100. The cross-linking density could be varied by choosing different polymerization techniques. Electron micrographs of the cross-linked polymeric vesicles showed they could retain their size and shape after freeze-drying and re-dispersal in water. The surface of the cross-linked vesicles could be modified for many applications.

CHAPTER 1

INTRODUCTION

1.1 Overview: Supramolecular Assemblies of Hydrated Amphiphiles

In recent years, the area of molecular self-assembly has drawn much scientific attention as a convenient tool for building functional assemblies. Self-assembly of molecules involves spontaneous association of molecules under equilibrium conditions into stable and structurally well-defined aggregates joined by non-covalent bonds (e.g., hydrogen bonds). The resulting structures are often termed "supramolecular assemblies". Self-assembly of molecules is not only of laboratory interest, but this concept is also commonly used in the formation in many complex biological structures such as DNA, proteins, and lipid bilayers. Molecular self-assembly is a new strategy in chemical synthesis. The structures prepared by conventional chemical synthesis are mainly in the 0.1 to 2 nm range while both biology and microfabrication provide structures with dimensions ranging from 1 to 10^4 nm. Self-assembly may make possible the synthesis of structures that are 10 to 10^3 nm in size (with molecular weights of 10^4 to 10^{10} daltons). The ability to prepare such large assemblies would open a route to structures comparable or smaller in size (and perhaps complementary in function) to those that can be prepared by microlithography and other techniques of microfabrication. Also structures that are bigger than ordinary molecules but too small for microfabrication can be synthesized in a simple manner.

For the final assembly to be stable and have well-defined shape, the noncovalent interactions between the molecules must be stable. The strengths of individual van der Waals interactions and hydrogen bonds are weak (0.1 to 5 kcal/mol) relative to typical covalent bonds (40 to 100 kcal/mol) and comparable to thermal energies (RT = 0.6 kcal/mol at 300 K). Since supramolecular assemblies are composed of noncovalently associated molecules, they are often unstable and prone to change when the conditions (e.g. temperature, concentration, and additives) are changed. Therefore certain long-term applications are limited. Polymerization of supramolecular assemblies is an effective method to modify their chemical and physical properties and to stabilize them.

In this dissertation the synthesis and characterization of cross-linked supramolecular lipid assemblies is described. The potential applications for polymeric lipid assemblies are in biotechnology and materials science such as diagnostics, controlled delivery of reagents and drugs,[1,2] preparation of membrane mimics,[3] separation of biomolecules,[4] transduction of light energy,[5-7] modification of surfaces,[8] and as organic zeolites.[9]

1.1.1 Structure and Self-Assembly of Amphiphiles

Many amphiphiles with a hydrophilic head group and a hydrophobic tail self-organize into supramolecular structures. A typical structure is shown in Figure 1-1.

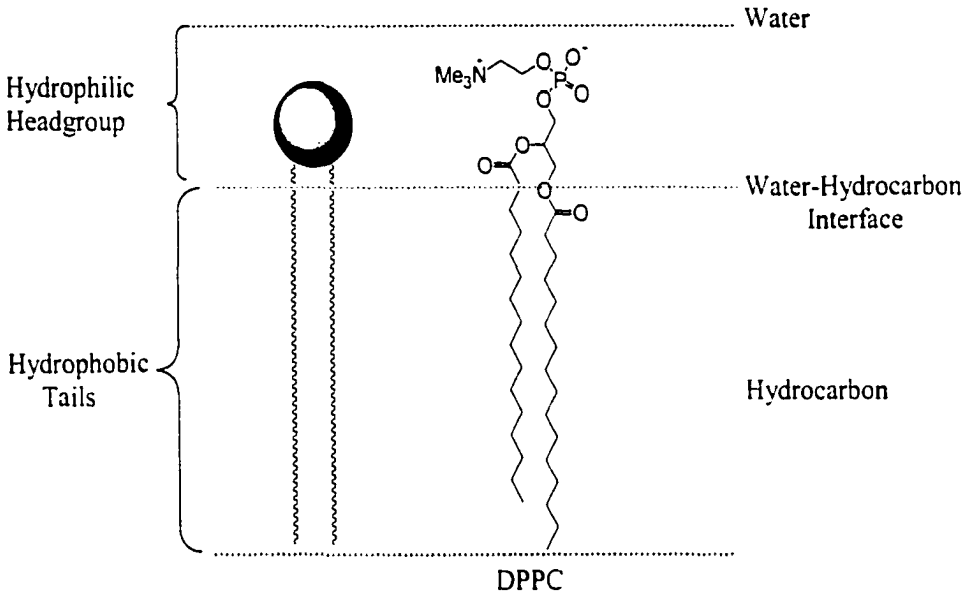

Figure 1-1. Schematic representation of an amphiphile and the phospholipid dipalmitoylphosphatidylcholine (DPPC) is an example. The hydrophilic headgroup is represented by a circle and the hydrophobic hydrocarbon chains by wavy lines.

Examples of amphiphiles include lipids, detergents, and fatty acids. The formation of these assemblies in aqueous media is favored by the hydrophobic effect:[10,11] amphiphiles interact with one another to exclude water from the hydrophobic tails and promote optimum hydration of the hydrophilic head groups. The contact between water and the hydrophobic chains of an amphiphile is minimized by the formation of assemblies.

A variety of different supramolecular assemblies can be formed based on the chemical/physical nature of the polar and non-polar moieties (Figure 1-2).[12-14] They can be classified as self-supported assemblies and supported assemblies. Self-supported structures can be either lamellar, e.g., bilayers and vesicles, or non-lamellar, e.g.,

hexagonal, cubic and tubules. Supported structures can be Langmuir-Blodgett (LB) multilayers and self-assembled monolayers (SAM).

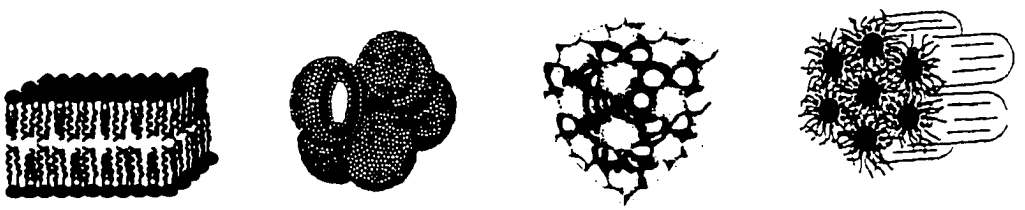

Bilayers | Vesicles[15] | Cubic Phase (G) | Inverted Hexagonal Phase (H_{II})

Figure 1-2. Schematic representation of supramolecular assemblies.

1.1.2 Bilayer Vesicles (Liposomes)

Bilayer vesicles are self-supported supramolecular assemblies. Vesicles are composed of a lipid bilayer that encloses an aqueous interior volume (Figure 1-3). The lipid bilayer structure can be composed of tens of thousands of lipid molecules arranged with their hydrophilic head groups exposed to water and the hydrophobic tails aggregated to exclude water. The bilayer structure is highly ordered but the lipid molecules are free to diffuse laterally in the lipid matrix. The lipids used to form vesicles are generally double chain amphiphiles (with two tails). However, certain single chain surfactant[16-18] and ion-pairs of oppositely charged amphiphiles[19] can also form vesicles. Vesicles composed of naturally occurring or synthetic phospholipids are referred to as liposomes.

In contrast, those formed from completely synthetic amphiphiles are to be designated as vesicles.[20]

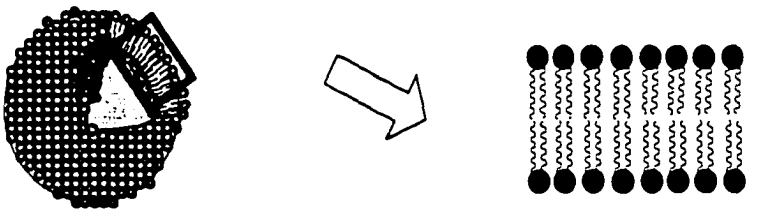

Unilamellar Vesicle Bilayer

Figure 1-3. Schematic representation of unilamellar vesicle and bilayer formed from lipid molecules.

Bilayer vesicles have attracted a great deal of scientific interest in two quite distinct roles. First, vesicles can provide an excellent model for cell membranes, allowing exploration of questions concerning membrane lipid chemistry, lipid-protein interactions, transport phenomena, and ligand binding to membranes.[1,21-24] Second, vesicles are being developed as controlled delivery systems for therapeutic agents.[25-29]

Biological cell membranes are composed of lipids, proteins, and carbohydrates. During the early 1960s researchers demonstrated that certain classes of lipids could be used to form protein- and carbohydrate-free model membranes. The most common lipid components of cell membranes are phospholipids. Vesicles are the nearest approach to biomembranes. Their membrane properties make them suitable for a large number of applications, e.g., encapsulation and controlled release as drug carriers,[26,30,31]

functional incorporation of proteins,[23,32] the study of surface recognition reaction,[32,33] and dynamic membrane processes.[23,33,34]

The preparation of vesicles of defined and variable size is an important objective for the study of vesicles as drug carriers and model membranes. In general, there are two types of vesicles based on number of bilayers (lamellar) per vesicle: multilamellar vesicles and unilamellar vesicles. Multilamellar vesicles (MLV > 100 nm) are prepared by hydration of dried lipids. This method, developed by Bangham,[35] gives multilayer structures of varying size with diameters in the range of 0.2-5 μm. The major advantage of MLV preparation is the simplicity of the procedure. However, the multilamellar character and heterogeneity of MLV is a distinct disadvantage in many applications.

Single unilamellar vesicles of uniform size distribution are better suited for physical and chemical investigations than MLV. The early and most widely used method for forming small unilamellar vesicles (SUV) is sonication.[36] Either a probe or a bath-type sonicator can be used. Sonication of MLV produces SUV (20-100 nm) with a very homogeneous in size distribution which have been used extensively as model membrane systems. However, their relatively small enclosed aqueous space produces serious limitations for their potentional use as drug carriers. In the 1970s, several methods were developed to prepare large unilamellar vesicles (LUV, 100-1000 nm). There are three commonly used methods: infusion, reverse-phase evaporation, and detergent dilution. In the infusion method,[37,38] a lipid solution in a nonpolar solvent is infused into an aqueous solution under conditions that cause the solvent to vaporize, resulting in the formation of vesicles. The advantage of the infusion procedure is that it is applicable to a

wide variety of lipids and can be completed in less than an hour. The main limitation is that the resulting preparations are relatively dilute so that the encapsulation efficiency is low. In the reverse-phase evaporation (REV) method,[39] a dispersion of inverted micelles of lipid is produced in a system containing mixed organic and aqueous phases. As the solvent is evaporated away, the micelles coalesce to form large unilamellar vesicles. The REV method has the distinct advantages of being applicable to a range of volumes (as little as 0.2 ml) and being able to encapsulate a large fraction of the original volume. The disadvantages are that components are exposed to organic solvents and sonication which may be damaging and that the lipid requirement (10 mg per 0.2 ml of solution) is relatively large. In the detergent dilution method, lipids are cosolubilized by a detergent that is subsequently removed by gel filtration[40] or by dialysis.[41-43] The detergent dilution method is widely applicable in vesicle preparations, particularly when proteins are to be reconstituted into the resulting membrane. This method is applied in the first commercially available vesicle preparation apparatus, called Lipoprep. A limitation of this method is that preparations using dialysis require hours or even days to be completed, and if the solute to be entrapped is dialysis membrane permeable, the encapsulation efficiency is very low.

The extrusion method proposed by Hope et al.[44] provided a rapid and easy way to prepare large unilamellar vesicles (LUV) with defined size and homogeneity. MLV, prepared by repeated freeze-thaw protocols, were sequentially extruded through polycarbonate membranes with pore diameters of 1.0 to 0.1 μm, under moderate pressures (< 500 lb / in^2). Passage through the membrane pores resulted in progressively

smaller and less polydisperse vesicles. This technique provides a reproducible protocol for the formation of LUV of intermediate size (60-100 nm) and relatively high trapping efficiencies (up to 30%). This procedure is relatively simple, rapid (≤ 10 min preparation time), and can be employed to generate LUV from a variety of lipid species and mixtures. No organic solvents or detergents are encountered. However, filtration has to be carried out above the phase transition temperature since below the phase transition temperature vesicles are not filterable.[45]

In this research, we used unilamellar vesicles (LUV) prepared by thte extrusion method as a convenient form of the lamellar phase for all the studies.

1.2 Stabilization of Supramolecular Assemblies

Because of the long-term instability of membrane structures for supramolecular assemblies, the use of supramolecular assemblies in mechanistic studies and practical applications is seriously restricted. The synthesis of more stable model membranes in order to be used in biological process study has been a scientific goal for quite a long time. In the last two decades, numerous methods to stabilize these model membranes have been developed.

The polymerization of lipids before or after their orientation in model membranes has been studied most intensively. Besides polyaddition, polycondensation has also been used for stabilizing model membrane systems.[46] These polymerization methods form covalent binding inside lipid membranes. Other methods to stabilize lipid bilayers based on noncovalent binding of polymers to the membrane surface are polymer adsorption,

polymerization of counterions, insertion of hydrophobic anchor groups, and the incorporation of membrane-spanning lipids into the bilayer.

1.3 Polymerization of Hydrated Lipid Bilayers

The polymerization of lipid assemblies was first demonstrated in monolayers,[15,47-50] vesicles and extended bilayers[15,51-56] and subsequently in cast multilayers,[57] bilayer lipid membranes (BLMs), and nonlamellar phases.[9,58,59] There are two major approaches for the preparation of polymeric assemblies. The first approach involves formation of a supramolecular assembly from a polymerizable lipid and subsequent polymerization of the assembly. The second one is the polymerization of a suitably designed lipid in isotropic media, followed by assembly formation from the pre-polymerized lipid. This dissertation emphasizes the first approach.

1.3.1 Polymerizable Lipids

The use of polymerizable lipids represents a convenient method for lipid bilayer stabilization because this strategy does not rely on the addition of an extra component to the lipids. These polymerizable lipids exhibit physical properties that are similar to their non-polymerizable analogues before polymerization. Upon polymerization, the polymerizable lipids form covalent bonds with their next neighbor and stabilize the membrane. In the design of polymerizable lipids to build up membranes of high stability, the polymerizable group can be incorporated into different parts of the lipid molecule, i.e., into the hydrophobic region or the hydrophilic region (Figure 1-4, where x is the

polymerizable group). In Figure 1-4, types A and B have the polymerizable group attached to the chain terminal and near the backbone of the hydrocarbon chain respectively. Type C has the reactive group in the middle of a bola-amphiphile. In type D the polymerizable group is attached to the hydrophilic headgroup, and in type E the polymerizable group is electrostatically associated with a charged lipid. Polymerization of types A, B and C drastically decreases the mobility of the hydrocarbon core. Types D and E show little or no effect on bilayer mobility, but may change the hydration properties of the lipid headgroup.

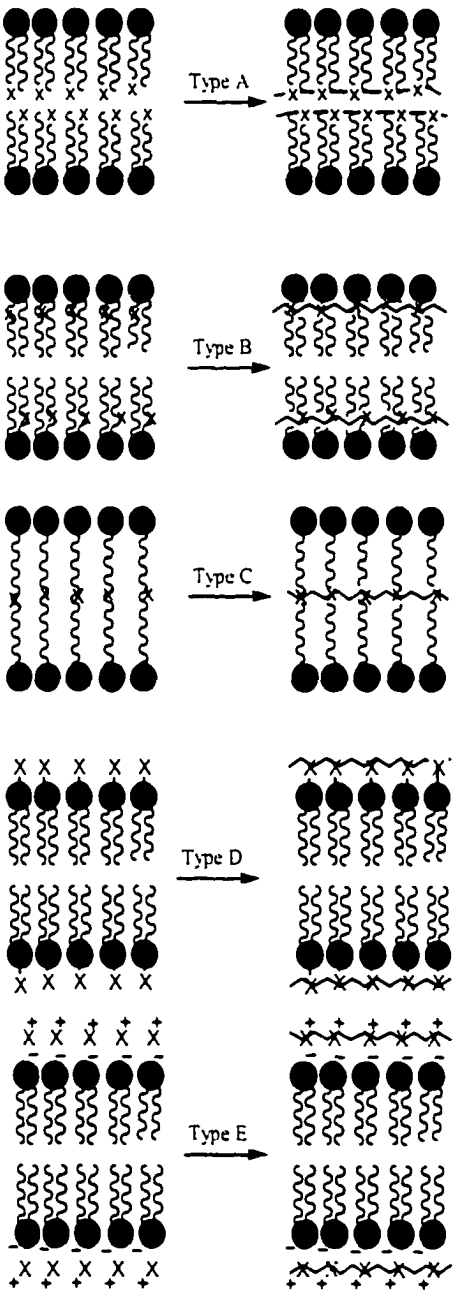

Figure 1-4. Location of polymerizable moieties in lipid molecules (x denotes the polymerizable group).

A variety of polymerizable groups have been successfully employed in lipid molecules.[33,60,61] In the early 1980s, the formation of polymerized vesicles by using methacryloyl[52] and diacetylene amphiphiles[47,51,53,62] was reported for the first time. Shortly after that, more groups reported the synthesis and polymerization of diacetylene lipids, dienoyl lipids, methacryloyl lipids and styryl lipids, etc. More recently, a variety of reactive groups have been incorporated into one or both acyl chains of amphiphiles including acryloyl, itaconyl, muconyl, vinyl, thiol, lipoyl, disulfide, diene and sorbyl (Figure 1-5).[15,32,33,60,61,63-66] Polymerization has been achieved photochemically, thermally and with redox initiators. Diacetylenic lipids are only polymerized efficiently in the solid-analogous phase (L_β)[53] or in other solid-like assemblies, e.g. tubules[67] and the condensed phase of Langmuir monolayers.[47] In contrast to the topochemical requirement of diacetylenes, other lipids such as methacryloylic and butadienic lipids are also polymerizable in the liquid-like phase (L_α). Compared to diacetylenes, methacryloylic and butadienic lipids exhibit a higher mobility of their polymer chains, and therefore are more suitable for the formation of flexible membranes.

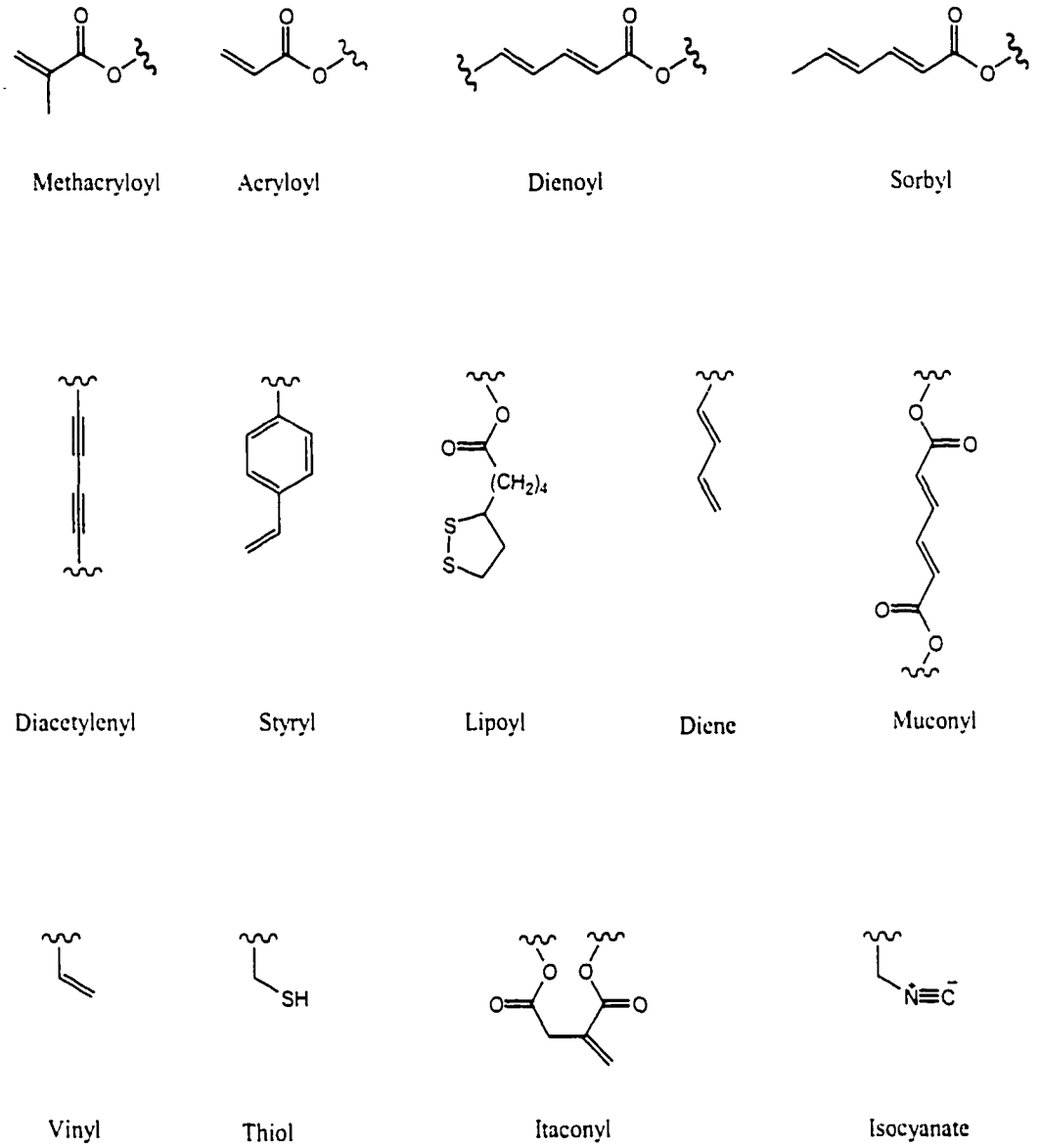

Figure 1-5. Examples of polymerizable groups which have been incorporated into polymerizable lipids.

1.3.2 Polymerization Methods

(a) UV polymerization. Extensive studies were carried out on the reactivity of polymerizable lipids. Lipids with unsaturated bonds can be polymerized by UV irradiation. In the case of diacetylenic lipids the transition from monomeric to polymeric bilayers can be observed visually and spectroscopically (blue intermediate: 620-630 nm; red polymer: 500-540 nm). This was first discussed by Day[47] and Chapman.[48] In the case of butadienic lipids, the polymerization was followed by a decrease of the strong monomer absorption (260 nm). Disappearance of vinyl protons in the ^{2}H NMR spectrum proved polymer formation for vesicles made from vinyl, acryloyl, and methacryloyl lipids. However, photopolymerization with short wavelength UV light can lead to polymer chain degradation in competition with chain growth. Sackmann and coworkers observed that the UV-induced polymerization of methacryloyl-substituted lipids produced long polymer chains at short exposure time. Continued irradiation of the sample caused a progressive decrease in the size of the poly(lipid).[68]

(b) Thermal polymerization. Water-insoluble azobis(isobutyronitrile (AIBN) and water-soluble azobis(2-amidinopropane) (AAPD) are two types of thermal initiators widely used in lipid polymerization studies. These initiators are decomposed to form radicals upon heating. The polymerization is performed at 50-70 °C in order to obtain reasonable rates of radical generation (half-lives of AIBN at 50 and 70 °C are 74 and 4.8 h, respectively).[69] Two of the factors controlling the polymer chain length in conventional three-dimensional polymerization are the ratio of monomer to initiator ([M]/[I]) and the monomer concentration. In particular, it has been found that decreasing

either of these quantities leads to formation of shorter polymer chains. Recent work on vesicles indicates that the same relationship applies to two-dimensional polymerization.[70-72] The polymer size (degree of polymerization, X_n) is sensitive to the relative stability of the propagating species in both bilayer and isotropic polymerization. For AIBN-initiated polymerization of a mono-Acryloyl substituted PC, the polymer chain length was found to decrease with decreasing [M]/[I] ratio. Moreover, decreasing the monomer concentration (by mixing into the vesicles variable amounts of a nonpolymerizable lipid) also led to shorter polymer chains. Finally, termination of the growing polymer chain was found to occur by primary termination, a process involving coupling of an initiator radical with the reactive polymer terminus.[70,72,73] This termination mechanism contrasts with the standard termination modes, coupling and/or disproportionation of two polymer chains, which are commonly observed in solution polymerization. This is probably due to the high initiator concentration and viscosity of the bilayer system, which limits the diffusion of the growing polymer chain ends in the constrained environment of the lipid bilayer.

(c) Redox polymerization. The polymerization of lipid assemblies can also be achieved by addition of a redox initiator. The lower energy of activation (40–80 kJ/mol) allows the redox polymerization to be carried out under milder conditions than thermal polymerization. The low-temperature polymerization lowers the possibility of side chain reactions and avoids the possible degradation of vesicle-encapsulated compounds such as dyes or enzymes.

The most common oxidants in these systems are hydrogen peroxide, potassium bromate, and potassium persulfate. Reducing agents are usually L-cysteine, sodium bisulfite, and ascorbic acid. As the strength of the oxidizing agent increases, the rate of polymerization also increases. The rate of polymerization for methyl methacrylate (MMA) with various oxidizing agents and L-cysteine as the reductants shows that the rate of polymerization increases in the order of $K_2S_2O_8 < H_2O_2 < KBrO_3$.[74] Further study revealed that the molecular weight increased when the [oxidant]/[reductant], [O]/[R] ratio was increased from one to ten. Tsuchida and coworker examined the polymerization of monoDenPC **2-11** and bisDenPC **2-12** by various redox initiator systems. The efficiency of polymerization found was in the following order: Fe^{2+} / *t*-BuOOH > $K_2S_2O_8$ / L-cysteine > $K_2S_2O_8$ / $NaHSO_3$, $K_2S_2O_8$ / ascorbic acid > H_2O_2 / L-cysteine.[75]

Redox systems produce radicals by the reaction of an oxidant with a reductant, which then initiate chain polymerization (Figure 1-6). As in Figure 1-6, initiation of polymerization can result from $HO^{\bullet}$, $RS^{\bullet}$ or $SO_4^{\bullet-}$ radicals depending on the reaction conditions, radicals and monomer reactivities chosen. The most common radical generated in redox systems is the hydroxyl radical. This is a hydrophilic species but it is small enough to diffuse across lipid bilayers. It can be used to initiate reactive moieties on both hydrophobic and hydrophilic regions in a lipid chain. Reactive groups that have been polymerized by redox systems in isotropic media are acryloyl, dienoyl, acrylamide, and styryl. In lipid bilayer systems, only dienoyl,[75,76] sorbyl, acryloyl,[77] and lipoyl groups[78] have been reported to be polymerized by redox initiators.

Figure 1-6. Mechanism for redox reactions that generate a hydroxyl radical.[79]

$K_2S_2O_8$ / $NaHSO_3$

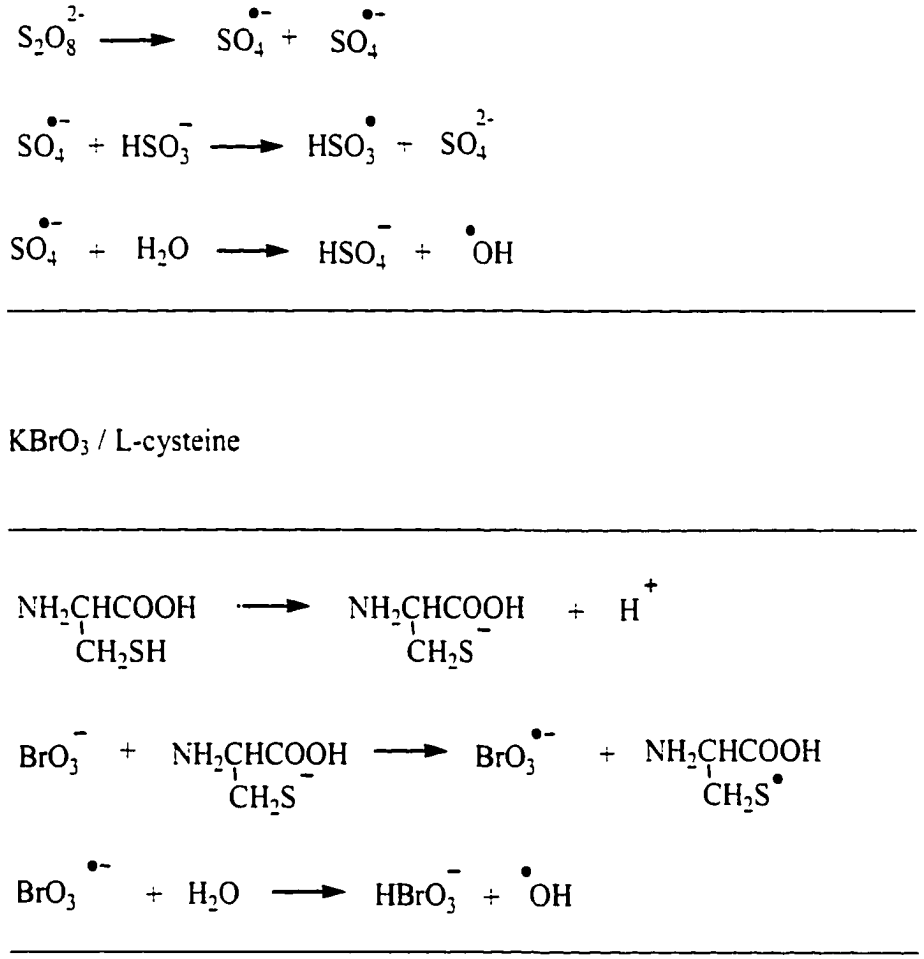

$KBrO_3$ / L-cysteine

1.3.3 Cross-linking Polymerization of Assemblies

A polymeric material can be linear or cross-linked depending on the number of reactive moieties in the monomers being polymerized. Homopolymerization of a

multifunctional monomer gives a cross-linked polymer; copolymerizaton of a monofunctional monomer with a multifunctional monomer can also yield cross-linking. In copolymerization, the multifunctional monomer serves as the cross-linking agent. Cross-linking occurs when two polymer chains become joined together by a branch, known as a crosslink.

The crosslinks between polymer chains can be of different length depending on the cross-linking method and the specific conditions employed. The number of crosslinks can also be varied to obtain lightly or highly cross-linked polymers. When the number of crosslinks is sufficiently high, a three-dimensional polymer is produced in which all the polymer chains in a sample have been linked together to form one giant network. Light cross-linking is used for polymers carrying good elastic properties such as rubbers. High degrees of cross-linking are used to impart rigidity and dimensional stability.

Cross-linking is characterized by the occurrence of gelation at some point in the polymerization. At this point, termed the gel point, the polymer undergoes a drastic change in physical properties, e.g. solubility, T_m, viscosity. Once the gel point is reached the system loses fluidity, the viscosity approaches infinity, and the gel is insoluble in all solvents at elevated temperatures under conditions where polymer degradation does not occur.[69]

Cross-linked polymers are remarkably important due to their unique properties. In comparison to linear polymers, cross-linked polymers have high chemical, thermal,

and mechanical stability. They are also generally stable even under high temperature and physical stress.

Many of the same principles which govern polymerization in three dimensions (isotropic solution or bulk systems in the melt) are also applicable to the two-dimensional environment of lipid bilayers.[69] Polymerization of monomeric lipids in an assembly proceeds in either a linear or a cross-linking manner dependent on the number of polymerizable groups per monomeric lipid. Lipids that contain a single reactive moiety in either of the hydrophobic tails or the hydrophilic headgroups yield linear polymer. Polymerization of lipids with two reactive groups in a lipid generally yields cross-linked polymers.[56,80,81] Other cross-linking strategies employed in two-dimensional assemblies include the addition of small molecule crosslinkers[82] and the use of bifunctional amphiphiles.[83]

O'Brien's group has focused on two approaches to achieve cross-linking in lipid assemblies. One approach is by addition of homobifunctional lipids, i.e. lipids with two polymerizable groups, one on each of the two hydrophobic chains.[76,81] These homobifunctional lipids can serve as cross-linking agents (Figure 1-7). The cross-linking density of the assemblies can be adjusted by varying the amount of homobifunctional lipid.

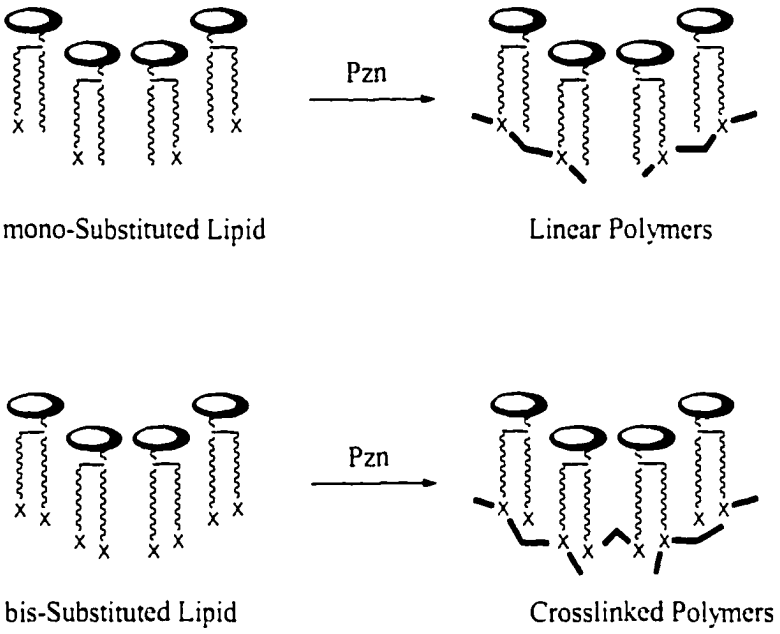

Figure 1-7. Schematic representation of the formation of linear and crosslinked polymer.

Another approach to accomplish cross-linking utilizes heterobifunctional monomers (Figure 1-8). These monomers have two different polymerizable groups in one lipid tail. The two reactive moieties have different reactivities resulting in differences in the rate and degree of polymerization as well as the type of initiators required. Selective polymerization of one reactive group in the presence of another is possible if the initiation chemistry favors only one polymerizable group. Post-polymerization modification can then be performed on the prepolymer by changing the initiation conditions to favor a subsequent transformation. The design of

heterobifunctional monomers permits either simultaneous or selective and sequential polymerization. Moreover, the two reactive groups are located in the same tail of the lipid, so it is also possible that the groups could form either cross-linked or linear-ladder polymers (Figure 1-8). The spacer length between the two reactive groups as well as the flexibility of the spacer groups that separates two reactive moieties determines if a linear-ladder or a cross-linked polymer is formed.[Liu, 2001 #45; Srisiri, 1996 #299; Sisson, 1998 #52]

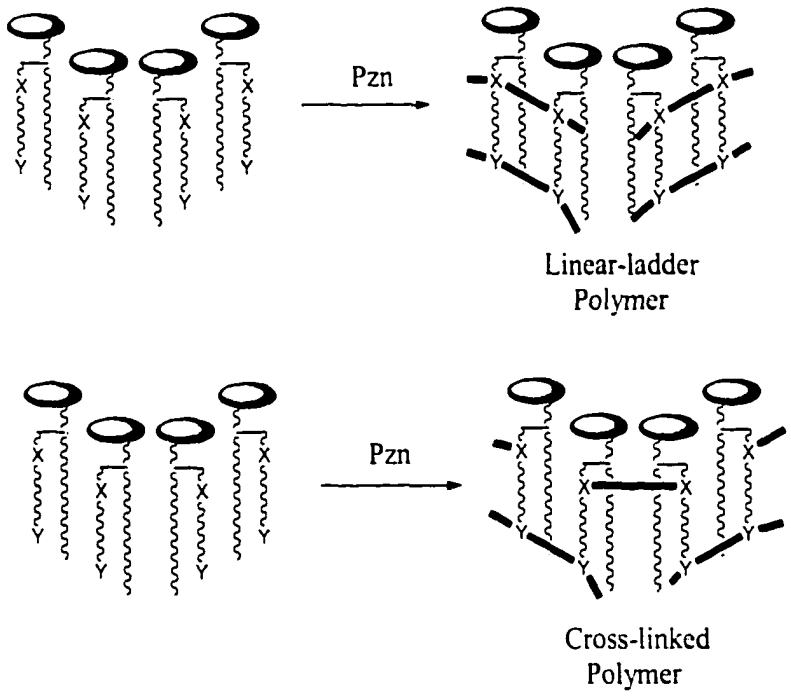

Figure 1-8. Schematic representation of the formation of linear-ladder polymer and cross-linked polymer.

1.4 Physical Properties of Lipid Bilayer Assemblies

1.4.1 Main Phase Transition Temperature (T_m).

Synthetic phospholipids, particularly phosphatidylcholines, have received considerable attention because of their ability to produce a variety of morphologies. The saturated diacyl phosphatidylcholines having fatty acyl chains 15-22 carbon atoms long are characterized by a relatively rich polymorphism. Studies show that there are three major first-order transitions with increasing temperature: sub-, pre-, and main phase transition (Figure 1-9). Following low-temperature equilibration, they form the lamellar crystalline (subgel, L_c) phase with hydrocarbon chains tilted with respect to the bilayer normal and the long axis of the head group oriented parallel to the bilayer plane. The L_c phase transforms to a lamellar gel phase ($L_{\beta'}$) with reduced chain tilt and increased hydration upon heating. This low-temperature $L_c \rightarrow L_{\beta'}$ transition is referred to as a subtransition. At higher temperatures, an interconversion between two different gel phases takes place during the so-called pretransition, i.e., the $L_{\beta'}$ phase transforms to the rippled gel ($P_{\beta'}$) phase. Upon further heating, the $P_{\beta'}$ phase undergoes a highly cooperative transition to a lamellar liquid crystalline (L_α) phase (the so-called main or chain order / disorder transition).

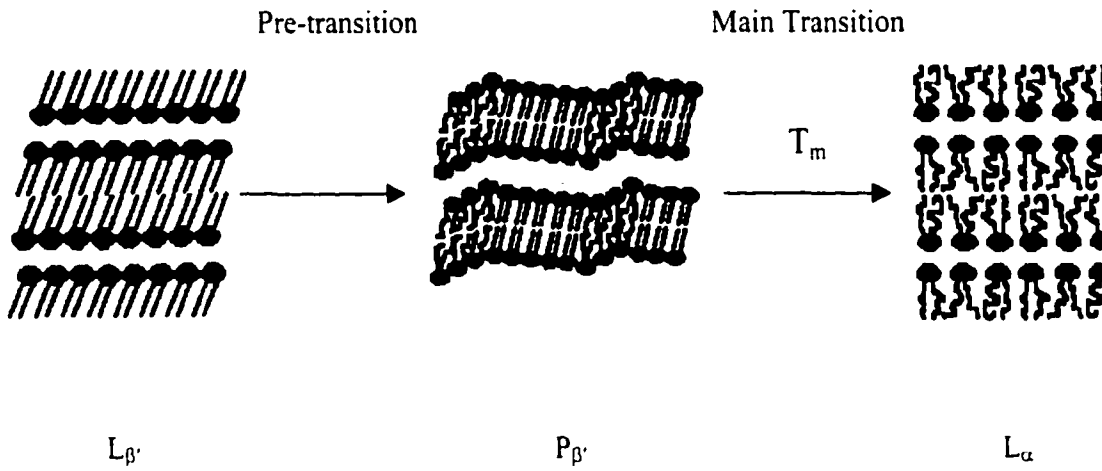

Figure 1-9. Schematic of the lipid bilayer undergoing phase transition.

Not every phospholipid shows all three phase transitions. Since the main phase transition was observed in most of the lipid systems, the main phase transition temperature (T_m) was used as a characteristic of the lipid properties. In general, the main lipid bilayer phase transition temperature (T_m), also called the melting temperature, is the equilibrium temperature between the lipid solid-like phase (gel phase, L_β) and the liquid-analogous phase (liquid-crystalline, L_α). At gel phase, the hydrophobic lipid chains exist in an ordered state where all of the C-C bonds are in the trans conformation. However, as the temperature increases, the gel phase becomes a more disordered and fluid liquid-crystalline phase where some C-C bonds are in the gauche conformation.

A variety of techniques can be used to monitor the phase transitions: ^2H- and ^{31}P-NMR, ESR, FT-IR, fluorescence,[84,85] and differential scanning calorimetry (DSC), among others.

DSC is the most direct technique, measuring the change in heat capacity as the sample undergoes an endothermic (or exothermic) phase transition. It has become a primary tool in studies of the thermotropic behavior of lipid bilayer since its inception in the late 1960's by Chapman.[86-89] The DSC experiments do not perturb the structure of the membrane. The advantage of high sensitivity DSC in the mid-1970's by Sturtevant permitted the direct study of lipids at dilute concentrations that are comparable to those used in many vesicle studies.[90-92]

In DSC experiments, the excess heat capacity of an aqueous bilayer dispersion relative to that of pure water is monitored accurately. The experiment not only provides T_m, but also the calorimetric enthalpy of the melting transition (ΔH_{cal}), the van't Hoff enthalpy (ΔH_{vH}), and the cooperative unit (CU). The heat capacity of the bilayer system is significantly increased at the T_m. The change in heat capacity at the phase transition is integrated to give the calorimetric enthalpy (ΔH_{cal}) for the process of the bilayer system (equation 1):

$$\Delta H_{cal} = M \int_{T_1}^{T_2} C_{ex}\, d\,T \qquad (1)$$

where M is the molecular weight of the lipid; c_{ex} the excess specific heat; and T_1 and T_2 are the temperatures at the initial and final transition respectively. Therefore ΔH_{cal} is determined by the area under the transition peak.

If the lipid transition is assumed to be a two-state process, the equilibrium constant (K) is represented by equation 2, which is the van't Hoff equation:

$$(\partial \ln K / \partial T)_p = \Delta H_{vH} / RT^2 \qquad (2)$$

The van't Hoff enthalpy is obtained from equation 3 where ΔCp is the excess heat capacity and T_m is the temperature at the maximum in the excess heat capacity profile:

$$\Delta H_{vH} = [(\Delta Cp)_{max} 4RT_m^2]^{0.5} \qquad (3)$$

The gel-to-liquid-crystalline transition in lipid bilayers is intermolecular cooperative. The cooperative unit (CU) of the transition, which is the number of molecules undergoing the transition at the same time, is obtained from a comparison of the calorimetric enthalpy with the van't Hoff enthalpy (equation 4):

$$CU = \Delta H_{vH} / \Delta H_{cal} \qquad (4)$$

For any strictly two-state process, the value of CU must equal unity; for any process involving independent molecules, $CU \leq 1$. However, for the bilayer system of 16:0/16:0PC (DPPC), the CU number can be as high as 1000.

The phase behavior of lipids is highly affected by the molecular structures of the lipids. The changes in lipid chain length, unsaturation (number, isomeric type and position of double bonds), asymmetry and branching, type of chain–glycerol linkage (ester, ether, amide), position of chain attachment to the glycerol backbone (1,2- vs. 1,3-) and head group modification all affect the value of T_m.

In general, T_m values decrease with decreasing chain length and with increasing asymmetry of the alkyl chains. The presence of branched chains or bulky side groups

also decreases the T_m. The transition temperature data for the saturated diacyl phosphatidylcholines as a function of chain length are shown in Figure 1-10a. With increasing chain length, the T_m increases. If the T_m is plotted vs. the reciprocal of chain length (Figure 1-11), it is clear that the chain length dependence of transition temperature is linear. An extrapolation of the straight line gives 430 K (153 °C) at $n \rightarrow \infty$, a temperature close to the melting temperature of polyethylene.[93] The dependence of the enthalpy change on chain length is shown in Figure 1-10b. The main transition enthalpy for chain lengths between 13 and 21 carbons depends almost linearly on the chain length. The slope of the ΔH, which indicates the enthalpy per $-CH_2-$ group, is 0.56 kcal/mol in this range.[94]

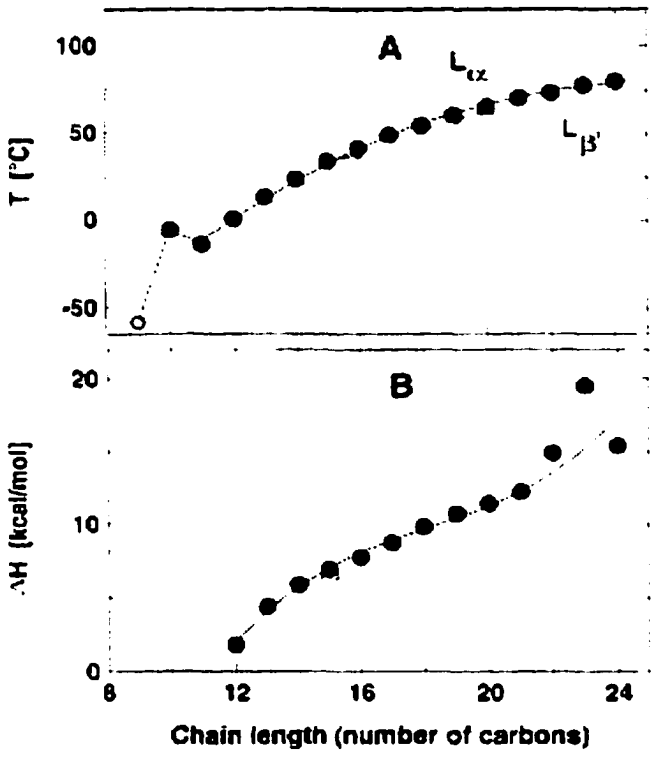

Figure 1-10. Dependence of the main phase transition temperature T_m (A) and enthalpy change (B) on the fatty acyl chain length (in units of number of carbon atoms) of the fully hydrated diacyl phosphatidylcholines (calculated value).
Adapted from Finegold[95]

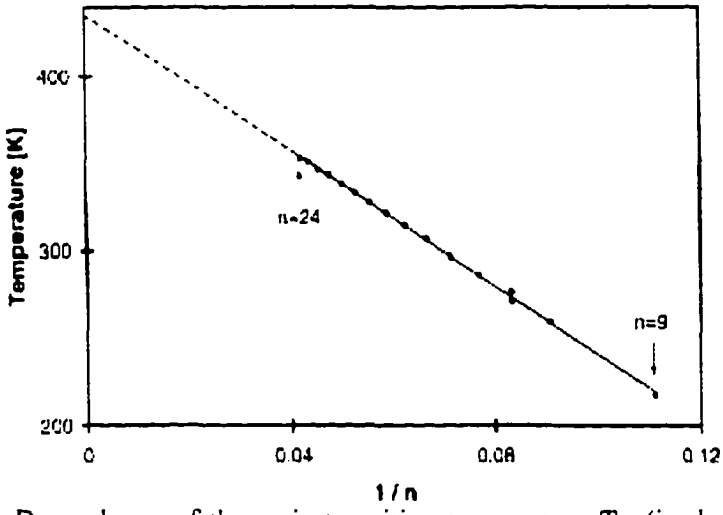

Figure 1-11. Dependence of the main transition temperature T_m (in degrees Kelvin) of the fully hydrated diacyl phosphatidylcholines on the reciprocal of hydrocarbon chain length (in number of carbon atoms, n).[96]

The T_m for phosphatidylcholines with one or two unsaturated double bonds in the fatty acyl chain are shown in Figure 1-12.

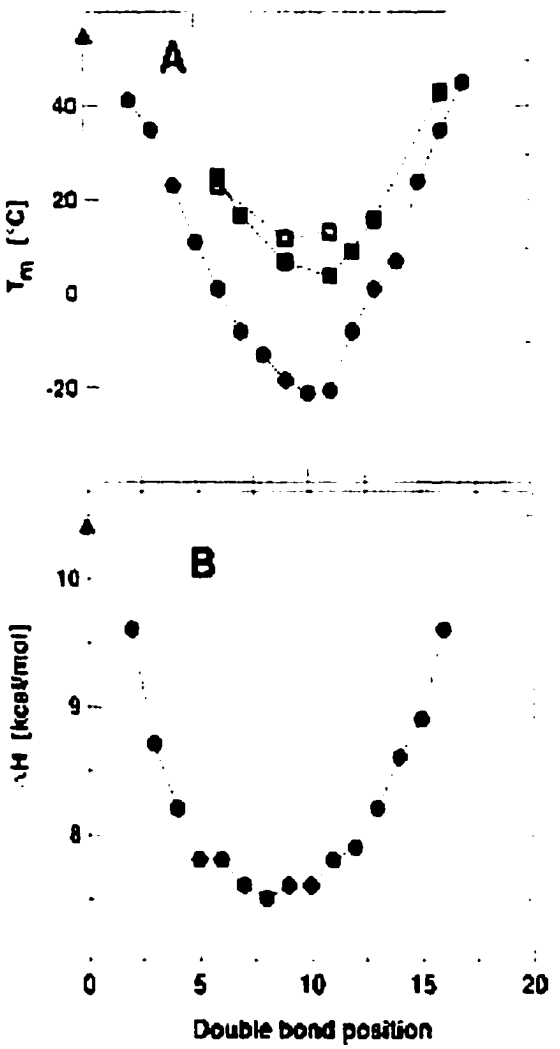

Figure 1-12. Dependence of T_m (A) and enthalpy change (B) on the position of the double bond in the fatty acyl chain of the fully hydrated diacyl phosphatidylcholines: (•) 18:1cX / 18:1cX PC; ( ) 18:0 / 18:1cX PC; ( ) 18:1tX / 18:1tX PC (X denotes the position of the double bond). The transition temperature and enthalpy change of fully hydrated 18:0 / 18:0 PC are included for comparison ( ).[97]

The data in Figure 1-12 show that introducing a single site of *cis*-unsaturation on the *sn*-2 chain only and in both chains of an 18-carbon phosphatidylcholine can lower the chain melting transition temperature by 50 and 75 °C, respectively. In contrast, when the double bond is of the *trans* type, the effect is considerably lessened. Thus, in the case of 18:0/18:0 PC, the gel – liquid crystalline transition temperature is 54 °C. The same transition occurs at 6.9 °C in 18:0/18:1c9 PC, at -18.3 °C in 18:1c9/18:1c9 PC, and at 12 °C in 18:1t9/18:1t9 PC. Further, T_m and ΔH depend strongly on the position of the *cis*-double bond. Specifically, T_m and ΔH are minimized when the double bond is located near the geometric center of the hydrocarbon chain, and progressively increase as the double bond migrates toward either end of the chain. These dependencies apply when the double bond is present in the *sn*-2 chain only or in both chains of phosphatidylcholine. This dependence is explained by the perturbation on chain packing. With double bonds positioned at the center of the chain, the local perturbation of the van der Waals chain – chain interaction is maximized since the chain is separated into two relatively small segments. In contrast, when the double bond is positioned close to either end of the chain, the relatively long saturated segment on the one side of the double bond packs tightly with neighboring chains and so increases gel phase stability and the chain melting transition temperature and enthalpy change.

O'Brien's group reported the first systematic study of the thermotropic behavior of chain-substituted polymerizable lipids.[98] The phase behavior of hydrated bilayers of mono- and bis-substituted phosphatidylcholines (PC) containing either acryloyl,

methacryloyl, or sorbyl ester groups at the chain end and the dienoyl group at the top of the tail was studied by DSC (Table 1-1).

Table 1-1. Main phase transition temperature and enthalpy of polymerizable lipids.[98]

Lipid	T_m (°C)	ΔH (kcal/mol)
bis-SorbPC$_{15,15}$	18.5	9.98 ± 0.85
bis-SorbPC$_{16,16}$	6.9	6.77 ± 0.14
bis-SorbPC$_{17,17}$	28.8	7.48 ± 0.16
bis-SorbPC$_{18,18}$	30.3	10.83 ± 0.14
bis-SorbPC$_{19,19}$	42.5	10.83 ± 0.14
mono-SorbPC$_{14,15}$	11.0	6.99 ± 0.62
mono-SorbPC$_{16,17}$	36.1	10.5 ± 0.29
bis-DenPC$_{18,18}$	20.1	7.44 ± 0.14
mono-DenPC$_{16,18}$	26.2	7.02 ± 0.29
bis-AcrylPC$_{16,16}$	30.0	6.90 ± 0.59
mono-AcrylPC$_{16,16}$	31.8	8.90 ± 0.42
bis-MethPC$_{16,16}$	-4.4	5.30 ± 0.26
mono-MethPC$_{16,16}$	11.4	10.50 ± 0.25

It was found that the T_m is sensitive to both the type and location of the functional group along the chain as well as the orientation of branching substituents. All the results

showed a lower phase transition of the polymerizable lipids than of the corresponding linear saturated chain PCs (Figure 1-13A). The T_m values of acryloyl-substituted PCs were somewhat higher than those of comparable chain-length sorbyl-substituted PCs. The addition of an isomethyl to the acryloyl group, i.e., methacryloyl, significantly depressed the T_m values. The effect of the unsaturated group is also dependent on its position. When it is near the headgroup (e.g. DenPC), it has much more effect on the chain packing and lowered the T_m more than if it is located at the chain termini (SorbPC), as discussed above. The odd/even alternation of the T_m of sorbylPCs at different chain lengths revealed the possibility of chain orientation in ester lipids (Figure 1-13b). The interaction of the sorbyl ester carbonyl group on *sn*-2 chain with neighboring methylene chains could be either inter- or intramolecular. This is dependent on whether the chain length is even or odd and intermolecular interaction is expected to decrease the T_m to a greater extent than intramolecular interaction. These systematic thermotropic studies of polymerizable lipids provide new insights into the relationship of lipid phase behavior and lipid chain substitution patterns, and facilitate the design of novel lipids and materials to form supramolecular assemblies with desired properties.

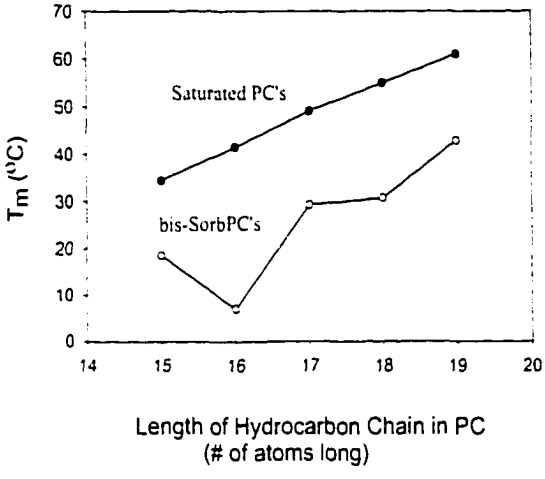

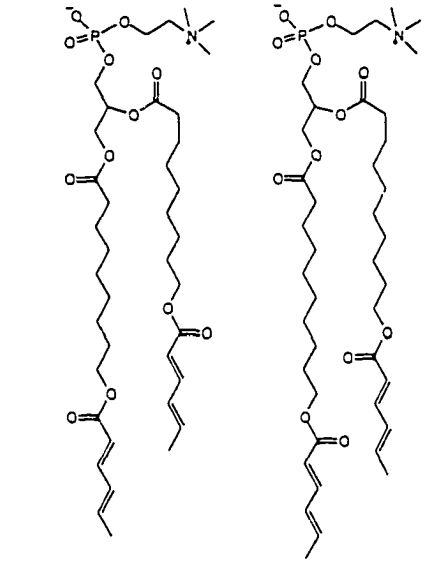

A B

bis-SorbPC$_{16.16}$ bisSorbPC$_{17.17}$

Figure 1-13. (A) chain-length dependence of the gel/liquid-crystalline phase transition temperature T_m of bis-SorbPCs. (B) Chain orientation of the ester group in all-trans extended conformations of bis-SorbPC$_{16.16}$ and bis-SorbPC$_{17.17}$.[98]

The morphology of the lipid aggregates (unilamellar and multilamellar vesicles) also affects their phase behavior. Examples of T_m and enthalpy of diacyl phosphatidylcholines under different preparation conditions are shown in Table 1-2. The table indicates that for unilamellar vesicles of 16:0/16:0 PC, the phase transition parameters depend on vesicle size. Vesicles with diameters below ~35 nm undergo a chain melting transition at 37-37.5 °C. For larger vesicles (35-70 nm), the transition temperature increases from 37 to 41 °C as vesicle size increases. Larger vesicles

(diameters > 70 nm) undergo the transition at 41 °C, essentially independent of size. Also, the chain melting transition of small unilamellar vesicles (SUV) with diameters below 30-50 nm are considerably broader than those observed for MLV ($T_{1/2}$ = 3.5 °C for SUV vs. ~ 0.1°C for MLV). Further, the enthalpy change of the transition in SUVs is smaller than that in MLVs. The difference is attributed to a sensitivity of the enthalpy level of the gel phase lipid to vesicle size.

Table 1-2. Thermodynamic parameters of the phase transitions undergone by saturated diacyl phosphatidylcholines in different vesicle preparations.[94]

Lipid chains	Vesicle preparation	T_m (°C)	ΔH (kcal/mol)
14:0 / 14:0	MLV	23.6 ± 1.5	6.0 ± 2.4
	SUV	22.2 ± 2.0	4.1 ± 0.9
16:0 / 16:0	MLV	41.3 ± 1.8	8.2 ± 1.4
	LUV	41.1 ± 0.1	7.5 ± 0.5
	SUV	37.8 ± 1.0	5.9 ± 1.3
18:0 / 18:0	MLV	54.5 ± 1.5	10.4 ± 1.6
	SUV	51.8 ± 1.1	9.0

* adapted from [94]

** SUV, small unilamellar vesicles (diameter < 100 nm); LUV, large unilamellar vesicles (diameter > 100 nm); MLV, multilamellar vesicles.

1.4.1 Membrane Permeability.

One of the most important properties of membranes is their ability to control the rate of permeation of different species. The diffusion model is used to explain the mechanism. In this solution-diffusion mode, the permeants dissolve in the membrane and then diffuse through the membrane by a concentration gradient (Figure 1-14). This process can be expressed by Fick's law of diffusion:

$$J_i = -D_i (dc_i / dx)$$

where J_i is the rate of transfer of component i, or flux [g/(cm^2/s)] and dc_i/dx is the concentration gradient of component i. The term D_i is called the diffusion coefficient (cm^2/s) and is a measure of the mobility of the individual molecules. The minus sign reflects that the direction of diffusion is down the concentration gradient.

Fick's law, as applied to passive diffusion, is usually written:

$$J = - P \Delta C$$

where $P = D/\Delta x$, the permeability coefficient.

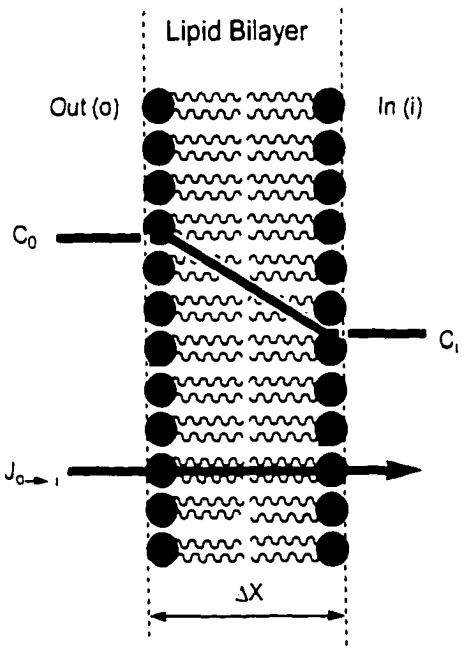

Figure 1-14. Membrane transport. C and J donate concentration and molecular flux, respectively. Subscripts: o = outside, i = inside. ΔX = membrane thickness (~ 5 nm for lipid bilayer).

One of the characteristics of phospholipid membranes is their extreme impermeability to cations. Studies with phospholipid vesicles have given values of permeability coefficients in the range of 10^{-13} to 10^{-14} cm/sec for monovalent cations (e.g. K^+, Na^+).[99-101] The diffusion rates of anions (e.g. Cl^-) measured by Bangham et al. were found to be 2 to 3 orders of magnitude larger than that for cations.[35] The enhanced permeability of anions over cations has been ascribed to the positive membrane potential of the lipid bilayer.[102] In contrast to the low permeability to ions, phospholipid bilayer membranes exhibit considerable permeability to water, ranging from 10^{-2} - 10^{-4} cm/sec.[103] The rate of permeation of most nonelectrolytes across cell membranes is

governed by their lipid solubility relative to their water solubility,[104-106] so P increases with increasing partition coefficient. Table 1-3 shows that the permeability coefficient of egg lecithins is directly related to the partition in the hydrocarbon-like phase. The permeation rate of polar nonelectrolytes across BLMs is appreciably lower than that of water. Permeability coefficients of such solutes as glucose, ribose, sucrose, glycerol, urea, thiourea, and indiles in BLMs range between 10^{-5}-10^{-8} cm/sec.[107,108] Small molecules permeate more rapidly than large or branched molecules. The difference in permeability depends significantly upon the physical and chemical nature of the molecule.[109,110] In general the permeability of various molecules through the bilayer occurs in the following order: water > small nonelectrolytes > anions > cations.

Table 1-3. Permeability coefficient (P) of egg lecithins as a function of the partition coefficient (K).[22]

Compound	P x 10^4 (cm sec^{-1})	$K_{octanol}$
Formid acid	2.34	0.29
Acetic acid	2.38	0.49
Propionic acid	6.1	1.8
Butyric acid	11.5	6.2

Several methods have been described for the study of the permeability properties of lipid vesicles. The original method introduced by Bangham et al.[35] involves isotope

tracers and has been used extensively for the study of efflux rates for ^{22}Na, ^{42}K, ^{36}Cl, ^{86}Rb, and ^{14}C-glucose. The tracer is added in the salt solution during the formation of the vesicles when it can be trapped within the aqueous interior of the closed membranes. The vesicles with trapped tracer are then separated from the untrapped species either by dialysis or by passage through a gel-filtration column (usually Sephadex G-50). The efflux of the trapped tracers is then followed by sequential dialysis of the vesicles against the same salt solution. This method is particularly suited for studying the efflux of slowly diffusing solutes.[101]

A modification of this method has been used by Kinsky and his colleagues, who measured the efflux of glucose by following spectrophotometrically the reduction of DNA with suitable enzyme systems utilizing glucose as substrate.[111]

A method particularly suited to fast-diffusing solutes, such as water, glycerol, and urea was developed by Bangham.[112] It depends on measurements of the change in optical density of vesicle suspensions as the osmolarity of the aqueous environment changes in respect to the interior of the vesicles. Shrinking (in hypertonic solutions) and swelling (in hypotonic solutions) is accompanied by an increase and decrease in optical density, respectively. This method was used extensively by DeGier and colleagues in studies of glycerol and glycol permeability of vesicles of different fatty acid chains.[113]

Both composition and thermotropic state of the bilayer play important roles in membrane permeability. The structure of the fatty acyl chains of phospholipids determined diffusion rates. Van Deenen and coworkers have reported studies on the permeability of vesicles composed of phospholipids with well-defined fatty acyl chains.

They found that the permeability of vesicles generally increased with increasing unsaturation and decreasing chain length.[113,114] The effect of increased unsaturation resulting in higher permeability rates was also observed by Klein[115] and Papahadjopoulos et al.[116]

The role of phase transition in the permeability of phospholipid membrane was studied by Papahadjopoulos and coworkers.[116] The melting of the acyl chains at phase transition temperature could be related to the higher frequency of kinks induced by the melting of the chains, which resulted in decreased order within the interior of the bilayer. Studies also showed[110,117,118] that at temperatures in the vicinity of the gel/liquid-crystalline transition, the packing defects between gel and liquid-crystalline domains as well as the decrease of lateral compressibility of the bilayer may open up spaces between headgroups, which resulted in a significant increase in membrane permeability.

Membrane permeability of vesicles can be measured with any water-soluble marker. Both encapsulated fluorescent and radiochemical labels are commonly used to evaluate permeability. Useful detection methods based on fluorescence, enzymatic, redox, electron paramagnetic resonance, and radiochemical techniques are commonly used. A convenient method monitors the increase in fluorescence of an encapsulated self-quenching dye, e.g. carboxyfluorescein (CF), calcein, or [^{3}H]-glucose as it escapes the vesicles.[80,119]

The introduction of polymerizable groups into lipids can cause drastic changes in membrane permeability.[15,120] Polymerization of bilayers decreases the bilayer

permeability to encapsulated aqueous markers. The formation of linear polymers changes the bilayer permeability by 0.2-0.5, whereas the formation of a cross-linked polymer network in the bilayer can decrease the permeability by at least 2 orders of magnitude.[80,121]

1.5 Characterization of Cross-linked Lipid Bilayer Vesicles

Polymerization of lipid vesicles alters the assembly characteristics. Preliminary characterization of the resulting vesicles includes determination of their size and shape, and phase behavior.

It is necessary to demonstrate that the vesicle size and shape are not significantly changed by the polymerization. Electron microscopy and laser light scattering are commonly used for these purposes. Electron microscopy provides direct evidence that the polymerized dispersions still contain spherical vesicles. Laser light scattering measurements also demonstrate that the size distribution of vesicles is not significantly altered by polymerization.

However, polymerization of a vesicle can have dramatic effects on the physical properties of the bilayer, particularly when the polymerizable groups are located in the lipid tails. Polymerization leads to a decrease in the fluidity of the membrane, as indicated by retarded lateral diffusion of the lipids within the bilayer. Modest reductions are observed for monofunctional lipids, but diffusion of a small molecule probe is decreased by two orders of magnitude with polymerization of bifunctional lipids.[122] This is due to the effect of cross-linking in the system.

Polymerization of the lipid tails usually leads to a broadening or even abolition of the main phase transition of the bilayer.[32,123,124] Covalent linkage of the lipid tails inhibits the formation of the gauche rotamers and the cooperativity typically observed as unpolymerized bilayers pass through the phase transition. The loss of the phase transition is correlated to an increase in the chemical and physical stability of vesicles after polymerization. Polymerized vesicles generally exhibit enhanced stability to organic solvents and detergents,[56,78,124] longer shell-life,[55,125] and decreased permeability to water-soluble molecules.[55,56,80,124,126]

1.5.1 Surfactant Dissolution (Triton X-100) of Vesicles

Regen and coworkers reported that the stability of vesicles towards surfactant treatment increases in the following order: unpolymerized < linearly polymerized < cross-linked.[56] The increased stability to surfactant has been attributed to the cross-linking of the lipids into a covalently linked monodomain polymeric vesicle. It has long been known that surfactant micelles are effective in solubilizing lipids and other biomembrane components. Surfactant solubilization of vesicles is a common method to characterize the colloid stability in aqueous suspension as long as the polymer chains are short enough to be incorporated into a mixed micelle.[81] The mechanism of surfactant solubilization (lysis) of bilayers involves the incorporation of surfactant molecules into the bilayer. The effective solubilization of lipids into micelles requires that the surfactant concentration be greater than its critical micelle concentration (CMC) and that the surfactant to lipid molar ratio be ca. 3 to 5. When the surfactant concentration

predominates, the lipids no longer exist in a vesicle but are incorporated into a mixed micelle of lipid and surfactant. If the lipids are cross-linked in a polymerized vesicle, they cannot be readily extracted by surfactant. This concept is shown in Figure 1-15 with cross-linked vesicles being stable in the presence of a surfactant while linear poly(lipid) vesicles and unpolymerized vesicles are lysed and solubilized by the surfactant, forming mixed micelles.

Figure 1-15. Vesicle Dissolution by Triton X-100.

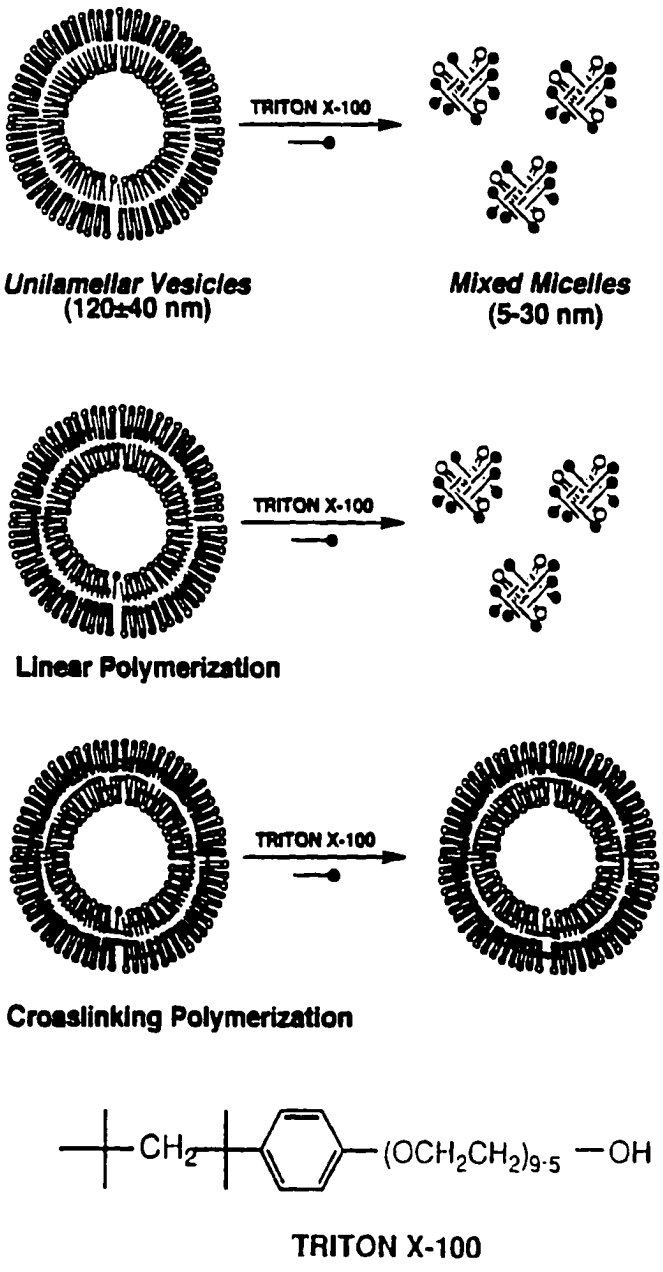

The extent of vesicle lysis by TX-100 was determined by quasi-elastic light scattering (QELS). In the QELS experiment, the intensity of the scattered light (in photons/sec) is measured and the average mean diameter of the particle calculated. The diameter of the vesicle/particle was determined by a variety of different mathematical algorithms (based on a spherical model), which analyze the measured autocorrelation function. Thus, the lysis of poly(lipid) vesicles with surfactant results in decreased particle size since the lipids are now solubilized as mixed micelles. The light scattering intensity decreased due to the smaller particle diameter if the vesicles were dissolved to form mixed micelles. Previous experiments[75,76,81] showed that unpolymerized and linear polymerized lipid vesicles were lysed after addition of 2-4 equivalents of TX-100, whereas the average mean diameter for crosslinked lipid vesicles remained constant up to at least 15 equivalents of TX-100. At high surfactant concentrations, two different size particles could be observed at ca. 110 and 5-10 nm due to the polymerized vesicles and TX-100 micelles, respectively. After cross-linked vesicles become saturated with TX-100, excess surfactant forms micelles in the presence of the stabilized vesicles. Measuring scattering intensities is a common method to show the chemical stability of cross-linked vesicles. Since the total scattering intensity is varied at different concentrations, normalized scattering intensity is used as described in Section 2.2.

1.5.2 Solubility in Organic Solvents

Cross-linking is associated with a gel point, i.e., the point of polymer insolubility, so the solubility characteristics of a polymer provide strong evidence about whether a

polymer is cross-linked or linear. If cross-linked vesicles are freeze-dried, the resulting dry polymer exhibits general insolubility in organic solvents.

Weight percent solubility is frequently used to determine whether a polymer is cross-linked.[56,127] The polymerized lipids are recovered from the hydrated bilayer by freeze-drying the sample after completion of the polymerization, then dispersing the remaining solid in an organic solvent in an attempt to dissolve the polymer. A preliminary examination of the effectiveness of various solvents for polymerized zwitterionic PC lipids indicated that 1,1,1,3,3,3-hexafluoro-2-propanol (HFIP) was the most effective solvent for these polymers. HFIP is an excellent hydrogen-bond donor. Therefore, it can interact strongly with the carbonyl functional groups of the polymeric lipids.[128-130] Furthermore its low self-association makes it a good solvent for a variety of zwitterionic polymers.[131] The solubility of linearly polymerized phospholipids in HFIP is great enough to permit the effective use of poly(lipid) solubility to estimate the reach of cross-linking inside the bilayer. HFIP has been used as a solvent for polymers which contain a phosphocholine moiety such as those used in this study.[81,131]

However, the solubility method is limited by the molecular weight of the polymer. The HFIP solubility protocol is most effective with poly(lipid) chains that have a degree of polymerization less than ca. 10^3.[81] As long as this possible limitation is given proper consideration, the HFIP procedure appears to have broad applicability for the determination of gelation of polymerized assemblies.

The objectives of this work include the design and synthesize novel polymerizable lipids, both homobifunctional and heterobifunctional lipids, and the characterization of their polymerization in large unilamellar vesicles. We are particularly interested in cross-linking polymerization to increase the stability of the assemblies.

In this dissertation, Chapter 1 describes the general concepts of physical properties of lipids and their assemblies, methods used to stabilize supramolecular assemblies, and the design of polymerizable lipids. Chapter 2 focuses on the cross-linking polymerization of lipid bilayers by homobifunctional lipids and Chapter 3 on cross-linking by heterobifunctional lipids. The ability to freeze-dry and redisperse cross-linked polymerized vesicles is demostrated in Chapter 4.

CHAPTER 2

CROSS-LINKING POLYMERIZATION OF ASSEMBLIES WITH HOMOBIFUNCTIONAL LIPIDS

2.1 Introduction

One of the first examples of polymerizable bilayer vesicles was designed by Regen and coworkers. In the early 1980s, Regen et al. introduced the concept of polymerized vesicles by incorporating a methacryloyl group into an ammonium amphiphile **2-1**:[52]

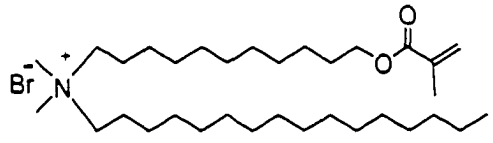

2-1

Small bilayer vesicles (20-70 nm) of **2-1** were prepared by sonication and then polymerized by addition of 5 mol% of AIBN. TEM of the polymerized vesicles confirmed the presence of closed, spherical vesicles. These vesicles retained sucrose and were stable in the presence of 25% ethanol while monomeric vesicles would precipitate if the solution contained more than 10% ethanol. Two years later a methacryloyl group was introduced into phosphatidylcholine (PC) analogues, and mono-methacryloyl-substituted PC **2-2** and bis-methacryloyl PC **2-3** were synthesized.[56] Vesicles were polymerized by direct UV irradiation. It was shown that the polymerization of these vesicles increased

the stability of the vesicles for long-term storage as well as in 20% ethanol. Leakage rate measurements for polymerized vesicles showed that poly-**2-3** had a greater retention of [^{14}C] sucrose than poly-**2-2**. The polymerized vesicles of **2-3** could not be solubilized with chloroform. All these results indicated the formation of cross-linking polymerizaton by lipid **2-3**. The copolymerization of 20% **2-3** with 80% **2-2** gave a decreased leakage rate similar to pure polymer **2-3**. This suggested that 20% of the bis-substituted lipid **2-3** as a cross-linking agent was enough to achieve cross-linking.

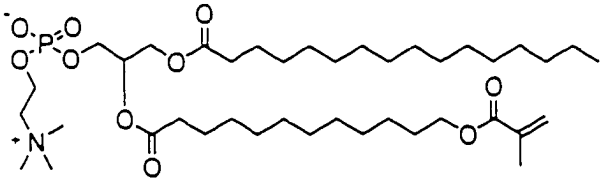

2-2

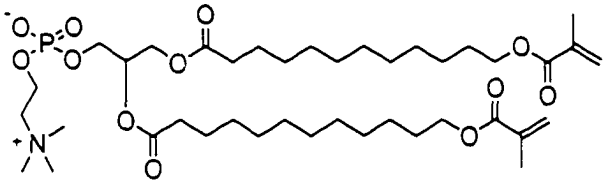

2-3

Other polymerizable lipids synthesized by Regen and coworkers were lipoyl-substituted phospholipids: 1-palmitoyl-2-[12-(lipoyloxy)dodecanoyl]-*sn*-glycero-3-phosphocholine **2-4** and 1,2-bis[12-(lipoyloxy)dodecanoyl]-*sn*-glycero-3-phosphocholine **2-5**.[121] Polymerization was performed on pure **2-4** and **2-5** and mixtures of **2-4** and **2-5** with the addition of catalytic amounts of DTT.

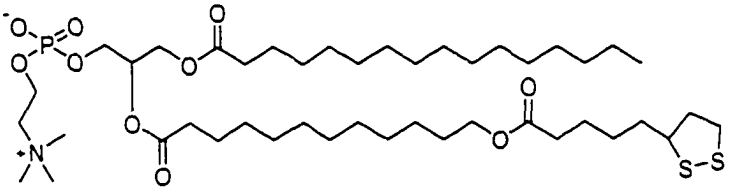

2-4

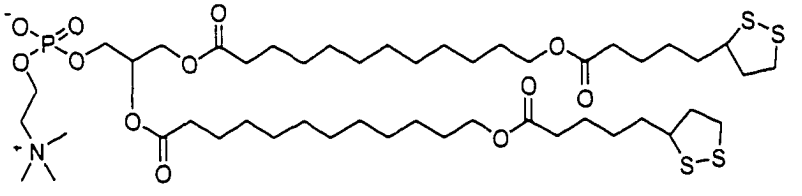

2-5

The results showed that polymerized vesicles from pure **2-5** were insoluble in chloroform and chloroform/ethanol (1/1, v/v) while those from pure **2-4** were soluble in those solvents. Increasing the mole percentage of **2-5** in mixed polymerized vesicles resulted in a reduction in bilayer permeability. The cross-linked vesicles from **2-5** had 0.02 the permeability to sucrose of the monomeric ones.

Dorn et al. synthesized butadiene lipids **2-6** and **2-7**, each of which has a dienoyl group in both hydrophobic chains.[80] UV polymerization of **2-6** yielded membrane vesicles that were about 0.5 as permeable to [^{3}H]glucose as the monomeric **2-6**. A similar experiment with **2-7** resulted in a decrease in glucose permeability to about 30% of that of the monomeric vesicles. The greater reduction of glucose permeability in poly-**2-7** compared with poly-**2-6** was assigned to the formation of cross-linking in lipid **2-7**. The α- and β-chain dienoyl groups in **2-7** are not likely to react with one another since the two fatty acid chains extend unequal distances into the membrane bilayer. Therefore, poly-**2-7** could be highly cross-linked. On the other hand, the fatty acid chains in

symmetrical lipid **2-6** extend equally into the bilayer, and are likely to react with each other to form linear polymers.

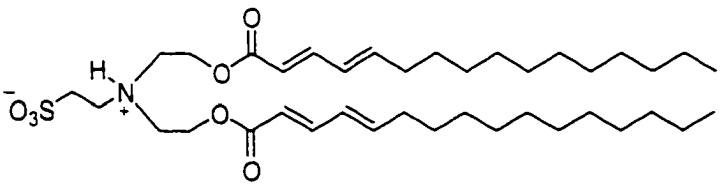

2-6

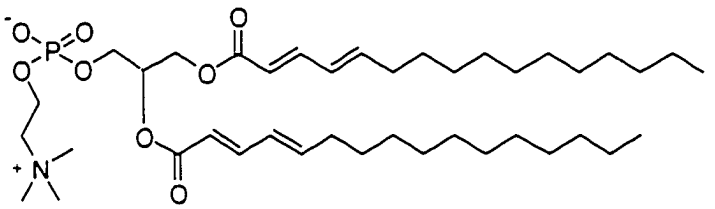

2-7

These early studies provided the initial evidence that cross-linked bilayer vesicles possess different properties than linear polymeric vesicles, and the cross-linking polymerization of bilayer vesicles can be introduced by bis-substituted functional groups, i.e. homobifunctional lipids.

Diacetylene lipids are another type of polymerizable lipids that has drawn much attention because the conversion from monomeric to polymeric vesicles can be observed visually and spectroscopically by a color change. The colorless monomer solution is converted into deep-blue or brilliant red polymer with the formation of poly(diacetylene) (PDA). Phospholipids containing single or double diacetylene groups have been studied by the Ringsdorf[15,47,124], Chapman[48,51,132] and O'Brien[53,54] groups. Bilayer vesicles were readily formed from hydrated diacetylenic lipids by sonication. The

multilayered vesicles formed from the dialkyl methylammonium salt **2-8**[47] by sonication has a diameter of about 400 nm.

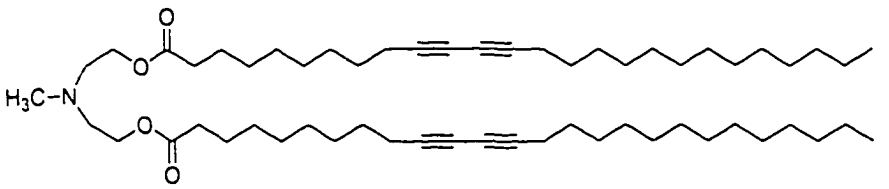

2-8

Polymerization of these vesicles by UV irradiation under nitrogen initially gave a blue (absorbing around 620-630 nm) product that changed to red (absorbing at 500-541 nm) upon prolonged irradiation or at high temperatures. Electron microscopy provided the evidence that the polymers were vesicles. Monomeric and polymeric vesicles had essentially the same size. Multilamellar vesicles of phospholipids **2-9** and **2-10** were also prepared[132] and reddish products were obtained upon UV irradiation:

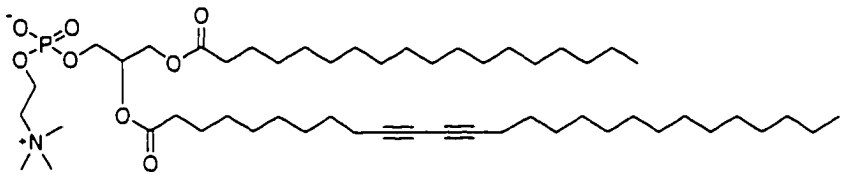

2-9

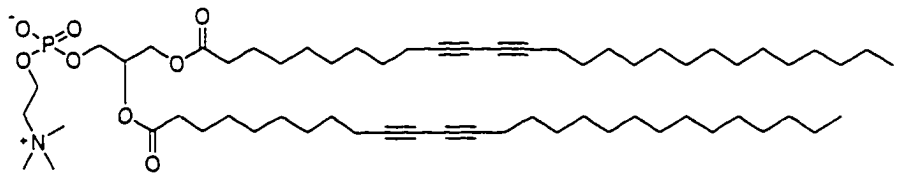

2-10

The permeability of the vesicles to glycerol decreased considerably after polymerization. Polymerization also markedly enhanced the stability of vesicles to precipitation at 4 or 20 °C. The unpolymerized vesicle dispersions precipitated within 1 h and the rate of

precipitation was temperature independent. The precipitation from polymeric vesicles only became apparent after 24 h at 20 °C and after 7 days at 4 °C for both lipids. On the other hand, only the polymerization of the bis-substituted analogue **2-10** led to an insoluble polymer, indicating the formation of a cross-linked material.

The polymerization of diacetylene-containing monomers occurred only when the lipids were well packed in a solid-like phase (below the main phase transition temperature of the lipids) and by photopolymerization. The polymerization efficiency depends on the correct alignment of the monomeric units. The polymerization of symmetrical diacetylene lipids was much more efficient than that of asymmetrical lipids.[54] The topotactic requirements for the polymerization of diacetylene lipids limit the choices of lipid structures as well as polymerization methods.

Diene lipids are another type of polymerizable lipids widely studied by researchers. They are normally easy to cross-link, either through the use of bis-diene comonomers in the original polymerization or by post-polymerization reaction of the double bond that remains after the initial polymerization. Photopolymerization, thermal initiation, and redox initiation can be usefully employed to polymerize bilayer membranes of diene monomers.

Tsuchida et al.[75,127,133-138] carried out extensive studies on the polymerization of mono- and bis-substituted diene lipids **2-11** and **2-12** with different initiation methods. They found that UV- polymerized poly-**2-12** only resulted in oligomers with X_n around 6 and soluble in organic solvents such as chloroform or ethanol. Polymerization by addition of radical initiator (AIBN or AAPD) gave 50-60 % polymerization conversion at

60 °C. Complete polymerization was performed by the use of AIBN and AAPD simultaneously.[135]

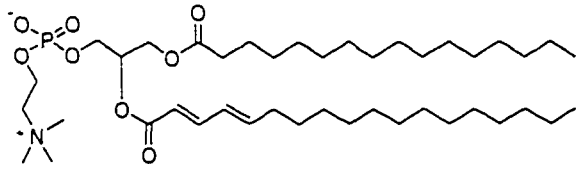

2-11

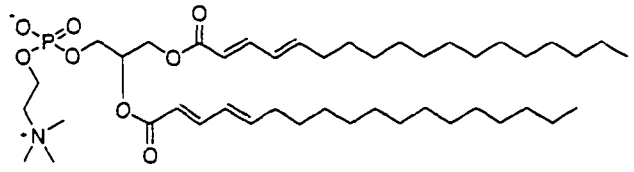

2-12

From these results, they proved the nonequivalent acyl chain packing of phospholipids in bilayer membranes that had been proposed by O'Brien et al.[54] and Chapman et al.[139] The diene group in the 1-acyl chain locates in the more hydrophobic region of the bilayer and could only be polymerized by a water-insoluble initiator (AIBN), while the 2-acyl chain is close to the aqueous phase, and therefore could be initiated by a water-soluble radical initiator (AAPD). The vesicles polymerized by AIBN or AAPD were partially soluble in organic solvents (methanol, ethanol, and chloroform) while polymers initiated by both AIBN and AAPD were insoluble in the same solvents.[135] This indicated a cross-linked polymeric membrane structure. The simultaneous polymerization of both diene groups on *sn*-1 and *sn*-2 chains could also be achieved by redox initiation or γ-irradiation.[75]

It is clear that cross-linking polymerization of vesicles increases the stability drastically. In contrast to monomeric vesicles, the polymeric vesicle suspensions remain

stable for weeks. Entrapped substances are released to a much smaller extent from polymeric vesicles than from monomeric ones. Vesicle solutions can be diluted with ethanol without precipitation. The polymeric vesicles were not destroyed osmotically after addition of salts, e.g. KCl. Electron micrographs of the precipitate still showed spherical vesicles. Another indication of the high stability of polymeric vesicles was obtained by scanning electron microscopy (SEM). While monomeric vesicles are destroyed due to the drastic preparation conditions (high vacuum), spherical structures of polymeric vesicles could be obtained.[134] The size of the polymerized vesicles was not changed even after repeated freeze-thaw treatment of the aqueous dispersion.[75]

Anikin and coworkers synthesized a novel polymerizable phospholipid with conjugated diene groups at the hydrocarbon chain ends, 1.2-bis(11,13-tetradecadienoyl)-sn-glycero-3-phosphocholine **2-13**.[140] This lipid formed vesicles which could be polymerized upon γ- and UV-irradiation. The polymerized vesicles were detergent-resistant and retained their structure under ultrasonic treatment and in organic solvent. The high stability of polymeric vesicles was apparently caused by the formation of cross-linking covalent bonds between two monolayers in polymerized membranes.

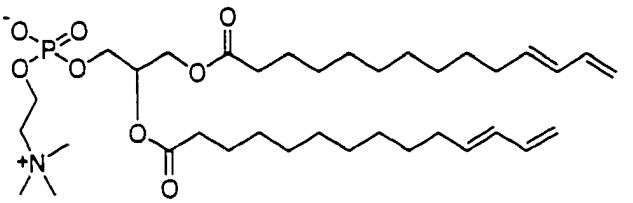

2-13

O'Brien's group did a systematic study on the cross-linking behavior introduced by homobifunctional lipids. Sisson et al.[81] examined the cross-linking of bilayers as a function of the mole fraction of bis-substituted lipids, using mono- and bis-acryloyl PC **2-14**, **2-15** as well as mono- and bis-sorbyl PC **2-16**, **2-17**. In each lipid the reactive group(s) was located at the hydrophobic end of the lipid tails. The onset of cross-linking of both acryloyl (AcrylPC) and sorbyl (SorbPC) lipids was determined by changes in lipid lateral diffusion, bilayer vesicle stability, and polymer solubility. Each method indicated that a substantial mole fraction (0.30 ± 0.05) of the bis-substituted lipid was necessary to cross-link bilayer membranes.

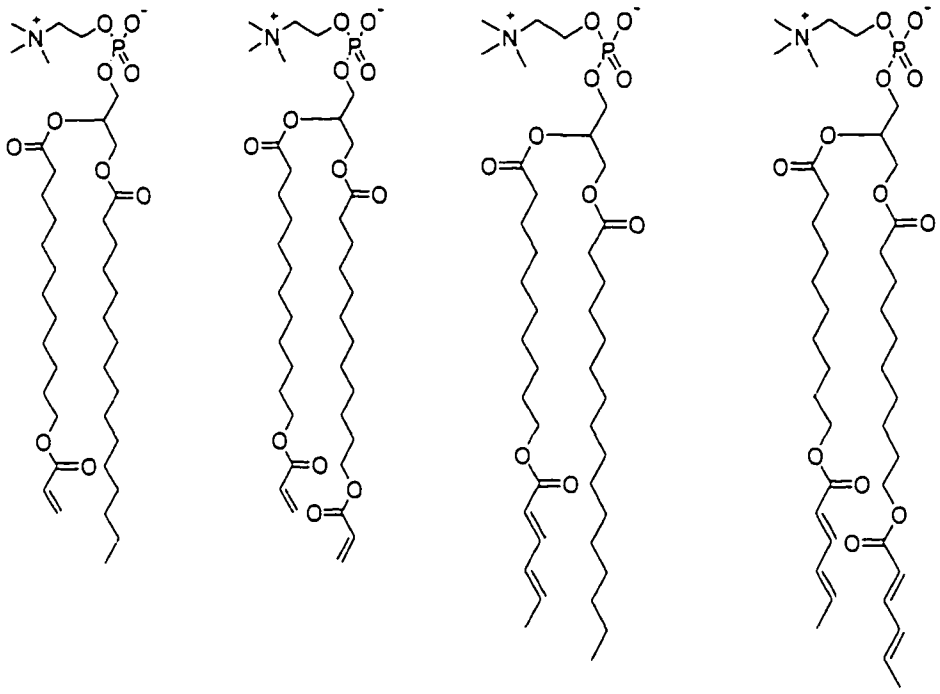

2-14 **2-15** **2-16** **2-17**

The study by Sisson et al. provided the initial insight into the nature of cross-linking in the constrained environment of organized assemblies and how it differs from isotropic polymerizations.[81] Significant differences between bilayer and solution or bulk polymerizations were previously revealed through systematic investigations of radical-initiated polymerizations in bilayers composed of acryloyl-, methacryloyl-, and sorbyl-substituted lipids.[70,72,73] At high conversions the polymer chains were likely to be terminated by reaction with initiator fragments, i.e., primary radical termination. Relatively large degrees of polymerizations, X_n, were observed for the radical polymerizations of acryloyl-, methacryloyl-, and sorbyl-substituted lipids in bilayers.

Differences in reactivity of the propagating radical were also reflected in the size of the polymers obtained from the polymerization of bilayers of AcrylPC and SorbPC.[70,72] However, these experimentally observed differences did not account for the significant inefficiency in bilayer cross-linking of these amphiphiles. An analysis of the cross-linking and competing processes suggested that the location of the reactive group, i.e., reaction site, in the amphiphile and therefore within the bilayer assembly could influence the cross-linking efficiency.[141] To assess this possibility, the cross-linking of binary mixtures of dienoyl-substituted lipids, (*E,E*)-DenPC **2-11**, **2-12**, where the reactive diene was located near the glycerol backbone of the lipid, was compared with the cross-linking of SorbPC **2-16**, **2-17**, where the reactive group was at the end of the lipid tail.

2.2 Experimental

2.2.1 Materials

1-Tetradecanol, pyridinium dichromate (PDC), dicyclohexylcarbodiimide (DCC), sodium hydride (60% dispersion in mineral oil), 4-(dimethylamino)pyridine (DMAP), potassium persulfate, sodium bisulfite, and Triton X-100 (TX-100) were obtained from Aldrich Chemicals. Trimethyl 4-phosphonocrotonate was purchased from Lancaster Synthesis Inc. 1-Palmitoyl-2-hydroxy-*sn*-glycerol-3-phosphocholine ($LysoPC_{16}$) and L-α-glycerophosphorylcholine:cadmium chloride (1:1) adduct (GPC) were from Avanti Polar Lipids Co. DMAP was recrystallized from $CHCl_3$/ether (1:1), and the others were used without further purification. THF was distilled from sodium benzophenone ketyl. $CHCl_3$ and CH_2Cl_2 were distilled from CaH_2 under argon. The reactions were monitored

by TLC visualized by a UV lamp or phosphomolybdic acid dye. The lipids were hydrated in Milli-Q water, Millipore Inc.

2.2.2 Synthesis of mono- and bis-DenPC

2.2.2.1 Tetradecanal (**2-18**)

PDC (13 g, 34 mmol) was added to a solution of 1-tetradecanol (5 g, 22.6 mmol) in 500 mL of CH_2Cl_2. The reaction was stirred at room temperature overnight, and the mixture was filtered through silica gel to remove the PDC. The filtrate was concentrated, and the crude product was purified by column chromatography with hexane/EtOAc (95/5). A yield of 3.6 g (75%) was obtained. ^{1}H NMR ($CDCl_3$): 9.74-9.73 (t, J = 1.8 Hz, 1H), 2.42-2.36 (dt, J = 7.4, 1.8 Hz, 2H), 1.63-1.54 (m, 2H), 1.27-1.16 (b, 20H), 0.87-0.82 (t, J = 6.6 Hz, 3H) ppm. ^{13}C NMR ($CDCl_3$): 202.96, 43.90, 31.89, 29.62 (3), 29.56, 29.41, 29.33 (2), 29.14, 22.67, 22.07, 14.09.

2.2.2.2 Methyl 2,4-Octadecadienoate (**2-19**)

Trimethyl 4-phosphonocrotonate (4.2 g, 20 mmol) in 50 mL of THF was added slowly to a suspension of NaH (60% dispersion in mineral oil, 1.4 g, 34 mmol) in 150 mL of THF at 0 °C under argon. The suspension was stirred until no evolution of gas was observed. Tetradecanal **2-18** (3.6 g, 17 mmol) in 100 mL of THF was added dropwise at 0 °C. The reaction was allowed to warm to room temperature and monitored by TLC with hexane/EtOAc (98/2) as the mobile phase. Excess NaH was quenched by slow addition of cold water. The THF was evaporated and the residue was taken up in diethyl

ether and washed several times with water and brine. The organic layer was dried with anhydrous $MgSO_4$ and concentrated. The crude ester was purified by column chromatography using hexane/EtOAc (98/2), affording 2.4 g of compound **2-19** (48% yield).

The ratio of (*E,E*)-2,4-dienoyl ester to its (*E,Z*)-isomer was determined by ^1H NMR to be 1/1. ^1H NMR ($CDCl_3$; peaks in *italics* are from *E,Z* isomer.): 7.67-7.56 (dd, *J* = 15.2, 11.7 Hz, (*E,Z*)-isomer, 0.5H) and 7.32-7.22 (m, (*E,E*)-isomer, 0.5H), 6.17-6.07 (m, 1.6H), 5.91-5.76 (m, 1.4H), 3.75 (s, (*E,Z*)-isomer, 1.2H) and 3.74 (s, (*E,E*)-isomer, 1.8H), 2.31-2.25 (m, (*E,Z*)-isomer, 1H), 2.20-2.12 (m, (*E,E*)-isomer, 1H), 1.42-1.20 (b, 22H), and 0.9-0.85 (t, *J* = 6.6 Hz, 3H) ppm. ^{13}C NMR ($CDCl_3$): 167.75, 145.41, 145.02, *141.92*, *139.79*, 128.26, *126.35*, *120.63*, 118.61, 51.41, 32.99, 31.91, 29.64, 29.55, *29.45*, 29.42, 29.35, 29.17, 28.68, *28.29*, 22.68, 14.10.

2.2.2.3 Methyl (*E,E*)-2,4-Octadecadienoate (**2-20**)

A well-stirred solution of urea (4.4 g, 73 mmol) in 220 mL of methanol was treated with ester **2-19** (2.4 g, 4.1 mmol). The solution was kept at 0 °C overnight. The needlelike crystals were filtered, washed with cold methanol, and dried under vacuum. These crystals were dissolved in ether and washed several times with water. The organic layer was combined and dried with anhydrous $MgSO_4$. After evaporation of ether, 1.2 g of the purified *E,E*-isomer **2-20** was obtained. ^1H NMR ($CDCl_3$): 7.32-7.22 (m, 1H), 6.17-6.12 (m, 2H), 5.82-5.76 (d, *J* = 15.4 Hz, 1H), 3.74 (s, 3H), 2.20-2.12 (m, 2H), 1.42-1.20 (b, 22H), 0.90-0.85 (t, *J* = 6.6 Hz, 3H) ppm. ^{13}C NMR ($CDCl_3$): 167.74, 145.40,

145.01, 128.26, 118.61, 51.40, 32.99, 31.91, 29.64 (4), 29.54, 29.42, 29.35, 29.17, 28.67, 22.67, 14.10.

2.2.2.4 2,4-(*E,E*)-Octadecadienoic Acid (**2-21**)

A methanol solution of methyl ester **2-20** (1.2 g, 4.1 mmol) in 50 mL of MeOH was treated with 1.5 mol equiv of 85% aqueous solution of KOH. The mixture was refluxed overnight until the reaction was complete as determined by TLC with hexane/EtOAc (95/5). The MeOH solution was evaporated and ether was added. After the solution was acidified to pH 3 with dilute HCl solution, it was extracted several times with water. The organic layer was dried with anhydrous $MgSO_4$ and concentrated. The crude acid was purified by recrystallization from hexane at -30 °C, giving 0.66 g (57%) of acid **2-21**. ^{1}H NMR (CD_2Cl_2): 7.40-7.30 (m, 1H), 6.24-6.22 (m, 2H), 5.81-5.75 (d, J = 15.3 Hz, 1H), 2.22-2.15 (m, 2H), 1.43-1.20 (b, 22H), 0.90-0.85 (t, J = 6.5 Hz, 3H) ppm. ^{13}C NMR (CD_2Cl_2): 172.91, 148.06, 147.11, 128.46, 118.31, 33.44, 32.32, 30.04 (4), 29.95, 29.80, 29.75, 29.57, 29.01, 23.08, 14.26.

2.2.2.5 1-Palmitoyl-2-(2,4-(*E,E*)-octadecadienoyl)-*sn*-glycero-3-phosphocholine (**2-11**)

LysoPC_{16} (265.3 mg, 0.54 mmol), fatty acid **2-21** (100 mg, 0.36 mmol), and DMAP (43.6 mg, 0.36 mmol) were mixed in a flask with 5 mL of CH_2Cl_2. DCC (73.6 mg, 0.36 mmol) in 5 mL of CH_2Cl_2 was added to the suspension. The reaction mixture was kept in the dark for 3 days and then worked up as above to give 44 mg of product (16%). ^{1}H NMR (CD_2Cl_2): 7.32-7.20 (m, 1H), 6.27-6.18 (m, 2H), 5.82-5.75 (dd, J =

15.0, 6.3 Hz, 1H), 5.24 (b, 1H), 4.44-4.17 (m, 4H), 3.95 (b, 2H), 3.76 (b, 2H), 3.34 (s, 9H), 2.34-2.26 (m, 4H), 1.61-1.54 (m, 2H), 1.45-1.38 (b, 2H), 1.27 (bs, 44H), 0.91-0.87 (t, J = 6.5 Hz, 6H) ppm. FAB-MS *m/z*: calcd for $C_{42}H_{81}O_8NP$, 758.5700; found, 758.5710.

2.2.2.6 1,2-Bis[2,4-(*E,E*)-octadecadienoyl]-*sn*-glycero-3-phosphocholine (**2-12**)

GPC (94.3 mg, 0.21 mmol), fatty acid **2-21** (100 mg, 0.36 mmol), and DMAP (43.6 mg, 0.36 mmol) were dissolved in 5 mL of CH_2Cl_2. DCC (73.6 mg, 0.36 mmol) in 5 mL of CH_2Cl_2 was added. The mixture was stirred at room temperature in the dark for 3 days under argon. The white suspension was filtered to remove urea. 3 g of Bio-Rad AG 501-X8 ion-exchange resin was added to the filtrate and stirred for 10 min. The resin was removed by vacuum filtration, the filtrate was concentrated, and the crude product was purified by column chromatography using hexane/EtOAc (9/1) followed by $CHCl_3$/MeOH/H_2O (65/25/2), giving 28 mg of lipid (20%). ^{1}H NMR (CD_2Cl_2): 7.33-7.21 (m, 2H), 6.27-6.14 (m, 4H), 5.83-5.76 (dd, J = 12.5, 6.4 Hz, 2H), 5.29 (b, 1H), 4.46-4.23 (m, 4H), 4.02-3.98 (m, 2H), 3.71 (b, 2H), 3.32 (bs, 9H), 2.17 (b, 4H), 1.45-1.38 (b, 4H), 1.28 (bs, 40H), 0.91-0.87 (t, J = 6.5 Hz, 6H) ppm. FAB-MS *m/z*: calcd for $C_{44}H_{81}O_8NP$, 782.5700; found, 782.5725.

2.2.3 Methods

2.2.3.1 Instruments

Compounds containing UV-sensitive groups were handled under yellow lights. ^{1}H NMR spectra were acquired on a Bruker AM-250 magnetic resonance spectrometer in chloroform-*d* or methylene chloride-d_2. The chemial shifts were referenced to TMS in chloroform-*d* and to solvent peak in all other cases. The digital resolution was 0.4 and 0.9 Hz for ^{1}H and ^{13}C NMR respectively. UV/vis absorption spectra were recorded on a Varian DMS 200 spectrophotometer. Quasi-elastic light scattering (QELS) was performed with a BI 8000 autocorrelator from Brookhaven Instrument Corp., and particle sizes were calculated with the software accompanying the instrument.

2.2.3.2 Calorimetry

The lipids were lyophilized from benzene stock solution to a loose powder and hydrated to a concentration of 2.0 mM by 3 freeze-thaw-votex cycles (-78 → 35 °C) followed by extrusion 5 times (2 x 0.6 μM + 3 x 0.1 μM). A Microcal Inc., model MC-2 differential scanning calorimeter (DSC) was used for thermotropic studies. Thermograms were obtained at a scan rate of 10 °/h.

2.2.3.3 Vesicle Polymerization

Vesicle Preparation. Large unilamellar vesicles (LUV) of polymerizable lipid were prepared as follow: A total of 0.5 mL of lipids from stock solutions (1 mM in water) was mixed and freeze-dried under high vacuum for 4 h. The dried lipid was hydrated with deoxygenated Milli-Q water to a final concentration of 200 μM. Samples were vortexed to uniformity and subjected to five freeze-thaw-vortex cycles (-78 → 30 °C).

The lipid suspension was extruded 5 times (2 × 0.2 μm + 3 × 0.1 μm) through two stacked Nuclepore polycarbonate filters at 35 °C using a stainless steel extruder from Lipex Biomembranes.

Redox Initiation. The redox initiator was prepared from $K_2S_2O_8$ (27.0 mg, 0.1 mmol) and $NaHSO_3$ (10.4 mg, 0.1 mmol), which were weighed into a 10 mL volumetric flask and diluted. An aliquot (10 μL) was added to the LUV suspension, giving a [M]/[I] ratio of 5. The sample was sealed in an ampoule with a septum and flushed with argon for 0.5 h. Polymerization was performed at 60 ± 2 °C in a water-circulating bath under a positive argon pressure for 18 h. Polymerization was monitored by UV absorption spectroscopy of aliquots diluted with Milli-Q water to ca. 60 μM.

Photopolymerization. The LUV, prepared as above, were placed in a Pyrex tube, thermostated at 40 °C and 18.5 cm from a high-pressure Hg/Xe light source. A Corning CS-056 cut-off filter which cut off wavelengths shorter than 300 nm was placed between the sample and the light source. UV irradiation lasted for 4 h and was monitored by UV absorption spectroscopy as above.

2.2.3.4 Surfactant Dissolution of Vesicles

The LUV were prepared as described above. After polymerization, the LUV were characterized by QELS as 2 mL samples with lipid concentrations of 150 μM. An aliquot of 42.86 mM TX-100 solution was added. Each aliquot was equal to 2 equiv of lipid. The light-scattering intensities were determined again by QELS. TX-100 was added in 2 equiv increments up to a total of 12 equiv. Measurements at each concentration of TX-

100 were performed at least three times. Light scattered (in photons/second) varied for each sample and was normalized as described by the following expression:

$$\text{normalized light scattering intensity} = (I - I_\infty)/(I_0 - I_\infty)$$

where I is the intensity of photons scattered after the addition of each equivalent of TX-100, I_∞ is the intensity of photons scattered by a micellar suspension of TX-100 at a similar concentration, and I_0 is the intensity of photons scattered by vesicles in the absence of TX-100. The average mean diameter of vesicles/particles was calculated by a nonnegatively constrained least-squares mathematical procedure.

2.3 Results and Discussion

2.3.1 Lipid Synthesis

Both the mono- and bis-substituted dienoyl lipids were prepared from the dienoyl (Den) fatty acid **2-21** (Scheme 2-1), which was synthesized from the commercially available 1-tetradecanol. The alcohol was oxidized to the corresponding aldehyde (**2-18**) using pyridinium dichromate in CH_2Cl_2. The Wittig-Horner reaction of **2-18** and trimethyl 4-phosphonocrotonate gave a mixture of (*E,E*)- and (*E,Z*)-methyl dienoate (**2-19**). The (*E,E*)-Den acid **2-21** was obtained by basic hydrolysis of the (*E,E*)-ester **2-20** after its separation from its (*E,Z*)-isomer by urea inclusion.[58] Den acid (**2-21**) was used to acylate both $LysoPC_{16}$ and GPC to obtain $monoDenPC_{16,18}$ **2-11** and $bisDenPC_{18,18}$ **2-12**, respectively. The monoDenPC **2-11** bears the reactive group on the *sn*-2 chain.

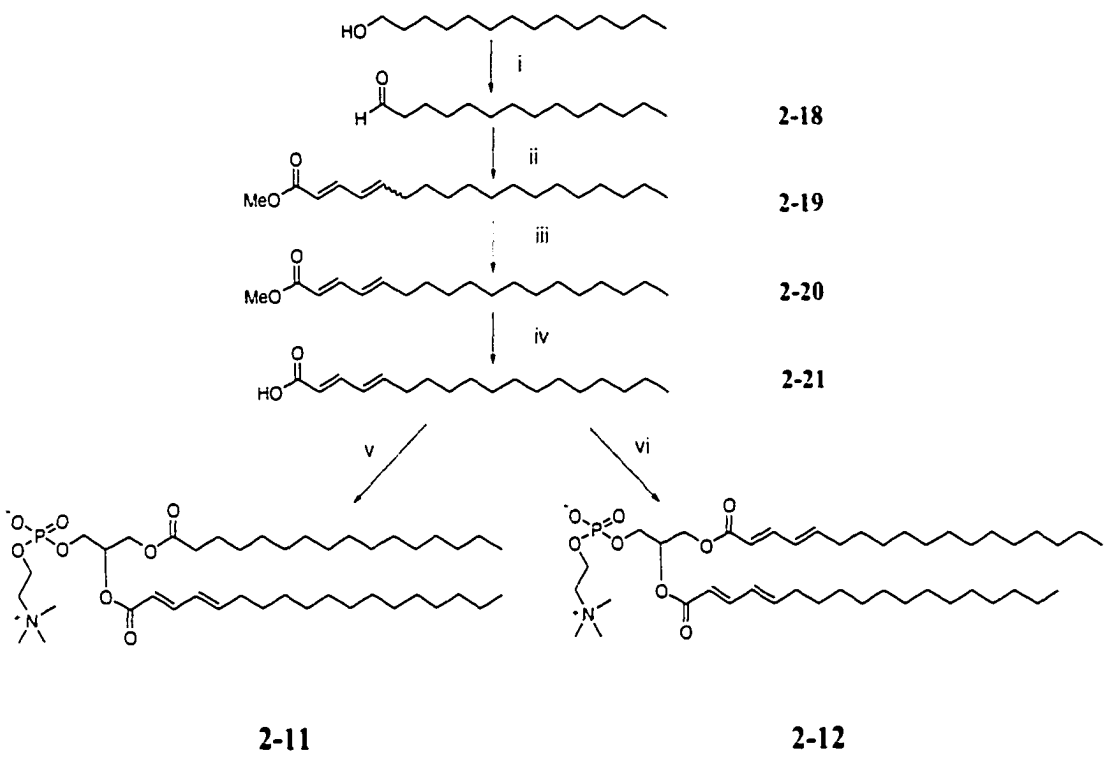

Scheme 2-1. Synyhrsis of mono- and bis-DenPC. (i) PDC, CH_2Cl_2; (ii) NaH, trimethyl phosphonocrotonate, THF; (iii) urea inclusion; (iv) KOH, MeOH; (v) $LysoPC_{16}$, DCC, DMAP, CH_2Cl_2; (vi) GPC, DCC, DMAP, CH_2Cl_2.

2.3.2 Differential Scanning Calorimetry (DSC)

DSC heating curves were obtained for each of the lipids **2-11** and **2-12** (Figure 2-1). The main phase transition temperature T_m, peak width at half height $T_{1/2}$, calorimetric enthalpy ΔH, and cooperative unit are reported in Table 2-1. The T_m was 26.1 °C for monoDenPC **2-11** and 20.2 °C for bisDenPC **2-12**. For the mixture of mono/bis 90/10, the T_m is 25.6 °C. The plot of T_m as a function of percent of bisDenPC **2-12** (Figure 2-2) gave a straight line which indicates ideal mixing between the two lipids.

Table 2-1. Thermodynamic characteristics of the heating endotherms of hydrated bilayers of mono/bisDenPC **2-11** and **2-12**

Lipid	T_m (°C)	$T_{1/2}$	ΔH (kcal/mol)	CU
$MonoDenPC_{16.18}$	26.15 ± 0.04	1.36	7.02 ± 0.29	71 ± 3
$MonoDenPC^{*}_{16.18}$	28.11 ± 0.26	5.32	5.12 ± 0.07	25 ± 2
$BisDenPC_{18.18}$	20.13 ± 0.03	0.87	7.44 ± 0.14	75 ± 3
Mono/bis 90/10	25.56 ± 0.03	1.97	5.39 0.06	58 ± 2
$MonoSorb_{PC16.17}$	34.11 ± 0.07	1.61	4.98 ± 0.10	81 ± 2
$PC^{**}_{16.17}$	46.20			
$PC^{**}_{16.18}$	49.00			

* UV polymerization at 40 °C / 4 h.

** From Ref.[142]

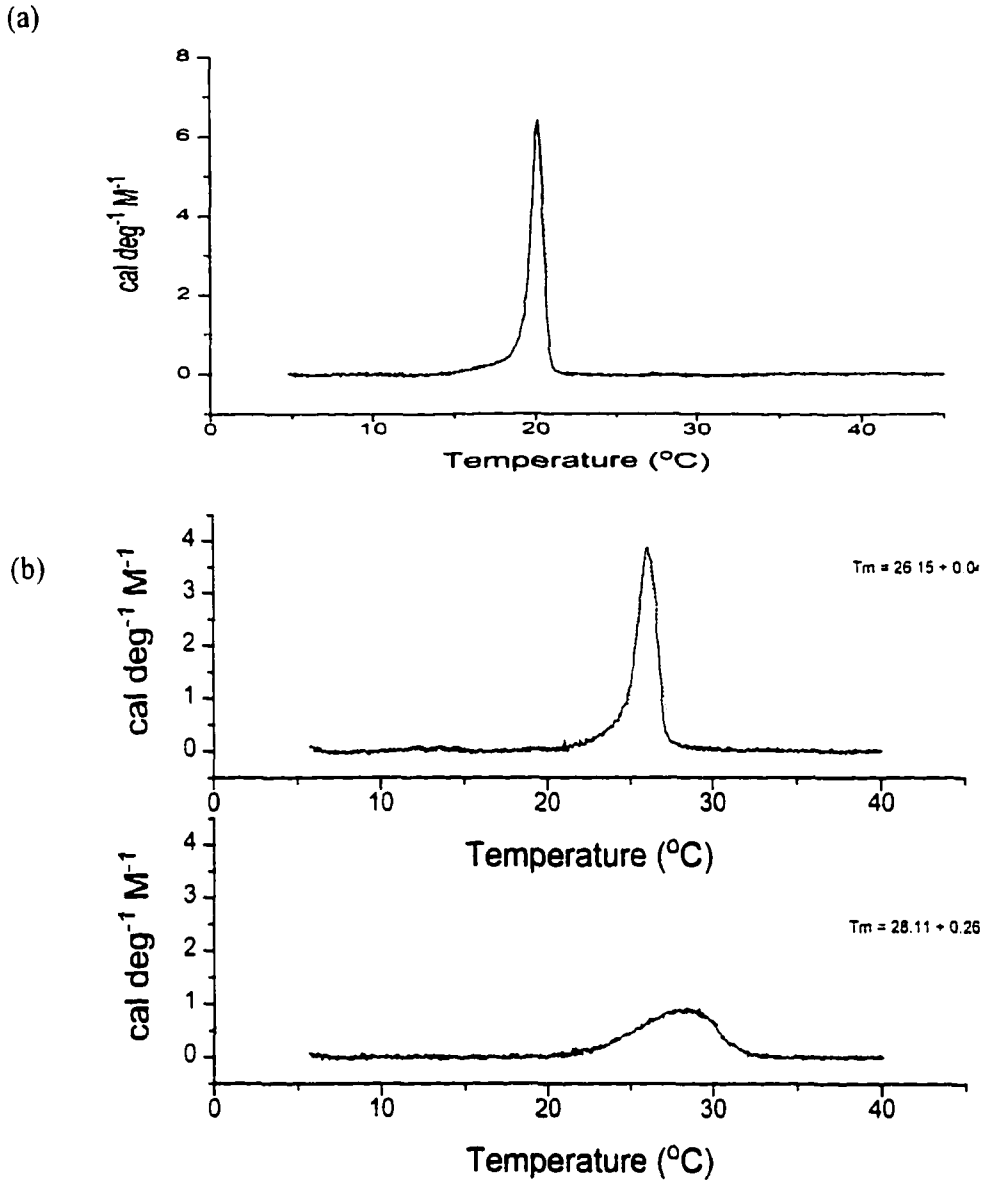

Figure 2-1. DSC heating thermograms of lipid vesicles in water: (a) bisDenPC **2-12**; (b) monoDenPC **2-11** before and after UV polymerization.

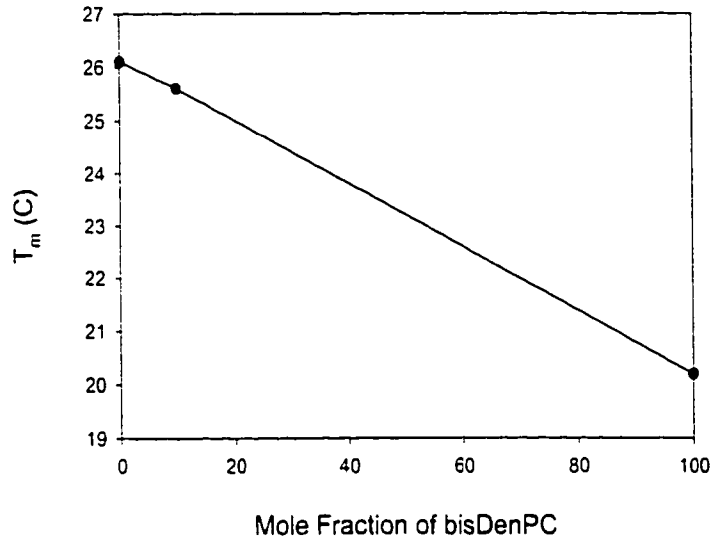

Figure 2-2. T_m as a function of mole fraction of bisDenPC **2-12** in the lipid mixture.

The DSC of the monoDenPC$_{16.18}$ **2-11** after UV polymerization was also measured and compared with that of monoSorbPC$_{16.17}$ **2-16**. As shown in Table 2-1, after polymerization, the T_m of monoDenPC **2-11** was 28.1, a 2 °C increase. Figure 2-1 shows that the peak was broadened and CU was decreased. The T_m of monoSorbPC **2-16** was totally eliminated after polymerization.

The formation of polymer chains in the membrane increased the viscosity and thus reduced flexibility. Whether polymerized bilayer membranes are too rigid to show a phase transition strongly depends on the type of polymerizable lipid used. In the case of

diacetylenic lipids, a loss of phase transition can be expected due to the formation of the rigid fully conjugated polymer backbone.[48,143] This is confirmed by DSC measurements with the diacetylenic sulfolipid **2-22**. Ringsdorf and coworkers measured the phase transition behavior of lipids **2-22** as a function of the polymerization time. The monomeric **2-22** showed a transition temperature of 53 °C. During polymerization a decrease in phase transition enthalpy indicated a restricted mobility of the polymerized hydrocarbon core. The phase transition eventually disappeared after complete polymerization of the monomer.[123]

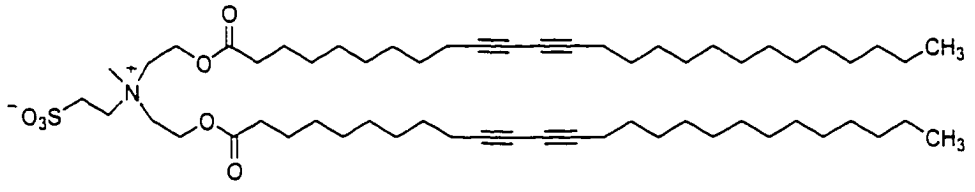

2-22

In contrast, the phase transition of polymeric liposomes is retained if the polymer chain is more flexible or located on the surface of the vesicles instead within the hydrophobic core. Polymerized vesicles of methacrylamide **2-23** showed a phase transition temperature (33 °C) which was 7° lower than the one for the corresponding monomeric vesicles (40 °C).[32] This was explained by a disordering influence of the polymer chain on the head group packing.[80]

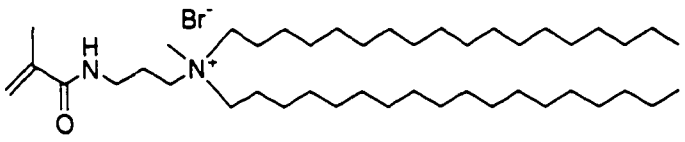

2-23

Methacryloylic lipid **2-24** was polymerized in the hydrophobic part of the molecules.[32] The phase transition temperature of the polymeric vesicles (10 °C) was decreased compared to the non-polymerized vesicle (24 °C). The difference between the phase transition temperatures of monomer and polymer was somewhat larger (14 °C) than in the case of **2-23**. This indicates that a polymer chain formed in the hydrophobic core of a membrane decreases membrane order to a larger extent than a polymer chain formed on the membrane surface.

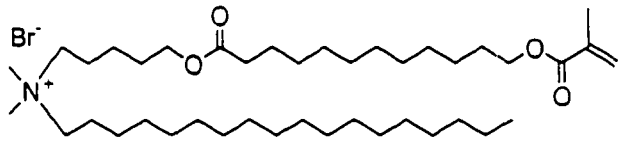

2-24

Sackmann et al. studied the phase transition temperature of a butadiene lipid (**2-25**) before and after UV polymerization.[144] They found that the T_m was 31 °C before polymerization and shifted to a slightly higher temperature (34 °C) upon polymerization.

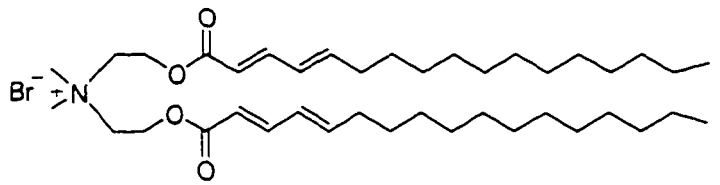

2-25

All these results imply that the type and location of the polymerizable group has a large effect on the phase transition temperature after polymerization. In our study, SorbPC **2-16**, where the polymerizable groups were in the hydrophobic chain ends, polymerization would have a much bigger effect on the chain movements than that of DenPC **2-11** where the polymerizable groups were close to the hydrophilic headgroup.

A comparison of T_m values for monoDenPC **2-11** and monoSorbPC **2-16** with the corresponding saturated chain PCs of the same chain length showed big decreases in T_m. The introduction of dienoyl groups at the tops of hydrophobic tails decreased the T_m about 20 °C, but only 12 °C if they were at the end of the tail.

2.3.3 Surfactant Solubilization of Vesicles

The previous studies by Sisson et al. demonstrated that cross-linked lipid vesicles are stable in the presence of excess surfactant, whereas unpolymerized or linearly polymerized vesicles are dissolved by surfactant.[81] At concentrations above the critical micellar concentration (cmc) a surfactant partitions into the lipid bilayer and eventually forms mixed micelles of surfactant and lipid.[145] The same process occurs with polymerized vesicles. However, cross-linked vesicles are not solubilized by added surfactant. If the vesicles are not cross-linked, they will be destabilized and form mixed micelles of poly(lipid) and surfactant. Because mixed micelles of lipid and surfactants, such as T X-100, are usually spherical and less than 10 nm in diameter, they can be readily distinguished from lipid vesicles (ca. 100 nm diameter) by light scattering. If the poly(lipid) chains are not too long, then mixed micelles of the poly(lipid) and TX-100 are

also small and readily distinguished from vesicles.[81] However, as a linear poly(lipid) increases in length, the mixed micelle increases in size and may change from spherical to rodlike. Consequently, it is desirable to use polymerization conditions that yield poly(lipids) of only moderate length in order to effectively use light scattering to differentiate between cross-linked and non-cross-linked vesicles.

Large unilamellar vesicles (LUV) composed of different mole fractions of mono- and bisDenPC – 100/0, 90/10, 85/15, 80/20, 70/30, and 0/100 – in Milli-Q water were prepared by standard extrusion protocols.[44] The mean diameter of the LUV was determined by QELS to be 120 ± 10 nm. After preparation, the LUV were incubated at 60 °C for polymerization. At this temperature, both zwitterionic lipids are in the liquid crystalline phase, and the various mixtures used in this study are expected to be random distributions of the two lipids.

The polymerization of each LUV sample composed of mono- and bis-DenPC **2-11** and **2-12** was initiated by an equimolar mixture of potassium persulfate and sodium bisulfite at 60 °C.[9] The progress of the polymerization was monitored by changes in the monomer absorption at 260 nm (Figure 2-3).

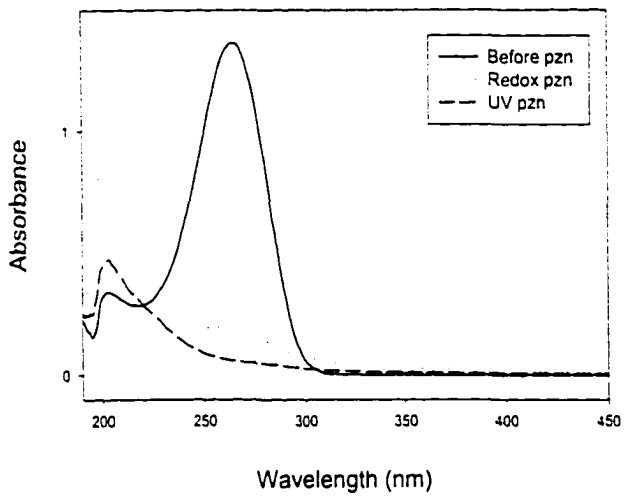

Figure 2-3. Absorbance spectra of a methanol extract of vesicles composed of mono/bisDenPC **2-11** and **2-12** (90/10) before and after polymerization.

After 90% conversion, usually 18 h, the sample was cooled to room temperature and examined by quasi-elastic light scattering (QELS).[146] The degree of polymerization, X_n, which was determined by the methods previously described,[70] was controlled by selection of a [M]/[I] ratio of 5. Under these conditions the poly(lipid) formed from LUV of monoDenPC **2-11** are short enough to be incorporated into mixed micelles when treated with Triton X-100. The apparent diameter of these micelles is 10 nm (Figure 2-4). The stability of polymerized LUV to TX-100 is dependent on the initial composition of the LUV. Figure 2-4 shows the normalized scattering intensity and Figure 2-5 the

calculated mean diameter of the samples as a function of the molar ratio of [TX-100]/[lipid]. The light scattering intensity as well as the diameter of polymerized monoDenPC **2-11** LUV is substantially decreased upon addition of 2 equiv of TX-100. Further addition of TX-100 appears to have completely lysed the vesicles.

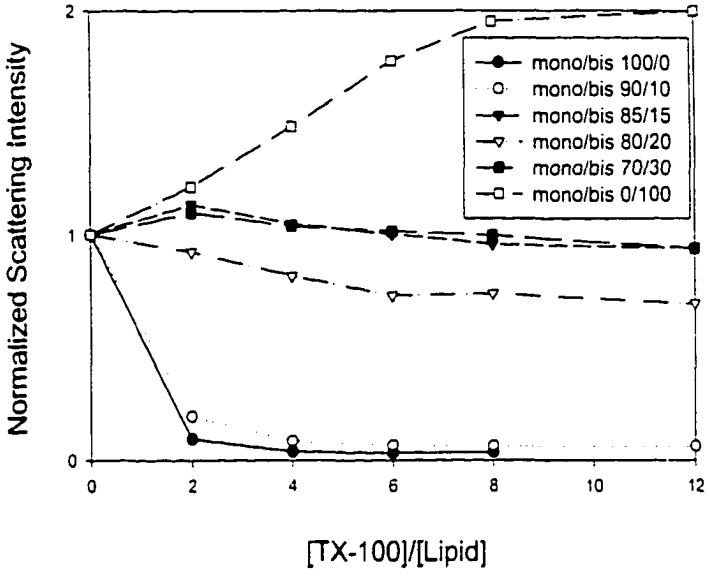

Figure 2-4. Normalized scattering intensity of polymerized vesicles composed of the indicated molar ratios of mono- and bis-DenPC **2-11** and **2-12** as a function of added equivalents of the surfactant TX-100.

The polymerized LUV composed of a 9/1 molar ratio of monoDenPC **2-11** and bisDenPC **2-12** shows a similar sensitivity to the addition of Triton X-100. In contrast to these observations, polymerized LUV comprised of 15 mol % or more bisDenPC **2-12**

are essentially unchanged in size by the addition of up to 12 equiv of TX-100.

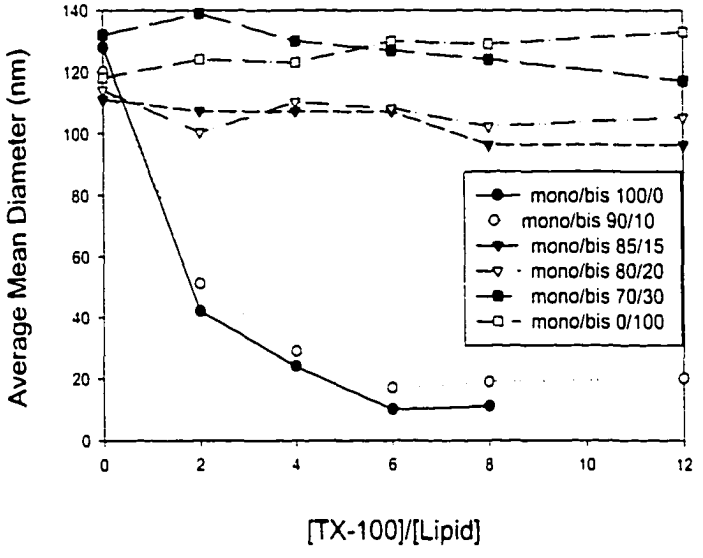

Figure 2-5. Average mean diameter (nm) of polymerized vesicles composed of the indicated molar ratios of mono- and bis-DenPC **2-11** and **2-12** as a function of added equivalents of TX-100.

The mean diameter of the polymerized LUV after addition of 8 equiv of TX-100 is plotted as a function of mole fraction of bisDenPC **2-12** in the bilayer at the time of the polymerization (Figure 2-6). These data show that the polymerized LUV sensitivity to surfactant lysis is dramatically different if the initial mole fraction of bisDenPC **2-12** is 0.10 (soluble) as opposed to 0.15 (insoluble). This suggests that at high conversion to

polymer the LUV will be cross-linked if the initial mole fraction of bisDenPC **2-12** is greater than 0.10 yet less than or equal to 0.15.

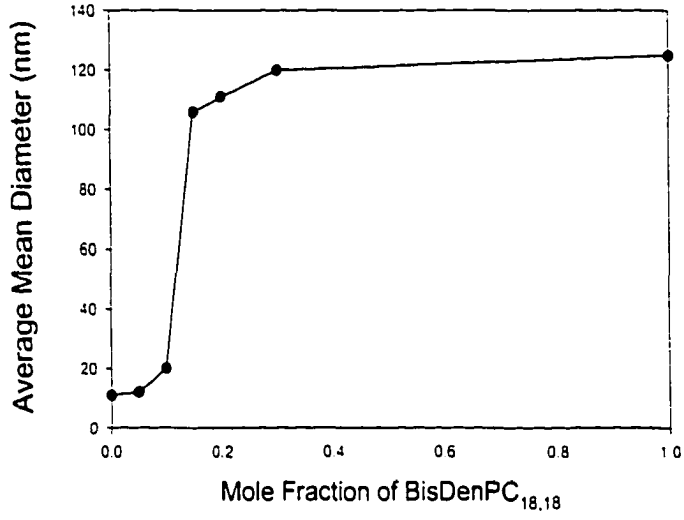

Figure 2-6. Average mean diameter (nm) of polymerized vesicles plus 8 equiv of TX-100 as a function of the mole fraction of bisDenPC **2-12** in monoDenPC **2-11** /bisDenPC **2-12** vesicles.

2.4 General Discussion

Our previous studies found effective cross-linking of hydrated lipid bilayer membranes of AcrylPC and SorbPC requires a high (0.30 ± 0.05) mole fraction of the respective bis-substituted lipid.[81,141] This contrasts with the normal situation in isotropic media where quite low mole fractions of the bis-monomers are necessary for

cross-linking. Inefficient cross-linking could be due to low conversion of monomers to polymers, significant differences in chemical reactivity of the monomers, and/or small degrees of polymerization. However, each of these appears unlikely to be a major contributor to the inefficient cross-linking, because the polymerization were taken to high conversion; the relative reactivity of mono- and bis-SorbPC (as well as mono- and bis-AcrylPC) should be quite similar because the reactive group is the same in each monomer. Moreover, although the degrees of polymerization of mono-AcrylPC and mono-SorbPC differed, the cross-linking efficiency of each mono and bis pair of monomers was similar. Consequently, other explanations for the observed inefficiency in cross-linking of chain terminal substituted monomeric lipids were considered.

The high mole fraction of the bis-substituted lipid necessary for cross-linking could be due to the conformation of the lipids in the bilayer. The glycerol backbone of phospholipids in the L_β phase present when the sample temperature is less than the T_m, is perpendicular to the plane of the bilayer[135,147,148] as represented in Figure 2-7. Therefore, when each lipid tail has the same length, the *sn*-1 chain penetrates deeper into the bilayer than the *sn*-2 chain. At temperatures above the T_m the motions of the lipid tails are more dynamic, especially for the portion of the lipid tail distal from the lipid headgroup. Both molecular simulations of PC bilayers and experimentally determined NMR order parameters of the individual carbons along the lipid chain indicate that the distal portion of the lipid chains exhibit considerably more disorder at temperatures above the T_m than below it.[Heller, 1993 #158; Seelig, 1977 #159; Brown, 1984 #160]

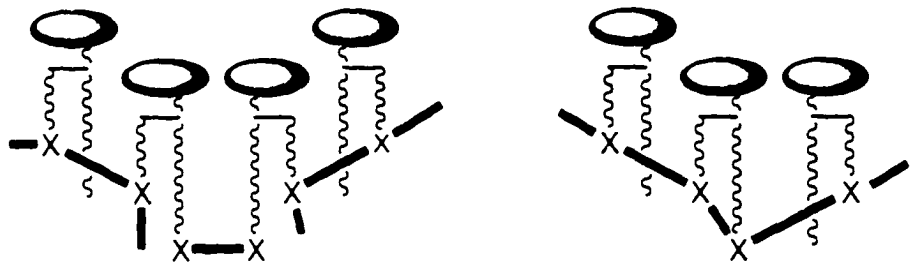

a b

Figure 2-7. Schematic representation of a small portion of half a bilayer of mono-SorbPC and bis-SorbPC where the reactive groups in the *sn*-1 chains of the bis-SorbPC react to form a link between poly(SorbPC) chains (a) and where the competitive macrocyclization of the bis-SorbPC yields a linear polymer chain segment (b).

The reactive groups on each lipid tail of a polymerizable lipid, such as bis-SorbPC, are positionally unequivalent even though they have the same chemical composition. This suggests that bis-SorbPC could function as an AB type cross-linker (Figure 2-7a) that can react with the mono-SorbPC primarily through the respective *sn*-2 chains. Under these circumstances a cross-link between polymer chains occurs when a reactive group on the *sn*-1 chain of a bis-SorbPC reacts with a similar group in a neighboring chain. Dimerization of *sn*-1 chains of bis-substituted lipids provides a mechanism to cross-link the linear polymer chains formed by reaction at the *sn*-2 chains. Such a link between polymer chains may not always occur as shown in Figure 2-7a. It may be possible for the reactive group on the *sn*-1 chain of bis-SorbPC to react with mono-SorbPC to form a longer bridge between polymer chains. Because a 100 nm

diameter vesicle is composed of ca. 8×10^4 lipids, high conversion of mono-PC to polymers with a degree of polymerization of ca. 10^2 yields at least hundreds of polymer chains. If each bis-substituted lipid in the chain efficiently formed a link with a bis-substituted lipid on a neighboring chain, then only a few mole percent of the lipids would need to be bis-substituted. However, nearly one in three of the SorbPC lipids must be bis-substituted to achieve cross-linking. This suggests that most of the bis-substituted lipids fail to create links between chains either because they preferentially react with other bis-substituted lipids in the same chain or because of other competitive reactions. Sisson et al. reported evidence that is consistent with macrocyclization of bis-SorbPC lipids.[141] Intramolecular macrocyclization of the *sn*-1 and *sn*-2 reactive groups in the same lipid connects both lipid tails in a linear polymer (Figure 2-7b). The constrained nature of hydrated lipid assemblies reduces the number of conformations of lipid tails in a manner that increases the probability of macrocyclization in direct competition with cross-linking.

The cross-linking of DenPC lipids is significantly more efficient than with the SorbPC lipids. The location of the dienoyl groups adjacent to the glycerol backbone was expected to be more favorable than SorbPC for cross-linking because the probability of macrocyclization is diminished when the reactive groups are in a more ordered region of the lipid molecule. When approximately one in eight DenPC lipids was a bis-substituted lipid, then cross-linking was observed. Since the degree of polymerization of polymer chains from monoDenPC **2-11** would be less than 50 for the polymerization conditions used in this study, and the minimum number of bis-substituted lipids per polymer chain

necessary for cross-linking is two, then the minimum mole fraction of bis-substituted lipids required to observe cross-linking is >0.04. This suggests that under the experimental conditions employed here about a third of the bisDenPC **2-12** lipids react in a manner to cross-link poly(DenPC) chains.

Dienoyl lipids have been successfully used in the polymerization of bicontinuous cubic (Q_{II}) phases of hydrated lipids. Lee et al. employed a 3:1 molar mixture of a mono-DenPE and a bis-DenPC to form a Q_{II} phase at temperatures greater than 55 °C and then polymerized the Q_{II} phase in a manner that increased its thermal and chemical stability.[9] The poly(lipid) structure was not disrupted by organic solvents. Further support for the original suggestion that the poly-Q_{II} phase was cross-linked is provided by the current observations that indicate about one in eight of the dienoyl lipids must be bis-substituted to achieve cross-linking. Recently, Srisiri et al. described the formation and polymerization of a Q_{II} phase with *Ia3d* symmetry from a 9:1 molar mixture of a mono-Den monoacylglycerol and a bis-Den diacylglycerol.[59] Again the polymerization proceeded with retention of the Q_{II} phase; however, the poly(lipid) structure was soluble in selected organic solvents, indicating a lack of cross-linking of the Q_{II} phase. These data are consistent with the current study, which found that one bis-Den lipid in 10 Den-lipids is insufficient to achieve cross-linking.

2.5 Conclusions

The cross-linking polymerization of hydrated lipids in monolayers, bilayers, and nonlamellar phases, i.e., bicontinuous cubic and the inverted hexagonal phases, is an

effective method to modify their properties. Polymerization of monomeric lipids in an assembly proceeds in a linear or cross-linked manner depending on the number and location of polymerizable groups per monomer. Polymerization of bilayers composed of lipids containing a single reactive moiety in either of the hydrophobic tails or associated with the hydrophilic headgroup (monosubstituted lipids) yields linear polymers. Polymerization of lipids with reactive groups in each hydrophobic tail generally yields cross-linked polymers.

This chapter described the approach of cross-linking polymerization of lipid bilayer vesicles with homobifunctional lipids. Homobifunctional lipids, i.e., lipids with two polymerizable groups in each hydrophobic chain, served as cross-linking agents. Previous studies by Sisson et al.[81] examined the cross-linking of bilayers as a function of the mole fraction of bis-substituted lipids (bis-SorbPC), where the reactive groups were located at the end of the lipid tails. The onset of cross-linking was determined by changes in lipid lateral diffusion, bilayer vesicle stability, and polymer solubility. These data indicated that a substantial mole fraction (0.30 ± 0.05) of the bis-substituted lipid was necessary for bilayer cross-linking.

The lipids selected for this study were monoDenPC **2-11** and bisDenPC **2-12** where the polymerizable groups were located near the glycerol backbone of the lipid. The bilayer composition was varied with increasing mole fraction of the homobifunctional lipids. LUV were polymerized by redox initiation with $K_2S_2O_8$ and $NaHSO_3$. The polymerization condition was chosen so that the linear or cross-linking of the resulting polymers could be easily distinguished by the vesicle stability towards

addition of surfactant TX-100. The results showed that 15% of bisDenPC lipid was necessary for cross-linking. Compared to SorbPC lipids, where 30% of the bis-substituted lipid was needed for bilayer cross-linking. The cross-linking of DenPC was thus found to be substantially more efficient than that of SorbPC. It was proposed that this effect was partly a consequence of the relative probability of macrocyclization and cross-linking reactions. It was suggested that the location of the reactive group, i.e., reaction site, in the lipid and therefore within the bilayer assembly influenced the cross-linking efficiency. The dienoyl group was located in a more ordered region of the lipid molecule, and was expected to be more favorable for cross-linking than macrocyclization.

The development of methods to polymerize hydrated lipid mesophases, i.e., lamellar, bicontinuous cubic, hexagonal, etc., can now be used to create new polymeric materials with novel properties.[66] Cross-linking polymerization can substantially enhance the chemical and thermal stability of these materials. The capability of varying the cross-link density in these poly(lipid) structures by the use of mixtures of mono- and bis-substituted amphiphiles provides researchers with a means to further modify the physical properties of these polymers. Moreover, the ability to use high molar fractions of the monosubstituted lipids and still obtain cross-linked polymeric phases makes it straightforward to introduce various amounts of additional monosubstituted lipids that can subsequently be elaborated to create surface sites for the binding of molecules or ions for various biological or materials objectives.

CHAPTER 3

CROSS-LINKING POLYMERIZATION OF ASSEMBLIES WITH HETEROBIFUNCTIONAL LIPIDS

3.1 Introduction

In the previous chapter we concluded that the polymerization of supramolecular assemblies of hydrated amphiphiles is an effective way to modify the chemical and physical properties of the assembly and stabilize it.[66,76] The polymerization in a lipid assembly can proceed in a linear or cross-linked manner depending on the number of polymerizable groups in the monomeric lipid. It is known that the polymerization of hydrated lipids with a single reactive moiety in either the hydrophobic tails or the lipid headgroup yields linear polymers, whereas polymerization of lipids with reactive groups in both tails yields cross-linked polymers.[56,80,121,124,135] In the last chapter, the cross-linking was introduced by using homobifunctional lipids, i.e. bis-substituted lipids in which both functionalities are the same. The polymerizable groups are incorporated either close to the lipid backbone or at the hydrophobic termini. However, for homobifunctional lipids, it is not known if the occurrence of the cross-linking reaction depends on the location of the two reactive groups in each lipid. To address that question, we designed heterobifunctional lipids with two different reactive groups in one of the tails and different separation distances between the two groups.

In bilayer assemblies, the lipid molecules are well-aligned with each other. The distinct location of each reactive group within the assembly inhibits copolymerization between two different groups even if they have similar reactivities. For monomers containing at least two polymerizable groups that are well aligned in separate planes, parallel polymerization occurs in each plane. If both reactive groups prefer to react with the same lipid neighbor, then linear-ladder polymers form (Figure 1-9). Compared to conventional cross-linked polymers, ladder polymers behave somewhat differently. These polymers are sometimes called "double-stranded," "ordered linear network," and "nonrandom cross-linked" polymers. Their architecture is between that of linear and cross-linked polymers and may possess some properties of each. For example, they are resistant to degradation but still soluble in organic solvents. They can exhibit liquid crystalline behavior because of their stiffness and restriction to rotation.[149,150]

Alternatively, if the two reactive groups tend to react with different lipid neighbors, a cross-linked polymer forms (Figure 1-9). Decorrelation of the direction of polymerization in the two different reactive planes results in the formation of cross-linked polymers.

Heterobifunctional lipid monomers designed in our group have two reactive moieties with distinct reactivities, which could result in differences in the rate and degree of polymerization. Moreover, since the two reactive groups are located in the same tail of the lipid, there is the additional possibility that the groups could form cross-linked or linear-ladder polymers.

The introduction of two different polymerizable groups into a single tail started with single-chain amphiphiles. In the 1980s, Ringsdorf and coworkers synthesized bipolymerizable amphiphiles, which contained two different polymerizable moieties, one in the hydrophilic headgroup and one in the hydrophobic tail.[83] They incorporated acrylic, dienoyl, diyne and cinnamoyl groups into diacetylic fatty acids (**3-1** – **3-4**) and studied their polymerization on LB multilayers with UV light. The results showed that **3-3** did not form a stable monolayer, and could not be polymerized by UV light. Electron micrographs of the polymeric multilayers revealed defects. This means that the polymerization of the multilayers leads to a change of the layer spacings that can cause the formation of defects in the multilayers.

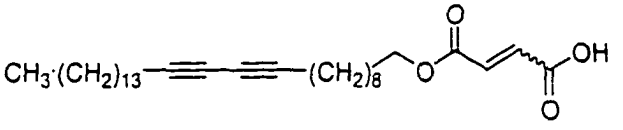

3-1

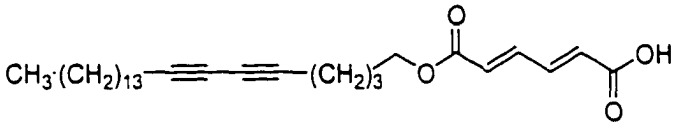

3-2

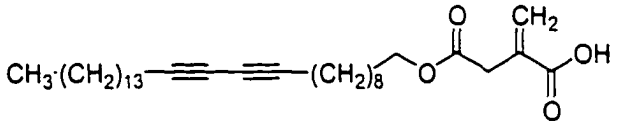

3-3

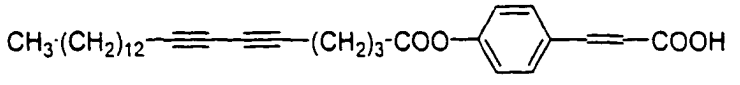

3-4

Nezu and Lando reported another heterobifunctional single-chain diacetylene amphiphile that contains an acetylene group at the hydrophobic end (**3-5**).[151] The solid-

state polymerization of monolayers on the gas-water interface and multilayers were investigated. The diacetylene group could be polymerized by UV or γ-irradiation. However, the terminal acetylene groups did not polymerize under these conditions.

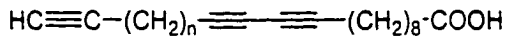

3-5

n = 6, 12

Stupp and coworkers synthesized heterobifunctional oligomers with an acryloyl group at one terminus and a cyano group near the middle of the molecule (**3-6**).[152,153] The oligomers were rodlike mesogens that self-organize into layers that placed the reactive groups within specific planes. Polymerization in the smectic phase yielded bilayer 2D polymers of molecular weight on the order of millions and a monodisperse thickness of 5 nm. ^{1}H and ^{13}C NMR spectra indicated that both C=C and C≡N bonds reacted. However, the polymer was soluble in chloroform (90% w/w), which indicates that the system was not a 3D network of random cross-linked oligomers, but a 2D cross-linked polymer.

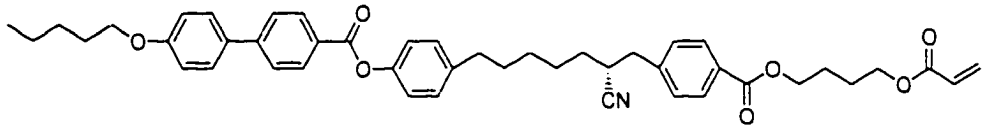

3-6

Another rodlike monomer designed in the Stupp group had a diacetylene group and a hydroxyl group capable of forming hydrogen bonds (**3-7**).[154] The monomer could self-assemble into a 2D polymer formed by both covalent bonds (the polydiacetylene backbone) and hydrogen bonds (formed among side chains). UV polymerization of the diacetylene resulted in a 2D cross-linked structure because of the polymeric hydrogen bonding inside the system.

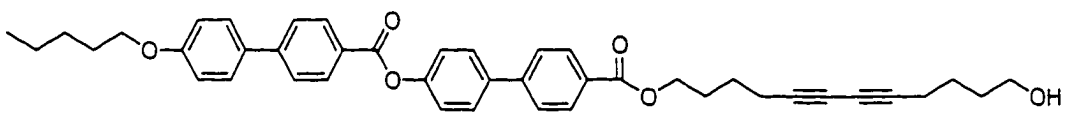

3-7

Singh et al. reported the synthesis of heterobifunctional phospholipids **3-8** and **3-9**.[155] These lipids contained either a vinyl or methacryloyl group at the acyl chain terminus in addition to a diacetylenic group to provide for additional polymerization in the lipid bilayer. Tubules with a diameter of 0.4-0.5 μm and up to 300 μm long were formed from **3-8** and **3-9**. Polymerization was carried out with UV and γ-irradiation. Tubules polymerized by a combination of UV and γ-irradiation retained their tubule morphology and were stable to ultrasonic agitation and lyophilization followed by redispersion.

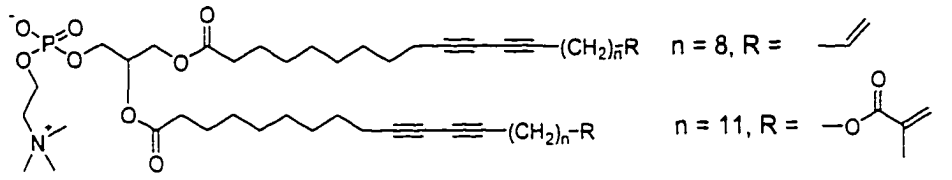

3-8

3-9

Srisiri et al. synthesized a novel heterobifunctional lipid, 1-palmitoyl-2-(2,4,12,14-tetraenehexadecanoyl)phosphatidylcholine (Double-dienePC) **3-10,** that contained a diene and a dienoyl group in the *sn*-2 acyl chain.[156,157] The dienoyl group was conjugated with the ester carbonyl of the fatty acid chain, and the diene group was located near the acyl chain terminus of the same chain. Because the two diene groups were located in regions of different polarity, it was possible to perform simultaneous or selective and sequential polymerization of these groups. The degree of polymerization depended on the initiation methods. Photopolymerization gave oligomers, whereas radical polymerization with redox initiators or AIBN afforded polymers with a number average degree of polymerization of 200-350. Polymeric vesicles obtained with both reactive groups polymerized were solubilized by TX-100, indicating a lack of polymer cross-linking. These results showed that both groups preferentially reacted with the same neighbor lipid and formed ladder-like polymers.

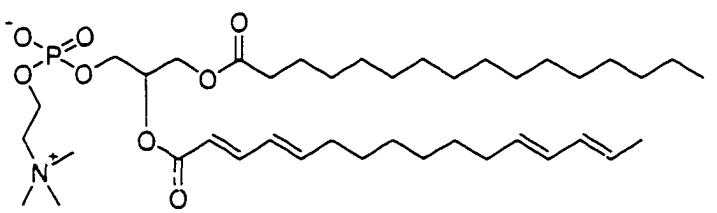

3-10

Several factors can influence the preferred course of polymerizations in organized media, such as thermotropic and lyotropic liquid crystals. These include the relative reactivity of the monomers, the percent conversion of the monomers, the distance between the reactive groups, and the flexibility of the spacer group that separates the monomers, among others. In monomer **3-10**, where the two diene groups were separated by only six methylenes, the preference for linear-ladder polymers in the polymerization of hydrated bilayers is attributed at least in part to the relatively short spacer length between the two reactive moieties. At some separation distance, the congruence of the preferred reactivity of the two groups will diminish to the point that the polymerization of both groups will be uncorrelated, resulting in cross-linked polymers instead of ladder-like polymers.

In this study, we examined the nature of the polymerization of hydrated bilayers, at high conversion, of two types of heterobifunctional lipids, each bearing a pair of reactive groups in the *sn*-2 tail that are separated by either 7, 9, or 11 atoms (Figure 3-1). The formation of cross-linked polymeric assemblies can be ascertained by the physical properties of the resulting assembly, including the chemical stability of the polymerized assembly toward added surfactant, general insolubility in organic solvents including hexafluoro-2-propanol (HFIP), and the rate of lateral diffusion of the lipids in the assembly.[81,122]

3.2 System Design

The key considerations in the design of a heterobifunctional lipid are the choice and location of the polymerizable groups in the lipid molecule. Reactive lipids may have polymerizable moieties located in the hydrophilic headgroup, near the lipid backbone, or in the hydrophobic lipid tail. The heterobifunctional lipids for this study contained two polymerizable groups in the *sn*-2 acyl chain of the lipid (Figure 3-1). One of the groups, i.e., dienoyl, was attached to the secondary oxygen of the glycerol backbone of the lipid, and the other was an acryloyl or sorbyl functional group located at the *sn*-2 chain terminus. These lipids could be polymerized in a bilayer by either radical initiation or direct photoactivation. Since the two reactive groups were in regions of different polarity, selective polymerization of one reactive group in the presence of the second was possible with a careful choice of initiation chemistry. The dienoyl (Den) group located near the lipid backbone could be polymerized by polar initiators, whereas the acryloyl (Acryl) or sorbyl (Sorb) groups located in the interior of the bilayer could be selectively polymerized by hydrophobic initiators.[157] The reactive groups were selected to yield one series of monomeric lipids with groups having similar reactivity, i.e., Sorb/Den, and a second series where the reactivity of the groups differ significantly, i.e., Acryl/Den.[70,72] These variations in molecular structure resulted in differences in the rate and degree of polymerization. This work focused on the effect of monomer structure on the architecture (linear or cross-linked) of the polymers formed. The properties of the resulting polymers were determined by polymer solubility and bilayer vesicle lysis techniques described in Section 1.5.

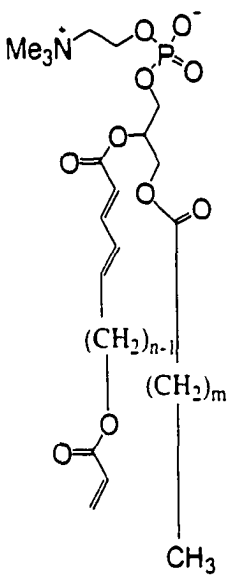

Acryl/DenPC

3-11

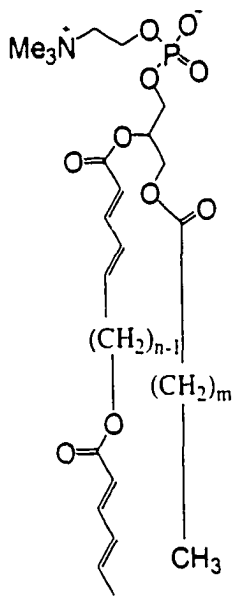

Sorb/DenPC

3-12

Figure 3-1. Structures of polymerizable heterobifunctional lipids. n = 6, 8, 10; m: to match the chain length on *sn*-2.

3.3 Experimental

3.3.1 Materials and Methods

All chemicals were obtained from Aldrich Chemical Corp., except for triethyl (trimethyl) 4-phosphonocrotonate (Lancaster Inc.), 1-palmitoyl-2-hydroxy-*sn*-glycerol-3-phosphocholine ($LysoPC_{16}$), and 1-oleoyl-2-hydroxy-*sn*-glycerol-3-phosphocholine ($LysoPC_{18}$); (Avanti Polar Lipids Co.). Solvents were dried and distilled prior to use. 4-

(Dimethylamino)pyridine (DMAP) was recrystallized from $CHCl_3$/ether (1:1). All other chemicals were used without further purification. The reactions were monitored by TLC visualized by an UV lamp and/or phosphomolybdic acid. The lipids were hydrated in Milli-Q water. Millipore Inc.

Compounds containing UV-sensitive groups were handled under yellow light. ^1H and ^{13}C NMR spectra were acquired on a Bruker AM-250 magnetic resonance spectrometer. High-resolution mass spectrometry was carried out on a JEOL HX110A sector instrument. UV/vis absorption spectra were recorded on a Varian DMS 200 spectrophotometer. Quasi-elastic light scattering (QELS) was performed with a BI 8000 autocorrelator from Brookhaven Instrument Corp., and particle sizes were calculated with the software accompanying the instrument. A Microcal, Inc., model MC-2 differential scanning calorimeter (DSC) was used for thermotropic studies.

3.3.2 Synthesis of Lipids

A general outline of the synthetic procedures is shown in Scheme 3-1 and a representative example is described for c.

3.3.2.1 10-(Acetyloxy)decan-1-ol (**3-13c**)

Acetyl chloride (3.6 mL, 0.05 mol) in THF (100 mL) was added dropwise to a solution of 1,10-decanediol (17.4 g, 0.1 mol) and pyridine (4.1 mL, 0.05 mol) in THF (250 mL) at 0 °C under argon. The reaction mixture was warmed slowly to room temperature and stirred overnight under a positive argon atmosphere. The mixture was

filtered and the solvent was removed by rotary evaporation. The crude product was dissolved in CH_2Cl_2 and cooled to -30 °C for 3 h. The unreacted diol was recrystallized and removed by vacuum filtration. After evaporation of CH_2Cl_2, the crude ester was purified by column chromatography using Hex/EtOAc (8/2), affording 10-(acetyloxy)-decan-1-ol. The yield was 7.7 g (71%). ^{1}H NMR ($CDCl_3$): 4.08-4.02 (t, J = 6.7 Hz, 2H, -OCOC$\underline{H}_2$-), 3.64-3.59 (t, J = 6.6 Hz, 2H, -C$\underline{H}_2$OH), 2.19 (br s, 1H, -OH), 2.05 (s, 3H, CH_3-), 1.64-1.53 (m, 4H, -COCH$_2$C$\underline{H}_2$, -C$\underline{H}_2$CH$_2$OH), 1.30 (br s, 12H, -CH_2-) ppm. ^{13}C NMR ($CDCl_3$): 171.21, 64.53, 62.68, 32.60, 29.35, 29.27 (2), 29.07, 28.43, 25.74, 25.61, 20.85 ppm.

6-(Acetyloxy)hexan-1-ol (**3-13a**). Acetyl chloride (5.0 mL, 0.07 mol), 1,6-hexanediol (16.4 g, 0.14 mol) and pyridine (5.6 mL, 0.07 mol). The yield was 9.3 g (83%). ^{1}H NMR ($CDCl_3$): 4.05-3.99 (t, J = 6.7 Hz, 2H), 3.63-3.57 (t, J = 6.5 Hz, 2H), 2.01 (s, 3H), 1.68 (s, 1H), 1.63-1.51 (m, 4H), 1.37-1.32 (m, 4H) ppm.

8-(Acetyloxy)octan-1-ol (**3-13b**). Acetyl chloride (3.6 mL, 0.05 mol), 1,8-octanediol (14.6 g, 0.1 mol) and pyridine (4.1 mL, 0.05 mol). The yield was 6.8 g (72%). ^{1}H NMR ($CDCl_3$): 4.08-4.03 (t, J = 6.7 Hz, 2H), 3.67-3.61 (t, J = 6.5 Hz, 2H), 2.05 (s, 3H), 1.65-1.51 (m, 4H), 1.45 (s, 1H), 1.34 (br s, 8H) ppm.

3.3.2.2 10-(Acetyloxy)decan-1-al (**3-14c**)

Dimethyl sulfoxide (5.6 mL, 78.4 mmol) in CH_2Cl_2 (60 mL) was added to a stirred oxalyl chloride (2.0 M in CH_2Cl_2, 19.6 mL, 39.2 mmol) solution in CH_2Cl_2 (140 mL) at –70 °C. The mixture was stirred for 5 min and 10-(acetyloxy) decan-1-ol **3-13c**

(7.7 g, 35.6 mmol) in CH_2Cl_2 (100 mL) was added within 5 min. The mixture was stirred for an additional 30 min. TEA (24.8 mL, 178 mmol) was added and the mixture was stirred for 10 min and allowed to warm to room temperature. Water (200 mL) was added and the aqueous layer was re-extracted with additional CH_2Cl_2 (60 mL) two times. The organic layers were combined and washed successively with dilute HCl (2%), brine, dilute Na_2CO_3 (5%) and brine until they were neutral. The solution was dried over $MgSO_4$. After filtration, the solvent was evaporated, giving a slightly yellow crude aldehyde, which was used without further purification. TLC with Hex/EtOAc (8/2) showed the major product at $R_f = 0.61$ with trace impurities. ^{1}H NMR showed less than 5% impurity. The yield was 7.4 g (97%). ^{1}H NMR ($CDCl_3$): 9.78-9.76 (t, J = 1.8 Hz, 1H, -CHO), 4.08-4.02 (t, J = 6.7 Hz, 2H, -OCOC$\underline{H}_2$-), 2.46-2.39 (td, J = 7.3, 1.8 Hz, 2H, -C$\underline{H}_2$CHO), 2.05 (s, 3H, -CH_3), 1.64-1.60 (m, 4H, -OCH$_2$C$\underline{H}_2$-, -C$\underline{H}_2$CH$_2$CHO), 1.30 (br s, 10H, -CH_2-) ppm.

6-(Acetyloxy)hexan-1-al (**3-14a**). Dimethyl sulfoxide (7.1 mL, 100.3 mmol), oxalyl chloride (4.4 mL, 50.1 mmol), 6-(acetyloxy) hexan-1-ol **3-13a** (7.3 g, 45.6 mmol). The yield was 6.5 g (90%). ^{1}H NMR ($CDCl_3$): 9.75-9.74 (t, J = 1.6 Hz, 1H), 4.06-4.01 (t, J = 6.6 Hz, 2H), 2.46-2.40 (td, J = 7.3, 1.6 Hz, 2H), 2.02 (s, 3H), 1.70-1.57 (m, 4H), 1.43-1.33 (m, 2H) ppm. ^{13}C NMR ($CDCl_3$): 202.19, 170.98, 64.00, 43.54, 28.24, 25.38, 21.50, 20.80 ppm.

8-(Acetyloxy)octan-1-al (**3-14b**). Dimethyl sulfoxide (5.6 mL, 79.6 mmol), oxalyl chloride (2.0 M in CH_2Cl_2, 19.9 mL, 39.8 mmol), 8-(acetyloxy)octan-1-ol **3-13b** (6.8 g, 36.2 mmol). The yield was 6.6 g (98%). ^{1}H NMR ($CDCl_3$): 9.78-9.76 (t, J = 1.8

Hz, 1H), 4.08-4.03 (t, J = 6.7 Hz, 2H), 2.47-2.40 (td, J = 7.3, 1.8 Hz, 2H), 2.05 (s, 3H), 1.64-1.60 (m, 4H), 1.35 (br s, 6H) ppm.

3.3.2.3 Ethyl 14-Acetyloxy-2,4-tetradecadienoate (**3-15c**)

A suspension of the aldehyde **3-14c** (7.4 g, 34.6 mmol), triethyl 4-phosphonocrotonate (9.5 g, 38.0 mmol), $LiOH{\cdot}H_2O$ (1.6 g, 38.0 mmol) and activated 4Å molecular sieves (10 g, 0.3 g/mmol of aldehyde) in THF (360 mL) was stirred at room temperature overnight under argon. The crude reaction mixture was filtered through a short plug of silica gel, eluting with ether. The mixture was concentrated and the residue was purified by column chromatography with Hex/EtOAc (9/1). The yield was 8.0 g (75%). The ratio of (*E,E*)-2,4-dienoyl ester to its (*E,Z*)-isomer was determined by ^{1}H NMR using peaks at 7.65-7.52 (*E,Z*) and 7.28-7.18 (*E,E*) (92/8), as well as by GC/MS (95/5).

^{1}H NMR (CD_2Cl_2, peaks in *italics* are from *E,Z* isomer): *7.64-7.53* (m, -C<u>H</u>=CHCOOH, 0.08H), 7.28-7.18 (dd, J = 15.4, 10.2 Hz, 0.92H, -C<u>H</u>=CHCOOH), 6.19-6.13 (m, 2H, -CH_2C<u>H</u>=C<u>H</u>-), 5.79-5.74 (d, J = 15.3 Hz, 1H, =C<u>H</u>COOH), 4.19-4.10 (q, J = 7.1 Hz, 2H, CH_3C<u>H_2</u>O-), 4.04-3.98 (t, J = 6.7 Hz, 2H, -OC<u>H_2</u>CH_2-), 2.32-2.12 (m, 2H, =CHC<u>H_2</u>-), 2.00 (s, 3H, CH_3CO-), 1.66-1.57 (m, 2H, -OCH_2C<u>H_2</u>CH_2-), 1.44-1.23 (m, 15H, -CH_2-, -CH_3) ppm. ^{13}C NMR (CD_2Cl_2): 171.25, 167.33, 145.25, 145.18, *141.97*, *139.63*, 128.64, *126.70, 121.60*, 119.54, 64.83, 60.42, 33.33, 29.79, 29.70, 29.59, 29.51, 29.08, 28.99, *28.61*, 26.26, 21.11, 14.48.

Methyl 10-Acetyloxy-2,4-decadienoate (**3-15a**). Aldehyde **3-14a** (3.4 g, 21.5 mmol), trimethyl 4-phosphonocrotonate (6.0 g, 25.8 mmol), lithium bis(trimethyl sily)amide (1.0 M in THF, 27.9mL, 27.9 mmol). The yield was 3.8 g (74%). The (*E,E*)/(*E,Z*)-isomer ratio was 83/17 by ^{1}H NMR. ^{1}H NMR (CD_2Cl_2): *7.64-7.53* (dd, *J* = 15.2, 11.6 Hz, 0.17H), 7.28-7.18 (dd, *J* = 15.3, 9.4 Hz, 0.83H), 6.24-6.06 (m, 2H), 5.89-5.74 (m, 1H), 4.03-3.98 (t, *J* = 6.6 Hz, 2H), *3.69* (s, 0.5H), 3.68 (s, 2.5H), 2.32-2.12 (m, 2H), 1.98 (s, 3H), 1.66-1.55 (m, 2H), 1.50-1.31 (m, 4H) ppm. ^{13}C NMR (CD_2Cl_2): 171.21, 167.71, 145.39, 144.87, *141.65*, *139.75*, 128.76, *126.84*, *121.24*, 119.18, 64.58, 51.57, 33.13, *29.31*, 28.77, 28.63, *28.46*, *25.86*, 25.81, 21.06.

Methyl 12-Acetyloxy-2,4-dodecadienoate (**3-15b**). Aldehyde **3-14b** (5.6 g, 30.1 mmol), trimethyl 4-phosphonocrotonate (7.7 g, 33.1 mmol), $LiOH{\cdot}H_2O$ (1.4 g, 33.1 mmol). The yield was 6.1 g (75%). The (*E,E*)/(*E,Z*)-isomer ratio was 92/8 by ^{1}H NMR and 94/6 by GC/MS. ^{1}H NMR (CD_2Cl_2): *7.65-7.54* (m, 0.04H), 7.29-7.19 (m, 0.96H), 6.19-6.14 (m, 2H), 5.81-5.75 (d, *J* = 15.3 Hz, 1H), 4.04-3.98 (t, *J* = 6.7 Hz, 2H), *3.71*-3.68 (m, 3H), *2.32*-2.13 (m, 2H), 2.00 (s, 3H), 1.70-1.54 (m, 2H), 1.48-1.32 (m, 8H) ppm. ^{13}C NMR (CD_2Cl_2): 171.23, 167.77, 145.51, 145.29, *142.06*, *139.87*, 128.64, *126.71*, *121.14*, 119.08, 64.77, 51.58, 33.28, *29.64*, 29.39 (2), 28.97 (2), *28.58*, 26.19, 21.10.

3.3.2.4 Ethyl 14-Acetyloxy-(*E,E*)-2,4-tetradecadienoate (**3-16c**)

A well-stirred solution of urea (13.8 g, 230.8 mmol) in methanol (140 mL) was treated with ester isomer **3-15c** (5.3 g, 17.1 mmol). The solution was kept at 0 °C overnight. The crystals of **3-16c** were filtered, washed with cold methanol, dried under

vacuum, dissolved in water and extracted several times with ether. The organic layer was combined and dried with $MgSO_4$. After evaporation of ether, pure (*E,E*)-isomer **3-16c** was obtained. ^{1}H NMR (CD_2Cl_2): 7.28-7.18 (m, 1H, -C<u>H</u>=CHCOOH), 6.24-6.13 (m, 2H, -CH_2C<u>H</u>=C<u>H</u>-), 5.80-5.73 (d, *J* = 15.3 Hz, 1H, =C<u>H</u>COOH), 4.19-4.10 (q, *J* = 7.2 Hz, 2H, $CH_3C\underline{H}_2O$-), 4.04-3.98 (t, *J* = 6.7 Hz, 2H, -O<u>CH_2</u>CH_2-), 2.20-2.12 (m, 2H, =CH<u>CH_2</u>-), 2.00 (s, 3H, CH_3CO-), 1.62-1.54 (m, 2H, -$OCH_2C\underline{H}_2CH_2$-), 1.45-1.23 (m, 15H, -$CH_2$-, -$CH_3$) ppm. ^{13}C NMR ($CD_2Cl_2$): 171.23, 167.33, 145.24, 145.18, 128.64, 119.54, 64.83, 60.41, 33.33, 29.79, 29.70, 29.59, 29.51, 29.08, 28.99, 26.26, 21.11, 14.48. FAB-MS *m/z*: calcd for $C_{18}H_{31}O_4$, 311.2222; found, 311.2219.

Methyl 10-Acetyloxy-(*E,E*)-2,4-decadienoate (**3-16a**). ^{1}H NMR (CD_2Cl_2): 7.29-7.19 (dd, *J* = 15.3, 9.2 Hz, 1H), 6.20-6.14 (m, 2H), 5.82-5.76 (d, *J* = 15.3 Hz, 1H), 4.04-3.99 (t, *J* = 6.6 Hz, 2H), 3.69 (s, 3H), 2.22-2.14 (m, 2H), 2.00 (s, 3H), 1.67-1.56 (m, 2H), 1.49-1.32 (m, 4H) ppm. ^{13}C NMR (CD_2Cl_2): 171.20, 167.72, 145.39, 144.86, 128.77, 119.18, 64.58, 51.57, 33.14, 28.76, 28.64, 25.82, 21.07.

Methyl 12-Acetyloxy-(*E,E*)-2,4-dodecadienoate (**3-16b**). ^{1}H NMR (CD_2Cl_2): 7.29-7.19 (m, 1H), 6.25-6.14 (m, 2H), 5.81-5.75 (d, *J* = 15.3 Hz, 1H), 4.04-3.98 (t, *J* = 6.7 Hz, 2H), 3.69 (s, 3H), 2.20-2.13 (m, 2H), 2.00 (s, 3H), 1.67-1.56 (m, 2H), 1.45-1.32 (m, 8H) ppm. ^{13}C NMR (CD_2Cl_2): 171.25, 167.78, 145.52, 145.31, 128.64, 119.07, 64.77, 51.58, 33.29, 29.39 (2), 28.97 (2), 26.19, 21.11.

3.3.2.5 14-(Hydroxy)-2,4-tetradecadienoic Acid (**3-17c**)

An aqueous solution of 1N KOH (50 mL, 50 mmol) was added to a methanol solution (50 mL) of ethyl ester **3-16c** (3.8 g, 12.25 mmol) and heated under refluxing conditions for 1 h. After the solution was acidified to pH 3 with dilute HCl solution, it was extracted several times with $CHCl_3$. The organic layer was dried with $MgSO_4$ and concentrated, affording the pure dienoic acid **3-17c**. The yield was 3.0 g (100%). ^{1}H NMR (methanol-d_4): 7.29-7.19 (dd, J = 15.4, 9.9 Hz, 1H, -C<u>H</u>=CHCOOH), 6.30-6.10 (m, 2H, -CH_2C<u>H</u>=C<u>H</u>-), 5.80-5.73 (d, J = 15.4 Hz, 1H, =C<u>H</u>COOH), 3.55-3.50 (t, J = 6.6 Hz, 2H, -CH_2OH), 2.22-2.14 (m, 2H, =CHC<u>H_2</u>-), 1.54-1.32 (m, 14H, -CH_2-) ppm. ^{13}C NMR (methanol-d_4): 170.76, 146.98, 145.94, 129.69, 120.34, 63.00, 33.96, 33.65, 30.65, 30.56, 30.49, 30.29, 29.87, 26.92. FAB-MS *m/z*: calcd for $C_{14}H_{25}O_3$, 241.1804; found, 241.1803.

10-(Hydroxy)-2,4-decadienoic Acid (**3-17a**). 1N KOH (17.5 mL, 17.5 mmol) methyl ester **3-16a** (1.4 g, 5.83 mmol). The yield was 1.0 g (93%). ^{1}H NMR (acetone-d_6): 7.30-7.20 (dd, J = 15.3, 9.7 Hz, 1H), 6.32-6.18 (m, 2H), 5.86-5.79 (d, J = 15.4 Hz, 1H), 3.56-3.51 (t, J = 6.2 Hz, 2H), 2.24-2.17 (m, 2H), 1.57-1.39 (m, 6H) ppm. ^{13}C NMR (acetone-d_6): 167.72, 145.88, 144.94, 129.15, 119.99, 62.08, 33.36, 33.26, 29.12, 26.02. EI-MS *m/z*: calcd for $C_{10}H_{16}O_3$, 184.1099; found, 184.1102.

12-(Hydroxy)-2,4-dodecadienoic Acid (**3-17b**). 1N KOH (53.7 mL, 53.7 mmol) methyl ester **3-16b** (4.8 g, 17.9 mmol). The yield was 3.4 g (89%). ^{1}H NMR (methanol-d_4): 7.29-7.19 (dd, J = 15.3, 9.8 Hz, 1H), 6.29-6.10 (m, 2H), 5.80-5.73 (d, J = 15.4 Hz, 1H), 3.56-3.50 (t, J = 6.5 Hz, 2H), 2.22-2.14 (m, 2H), 1.52-1.34 (m, 10H) ppm. ^{13}C

NMR (methanol-d_4): 170.80, 146.95, 145.88, 129.71, 120.39, 62.97, 33.96, 33.61, 30.36, 30.27, 29.82, 26.86. FAB-MS *m/z*: calcd for $C_{12}H_{21}O_3$, 213.1491; found, 213.1486.

3.3.2.6 14-Acryloxy-2,4-tetradecadienoic Acid (Acryl/Den Acid-18, **3-18c**)

Acryloyl chloride (0.53 mL, 6.5 mmol) in THF (30 mL) was added dropwise to a solution of 14-hydroxy-2,4-tetradecadienoic acid **3-17c** (1.2 g, 5.0 mmol) with pyridine (0.61 mL, 7.5 mmol) and one crystal of 2,6-di-*tert*-butyl-4-methylphenol in THF (120 mL) at 0 °C. The solution was allowed to warm to room temperature and stirred for another 2 h. The pyridine chloride was removed by vacuum filtration and the mixture was concentrated by rotary evaporation. The crude acid was purified by column chromatography using $CHCl_3$/MeOH (95/5), affording 14-acryloxy-2,4-tetradecadienoic acid **3-18c**. The yield was 0.89 g (60%). ^{1}H NMR ($CDCl_3$): 7.40-7.30 (m, 1H, -C<u>H</u>=CHCOOH), 6.44-6.36 (dd, J = 17.3, 1.6 Hz, 1H, <u>H</u>$_a$CH$_b$=), 6.21-6.06 (m, 3H, -CH$_2$C<u>H</u>=C<u>H</u>-, H$_a$C<u>H</u>$_b$=CHCOO-), 5.84-5.76 (m, 2H, CH$_2$=C<u>H</u>COO-, =C<u>H</u>COOH), 4.18-4.12 (t, J = 6.7 Hz, 2H, -CH$_2$O-), 2.22-2.14 (m, 2H, =CHC<u>H</u>$_2$-), 1.69-1.61 (m, 2H, -C<u>H</u>$_2$CH$_2$O-), 1.43-1.29 (m, 12H, -CH$_2$-) ppm. ^{13}C NMR ($CDCl_3$): 172.50, 166.35, 147.47, 146.17, 130.43, 128.62, 128.23, 118.23, 64.68, 33.02, 29.36, 29.29, 29.17, 29.11, 28.58 (2), 25.87. FAB-MS *m/z*: calcd for $C_{17}H_{27}O_4$, 295.1909; found, 295.1918.

10-Acryloxy-2,4-decadienoic Acid (Acryl/Den Acid-14, **3-18a**). Acryloyl chloride (0.58 mL, 7.2 mmol), 10-hydroxy-2,4-decadienoic acid **3-17a** (1.2 g, 6.5 mmol), pyridine (0.79 mL, 9.8 mmol). The yield was 0.90 g (60%). ^{1}H NMR ($CDCl_3$): 7.40-7.29 (m, 1H), 6.44-6.37 (dd, J = 17.3, 1.6 Hz, 1H), 6.21-6.07 (m, 3H), 5.85-5.76 (m, 2H),

4.19-4.13 (t, J = 6.6 Hz, 2H), 2.25-2.17 (m, 2H), 1.75-1.64 (m, 2H), 1.52-1.36 (m, 4H) ppm. ^{13}C NMR ($CDCl_3$): 172.28, 166.31, 147.21, 145.45, 130.58, 128.53, 128.49, 118.50, 64.40, 32.83, 28.38, 28.19, 25.48. FAB-MS *m/z*: calcd for $C_{13}H_{19}O_4$, 239.1283; found, 239.1282.

12-Acryloxy-2,4-dodecadienoic Acid (Acryl/Den Acid-16, **3-18b**). Acryloyl chloride (0.59 mL, 7.3 mmol), 12-hydroxy-2,4-dodecadienoic acid **3-17b** (1.4 g, 6.6 mmol), pyridine (0.80 mL, 9.9 mmol). The yield was 1.10 g (62%). ^{1}H NMR ($CDCl_3$): 7.40-7.29 (m, 1H), 6.44-6.37 (dd, J = 17.3, 1.64 Hz, 1H), 6.21-6.06 (m, 3H), 5.84-5.76 (m, 2H), 4.18-4.12 (t, J = 6.7 Hz, 2H), 2.20-2.14 (m, 2H), 1.70-1.61 (m, 2H), 1.48-1.34 (m, 8H) ppm. ^{13}C NMR ($CDCl_3$): 172.69, 166.27, 147.30, 145.90, 130.43, 128.48, 128.21, 118.32, 64.52, 32.88, 28.90 (2), 28.44, 28.40, 25.70. FAB-MS *m/z*: calcd for $C_{15}H_{23}O_4$, 267.1596; found, 267.1595.

3.3.2.7 14-Sorbyl-2,4-tetradecadienoic Acid (Sorb/Den Acid-21, **3-19c**)

Sorbyl chloride (0.75 g, 5.7 mmol) in THF (40 mL) was added dropwise to a solution of 14-hydroxy-2,4-tetradecadienoic acid **3-17c** (1.0 g, 4.2 mmol) and pyridine (0.46 mL, 5.7 mmol) in THF (100 mL) at 0 °C. The solution was allowed to warm to room temperature and stir overnight under argon. The mixture was filtered and concentrated. The crude acid was purified by reverse phase C-18 column chromatography using a gradient of MeOH/H_2O (1/1 to 7/3). The yield was 0.58 g (42%). ^{1}H NMR ($CDCl_3$): 7.40-7.20 (m, 2H, -C<u>H</u>=CHCOOH, CH_3CH=CHC<u>H</u>=), 6.21-6.12 (m, 4H, -CH_2C<u>H</u>=C<u>H</u>-, CH_3C<u>H</u>=C<u>H</u>-), 5.82-5.74 (2d, J = 15.3 Hz, 2H, =CHCO),

4.15-4.10 (t, J = 6.7 Hz, 2H, -CH_2O-), 2.19-2.14 (m, 2H, =CHC$\underline{H}_2$-), 1.86-1.84 (d, J = 5.3 Hz, 3H, CH_3-), 1.68-1.62 (m, 2H, -C$\underline{H}_2CH_2$O-), 1.42-1.29 (br s, 12H –CH_2-) ppm. ^{13}C NMR ($CDCl_3$): 172.38, 167.44, 147.48, 146.19, 144.89, 139.20, 129.78, 128.22, 119.03, 118.18, 64.38, 33.02, 29.36, 29.29, 29.18, 29.11, 28.67, 28.58, 25.90, 18.61. FAB-MS *m/z*: calcd for $C_{20}H_{31}O_4$, 335.2222; found, 335.2213.

10-Sorbyl-2,4-decadienoic Acid (Sorb/Den Acid-17, **3-19a**). Sorbyl chloride (0.43 g, 3.3 mmol), 10-hydroxy-2,4-decadienoic acid **3-17a** (0.3 g, 1.6 mmol) and pyridine (0.26 mL, 3.3 mmol). The yield was 0.244 g (40%). ^{1}H NMR ($CDCl_3$): 7.40-7.20 (m, 2H), 6.21-6.15 (m, 4H), 5.82-5.74 (2d, J = 15.2, 15.4 Hz, 2H), 4.16-4.11 (t, J = 6.6 Hz, 2H), 2.22-2.17 (m, 2H), 1.87-1.85 (d, J = 5.4 Hz, 3H), 1.70-1.62 (m, 2H,), 1.49-1.39 (m, 4H) ppm. ^{13}C NMR ($CDCl_3$): 172.22, 167.57, 147.35, 145.62, 145.03, 139.40, 129.75, 128.46, 118.89, 118.34, 64.09, 32.84, 28.47, 28.18, 25.51, 18.64. FAB-MS *m/z*: calcd for $C_{16}H_{23}O_4$, 279.1596; found: 279.1607.

12-Sorbyl-2,4-dodecadienoic Acid (Sorb/Den Acid-19, **3-19b**). Sorbyl chloride (0.37 g, 2.83 mmol), 12-hydroxy-2,4-dodecadienoic acid **3-17b** (0.61 g, 2.83 mmol) and pyridine (0.27 mL, 3.4 mmol). The yield was 0.41 g (46%). ^{1}H NMR ($CDCl_3$): 7.40-7.20 (m, 2H), 6.25-6.12 (m, 4H), 5.82-5.74 (2d, J = 15.2, 15.5 Hz, 2H), 4.16-4.10 (t, J = 6.7 Hz, 2H), 2.22-2.14 (m, 2H), 1.86-1.84 (d, J = 5.3 Hz, 3H), 1.68-1.60 (m, 2H,), 1.48-1.34 (m, 8H) ppm. ^{13}C NMR ($CDCl_3$): 172.67, 167.43, 147.40, 146.02, 144.93, 139.27, 129.74, 128.24, 118.93, 118.30, 64.28, 32.95, 28.97 (2), 28.60, 28.46, 25.79, 18.60. FAB-MS *m/z*: calcd for $C_{18}H_{27}O_4$, 307.1909; found: 307.1920.

3.3.2.8 1-Palmitoyl-2-[14-acryloxy-2,4-tetradecadienoic]-*sn*-glycero-3-phosphocholine (Acryl/Den $PC_{16.18}$, **3-11c**)

Lyso PC_{16} (0.808 g, 1.63 mmol), Acryl/Den acid **3-18c** (0.40 g, 1.36 mmol), dicyclohexylcarbodiimide (DCC, 0.336 g, 1.63 mmol), 4-(dimethylamino)pyridine (DMAP, 0.332 g, 2.72 mmol) and one crystal of 2,6-di-*tert*-butyl-4-methylphenol were added into a flask with $CHCl_3$ (8 mL). The mixture was stirred at room temperature in the dark for 3 days under argon. The white suspension was filtered and the solution was concentrated. The residue was dissolved in MeOH (20 mL) and stirred with Bio-Rad AG 501-X8 ion-exchange resin (5 g) for 15 min. The resin was removed by vacuum filtration and the filtrate was concentrated. The crude product was purified by column chromatography using $CHCl_3$/MeOH (9/1) followed by $CHCl_3$/MeOH/H_2O (65/25/4), giving 0.46 g of lipid (44%). ^{1}H NMR ($CDCl_3$): 7.29-7.19 (m, 1H, -C$\underline{H}$=CHCO-), 6.44-6.36 (dd, J = 17.3, 1.6 Hz, 1H, $\underline{H}_aCH_b$=), 6.17-6.06 (m, 3H, -$CH_2C\underline{H}$=C$\underline{H}$-, $H_aC\underline{H}_b$=CH-), 5.84-5.73 (m, 2H, =CHCOO-), 5.27 (br s, 1H, -$POCH_2C\underline{H}O$-), 4.42-4.19 (m, 4H, -$POC\underline{H}_2CH$-, -$CHC\underline{H}_2OCO$-), 4.17-4.12 (t, J = 6.7 Hz, 2H, -$OC\underline{H}_2CH_2$-), 4.01 (br s, 2H, -$NCH_2C\underline{H}_2$-), 3.82 (br s, 2H, -$NC\underline{H}_2CH_2$-), 3.38 (s, 9H, -NCH_3), 2.30-2.24 (t, J = 7.5 Hz, 2H, -CH_2COO-), 2.18-2.16 (m, 2H, =$CHC\underline{H}_2$-), 1.70-1.56 (m, 4H, -$OCH_2C\underline{H}_2$-, -$C\underline{H}_2CH_2COO$-), 1.48-1.18 (m, 36H, -CH_2-), 0.90-0.85 (t, J = 6.6 Hz, 3H, -CH_3) ppm. ^{13}C NMR ($CDCl_3$): 173.57, 166.50, 166.31, 146.02, 145.57, 130.40, 128.62, 128.20, 118.55, 70.78-70.65 ($J_{31p\text{-}c}$ = 7.7 Hz), 66.47-66.37 ($J_{31p\text{-}c}$ = 6.3 Hz), 64.64, 63.54-63.44 ($J_{31p\text{-}c}$ = 6.1 Hz), 63.01, 59.28-59.20 ($J_{31p\text{-}c}$ = 5.1 Hz), 54.49, 34.13, 33.03, 31.90, 29.68 (6), 29.64

(3), 29.49, 29.39, 29.33 (2), 29.19 (2), 29.13, 28.67, 28.58, 25.88, 24.88, 22.66, 14.10. FAB-MS *m/z*: calcd for $C_{41}H_{75}O_{10}PN$, 772.5129; found, 772.5110.

1-Palmitoyl-2-[10-acryloxy-2,4-decadienoic]-*sn*-glycero-3-phosphocholine (Acryl/Den $PC_{16:14}$, **3-11a**). Lyso PC_{16} (0.750 g, 1.51 mmol), Acryl/Den acid **3-18a** (0.30 g, 1.26 mmol), DCC (0.390 g, 1.89 mmol), DMAP (0.308 g, 2.52 mmol) were combined as in **3-11c** to give 0.40 g of lipid (44%). ^{1}H NMR ($CDCl_3$): 7.29-7.19 (m, 1H), 6.44-6.36 (dd, J = 17.3, 1.6 Hz, 1H), 6.18-6.06 (m, 3H), 5.85-5.74 (m, 2H), 5.28-5.26 (m, 1H), 4.41-4.21 (m, 4H), 4.18-4.13 (t, J = 6.6 Hz, 2H), 3.99 (br s, 2H), 3.85 (br s, 2H), 3.38 (s, 9H), 2.30-2.24 (t, J = 7.6, 2H), 2.21-2.19 (m, 2H), 1.72-1.66(m, 2H), 1.63-1.33 (m, 6H), 1.25 (br s, 24H), 0.90-0.85 (t, J = 6.6 Hz, 3H) ppm. ^{13}C NMR ($CDCl_3$): 173.60, 166.48, 166.26, 145.94, 145.02, 130.58, 128.53, 128.45, 118.74, 70.67, 66.41, 64.37, 63.53, 63.00, 59.16, 54.47, 34.11, 32.85, 31.90, 29.70 (8), 29.51, 29.34, 29.32, 29.14, 28.39, 28.27, 25.52, 24.88, 22.67, 14.11. FAB-MS *m/z*: calcd for $C_{37}H_{67}O_{10}PN$, 716.4503; found, 716.4508.

1-Palmitoyl-2-[12-acryloxy-2,4-dodecadienoic]-*sn*-glycero-3-phosphocholine (Acryl/Den $PC_{16:16}$, **3-11b**). Lyso PC_{16} (0.783 g, 1.58 mmol), Acryl/Den acid **3-18b** (0.35 g, 1.31 mmol), DCC (0.407 g, 1.97 mmol), DMAP (0.322 g, 2.63 mmol) were combined as in **3-11c** to give 0.276 g of lipid (28%). ^{1}H NMR ($CDCl_3$): 7.27-7.19 (m, 1H), 6.44-6.36 (dd, J = 17.3, 1.6 Hz, 1H), 6.17-6.06 (m, 3H), 5.84-5.74 (m, 2H), 5.25 (br s, 1H), 4.40-4.12 (m, 6H), 3.98 (br s, 2H), 3.83 (br s, 2H), 3.37 (br s, 9H), 2.30-2.24 (t, J = 7.5, 2H), 2.18-2.17 (m, 2H), 1.67-1.56 (m, 4H), 1.43-1.25 (m, 32H), 0.90-0.85 (t, J = 6.6 Hz, 3H) ppm. ^{13}C NMR ($CDCl_3$): 173.60, 166.48, 166.31, 146.08, 145.50, 130.45, 128.60,

128.26, 118.55, 70.62, 66.32, 64.56, 63.59, 63.00, 59.33, 54.44, 34.12, 33.00, 31.90, 29.70 (10), 29.52, 29.34, 29.15, 29.10, 29.02, 28.57, 25.83, 24.88, 22.66, 14.10. FAB-MS *m/z*: calcd for $C_{39}H_{71}O_{10}PN$, 744.4816; found, 744.4821.

3.3.2.9 1-Oleoyl-2-[14-sorbyl-2,4-tetradecadienoic]-*sn*-glycero-3-phosphocholine (Sorb/Den $PC_{18:21}$, **3-12c**)

Following the same procedure as in Acryl/Den $PC_{16:18}$ **3-11c**. LysoPC_{18} (0.56 g, 1.1 mmol), Sorb/Den acid **3-19c** (0.30 g, 0.9 mmol), DCC (0.22 g, 1.1 mmol) and DMAP (0.22 g, 1.8 mmol) afforded lipid **3-12c** with a yield of 0.55 g (73%). ^{1}H NMR ($CDCl_3$): 7.29-7.20 (m, 2H, -C<u>H</u>=CHCOO-), 6.19-6.12 (m, 4H, -CH_2C<u>H</u>=C<u>H</u>-, CH_3C<u>H</u>=C<u>H</u>-), 5.80-5.73 (d, *J* = 15.4 Hz, 2H, =CHCO-), 5.36-5.32 (m, 2H, -CH_2C<u>H</u>=C<u>H</u>CH_2-), 5.31-5.27 (br s, 1H, -$POCH_2$C<u>H</u>O), 4.40-4.19 (m, 4H, -POC<u>H_2</u>CH-, -CHC<u>H_2</u>OCO-), 4.15-4.10 (t, *J* = 6.7 Hz, 2H, -OC<u>H_2</u>CH_2-), 3.99 (br s, 2H, -NCH_2C<u>H_2</u>-), 3.84 (br s, 2H, -NC<u>H_2</u>CH_2-), 3.38 (s, 9H, -NCH_3), 2.30-2.24 (t, *J* = 7.5 Hz, 2H, -CH_2COO-), 2.18-2.15 (m, 2H, =CHC<u>H_2</u>-), 2.02-1.98 (m, 4H, -C<u>H_2</u>CH=CHC<u>H_2</u>-), 1.86-1.84 (d, *J* = 5.3 Hz, 3H, =CHC<u>H_3</u>), 1.70-1.52 (m, 4H, -OCH_2C<u>H_2</u>-, -C<u>H_2</u>CH_2COO-), 1.27 (br s, 32H, -CH_2-), 0.90-0.85 (t, *J* = 6.5 Hz, 3H, -CH_2C<u>H_3</u>). ^{13}C NMR ($CDCl_3$): 173.56, 166.51 (2), 146.09, 145.68, 144.86, 139.19, 129.98, 129.78, 129.70, 128.18, 119.03, 118.51, 70.77, 66.47, 64.35, 63.53, 63.04, 59.27-59.18 (J_{31p-c} = 5.4 Hz), 54.51, 34.10, 33.06, 31.88, 29.74 (2), 29.51, 29.42, 29.34, 29.30 (3), 29.22 (4), 29.14, 29.10, 28.69 (2), 27.20, 27.17, 25.92, 24.86, 22.66, 18.62, 14.10. FAB-MS *m/z*: calcd for $C_{46}H_{81}O_{10}PN$, 838.5598; found: 838.5607.

1-Palmitoyl-2-[10-sorbyl-2,4-decadienoic]-*sn*-glycero-3-phosphocholine (Sorb/Den $PC_{16.17}$, **3-12a**). $LysoPC_{16}$ (0.428 g, 0.86 mmol), Sorb/Den acid **3-19a** (0.20 g, 0.72 mmol), DCC (0.178 g, 0.86 mmol) and DMAP (0.176 g, 1.44 mmol) afforded lipid **3-12a** with a yield of 0.34 g (63%). ^{1}H NMR ($CDCl_3$): 7.29-7.19 (m, 2H), 6.19-6.15 (m, 4H), 5.80-5.74 (d, J = 15.4 Hz, 2H), 5.27 (br s, 1H), 4.41-4.21 (m, 4H), 4.15-4.10 (t, J = 6.6 Hz, 2H), 4.00 (m, 2H), 3.82 (br s, 2H), 3.37 (br s, 9H), 2.30-2.24 (t, J = 7.6 Hz, 2H), 2.20-2.18 (br s, 2H), 1.87-1.85 (d, J = 5.4 Hz, 3H), 1.70-1.36 (m, 8H), 1.25 (br s, 24H), 0.90-0.85 (t, J = 6.6 Hz, 3H) ppm. ^{13}C NMR ($CDCl_3$): 173.60, 166.47 (2), 145.91, 145.01 (2), 139.38, 129.75, 128.42, 118.89, 118.32, 70.51, 66.21, 64.09, 63.60, 62.99, 59.18, 54.52, 34.13, 32.87, 31.91, 29.70 (5), 29.66 (3), 29.51, 29.35, 29.30, 29.14, 28.51, 28.31, 25.58, 24.88, 22.68, 18.65, 14.11. FAB-MS *m/z*: calcd for $C_{40}H_{71}O_{10}PN$, 756.4816; found, 756.4818.

1-Palmitoyl-2-[12-sorbyl-2,4-dodecadienoic]-*sn*-glycero-3-phosphocholine (Sorb/Den $PC_{16.19}$, **3-12b**). $LysoPC_{16}$ (0.389 g, 0.78 mmol), Sorb/Den acid **3-19b** (0.20 g, 0.65 mmol), DCC (0.202 g, 0.98 mmol) and DMAP (0.160 g, 1.31 mmol) afforded lipid **3-12b** with a yield of 0.133 g (26%). ^{1}H NMR ($CDCl_3$): 7.29-7.19 (m, 2H), 6.19-6.12 (m, 4H), 5.80-5.73 (d, J = 15.6 Hz), 5.25 (br s, 1H), 4.40-4.19 (m, 4H), 4.15-4.10 (t, J = 6.7 Hz, 2H), 3.97 (br s, 2H), 3.83 (br s, 2H), 3.37 (br s, 9H), 2.30-2.24 (t, J = 7.5 Hz, 2H), 2.17 (br s, 2H), 1.86-1.84 (d, J = 5.3 Hz, 3H), 1.70-1.52 (m, 4H), 1.50-1.25 (m, 32H), 0.90-0.85 (t, J = 6.6 Hz, 3H) ppm. ^{13}C NMR (CD_2CH_2): 173.56, 166.50 (2), 146.12, 144.89, 139.22, 129.77 (2), 128.24, 119.00, 118.53, 70.87, 66.37, 64.27, 63.54, 63.00, 59.21, 54.45, 34.12, 33.02, 31.91, 29.70 (8), 29.53, 29.34 (2), 29.15 (2), 29.05, 28.67,

28.63, 25.86, 24.90, 22.67, 18.61, 14.10. FAB-MS *m/z*: calcd for $C_{42}H_{75}O_{10}PN$, 784.5129; found: 784.5141.

3.3.3 Calorimetry

The lipid was freeze-dried overnight and then hydrated with deoxygenated water to a concentration of 8 mM. The hydration of the lipid was done by heating to 45 °C, vortexing, and then cooling to -78 °C 10 times. The fully hydrated lipid bilayers were then transferred to a DSC cell. Thermograms were obtained at a scan rate of 10 °/h. and the phase transition temperature was measured from the point of maximum excess heat capacity. The cooperative unit (number of lipids undergoing the phase transition at the same time) was calculated by dividing the van't Hoff enthalpy by the calorimetric enthalpy.

3.3.4 Vesicle Polymerization

3.3.4.1 Simultaneous Polymerization

(a) Redox Initiation

Large unilamellar vesicles (LUV) of polymerizable lipid were prepared as follows: Approximately 6 mg of polymerizable lipid from a benzene stock solution (10 mg/mL) was freeze-dried under high vacuum for at least 4 h. The dried lipid was hydrated with deoxygenated Milli-Q water to a concentration of 0.6–2 mM. Samples were vortexed to uniformity and subjected to 10 freeze-thaw-vortex cycles (-77 to +45 °C). LUV with a diameter of ca. 100 nm were prepared by extrusion 10 times (4 × 0.2

μm + 6 × 0.1 μm) through two stacked Nuclepore polycarbonate filters at 45 °C using a stainless steel extruder from Lipex Biomembranes.[44]

The redox initiator was prepared from $KBrO_3$ (66.8 mg, 0.4 mmol) and L-cysteine hydrochloride hydrate (63.0 mg, 0.4 mmol), which were weighed into a 10 mL volumetric flask and diluted. An aliquot of $KBrO_3$/L-cysteine (1/1) was added to the vesicle suspension, giving a [M]/[I] ratio of 1. The sample was sealed in an ampule with a septum and flushed with argon for 0.5 h. Polymerization was performed at 60 ± 2 °C in a water-circulating bath under a positive argon pressure for 18 h. Polymerization was monitored by UV absorption spectroscopy of aliquots diluted with Milli-Q water to ca. 60 μM.

(b) UV Polymerization

The LUV, prepared as above, were placed into a 3 mL quartz cuvette equipped with a magnetic stir bar, and the cuvette was placed 1 cm in front of a low-pressure Hg vapor pen lamp. The polymerization was carried out at 40 °C and monitored by UV absorption spectroscopy as above.

3.3.4.2 Selective Polymerization

(a) Filtered UV Irradiation

The procedure was the same as in UV polymerization except that a CS9-54 filter, which has a cutoff wavelength shorter than 230 nm was placed between the sample and the light source.

(b) Thermal Radical Initiation

AIBN Radical Polymerization

An AIBN solution (1-1.5 mg/mL in benzene) was prepared. An aliquot was added to the lipid to give a [M]/[I] ratio of 5-20, and benzene was removed under vacuum. The sample was then hydrated with deoxygenated MilliQ water at a concentration of 1 mM through several freeze-thaw-vortex cycles. LUVs were prepared through extrusion as described above. The sample was then placed in an ampule sealed with a septum and flushed with argon for 1 h. Polymerization was performed at 60 °C in the absence of light for 3-5 days.

AAPD Polymerization

An AAPD stock solution (1.0 mg/mL in water) was prepared and the appropriate amount was added to the LUV. The system was flushed with argon for 1 h and the ampule was put in a 60 °C bath to polymerize for 2-3 days.

(c) Redox Initiation in Air

The same procedure as in Redox Initiation, except that the lipids were hydrated in nondeoxygenated MilliQ water and polymerization was conducted under air.

3.3.5 Surfactant Dissolution of Vesicles

The LUV were prepared as described above. After polymerization, the LUV were characterized by QELS for a 2 mL sample with a lipid concentration of 300 μM. Aliquots of 50 mM TX-100 solution, each 2 equiv. with respect to lipid, were added until the vesicles dissolved or 12 equiv. were added. The light-scattering intensities were determined again by QELS. Measurements at each concentration of TX-100 were

performed at least three times. The average mean diameter of vesicles/particles was calculated by a nonnegatively constrained least-squares program.

3.3.6 Weight Percent Solubility

Only samples with greater than 90% monomer conversion, as determined by UV/vis spectroscopy, were used in the solubility studies. Samples were lyophilized after polymerization. The lipid was weighed and HFIP added to a concentration of 2 mg/mL. The samples were shaken for 2 min and allowed to stand for at least 4 h. The solution was filtered through an Acrodisc CR PTFE filter with 0.2 μm pore size. The solvent was removed by lyophilization overnight, leaving the soluble polymer. The weight of the polymer was used to calculate the percent solubility.

3.4 Results and Discussion

3.4.1 Lipid Synthesis

The heterobifunctional lipids **3-11** and **3-12** of varying chain lengths were prepared by acylation of the appropriate fatty acid with either $LysoPC_{16}$ or $LysoPC_{18}$ in the presence of DMAP and DCC. Fatty acids **3-18** and **3-19** were synthesized from the commercially available α,ω-diol as shown in Scheme 3-1. The diol was monoprotected with acetyl chloride. The resulting alcohol **3-13** was oxidized to aldehyde **3-14** using a Swern oxidation.[158] The Horner-Wadsworth-Emmons olefination[159] of **3-14** with triethyl (or trimethyl) phosphonocrotonate gave ethyl (or methyl) dienoate **3-15** as a mixture of stereo isomers (83-95% *E,E*). Urea inclusion was used to separate the *E,E*

isomer **3-16** from the corresponding *E,Z* isomer.[160-163] The hydrolysis of the ethyl ester and the acetyl protecting group was accomplished with KOH in MeOH to afford the hydroxy dienoic acid **3-17**. Compound **3-17** was then reacted with either acryloyl chloride or sorbyl chloride to form the Acryl/Den acid **3-18** (30% overall yield) or the Sorb/Den acid **3-19** (21% overall yield).

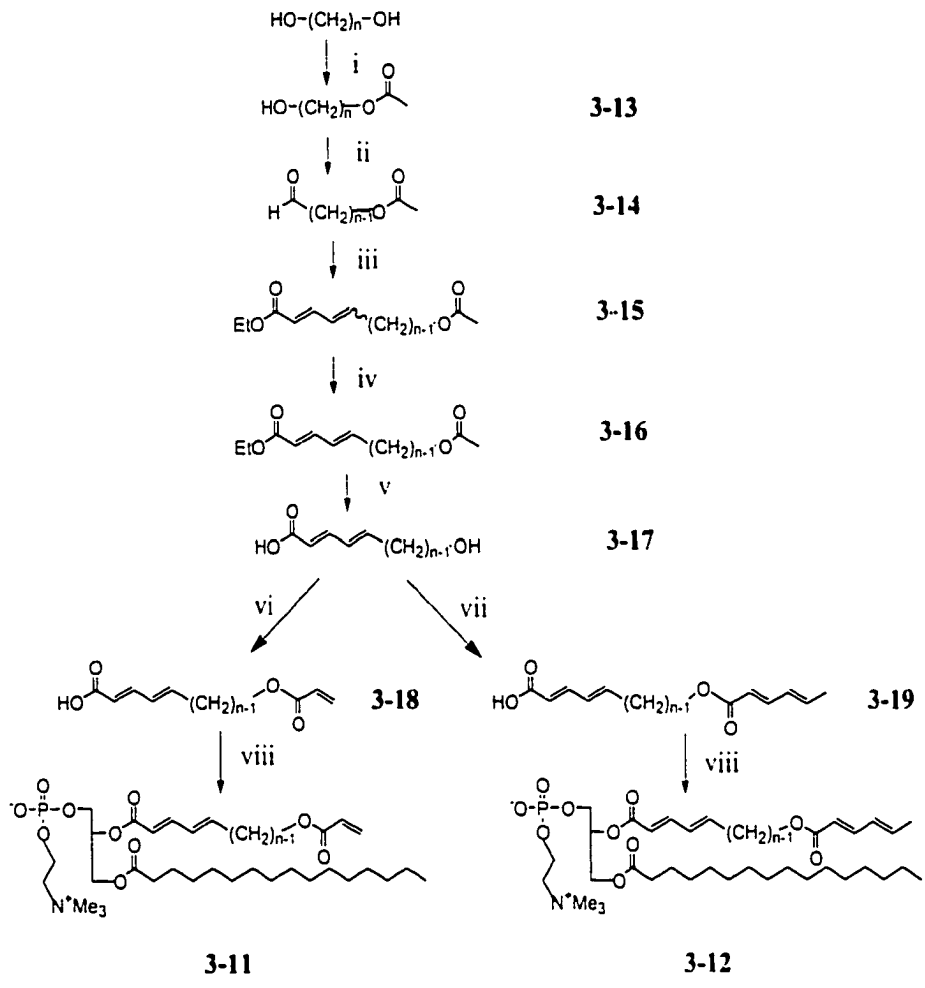

a: n = 6
b: n = 8
c: n = 10

Scheme 3-1. Synthesis of Acryl/DenPC **3-11** and Sorb/DenPC **3-12**. (i) acetyl chloride, pyridine; (ii) oxalyl chloride, DMSO; (iii) LiOH, triethylphosphonocrotonate; (iv) urea inclusion; (v) KOH, MeOH; (vi) acryloyl chloride, pyridine; (vii) sorbyl chloride, pyridine; (viii) LysoPC, DCC, DMAP.

3.4.2 Calorimetry

DSC heating curves were obtained for hydrated bilayers of each of the synthesized lipids **3-11** and **3-12** (Figure 3-2). The main phase transition temperature T_m, peak width at half-height $T_{1/2}$, calorimetric enthalpy ΔH, and cooperative unit (CU) are reported in Table 3-1. The T_m values range from less than 5 to 32 °C depending on chain length. Figure 3-2 shows that bilayers of Acryl/DenPC$_{16,18}$ **3-11c**, Sorb/DenPC$_{16,17}$ **3-12a**, or Sorb/DenPC$_{16,19}$ **3-12b** each exhibited a single sharp main transition. Acryl/DenPC$_{16,16}$ **3-11b** exhibited a broad main transition endotherm, which could be either a function of the lipid-phase behavior or due to the presence of isomer impurities. A phase transition was not observed between 6 and 60 °C for Acryl/DenPC$_{16,14}$ **3-11a**, Sorb/DenPC$_{18,21}$ **3-12c**, did not have a phase transition above 5 °C, presumably because of the *cis* double bond at the center of the *sn*-1 chain, which substantially lowers T_m values.

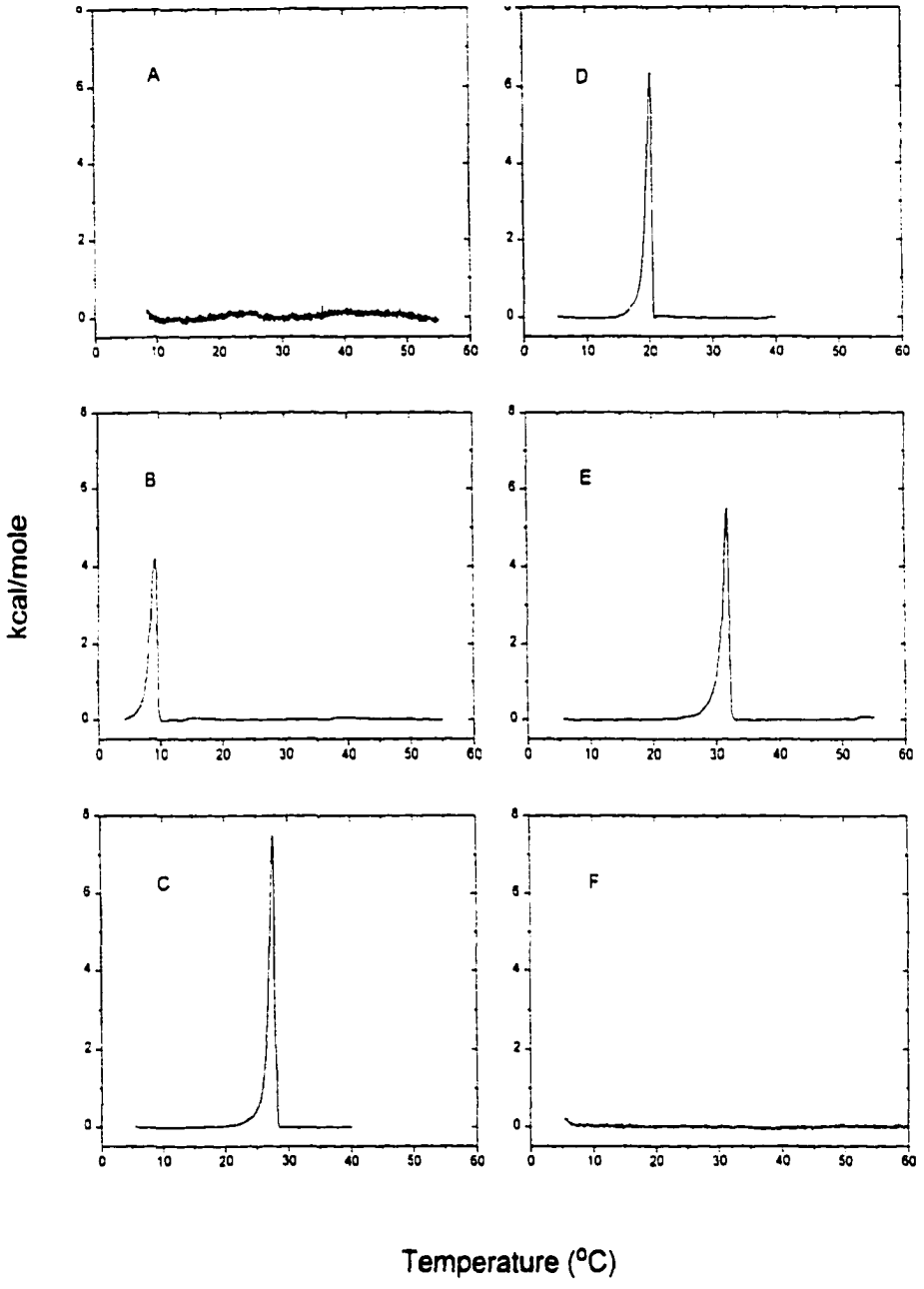

Figure 3-2. DSC heating thermograms of aqueous dispersions of Acryl/DenPCs **3-11** and Sorb/DenPCs **3-12**: (A) Acryl/DenPC$_{16.14}$; (B) Acryl/DenPC$_{16.16}$; (C) Acryl/DenPC$_{16.18}$; (D) Sorb/DenPC$_{16.17}$; (E) Sorb/DenPC$_{16.19}$; (F) Sorb/DenPC$_{18.21}$.

Table 3-1. Thermodynamic characteristics of the heating endotherms of hydrated bilayers of the Acryl/DenPC **3-11** and Sorb/DenPC **3-12**.

Lipid	T_m (°C)	$T_{1/2}$	ΔH (kcal/mol)	CU
Acryl/DenPC$_{16.16}$ (**3-11b**)	9.23	1.57	6.83 ± 0.15	53 ± 3
Acryl/DenPC$_{16.18}$ (**3-11c**)	27.7	0.99	9.86 ± 0.22	46 ± 2
Sorb/DenPC$_{16.17}$ (**3-12a**)	20.3	1.04	8.14 ± 0.13	47 ± 5
Sorb/DenPC$_{16.19}$ (**3-12b**)	31.9	1.08	8.48 ± 0.11	47 ± 3
Sorb/DenPC$_{18.21}$ (**3-12c**)	None (>5°C)			
monoAcrylPC*$_{16.16}$ (**2-14**)	31.8	-	8.90 ± 0.42	71 ± 10
monoSorbPC*$_{16.17}$ (**2-16**)	36.1	0.24	10.5 ± 0.3	202 ± 22
monoDenPC**$_{16.18}$ (**2-11**)	26.2	1.36	7.02 ± 0.29	71 ± 3

*All data are from ref.[122]

**LUV sample.

The main phase transition temperatures of Acryl/DenPCs **3-11** and Sorb/DenPCs **3-12** are plotted as a function of acyl chain length on *sn*-2 (*sn*-1 is 16 atoms long) in Figure 3-3. These data indicate that the T_m for Sorb/DenPC$_{16.15}$ will be near 10 °C. Similarly the T_m value for Acryl/DenPC$_{16.14}$ **3-11a** is far below zero. A comparison of T_m values for Acryl/DenPC and Sorb/DenPC and the corresponding saturated chain acylPCs of the same chain length[94] reveals a notable depression in T_m for all of these heterobifunctional lipids. The T_m values of monosubstituted PCs are also shown in Table

3-1.[98] Comparison of the T_m values for the monosubstituted PCs to those of the heterobifunctional lipids shows that the incorporation of the first acryloyl or sorbyl group into the terminus of the *sn*-2 chain decreases the T_m by ca. 10 °C. The incorporation of a dienoyl group at the top of an acyl chain causes a large decrease (23 °C) in the T_m. Thus, the effect of the unsaturated group is mainly dependent on its position. When it is near the headgroup, it disturbs the well-ordered packing of the lipid bilayer and decreases the phase transition. On the other hand, when it is on the relatively disordered chain termini, its effect on the chain packing is attenuated.

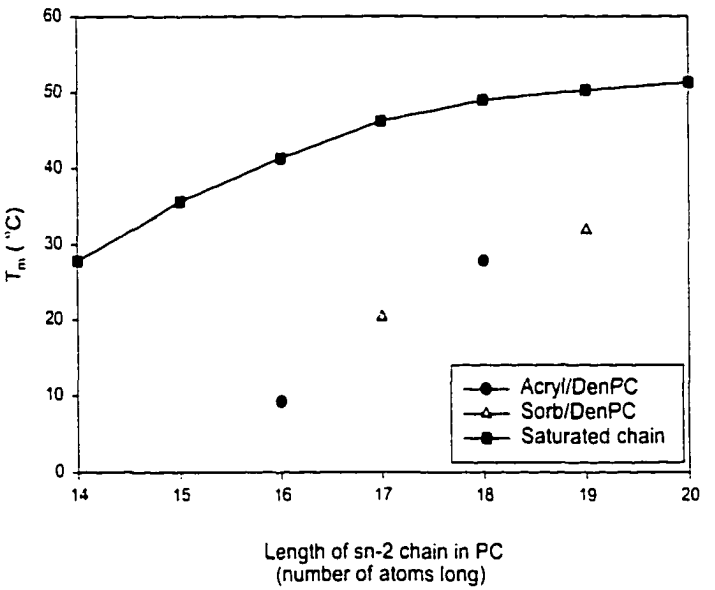

Figure 3-3. Chain-length dependence of the main phase transition temperature T_m of Acryl/DenPC **3-11** and Sorb/DenPCs **3-12**.

3.4.3 Polymerization of Bilayer Vesicles

Each of the lipids was hydrated and then extruded to give large unilamellar bilayer vesicles (LUV) with an average diameter of ca. 100 ± 10 nm as determined by quasielastic light scattering (QELS). The polymerization was performed under positive Ar(g) pressure under different initiation conditions described in the Experimental Section. During each polymerization, the average LUV size did not change, indicating that only intravesicle polymerization took place. The percent conversion of the monomer was determined by absorption spectroscopy, monitoring the decrease in monomer absorbance at various time intervals for both the dienoyl and sorbyl functionalities.

3.4.3.1 Simultaneous polymerization

Simultaneous polymerization of both reactive groups was achieved by either redox or direct UV photoirradiation. The term "simultaneous" means reactions of dienoyl and acryloyl/sorbyl groups in the bilayer were concurrent and happened with the same initiator. It does not necessarily imply that the two reactive groups were propagating at the same time.

(a) Redox Polymerization

The redox polymerizations were performed at 60 °C with a 1:1 mole ratio of $KBrO_3$/L-cysteine and a 1:1 mole ratio of monomer to oxidant. The nature of the resulting polymers, linear or cross-linked, could then be investigated by vesicle dissolution with TX-100 or by measuring the solubility of the isolated polymer in organic solvents.[164] Under the above conditions, both functional groups are expected to react,

since the redox system generates hydroxyl radicals, which can diffuse across the lipid bilayer and initiate the polymerization of reactive groups regardless of their location in the bilayer.[75] In Sorb/DenPC **3-12**, it was not possible to distinguish them by their UV/vis absorption since both the dienoyl and sorbyl group showed the same absorbance at 260 nm. However, the lack of an isosbestic point (Figure 3-4a) indicates that both functional groups were polymerized at the same time since the existence of an isosbestic point indicates the formation of a single product (as shown below in Figure 3-8 for UV polymerization of Acryl/DenPC **3-11c** with a filter). The reaction was fast and reached 99% conversion within 2 h (Figure 3-4b).

When $K_2S_2O_8$/L-cysteine was used as the initiator, the reaction was much slower (Figure 3-4b). The conversion only reached 42% within 2 h. After 13 h, only 80% of the monomers were consumed, and it was not possible to reach complete conversion.

a)

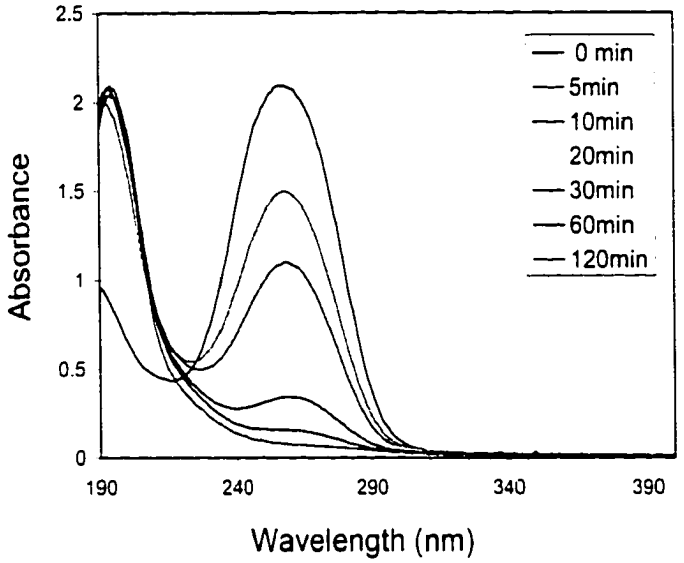

b)

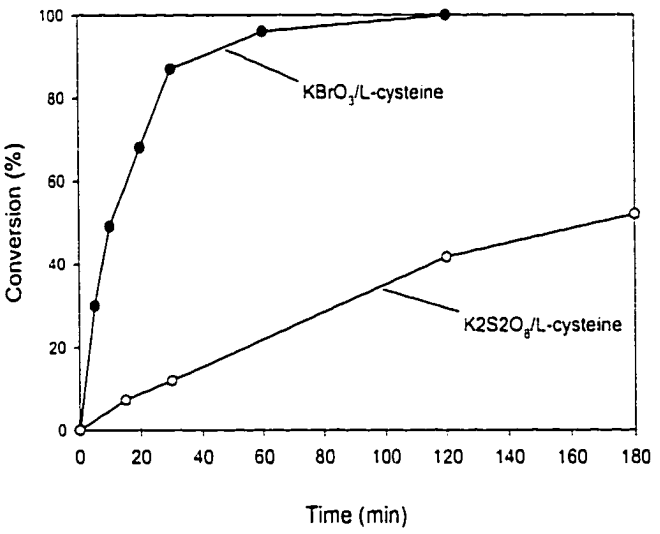

Figure 3-4. (a) Absorption spectra of Sorb/DenPC$_{18,21}$ **3-12c** LUV during redox polymerization. (b) Percent conversion of Sorb/DenPC$_{18,21}$ **3-12c** as a function of time for redox polymerization with [O]/[R] = 1/1, [M]/[O] = 1:1. [M] = 2 mM, 60 °C.

In Acryl/DenPC **3-11**, the percent conversion of the dienoyl group was greater than 95% as determined by UV/vis spectroscopy (Figure 3-5). However, the extent of conversion for the acryloyl group could not be determined due to overlap with the absorption of the isolated double bond of the poly(dienoyl). It is reasonable to assume that the conversion was at least 95%, since acryloyl is a more reactive group than dienoyl, and under similar conditions the extent of polymerization of mono-AcrylPC LUV was >95%.

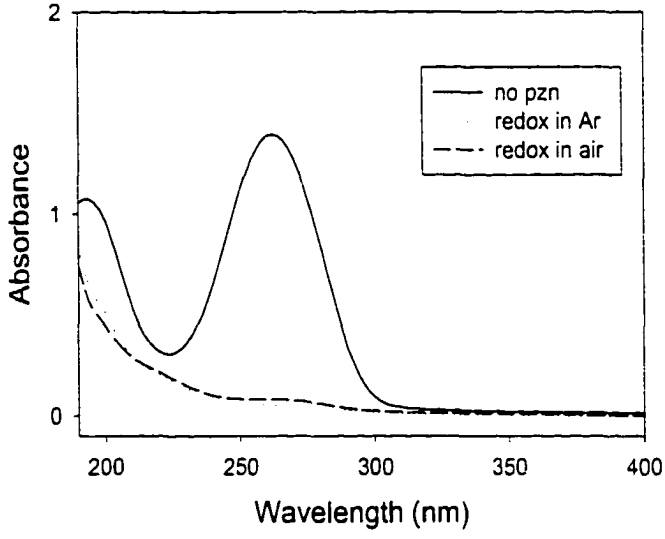

Figure 3-5. The absorbance spectra of Acryl/DenPC$_{16.18}$ **3-11c** LUV before and after redox polymerization with $KBrO_3$/L-cysteine (1/1), [M]/[O] = 1:1. [M] = 2 mM, 60 °C.

(b) UV Polymerization

LUV of Acryl/DenPC **3-11** were irradiated at 40 °C with a low-pressure Hg vapor lamp, and more than 90% conversion of the dienoyl group was achieved within the first 10 min (Figure 3-6). Further irradiation caused the decrease of the peak at 195 nm, which indicates the polymerization of the acryloyl groups. In this experiment the intensity of the light from the lamp was ca. 10 times greater at 260 nm than at 195 nm; therefore, under these conditions the dienoyl group polymerized faster than the acryloyl group.

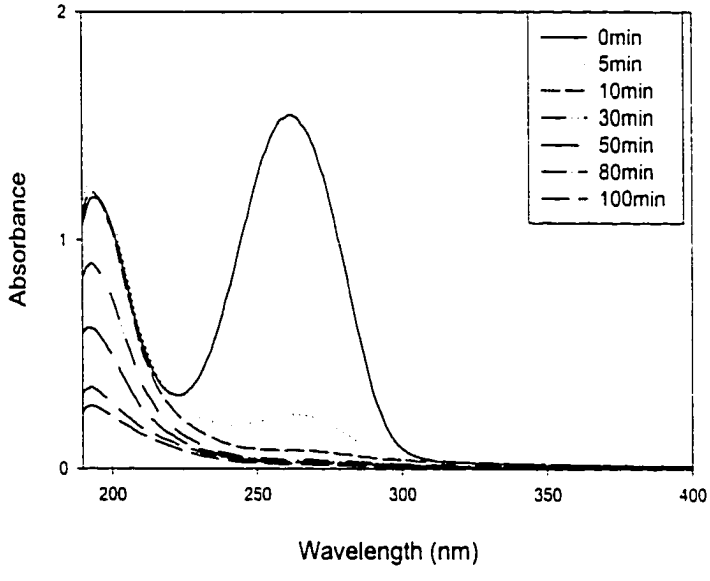

Figure 3-6. Absorption spectra of Acryl/ $DenPC_{16.16}$ **3-11b** LUV during UV polymerization at different times. [M] = 600 μM, 40 °C.

Simultaneous polymerization of Sorb/DenPC can be achieved either with or without a filter as shown in Figure 3-7a. High conversion (>95%) was reached at short times. UV irradiation of the sample without a cutoff filter eventually caused the disappearance of the peak at 195 nm, which suggests the occurrence of a second slower reaction of the nonconjugated double bond. The UV polymerization of Sorb/DenPC$_{18,21}$ **3-12c** was performed under argon, in air, and in oxygen and they all showed similar polymerization rates (Figure 3-7b).

(a)

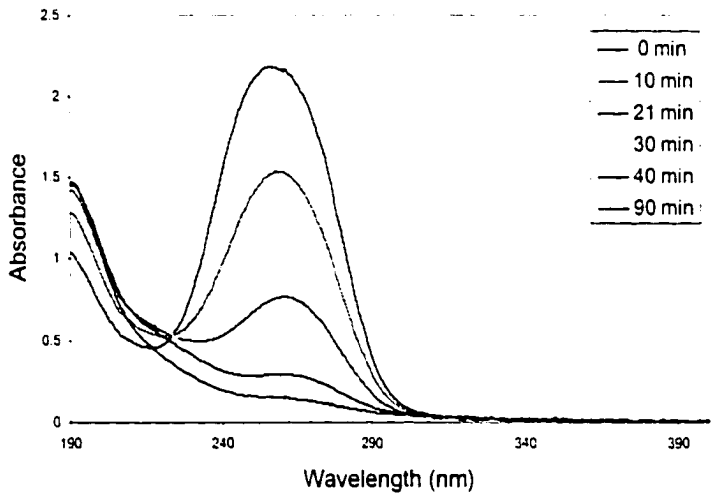

Figure 3-7. (a) Absorption spectra of Sorb/DenPC$_{18,21}$ **3-12c** LUV during UV polymerization (Ar) with a cutoff filter at different times.

(b)

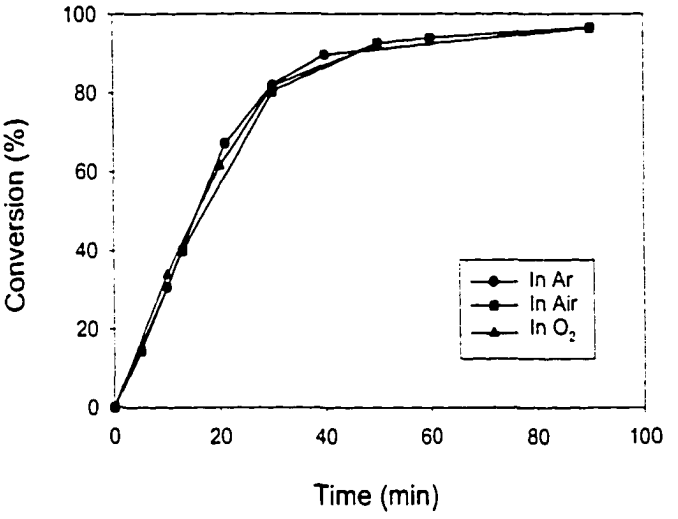

Figure 3-7. (b) Percent conversion of Sorb/Den $PC_{18,21}$ **3-12c** as a function of time for UV polymerization under argon, air, and O_2 with a CS9-54 filter (cutoff wavelength shorter than 230 nm). [M] = 2 mM, 40 °C.

3.4.3.2 Selective Polymerization

(a) Selective Polymerization by Filtered UV Irradiation

The dienoyl group of Acryl/DenPC **3-11** was selectively polymerized using filtered light from a low-pressure Hg vapor lamp. A CS9-54 filter, which has a cutoff wavelength shorter than 230 nm, was placed between the sample and the light source. As shown in Figure 3-8, the dienoyl absorption peak at 260 nm decreased, but the acryloyl absorption at 195 nm did not. A clean isosbestic point was observed and retained until almost the end of the polymerization. After 90 min, 98% conversion of dienoyl group was achieved, but a slight increase in the acryloyl peak at 195 nm was seen. This result indicates that dienoyl groups can be polymerized in the presence of acryloyl groups

because the cutoff filter prevented absorption of shorter wavelength light necessary for the photopolymerization of the acryloyl groups.

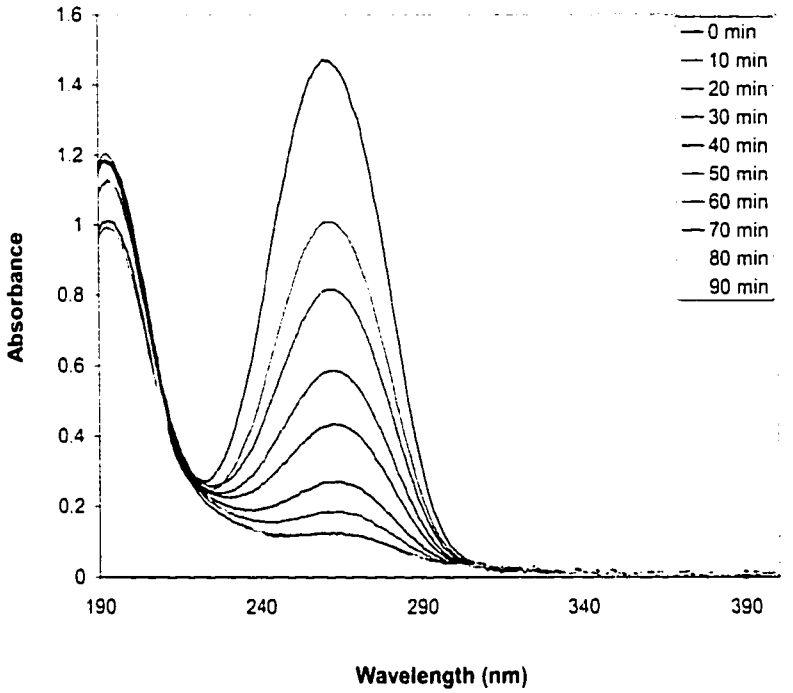

Figure 3-8. Absorption spectra of Acryl/DenPC$_{16.18}$ **3-11c** LUV at different photo-polymerization times. [M] = 4 mM, 40 °C.

(b) Selective Polymerization with AIBN or AAPD

Selective polymerization of one of the polymerizable groups was tried with either water-insoluble AIBN or water-soluble AAPD as the initiator. It was expected that the

dienoyl group which is located near the hydrophilic backbone could be polymerized by AAPD, while the acryloyl/sorbyl group which are located at the center of the hydrophobic region should be polymerized by AIBN.[135,136,157] AIBN or AAPD was introduced into the system in two different ways: (1) added to the lipid before freeze-thaw in order to incorporate the initiator into the appropriate region of the bilayer: (2) added to the vesicle suspension and incubated at 40 °C for 1 h to place the initiator into the inner phase of the vesicles, so there were initiators both inside and outside of the bilayer leaflet. The polymerization was carried out at 60 °C with a [M]/[I] equal to 5-20. The polymerization lasted for 3-5 days. For Acryl/DenPC$_{16,18}$ **3-11c** lipid, the peaks at 260 and 195 nm all decreased regardless whether the initiator used was AAPD or AIBN (Figure 3-9). The results indicated that both acyloyl and dienoyl groups were polymerized nonselectively. For Sorb/DenPC$_{18,21}$ **3-12c**, the conversion calculated from absorbance at 260 nm is much higher than 50% with either initiator (Figure 3-10).

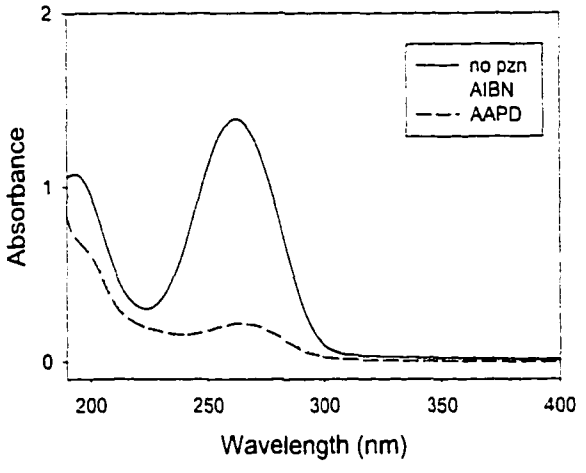

Figure 3-9. The absorbance spectra of Acryl/DenPC $_{16,18}$ **3-11c** LUV before and after thermal radical polymerization. [M]/[I] = 10:1. [M] = 2 mM, 60 °C/2 days.

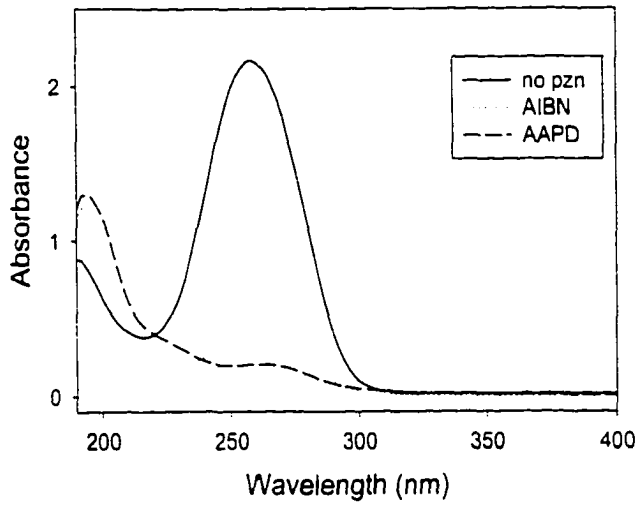

Figure 3-10. The absorbance spectra of Sorb/DenPC$_{18,21}$ **3-12c** LUV before and after thermal radical polymerization. [M]/[I] = 5:1. [M] = 1 mM, 60 °C/4 days.

To test the possibility that AAPD can initiate the reaction of the polymerizable groups located at the center of the hydrophobic region, mono- and bis-SorbPC (**2-16** and **2-17**) were used as model compounds. AAPD was added at varied concentrations between 2-40% of the monomer lipid and polymerizations were carried out at 60 °C, above the phase transition of both lipids (monoSorbPC$_{16,17}$, **2-16** T_m = 34.1 °C, bisSorbPC$_{17,17}$, **2-17** T_m = 28.8 °C). The results showed that 5% of AAPD is enough to achieve 80% conversion of bisSorbPC **2-17**. For monoSorbPC **2-16**, the number is slightly higher (<10% AAPD is needed; Figure 3-11).

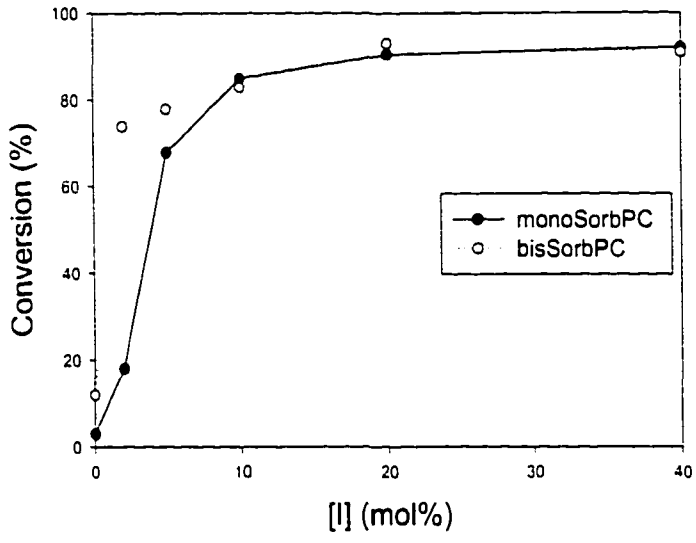

Figure 3-11. Effect of AAPD concentration on the polymerization conversion of mono-SorbPC$_{16,17}$ **3-16** and bis-SorbPC$_{17,17}$ **3-17**. [M] = 1 mM, 60 °C/3 days.

Selective polymerization of one group in heterobifunctional lipids was observed in the double-diene PC **3-10**.[156,157] In lipid **3-10**, the diene groups were selectively polymerized by AIBN, and the dienoyl groups were polymerized with filtered UV irradiation. The diene groups are located at the ends of the *sn*-2 chains in the hydrophobic region of the bilayer, a suitable environment for a polymerization with a hydrophobic initiator. In contrast, the dienoyl groups which near the lipid water interface, could not be polymerized by a hydrophobic initiator. This provides support for the hypothesis that the position of the polymerizable group governs the type of initiation that can be usefully employed.

Tsuchida and co-workers have worked on the selective polymerization of bisDenPC **2-12**.[127,135,138] They found that polymerizations by the addition of radical initiator AIBN or AAPD gave only 50-60% conversion at 60 °C. Complete polymerizations were achieved by the use of AIBN and AAPD simultaneously.[135] Further experiments with monoDenPC **2-11**, where the polymerizable group is located only on the *sn*-2 chain, found that monoDenPC **2-11** can be easily polymerized by AAPD, but not very effectively by AIBN.[136] The acyl chain packing of choline-type lipids in the bilayer membrane has already been discussed by Seelig et al. and it is well known that the two acyl chains do not extend equally into the lipid bilayer.[147,148,165,166] Thus they concluded that the two dienoyl groups in bisDenPC lipid were in a different chemical environment. The dienoyl group on *sn*-2 chain was closer to the hydrophilic region and, therefore, easily polymerized by a water-soluble radical initiator. On the other hand, the dienoyl group on the *sn*-1 chain was located in a more hydrophobic region and could only be initiated by a hydrophobic initiator. Polymerization of **2-12** was also performed with photosensitized AAPD added to the outer aqueous phase of the vesicles at different temperatures.[138] The conversion reached 50% above the T_m, but remained 27% below the T_m. These results indicate that AAPD molecules can penetrate through the lipid bilayer membrane at temperatures above the phase transition temperature. Nonselective polymerization of **2-12** was also observed by AAPD polymerization with SUVs.[127] The explanation for the nonselectivity is ascribed

to the disordered lipid packing, which permits invasion of water molecules deeper into the hydrophobic region of the lipid membrane.

The design of the heterobifunctional lipids, Acryl/DenPC **3-11** and Sorb/DenPC **3-12**, places an ester group at the end of a lipid tail. This ester group may disturb the tight packing of the lipid chain. This was examined by the surface pressure/area isotherms of the Sorb/DenPC$_{18,21}$ **3-12c** and Sorb/DenPC$_{16,19}$ **3-12b** compared with bisDenPC$_{18,18}$ **2-12** (Figure 3-12). The surface pressure/area diagrams of Sorb/DenPC$_{18,21}$ **3-12c** and bisSorbPC$_{17,17}$ **2-17** exhibited only an expanded phase, indicated the fluid phase behavior of the lipid at room temperature. The slopes of the isotherms for bisDenPC$_{18,18}$ **2-12** and Sorb/DenPC$_{16,19}$ **3-12b** were steeper, indicating their monolayers were less compressible. The surface pressure/area isotherms of bisDenPC$_{18,18}$ **2-12** and Sorb/DenPC$_{16,19}$ **3-12b** exhibit higher packing densities and collapse pressures than those of Sorb/DenPC$_{18,21}$ **3-12c** and bisSorbPC$_{17,17}$ **2-17**, indicating a higher film stability of these membranes. Obviously, in Sorb/DenPC$_{18,21}$ **3-12c**, the presence of a *cis* double bond at the *sn*-1 chain disturbs the packing. A major pertubation was also observed when two ester groups were located at the end of the lipid tail (bisSorbPC). The presence of one saturated chain (Sorb/DenPC$_{16,19}$ **3-12b**) helps the lipid pack into the more condensed phase. Loose packing of the lipid bilayer chains could favor penetration of initiator molecules into the membrane.

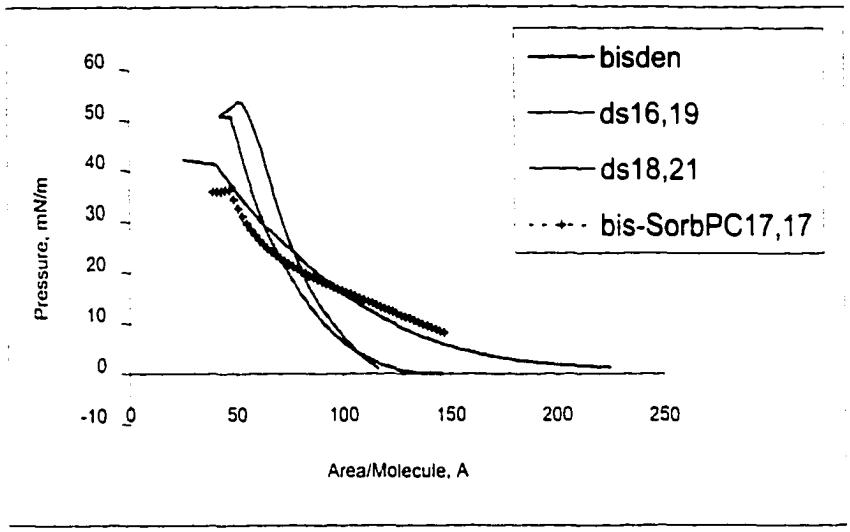

Figure 3-12. Surface pressure/area isotherms of Sorb/DenPC$_{16,19}$ **3-12b**, Sorb/DenPC$_{18,21}$ **3-12c**, bisDenPC$_{18,18}$ **2-12**, and bisSorbPC$_{17,17}$ **2-17** at 20 °C. (Data from Eric Ross in Dr Saavedra group)

Another reason for the nonselectivity of polymerization may be that the more hydrophilic ester group located at the hydrophobic region of the lipid reduces the efficiency of the initiator. AIBN is a hydrophobic initiator, which should be dissolved in the hydrophobic region of the bilayer.

Also, the nonselective polymerization could come from interdigited chain packing of the bilayer or the folding back of the *sn*-2 chain in the bilayer towards the headgroup. The real nature of the lipid bilayer packing needs to be clarified in the future.

(c) Selective Polymerization with Redox Initiator

The selective polymerization was also attempted with redox initiators in air. It is proposed that the dienoyl group can be polymerized in the presence of oxygen since it forms a copolymer with oxygen.[167] On the other hand, oxygen is an inhibitor for acryl radical polymerization. If this assumption is correct, we can use a redox initiator to polymerize the dienoyl group first in the presence of air and then, exclude oxygen to polymerize the acryloyl group. The experiment was performed with Acryl/DenPC hydrated in nondeoxygenated MilliQ water and polymerization in air. The results showed that the acryloyl group also polymerized and there is no difference between polymerizations conducted under argon or in air (Figure 3-5).

3.4.4 Molecular Weights of UV-Polymerized Lipids

Photoirradiation of dienoyl and sorbyl groups in lipid bilayers has previously been reported to yield oligomers (X_n of 3-10).[70,75] The direct UV polymerization of heterobifunctional double diene PC gave oligomers with X_n about 10.[157]

MALDI-TOF mass spectrometry was used to determine the molecular weight of the UV (with filter) polymers. The MALDI-TOF spectra showed only oligomers ($n \leq 5$) for samples polymerized in Ar, in air, or in O_2 (Figure 3-13). For Acryl/DenPC$_{16,18}$ **3-11c** peaks at 772.2 (monomer), 1545.4 (dimer), 2318.3 (trimer), 3091.3 (tetramer), and 3864.5 (pentamer) amu were found. For Sorb/DenPC$_{18,21}$ **3-12c** peaks at 838.3 (monomer), 1678.2 (dimer), 2517.8 (trimer), 3357.6 (tetramer), and 4193.2 (pentamer) amu were found. These results indicate that the polymerization is insensitive to oxygen.

They suggest that the excited state is a singlet and the photoreaction proceeds by photoactivated addition of the monomer..

a) Acryl/DenPC$_{16.18}$ **3-11c** b) Sorb/DenPC$_{18.21}$ **3-12c**

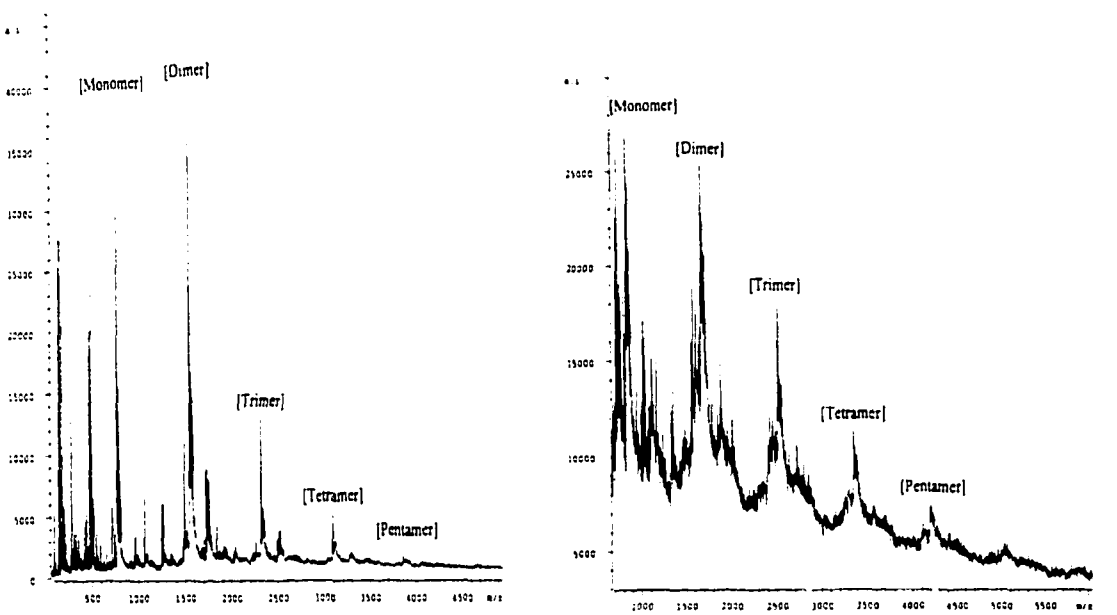

Figure 3-13. MALDI-TOF spectra for UV polymerized Acryl/DenPC$_{16.18}$ **3-11c** and Sorb/DenPC$_{18.21}$ **3-12c** with 2,5-dihydroxylbenzoic acid (DHB) as a matrix on addition of sodium salt.

3.4.5 Stabilities of the Vesicles toward Surfactant

Figure 3-14 shows the average diameter of Sorb/DenPC **3-12** LUV in comparison to the molar ratio of the surfactant TX-100 to lipid as measured by QELS. After addition of 2-6 equiv. of TX-100 per lipid to the UV polymerized Sorb/DenPC LUV, a sharp

decrease in the average mean diameter of the suspended vesicles was observed. On the other hand, the vesicles polymerized by a redox initiator were essentially unchanged in size by the addition of up to 12 equiv. of TX-100. Polymerized vesicles of Acryl/DenPC **3-11** showed similar trends (Figure 3-14).

a)

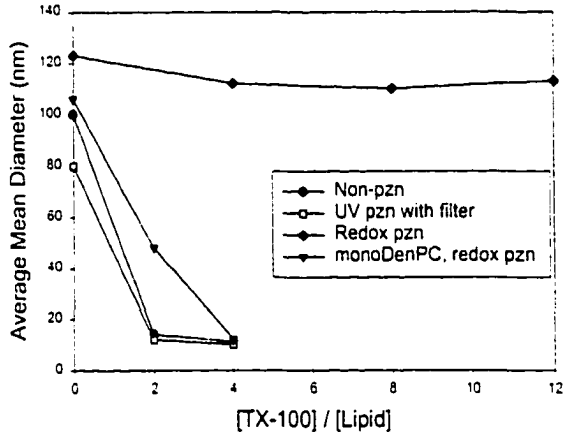

b)

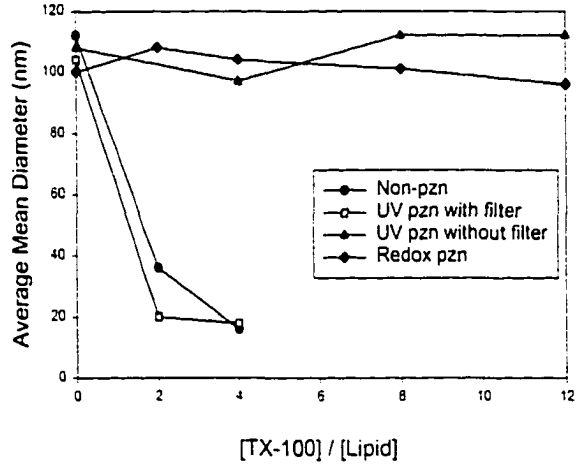

c)

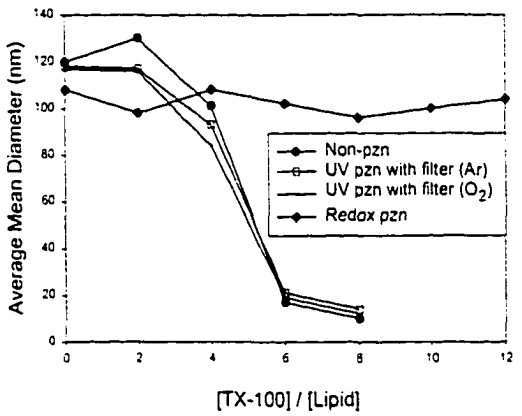

Figure 3-14. Average mean diameter of LUV composed of unpolymerized or polymerized Sorb/DenPC **3-12** or mono-DenPC$_{16.18}$ **2-11** as a function of added equivalents of Triton X-100: (a) Sorb/DenPC$_{16.17}$ **3-12a**; (b) Sorb/DenPC$_{16.19}$ **3-12b**; (c) Sorb/DenPC$_{18.21}$ **3-12c**.

a)

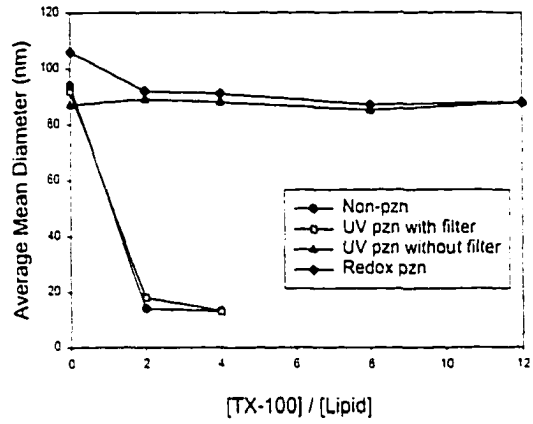

b)

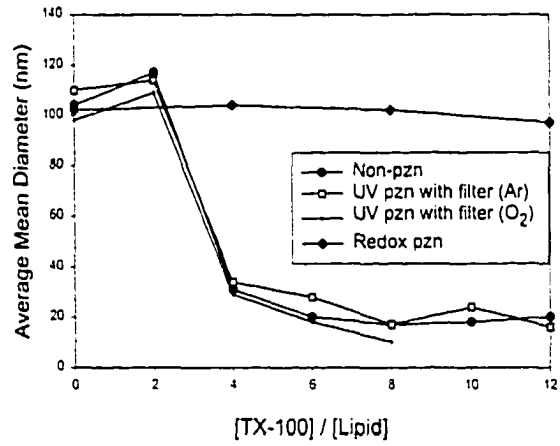

Figure 3-15. Average mean diameter of LUV composed of unpolymerized or polymerized Acryl/DenPC **3-11** as a function of added equivalents of Triton X-100: (a) Acryl/DenPC$_{16.16}$ **3-11b**; (b) Acryl/DenPC$_{16.18}$ **3-11c**.

Previous studies demonstrated that cross-linked lipid vesicles were stable in the presence of excess surfactant, whereas unpolymerized or linearly polymerized vesicles were dissolved by surfactant.[76,81] Further studies also showed that the surfactant

solubilization was dependent on the degree of polymerization, extent of cross-linking, and location of the reactive groups in the lipid. Vesicles composed of oligomers were efficiently dissolved with TX-100, while vesicles composed of longer linear polymeric lipids were less readily solubilized. In this study, UV polymerization of vesicles prepared from **3-11** or **3-12** did not stabilize the vesicles to TX-100, indicating the formation of oligomeric lipids. On the other hand, the stabilization of LUV toward addition of TX-100 after redox polymerization may indicate cross-linking or a higher degree of polymerization. To exclude the possibility that the effect was caused by a high degree of polymerization, the same redox condition was performed with monoDenPC$_{16,18}$ **2-11** vesicles, which generates linear polymers. As shown in Figure 3-14, the polymerized monoDenPC **2-11** LUV were not stable in the presence of TX-100. This demonstrates that the polymers obtained by redox initiation of heterobifunctional amphiphiles cannot be linear polymers.

3.4.6 Solubilities of Polymerized Lipids

Another effective way to distinguish a cross-linked polymer from a non-cross-linked one is to measure the polymer solubility. The polymerized lipids were recovered from the hydrated bilayer by freeze-drying, and then the polymeric solid was dispersed in different organic solvents. UV-polymerized Acryl/DenPC **3-11** and Sorb/DenPC **3-12**, as well as redox polymerized monoDenPC **2-11**, were soluble in various organic solvents, e.g. chloroform and benzene, whereas redox-polymerized Sorb/DenPC **3-12** and Acryl/DenPC **3-11** were insoluble in most organic solvents. The weight percent

solubility of redox polymerized lipids in HFIP was determined. Previous studies showed that HFIP was an excellent solvent for polymerized zwitterionic PC lipids.[128,131] In this study, the weight percent solubility of poly(Sorb/DenPC) and poly(Acryl/DenPC) in HFIP was no more than 30-40%. The weight percent solubilities for bisDenPC$_{18,18}$ **2-12** and bisSorbPC$_{17,17}$ **2-17**, as well as monoDenPC$_{16,18}$ **2-11** were also measured for comparison. The bis-substituted PCs form cross-linked polymers whereas mono-substituted PCs form linear polymers.[81] The solubilities of the two bis-substituted PCs **2-12** and **2-17** are 40 and 30%, respectively, whereas it was 86% for mono-DenPC **2-11** (Table 3-2). These data indicate that the majority of the polymers formed from Sorb/DenPC **3-12** and Acryl/DenPC **3-11** were cross-linked.

Table 3-2. Weight percent solubilities of polymerized lipids in HFIP

Sample	Weight % Solubility
monoDenPC$_{16,18}$ **2-11**	86
Sorb/DenPC$_{16,17}$ **3-12a**	35
Sorb/DenPC$_{16,19}$ **3-12b**	34
Sorb/DenPC$_{18,21}$ **3-12c**	40
Acryl/DenPC$_{16,16}$ **3-11b**	40
Acryl/DenPC$_{16,18}$ **3-11c**	38
bisDenPC$_{18,18}$ **2-12**	40
bisSorbPC$_{17,17}$ **2-17**	30

3.5 Conclusions

This chapter described the synthesis, characterization, and polymerization in lipid vesicles of two series of heterobifunctional phosphatidylcholine (PC) lipids with different separation distances between the two reactive groups. One of the groups, i.e., dienoyl (Den), is attached to the secondary oxygen of the glycerol backbone of the lipid, and the other is either an acryloyl (Acryl) or sorbyl (Sorb) functional group located at the *sn*-2 chain terminus. Polymerization of both reactive groups in Acryl/DenPC **3-11** or Sorb/DenPC **3-12** was achieved by either redox polymerization or direct photoirradiation. The degree of polymerization depended on the initiation chemistry. Photoirradiation

yielded oligomers that were insufficient to cross-link the vesicles, whereas redox-initiated radical polymerization afforded cross-linked polymeric vesicles.

Redox-initiated polymerization of bilayers of each of the compounds studied here resulted in the formation of cross-linked polymeric bilayers, regardless of whether the spacer length was 7, 9, or 11 atoms. Similar results were observed when the reactive groups had similar reactivities (Sorb/DenPC) or varied in reactivity (Acryl/DenPC). These data indicate that lipids of this general design can be employed to cross-link lipid assemblies of various types, including lamellar and perhaps nonlamellar phases[9,168] as well as bilayers on solid supports. The failure of photopolymerization of bilayers of the same monomeric lipids to yield cross-linked polymeric assemblies appears to be due to the formation of oligomers of insufficient length to create a polymeric network. The differences between the two modes of polymerization offer opportunities to control the materials properties of polymerized lipid assemblies.

Previously we reported that the redox-initiated polymerization of hydrated bilayers of 1-palmitoyl-2-(2,4,12,14-tetraenehexadecanoyl)phosphatidylcholine (**3-10**), where the two diene groups are separated by six methylene groups, did not yield cross-linked polymers.[156,157] These data suggested that a lipid monomer with a short spacer would prefer to react with the same neighboring lipid in a linear, ladder-like fashion. The contrasting behavior of bilayers of the lipid **3-10** and bilayers of Sorb/DenPC$_{16,17}$ **3-12a**, with a seven-atom spacer, is interesting. The current results suggest that at least one factor other than spacer length is crucial to the polymerization course. It is quite possible that this distinctive behavior, which warrants further examination, may be due to the

greater flexibility of a short spacer when the segment contains a oxygen as well as six methylenes (**3-12a**) vs six methylenes (**3-10**).

Selective polymerization of only one group in the heterobifunctional lipids **3-11** and **3-12** was examined with filtered UV polymerization, thermal radical initiation (AIBN or AAPD) and redox initiation in air. Filtered UV irradiation selectively polymerized acryloyl groups in Acryl/DenPC **3-11**. It was expected that the two reactive groups in these heterobifunctional lipids could be selectively polymerized since they were located in regions of different polarity in the bilayer assembly. However, polymerization with AIBN or AAPD showed no selectivity, as both groups were polymerized by either AIBN or AAPD. The nonselective polymerization with lipids **3-11** and **3-12** may relate to the structures of these lipids in the following way. The ester group, which is hydrophilic, is located at the end of the lipid tail, in a hydrophobic region. This inhibits the incorporation of hydrophobic initiator (e.g. AIBN) into this area. Moreover, the ester group at the center of the lipid bilayer may disturb the tight packing of the lipid chain and cause the easy penetration of hydrophilic initiator molecules (e.g. AAPD) through the membrane. This hypothesis can be proved by designing a heterobifunctional lipid with a more hydrophobic reactive group at the end of the tail, e.g. a vinyl or diene group, with a longer separation space between two reactive groups. It is our goal to be able to selectively polymerize one group to yield a prepolymerized assembly which is not cross-linked but could have valuable properties. Then, a second cross-linking reaction is introduced to further stabilize the assembly structures.

CHAPTER 4

LYOPHILIZATION AND REHYDRATION OF CROSS-LINKED LIPOSOMES

4.1 Introduction

4.1.1 Liposomes as Controlled Delivery System

Amphiphilic molecules such as phospholipids spontaneously form vesicular structures (i.e. liposomes) when dispersed into aqueous solution. The liposome is composed of an amphiphilic bilayer that encloses an aqueous interior volume.

Since they were introduced in the late 1960s, liposomes have been attractive delivery systems for drugs, vitamins, and cosmetic materials.[28,169-171] Liposomes are small, man-made spherical structure that can be produced from natural or synthetic phospholipids and cholesterol. Liposomes are extremely adaptable, and due to the diversity of their composition, they can be utilized for a large number of applications.[29,172] They can be custom designed for almost any need by varying the lipid constituents, size, surface charge, and method of preparation.

One of the prevailing interests in liposomes is their potential application as drug carriers.[25,26,170,173,174] Materials to be used for drug delivery must be biocompatible and have appropriate physical properties to provide controlled delivery. Other requirements include being stable under biological conditions, having minimal tissue reactions after implantation, and being nontoxic. If the material is biodegradable, the degradation products have to be readily excreted. The preferred method of drug delivery,

in many instances, is injection. This requires the development of drug microcapsules or microspheres. Liposomes as drug carriers fulfill many of those criteria. Liposomes are composed of natural body constituents and thus are biodegradable, and almost without intrinsic toxicity. One outstanding advantage of liposomes over other systems is that liposomes enable water-soluble and water-insoluble materials to be employed together in a formulation. Hydrophilic molecules can be encapsulated into the liposome internal aqueous volume whereas lipophilic ones can be incorporated in the lipid bilayer phase. These liposomes hold the normally immiscible materials together in a microsphere with controllable release of the encapsulated ingredients. As drug carriers, liposomes can be loaded with a great variety of molecules, such as proteins, nucleotides, small drug molecules, and plasmids. Current applications involve the specific targeting and delivery of informational molecules such as anti-sense oligonucleotides, DNA plasmids (i.e. genes), topical deliverors, vaccinators, and diagnosties. Other applications include the delivery of lipid-based carriers or anti-fungal agents by conventional liposomes, and systemic anti-cancer therapy using long-circulating sterically-stabilized liposomes.[27,29,171]

The studies on controlled release of drugs fall into two categories: long-term release[175] and triggered release.[176-179]

In long-term release, drug delivery systems aim to deliver the drug over an extended duration or at a specific time point. The drug release is typically diffusion regulated, which is also termed passive release. The drug is released by partitioning into the lipid bilayer and then diffusing through the membrane (Figure 4-1). As drug release is

dependent on partition and diffusion, drug release kinetics is predictable and determined by the physical properties of the bilayer membranes as well as the drug's size and lipophilicity. If polymers are formed within the bilayer membrane, the polymer chains such as those in a cross-linked network change the diffusion barrier presented by the lipid bilayer. In passive release, drug molecule diffusion within an aqueous solution is inhibited by the insoluble polymeric membrane, in which drug molecules must travel through tortuous pathways to exit the membrane. Thus, the rate of the release can be controlled by changing the size of the void, i.e., the cross-linking density.

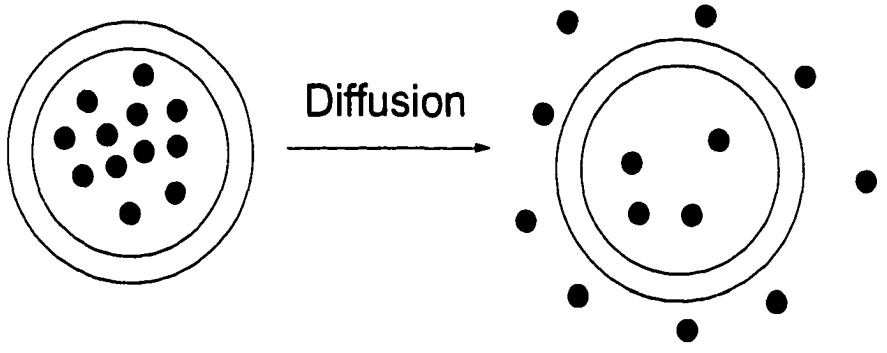

Figure 4-1. Mechanism of passive release.

Controlled release over an extended duration is highly beneficial for drugs that are rapidly metabolized and eliminated from the body after administration. With the controlled release system, the rate of drug release matches the rate of drug elimination and, therefore, the drug concentration is within the therapeutic window for the vast

majority of the period. Long-term release can be used in cases such as pain release, vaccines, birth-control, hormones, and immuno-suppressants.[180,181]

Triggered release drug delivery systems aim to release the drug in the vicinity of the target cells. Liposomes used for triggered release must have very low permeability to the encapsulated compounds, so that most of the contents remain encapsulated during several hours of circulation in the blood stream. This allows the delivery of the therapeutic agent to the desired site of action and prevents non-specific delivery, which can result in toxic side effects. Once liposomes reach the site of action, a stimulus is applied to release the contents (Figure 4-2). Several stimuli can be used to trigger the release of encapsulated drugs at the desired site of action. These include changes in pH, temperature, light, and ionizing radiation. The destabilization of liposomes by cross-linking polymerization has been extensively studied in O'Brien's group.[Lamparski, 1992 #249; Bondurant, 1998 #250; Bondurant, 2001 #251; Mueller, 2000 #252; Miller, 2000 #46; O'Brien, 2001 #268] The advantage of triggered release is that the side effects can be minimized. Current triggered release systems focus on chemotherapeutic drugs.[182]

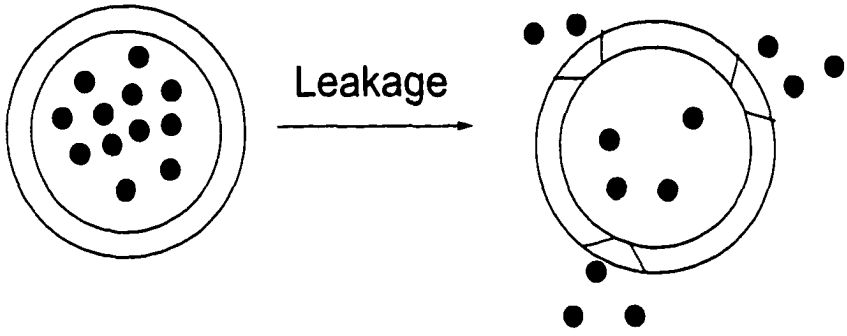

--Temperature, pH, or Light

Figure 4-2. Mechanism of leakage induced by stimulus.

4.1.2 Liposome Aggregation

Liposomes are dynamic structures which are fundamentally unstable. Colloidal particles in suspension attract each other by the ubiquitous van der Waals forces. If this attraction is not counterbalanced by any repulsive force, spontaneous aggregation of the particles occurs and the system flocculates. The strength of van der Waals attraction depends on the size and geometry of the particles and the chemical composition of the system.

One of the means to prevent the aggregation of colloidal suspensions in water is provided by the Coulomb repulsion between electrostatic charges which may be present on the particle surfaces.[183] The colloidal stability then depends critically on several parameters: ionic strength, surface potential or charge, and particle size. As a result the

method of electrostatic stabilization is restricted by the environmental conditions such as pH.

An alternative method to prevent aggregation is to use polymers.[184] The principle is simple: by attaching long flexible chains to the surface of colloidal particles, the approach of the surfaces gives rise to strong steric repulsion. There are two ways of attaching polymer chains onto a surface: by natural adsorption or by chemically grafting the chains to the surface. Sterically-stabilized liposomes (SSL) or 'PEG liposomes', with a phospholipid with poly(ethylene glycol) covalently attached to the polar headgroups, currently attract much interest.[27] In addition to their enhanced colloidal stability, a key feature of these PEG-liposomes is their greatly increased circulation time in blood compared to conventional liposomes. Studies have found that circulation time can be enhanced from hours to days by incorporating a small amount of PEG lipids into the liposomes.[185,186] The increased circulation time is believed to be due to steric stabilization of the liposomes by the grafted polymer, preventing their close approach to the membrane surface. It is also due to the immune system not recognizing the liposomes as a foreign body since it only sees the water shell. This has greatly expanded the potential of liposomes as drug carriers. The special properties of PEG: chemical inertness, biocompatibility, water solubility (hydrophilicity), insensitivity to changes in ionic conditions due to its nonionic character, and low protein adsorption have made it a particularly suitable polymer for use as a steric stabilizer in aqueous media. The length of the PEG chain and its density on the surface are both important in stabilizing the

liposomes. Studies showed that the optimal effect for a long $T_{1/2}$ is produced by a chain of approximately 2000 Da, at a density of about 5 to 8% of total phospholipid.[187-189]

4.1.3 Rehydration of Lyophilized Liposomes

In recent years, the storage of liposomes by freeze-drying has been examined both from a pharmaceutical and biological perspective. If rehydration and recovery of the liposomes after freeze-drying is possible, this increases the usefulness of liposomes as drug carriers, since freeze-drying improves the shelf life of the liposomes. Freeze-drying is a well-established technique in the pharmaceutical industry.

However, the conventional liposome structure is lost during the freeze-drying process. Liposome aggregates reorganize into large structures and cannot be redispersed as liposomes during rehydration. To protect the liposomes against the stress of drying (lyoprotection), many methods have been introduced.[190-192] One is to add sugars, which then form an amorphous, glassy matrix on the surface of the liposomes during freezing. The sugar coating on the surface of the liposomes imparts a low molecular mobility, which prevents damage by fusion processes or crystal formation after drying. In addition, the sugar coating also suppresses the possible phase transition of the lipid bilayer, which could lead to the leakage of the encapsulated compounds. Van Winden et al.[192] studied the stability of freeze-dried, lyoprotected liposomes. They studied the effect of heating freeze-dried liposomes on carboxyfluorescein (CF) retention and average liposome size after rehydration, which are dependent on the lipid composition and heating temperature. Freeze-drying and rehydration below the lipid phase transition

temperature resulted in a small increase of the average liposome size for most lipid compositions. The retention of the CF varied from 20-80% depending on the composition of the lipid. Heating the dried liposomes above their phase transition temperature resulted in pronounced leakage of CF from the liposomes after rehydration and an increase in the size of the liposomes. It was also shown that the freezing rate affected the retention of encapsulated compounds. DPPC liposomes can reach 75-90% CF retention by applying a slow freezing rate (0.5 °C/min) in the freeze-drying process.[193]

Tsuchida and coworkers studied the rehydration of linearly polymerized liposomes.[134] It was concluded that the polymerized liposomes after lyophilization were easily redispersed into water via extrusion. But the pore size of the applied filter should be larger than that of the filter for the preliminary preparation, since polymerized liposomes were stable against flow shear stress. Some of the polymerized liposomes have slightly larger radii than that of the filter pores, and therefore could not be passed through the filter. The leakage of the entrapped CF after rehydration was somewhat larger than the leakage from the original liposomes. On the other hand, sonication is usually a more effective method for dispersion. The data indicate that linearly polymerized LUV break up into SUV during sonication. There is no report on the behavior of cross-linked liposomes on freeze-drying and rehydration to date.

4.1.4 Permeability of Liposomes

Membrane permeability of liposomes can be measured with any water-soluble marker. Useful detection methods based on fluorescence, enzymes, redox, electron paramagnetic resonance, and radiochemical techniques are commonly used. A convenient method monitors the increase in fluorescence of an encapsulated self-quenching dye, e.g., 0.1 M CF or calcein, as it is diluted by escaping the liposomes. The CF fluorescence at concentrations less than 0.01 M is proportional to the CF concentration. At high concentrations self-quenching occurs. Thus, after removal of untrapped CF from liposome dispersion in a high CF concentration by gel filtration, the leakage rate of the liposomes can be determined by monitoring the increase of fluorescence.[120] [^{3}H]-Glucose is another label generally applied because it does not interact with charged lipid membrane surfaces and can be used at low ionic strength. [^{3}H]-Glucose release from liposomes was measured by Kinsky's spectrophotometric method.[194] This method is based on enzymatic oxidation of the carbohydrate with formation of NADPH, whose absorbance at 340 nm could be measured.

The introduction of polymerizable groups into lipids can cause drastic changes in membrane permeability. Entrapped substances are released to a much smaller extent from polymeric liposomes than from monomeric ones. Ringsdorf and coworkers described the permeability of polymerized liposomes.[15] They found that polymerization drastically decreased the leakage rate of liposomes from bisDenPC **2-12** lipid entrapping CF. At 20 °C, i.e., above T_m of **2-12**, unpolymerized liposomes released all trapped CF in approximately 50 h, whereas liposomes from DPPC (T_m = 41 °C) only released about 10% CF during the same time period. Polymeric liposomes of **2-12** did not appear to

release CF.[15] Further experiments showed that the polymerized liposomes also gave a much lower permeability rate in the presence of ethanol or surfactant.[124] While unpolymerized liposomes already exhibit a complete release of fluorescent dye at low concentration, polymeric **2-12** liposomes lose only 15% trapped CF on addition of 30% ethanol. Similar results were obtained on addition of the surfactant sodium dodecylsulfate (SDS) to the liposomes. 5% of SDS completely released the contents inside monomeric liposomes; however, even a large excess of SDS failed to destroy polymerized liposomes. The leakage was less than 10% after adding 2.0 mM SDS.

Regen et al. reported the permeability of [^{14}C] sucrose in methacryloyl-substituted phosphatidylcholine liposomes before and after UV polymerization. They found that polymerization decreased the leakage rate in water, NaCl solution (0.154 M), and 20% ethanol solution. After 4 h the percent of the sucrose released from polymerized liposomes decreased to about 0.5 of that of monomeric liposomes.[56]

O'Brien et al. presented the first kinetic analysis of the permeability of the bilayer membrane before and after polymerization.[80] They measured the permeability characteristics of polymeric bilayer membranes from methacryloyl and butadiene lipids. The results showed that for the methacryloyl-substituted lipids, which formed linear polymers after AIBN-initiated polymerization, the permeability of [^{3}H] glucose was about half that of the unpolymerized bilayers. When the lipid was bisDenPC$_{16,16}$, which forms cross-linked structures after polymerization, the polymeric liposomes showed a 30% decreased permeability in comparison to monomeric liposomes. Furthermore, after ca. 20% of the glucose escaped the polymerized liposomes, no further glucose was lost

even when the liposomes were treated with the surfactant TX-100 (0.1 wt.% concentration). These results indicate that cross-linked polymer networks in the membrane bilayer can significantly reduce the permeability of water-soluble uncharged species, e.g., glucose, through lipid liposomes.

Experiments performed by Stafely et al. with mono-lipoylPC **2-4** and bis-lipoylPC **2-5** also confirmed the effect of cross-linking on the membrane permeability.[121] Increasing the mole percentage of **2-5** in mixed polymerized liposomes resulted in a reduction in bilayer permeability to [^{3}H] glucose. The permeability rate of cross-linked **2-5** liposomes was decreased by a factor of ca. 50. These results demonstrated the feasibility of modulating liposome permeability by varying the percentage of cross-linkable and non-cross-linkable lipid employed.

Taken together, polymerization of bilayers decreases the bilayer permeability to encapsulated aqueous markers. The formation of linear polymers in each leaflet of the bilayer changes the permeability to 0.2-0.5 of the unpolymerized bilayers, whereas the formation of a cross-linked polymer network in the bilayer can decrease the permeability by at least 2 orders of magnitude.[80,121]

4.1.5 Purpose of Current Research

Liposomes have been considered as potential vehicles for drug delivery for a long time. The main disadvantage of conventional liposomes is their inherent mechanical instability in response to environmental changes. One potential solution to this problem is to use polymerizable lipids to stabilize preformed liposomes.[33,66] The polymerization

of supramolecular assemblies of hydrated lipids has proven to be an effective way to modify the chemical and physical properties of the assembly. Previous results demonstrated that linear and cross-linked polymeric assemblies have significantly different physical properties, e.g. permeability, chemical stability, and solubility.[56,66,76,77,81] In general, linear polymers provide some stabilization of the bilayers, but not as great as cross-linking polymerization.[81]

Progress in understanding the cross-linking polymerization of lipid bilayers now should make it possible to prepare sufficiently stable polymeric liposomes in water, then remove the water by freeze-drying without disruption of the polymeric membrane. In order to test this possibility the heterobifunctional lipids Acryl/DenPC **3-11** and Sorb/DenPC **3-12** were used. Previous polymerization studies of these two lipids illustrated that redox-initiated radical polymerization afforded cross-linked polymeric liposomes in water which were stable in the presence of surfactants.[77] It is shown in this work that the cross-linked liposomes are not destroyed upon complete drying and can be redispersed in water with no apparent change in microstructure. These observations may increase the range of applicability of these cross-linked liposomes and other cross-linked lipid structures, such as bicontinuous cubic phases and inverted hexagonal phases.

The current research focused on the redispersion of the polymerized liposomes after freeze-drying. The intervesicular aggregation depends on the surface properties, such as charges or steric effects of incorporated molecules. To increase the redispersion of the freeze-dried liposomes, two surface modifications were introduced. The first modification was the incorporation of the negatively charged lipid DOPA, which

produces an electrostatic repulsion between the liposomes. The second approach was based on steric stabilization by adding PEG-lipid. In recent years several groups have described methods to utilize PEG-conjugated phosphatidylethanolamine (PEG-PE) to sterically stabilize liposomes in order to increase their period of circulation. It is well established that PEG-grafted lipids in a liposomal bilayer membrane act as a highly hydrated steric barrier that prevents interaction with macromolecules such as proteins or other lipid surfaces.

4.2 Experimental

4.2.1 Materials

The polymerizable lipids Acryl/DenPC$_{16,18}$ **3-11c** and Sorb/DenPC$_{18,21}$ **3-12c**, were synthesized as described in Experimental Section 3.2.[77] 1,2-Dioleoyl-*sn*-glycero-3-phosphate (sodium salt) and 1,2-dioleoyl-*sn*-glycero-3-phosphoethanolamine-N-[poly(ethylene glycol) 2000] (DOPE-PEG$_{2000}$) were purchased from Avanti Polar Lipids Co. Lipid purity was evaluated by thin-layer chromatography (TLC) with chloroform/methanol/water (65/25/4 by volume) and visualized with a UV lamp. Potassium bromate, L-cysteine hydrochloride hydrate, and Triton X-100 were purchased from Aldrich Chemicals and used as received. The lipids were hydrated in Milli-Q water from Millipore Corp. Compounds containing UV-sensitive groups were handled under yellow light.

4.2.2 Preparation of Liposomes

Large unilamellar liposomes (LUV) of polymerizable lipid were prepared as follows: Approximately 5 mg of polymerizable lipid from a benzene stock solution (10 mg/mL) was freeze-dried under high vacuum for at least 4 h. The dried lipid was then hydrated with deoxygenated Milli-Q water to a concentration of 1 mM. Samples were vortexed to uniformity and subjected to ten freeze-thaw-vortex cycles (-77 → 45 °C). The LUV with a diameter of ca. 115 nm were prepared by extrusion 10 times (4 × 0.2 μm + 6 × 0.1 μm) through two stacked Nuclepore polycarbonate filters at 45 °C using a stainless steel extruder from Lipex Biomembranes.

Liposome mixture preparation. DOPE-PEG_{2000} and DOPA were each dried under an argon stream followed by drying under high vacuum for at least 3 h and then weighed. The appropriate amounts of Acry/DenPC **3-11c** and Sorb/DenPC **3-12c** were added to make the concentration of PEG or DOPA lipid 5% in total. The lipid mixtures were dried overnight.

Samples for leakage experiments were prepared as follows. Approximately 10 mg of Acry/DenPC **3-11c** lipid was freeze-dried and hydrated by an aqueous solution of PTSA (3 mM) / DPX (18 mM) to 10 mM lipid concentration. After extrusion, the PTSA/DPX containing LUV was eluted through a Sephadex G-50 column with an isoosmotic saline solution to remove unencapsulated PTSA/DPX.

4.2.3 Polymerization of Liposomes

The redox initiator was prepared from potassium bromate (33.4 mg, 0.2 mmol) and L-cysteine hydrochloride hydrate (31.5 mg, 0.2 mmol), which were weighed into a

10 mL volumetric flask and dissolved in water. An aliquot of potassium bromate/L-cysteine (1/1 mole/mole) solution was added to the liposome suspension, giving a [M]/[I] ratio of 1. The sample was sealed in an ampoule with a septum, and flushed with argon for 0.5 h. Polymerization was performed at 60 °C in a water-circulating bath under a positive argon pressure for 18 h (for leakage experiments, the liposomes were polymerized at room temperature). Polymerization was monitored by UV/vis absorption spectroscopy of aliquots diluted with Milli-Q water to ca. 60 μM. The UV absorption at 260 nm, attributed to the diene and/or sorbyl groups, was analyzed with a UV/vis spectrophotometer (Varian DMS 200) to determine the polymerization conversion of Acryl/DenPC **3-11c** or Sorb/DenPC **3-12c**.

4.2.4 Surfactant Dissolution of Liposomes

The LUV were prepared as described above. After polymerization, the LUV were characterized by QELS (BI 8000 autocorrelator from Brookhaven Instrument Corp.) for a 2 mL sample with a lipid concentration of 150-300 μM. Aliquots of 50 mM TX-100 solution, each 2 equiv. with respect to lipid, were added until the liposomes dissolved or 12 equiv. were added. The light-scattering intensities were determined at least three times at a 90° angle and room temperature by QELS at each concentration of TX-100. The average mean diameter of liposomes was calculated using a non-negatively constrained least squares program.

4.2.5 Redispersion of Lyophilized Liposomes

Only samples with greater than 90% monomer conversion, as determined by UV/vis spectroscopy, were used in these studies. Samples were lyophilized after polymerization. The residual solid was weighed and Milli-Q water was added to make the same concentration as that before freeze-drying. The samples were sonicated for 5-15 min with a bath sonicator (Branson 1200, 150 W) or mixed with 12 equiv. of TX-100 and allowed to stand for at least 30 min before the size of the dispersed LUV was measured by QELS.

4.2.6 Transmission Electron Microscopy (TEM)

A 30 μL aliquot of ammonium molybdate solution (11% w/w, pH = 7.2) was added to 100 μL of liposome suspension (150 μM). The solution was incubated for 5 h at room temperature. Then a small piece of carbon-coated mica sheet having one end pointed and the other one flat was immersed in the negative-stained sample. The carbon film was separated from the mica surface and floated on the surface of the sample solution. A freshly washed grid was placed underneath the floating specimen film and then raised with a pair of forceps to collect the sample and carbon film. The excess liquid was carefully removed with a pointed filter paper. The liposome suspensions were sandwiched between the copper grid and the carbon film. The sample was observed with a JEM-100CX II (JEOL) electron microscope operated at 80 kV.

4.2.7 Determination of Liposome Leakage

Fluorescence spectra were obtained with a SPEX FluoroLog2 fluorometer. The change in PTSA fluorescence emission over time was determined on a 1.0 mL, 60 μM solution with excitation at 357 nm and emission at 403 nm. The slit width for both excitation and emission monochrometers was 1 mm. Complete leakage was determined by addition of 50 μL of 50 mM aqueous TX-100 to the above sample. The fluorescence of each sample was measured over 30 s. The percent leakage at any time is given by the following expression:

$$\% \text{ leakage} = 100 \times (I_t - I_0)/(1.05I_{100} - I_0)$$

where I_t is the fluorescence intensity at time 't', I_0 is the fluorescence intensity immediately after column, I_{100} is the fluorescence intensity after addition of TX-100, and 1.05 is the dilution factor caused by addition of TX-100 solution.

4.3 Results and Discussion

4.3.1 Polymerization of Liposomes

Large unilamellar bilayer liposomes (LUV) with an average diameter of ca. 115 ± 10 nm were prepared by extrusion methods.[44] They were polymerized with a redox initiator to stabilize the lipid bilayer. The size of the liposomes was determined by QELS. The data showed only a slight decrease (< 10%) on the average mean diameter after polymerization (Table 4-1). The liposome's stability toward surfactant and their insolubility in organic solvents indicate the lipids were cross-linked.

Examination of the liposomes by negative staining TEM showed that the liposomes were generally smooth and spherical. Typical electron micrographs of liposomes before and after polymerization shown in Figure 4-3 indicate the liposomes were predominantly unilamellar. No significant change in the liposome appearance was caused by the cross-linking polymerization (Figure 4-3a b g j n p). The electron microscopy also reveals that cross-linked liposomes can be quite flexible. Several of the micrographs show collapsed structures, much like a partially deflated volleyball. The image in Figure 4-3c shows that the liposomes packed together in a manner that permits a cursory examination of the effect of liposome contact on liposome morphology. The image indicates that these cross-linked liposomes conform to the neighboring bilayers. Therefore the liposomes after cross-linking do not become hard spheres, but rather flexible nanostructures bounded by an elastomeric polymer.

Figure 4-3. TEM photographs of Acryl/DenPC and Sorb/DenPC liposomes negatively stained with ammonium molybdate. The bar is 100 nm (for h is 500 nm).

(a) Acryl/DenPC **3-11c**, before polymerization

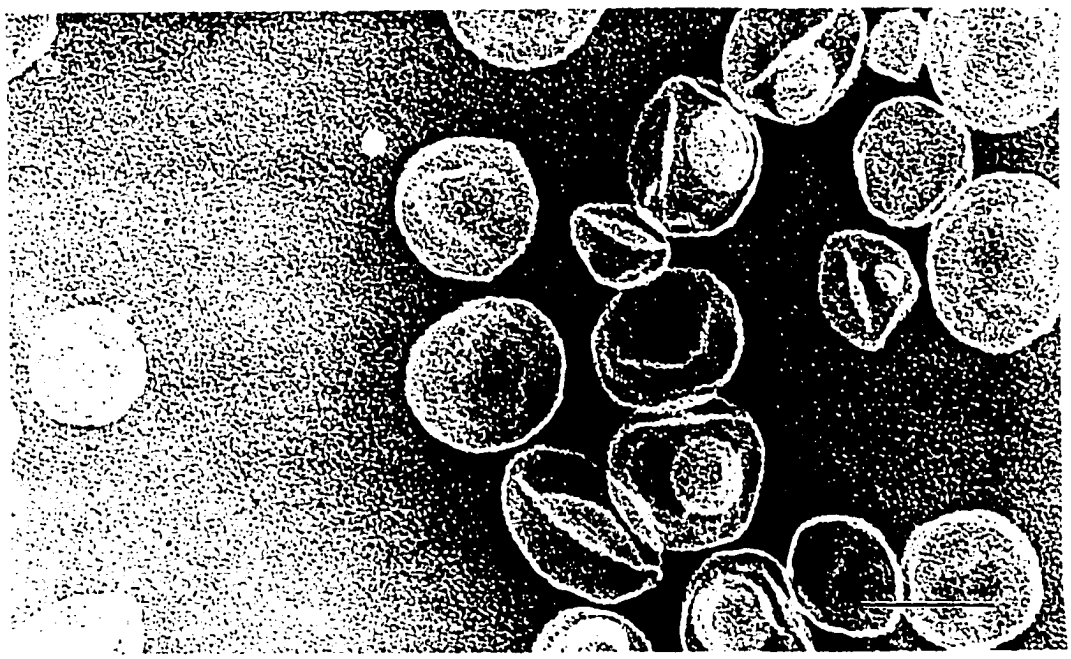

(b) Acryl/DenPC **3-11c**, after polymerization

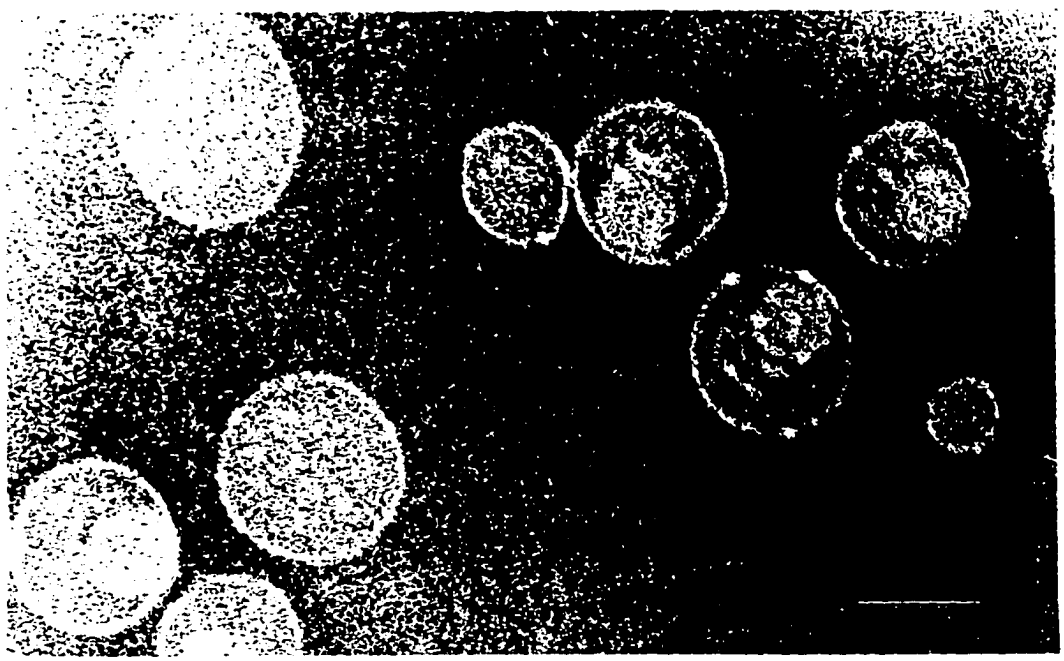

(c) Acryl/DenPC **3-11c**, after polymerization and in TX-100

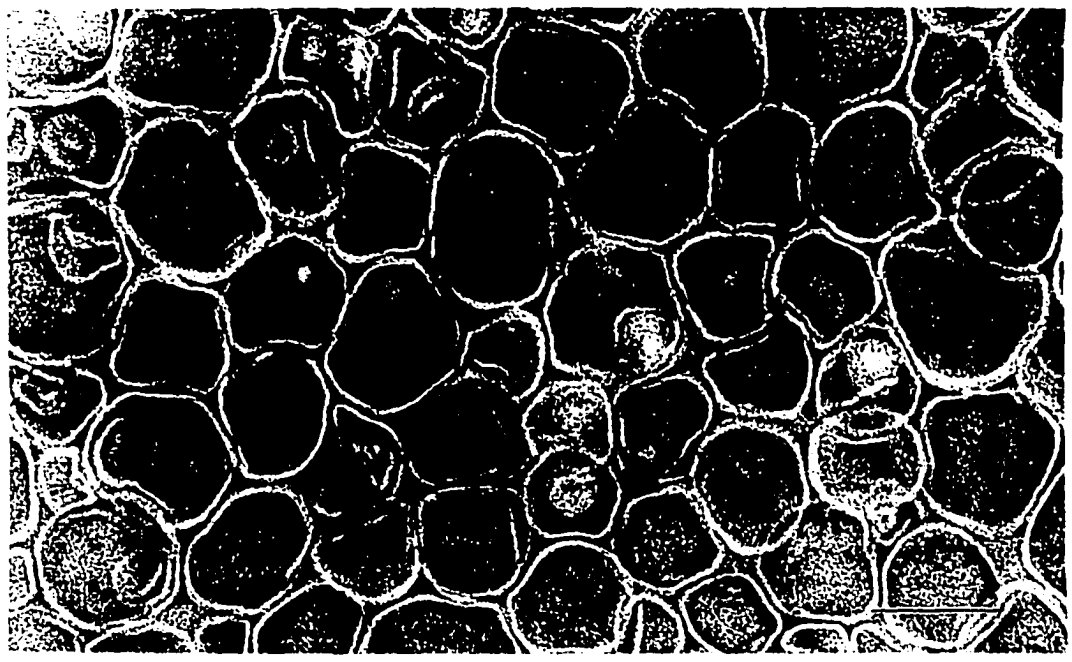

(d) Acryl/DenPC **3-11c**, after polymerization, in 50% MeOH

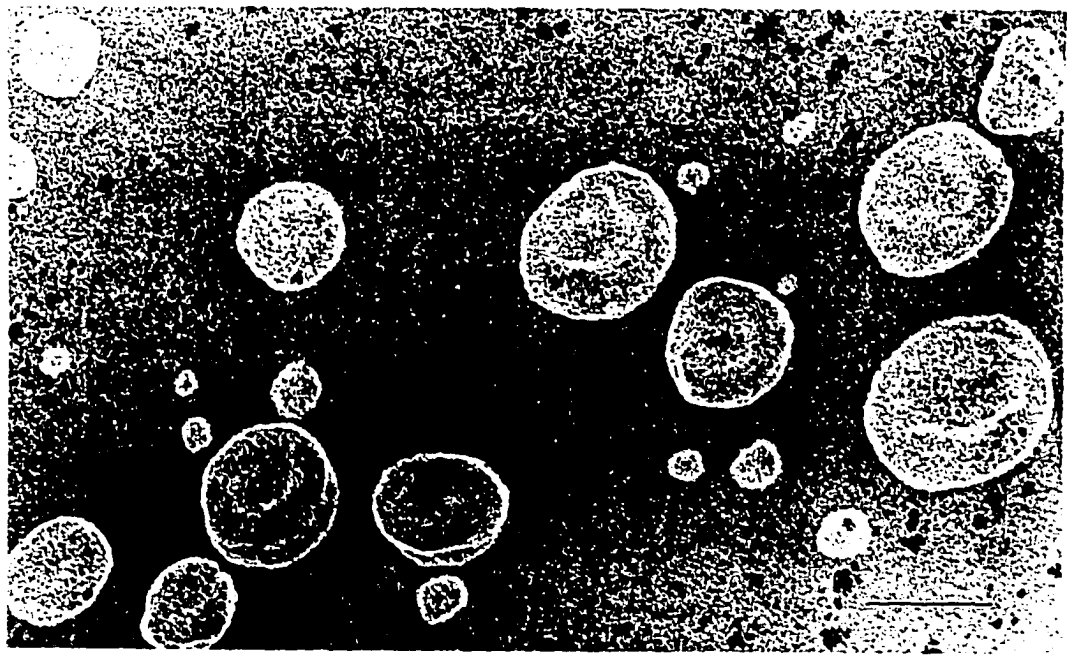

(e) Acryl/DenPC **3-11c**, after freeze-drying

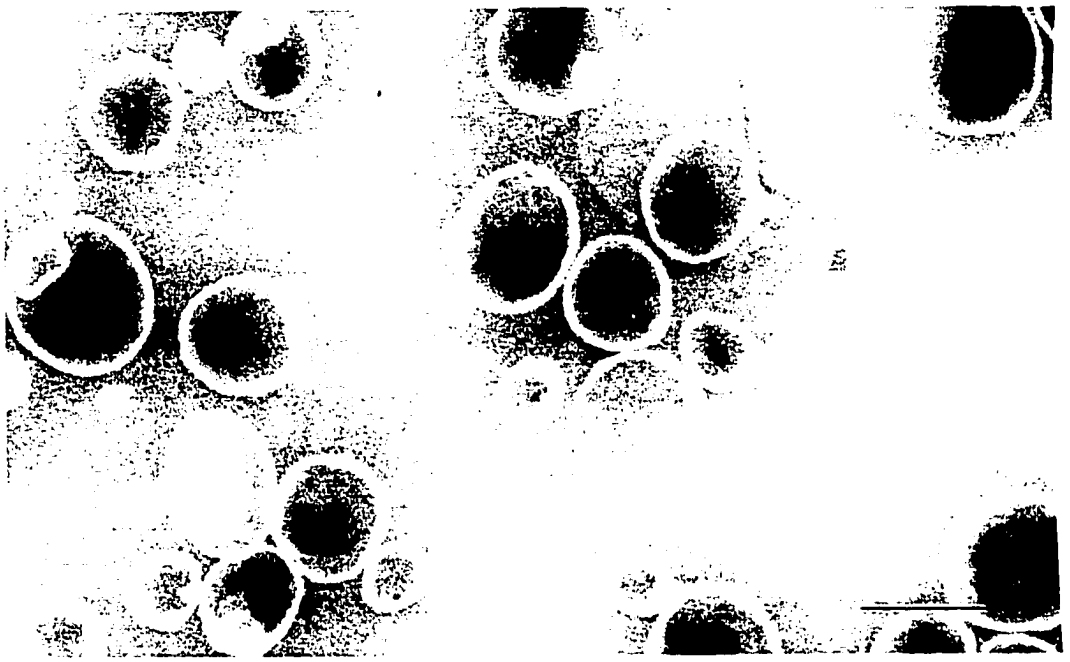

(f) Sorb/DenPC **3-12c**, after polymerization

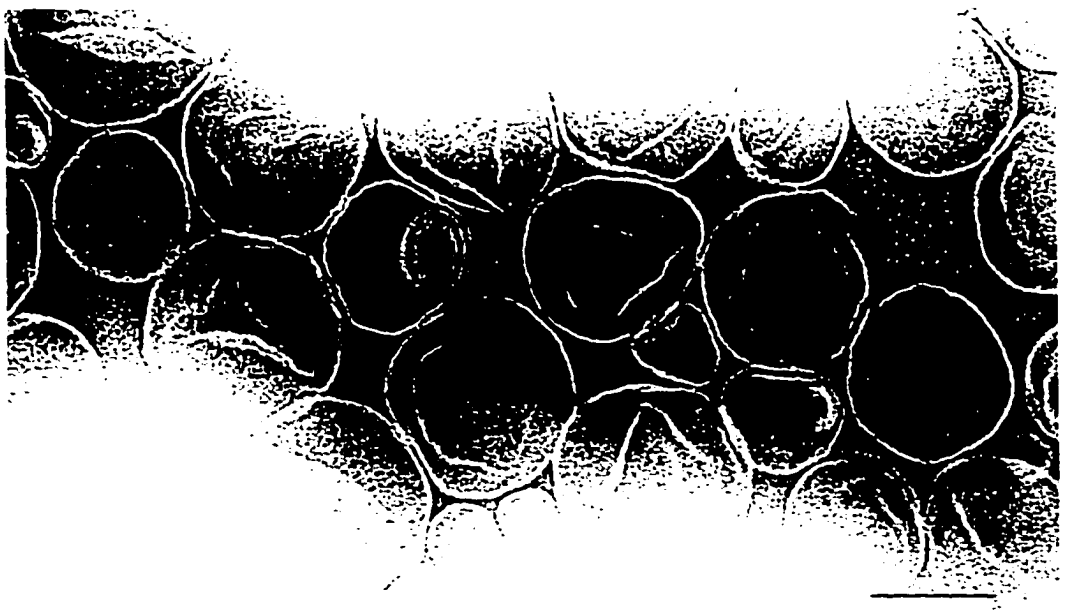

(g) Sorb/DenPC **3-12c**, after polymerization, in 50% MeOH

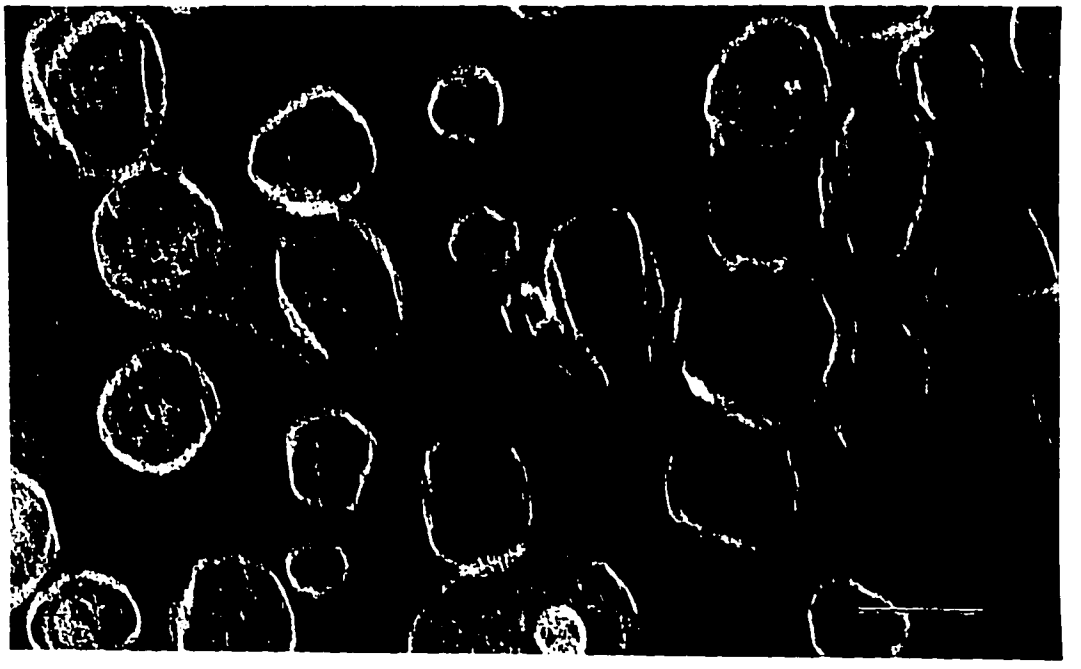

(h) Sorb/DenPC **3-12c**, Freeze-drying (20 K)

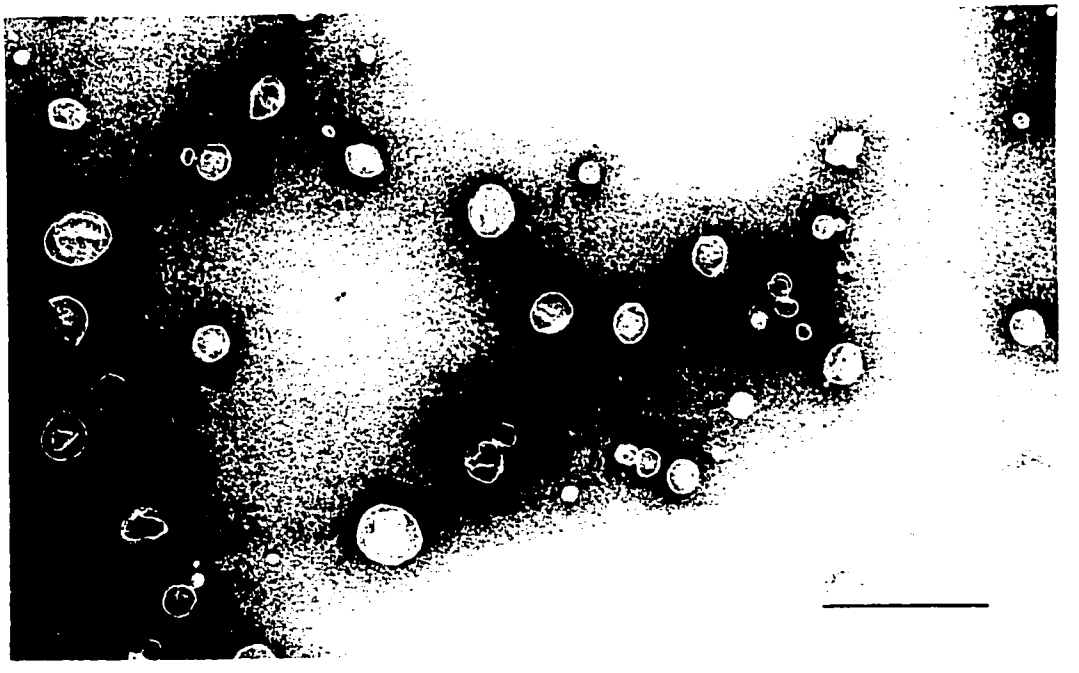

(i) Sorb/DenPC **3-12c**, Freeze-drying

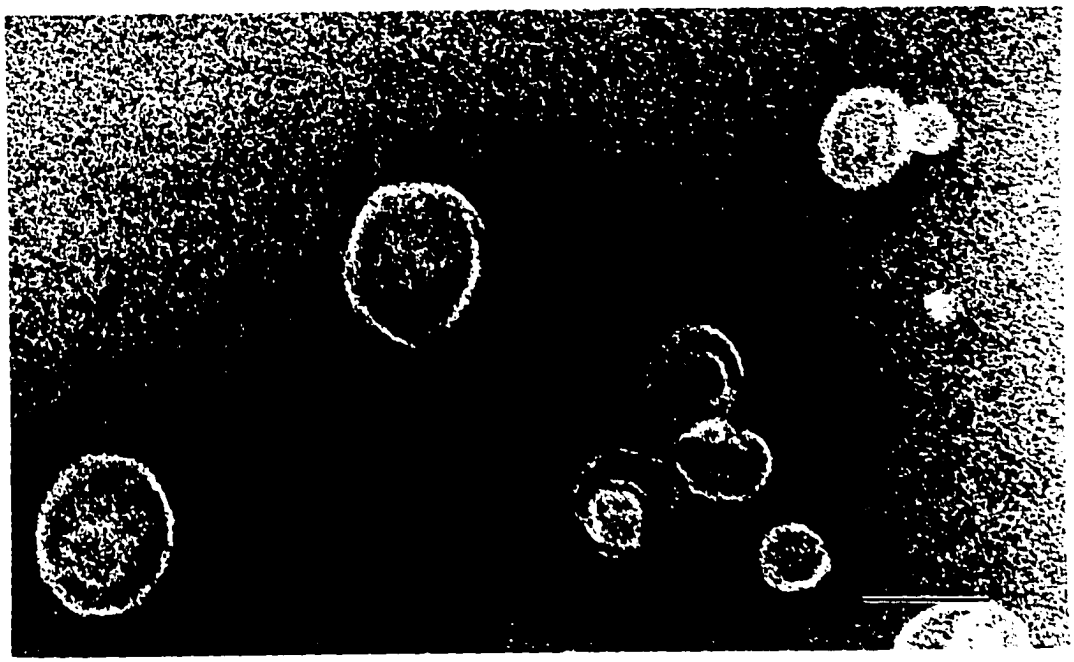

(j) Acryl/DenPC (**3-11c**)–PEG, after polymerization

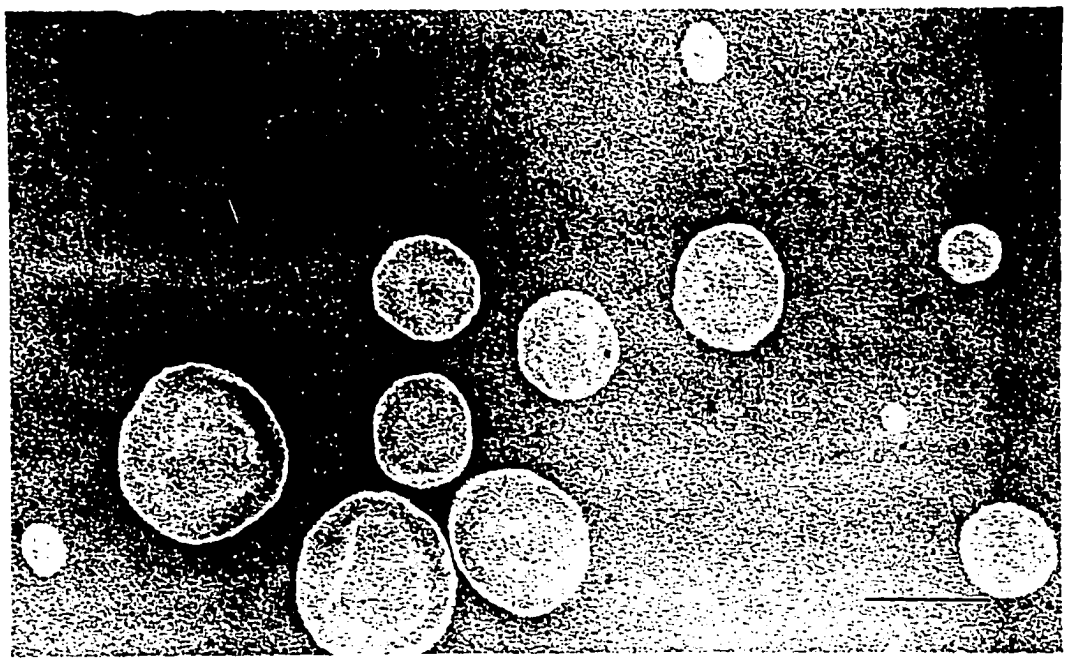

(k) Acryl/DenPC (**3-11c**)-PEG, after freeze-drying

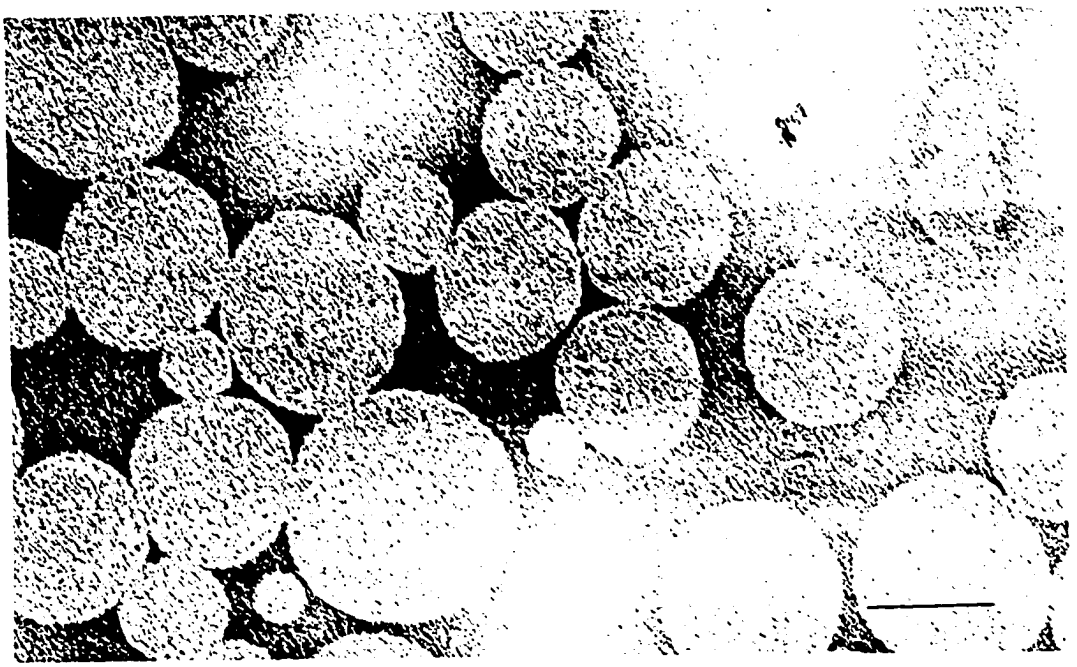

(l) Acryl/DenPC (**3-11c**)-DOPA, after polymerization, in 50% MeOH

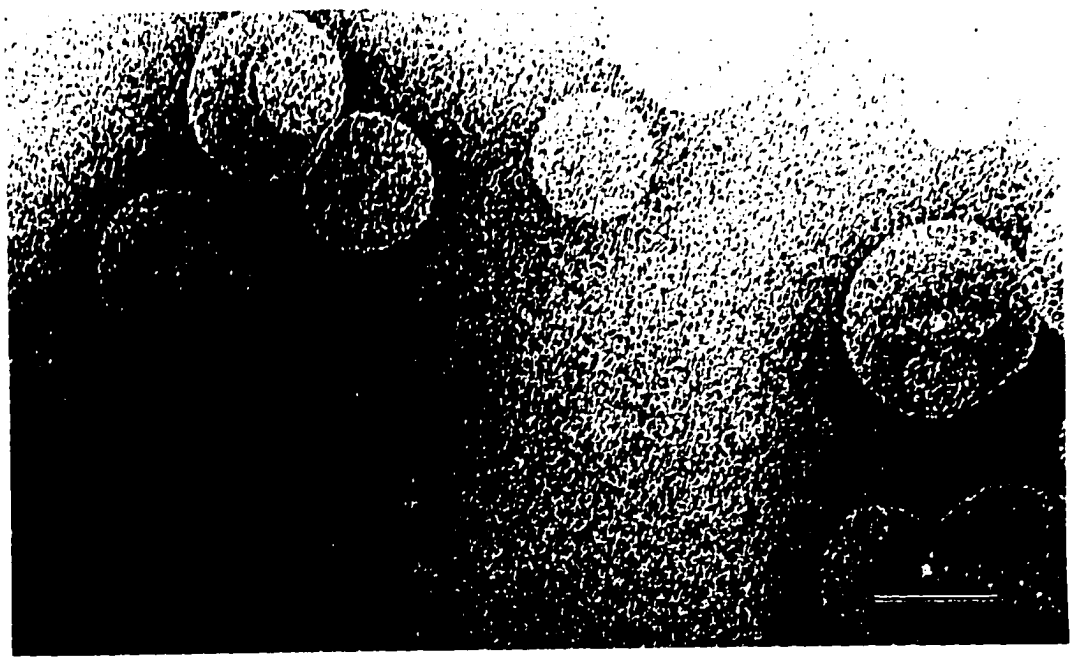

(m) Acryl/DenPC (**3-11c**)-DOPA, after freeze-drying

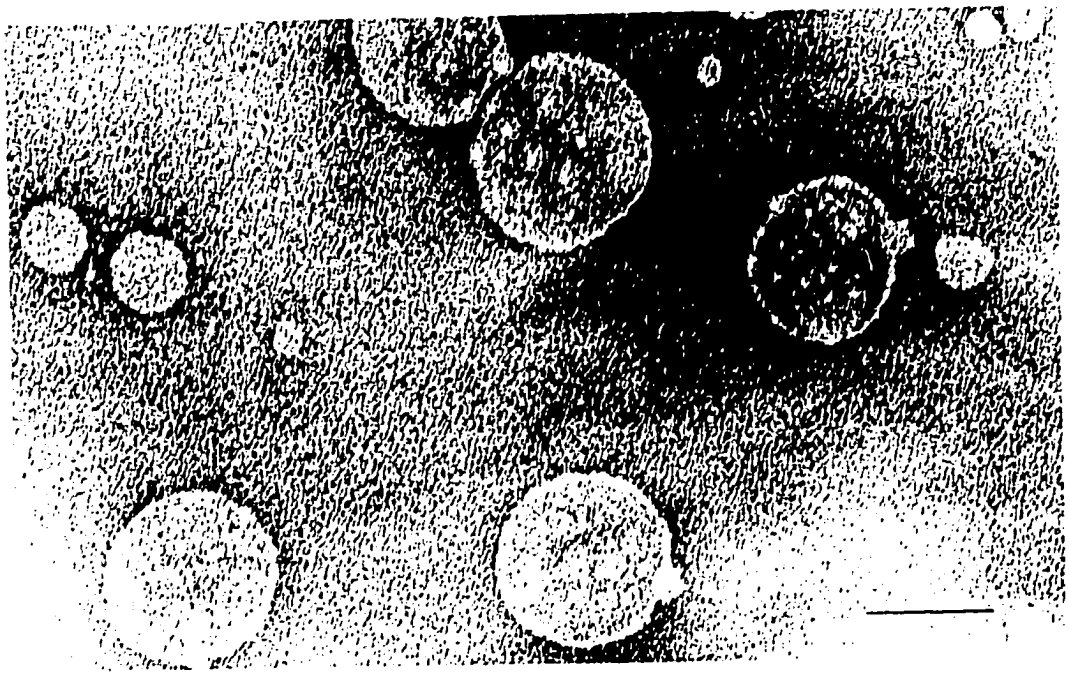

(n) Sorb/DenPC (**3-12c**)-DOPA, after polymerization

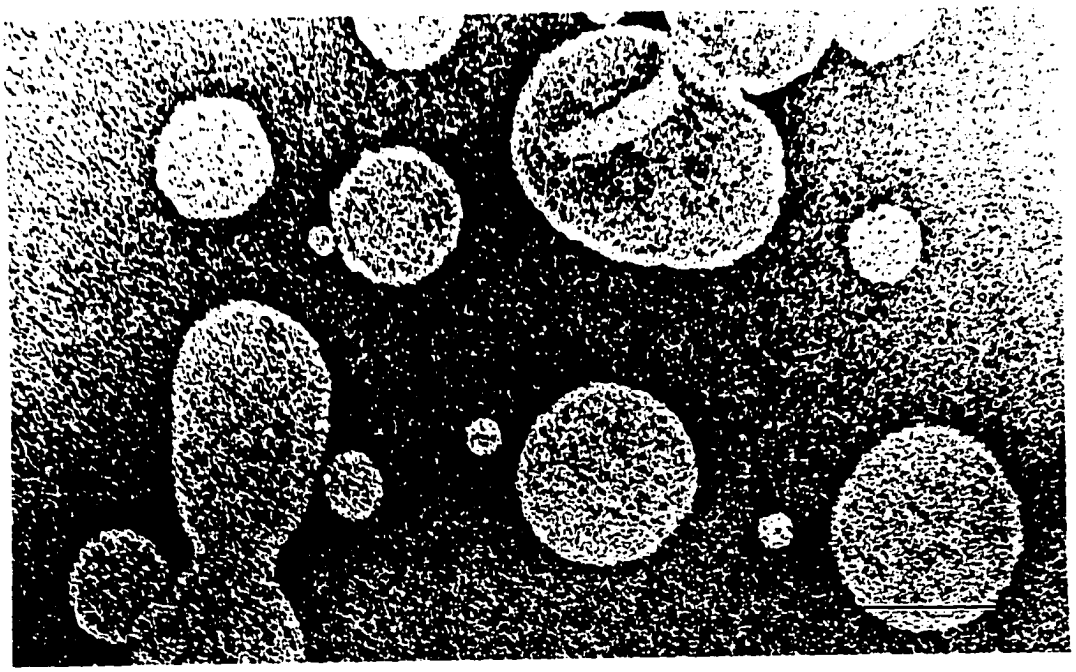

(o) Sorb/DenPC (**3-12c**)-DOPA, after freeze-drying

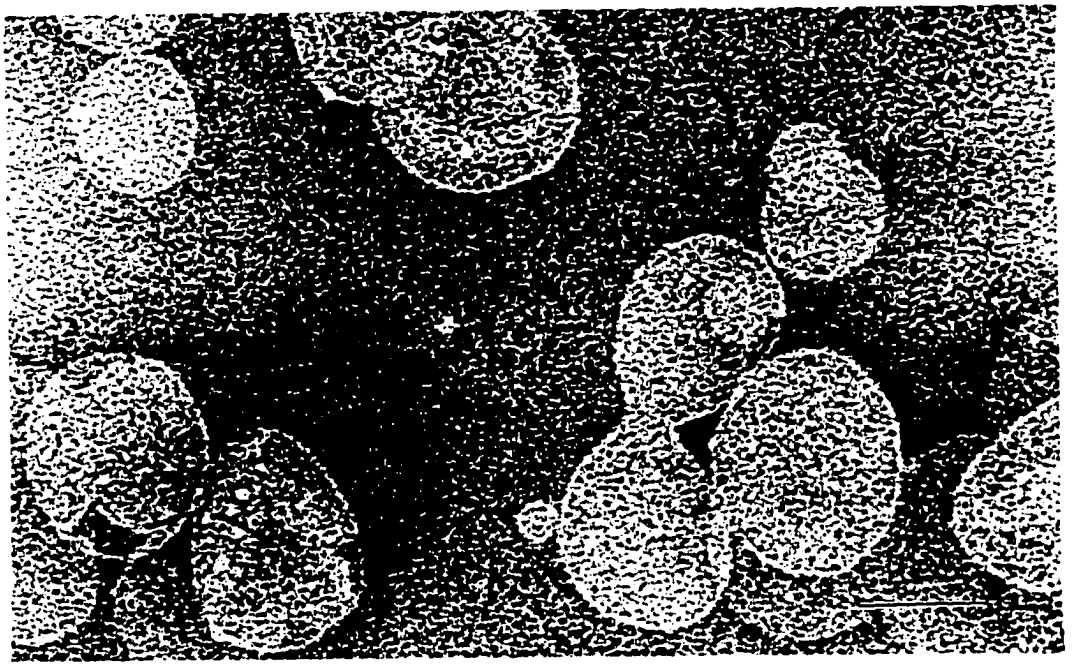

(p) Sorb/DenPC (**3-12c**)-PEG, after polymerization

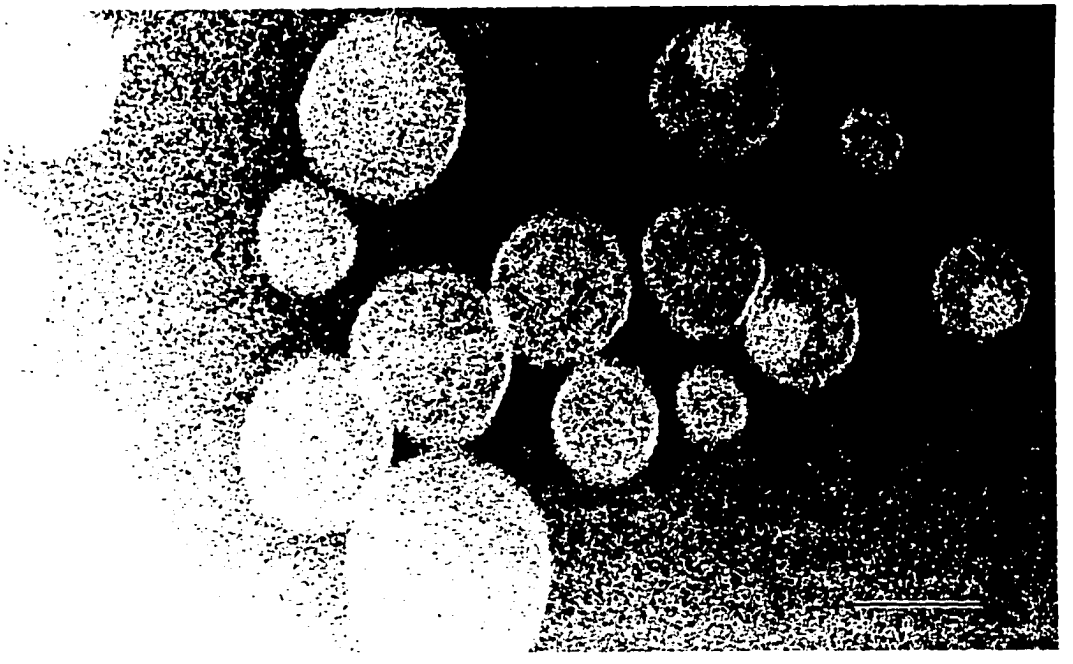

(q) Sorb/DenPC (**3-12c**)-PEG, after polymerization in 50% MeOH

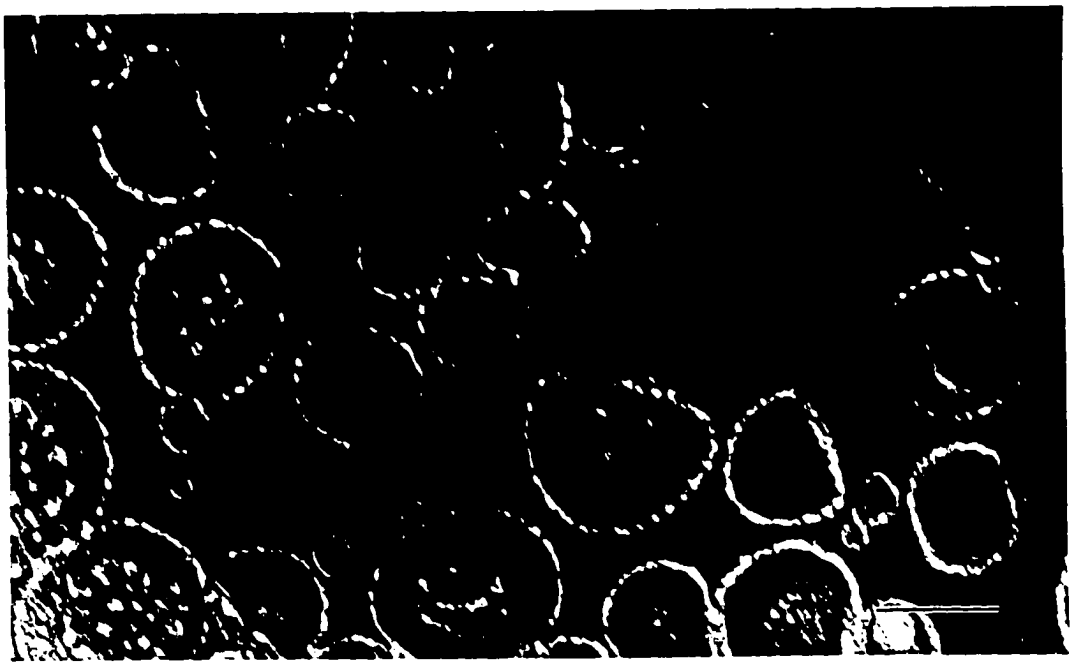

(r) Sorb/DenPC (**3-12c**)-PEG, after freeze-drying

4.3.2 Redispersion of Lyophilized Liposomes

The cross-linked liposomes were freeze-dried to obtain a white powder. The lyophilized liposomes, however, could not be fully redispersed but produced a mixture of suspended liposomes and larger aggregates by simple hydration in water. In order to reduce the size and proportion of the aggregates, bath sonication was utilized. The following procedure was adopted to redisperse the lyophilized LUV. The dried white powder was mixed with distilled water and then sonicated with a bench type bath sonicator for 5-15 min to obtain a homogeneous clear solution.

Table 4-1 shows the results of redispersion of the polymerized liposomes measured by QELS. The percent LUV redispersion is defined as the measured percent of redispersed particles that have a diameter of approximately 115 nm, which is taken to be the population of unaggregated liposomes. The rest of the light scattering particles were usually considerably greater than 200 nm in diameter. It is well known that larger particles scatter light more than smaller particles. Consequently, this analysis tends to understate the fraction of ca. 115 nm diameter liposomes that were successfully redispersed. More than 80% redispersion was observed for cross-linked liposomes prepared from either Acryl/DenPC$_{16.18}$ **3-11c** or Sorb/DenPC$_{18.21}$ **3-12c**. Examination of these redispersed liposomes by QELS indicated they had a similar size distribution before and after freeze-drying (Figure 4-3e f i k m o r). Addition of the surfactant TX-100 to the system increased the efficiency of redispersal of the freeze-dried liposomes. The measured redispersion increased to nearly 100% retention of liposome sizes and shapes.

Table 4-1. The average of the mean diameter (nm) of liposomes determined by QELS.

Lipid	Before pzn	After pzn	Pzn + TX-100	Freeze-dry (Sonication)		Freeze-dry (TX-100)	
				Size	Recovery	Size	Recovery
A/DPC	112	108	105	124	86%	122	100%
A/DPC+DOPA	118	102	105	128	55-75%	105	100%
A/DPC + PEG	112	102	103	122	100%	101	100%
S/DPC	122	121	117	117	90%	103	100%
S/DPC + DOPA	123	118	110	118	80-100%	99	100%
S/DPC + PEG	118	112	105	115	100%	113	100%

- The standard deviation was ± 10 nm.
- A/DPC: Acryl/DenPC$_{16,18}$ **3-11c**; S/DPC: Sorb/DenPC$_{18,21}$ **3-12c**;
- PEG: DOPE-PEG$_{2000}$

Liposomes that include 5% of the anionic lipid DOPA showed a small increase in percent redispersion for Sorb/DenPC$_{18,21}$ **3-12c** LUV (from 90 to 100% measured by QELS). However, a decrease of the percent redispersion was observed for

Acryl/DenPC$_{16.18}$ **3-11c** LUV. The amount of redispersion of DOPA-containing liposomes was dependent on the pH of the system. When the pH was less than 5 before freeze-drying, the amount of redispersion was only 55%, but when the pH was basic before freeze-drying, the redispersion increased to 75%. The redispersion of Sorb/DenPC-DOPA liposomes was 80% at pH less than 5 and nearly 100% under basic conditions. The dependence of the efficiency of redispersion on pH may be due to the amount of ionized DOPA in the liposomes. Certainly at basic pH all of the DOPA was ionized. Based on the known solution pK_a of phosphates most of the phosphatidic acid should be ionized at a pH of about 5. However, the effective pK_a of the DOPA phosphate group at the membrane surface may be greater than expected from solution values. When the DOPA was clearly deprotonated the electrostatic repulsion between the liposomes by the introduction of negative charge on the surface reduced the extent of liposome aggregation during redispersion. The decrease of redispersion of the Acryl/DenPC-DOPA system may be related to the large difference in the phase transition temperature (T_m) between Acryl/DenPC$_{16.18}$ **3-11c** (27.8 °C) and DOPA (-8 °C). These circumstances favor phase separation of any unionized DOPA from the polymerized lipid, which suggests these polymerized liposomes have domains of unpolymerized DOPA that would respond differently to freeze drying and rehydration than the cross-linked domains of the liposomes.

Addition of 5% of DOPE-PEG$_{2000}$ to the composition of polymerized liposomes resulted in a significant increase in percent and ease of redispersion (Figure 4-3k r). Liposomes from either of the polymerizable lipids were 100% redispersed with shorter

sonication times (5 instead of 15 min sonication). The redispersed liposome suspensions also have higher storage stability than those without PEG lipid.

4.3.3 Stability of Redispersed Liposomes

Surfactant solubilization is a useful method to evaluate liposome stability in solution. Figure 4-4 shows the average diameter of Sorb/DenPC$_{18,21}$ **3-12c** LUV as measured by QELS in comparison to the ratio of the surfactant TX-100 to lipid. When 4-6 equiv. of TX-100 were added to monomeric LUV, a sharp decrease in the average of the mean diameter of the suspended particles was observed which indicates the destruction of liposomes and the formation of micelles. On the other hand, the liposomes cross-linked by a redox initiator were essentially unchanged in size by the addition of up to 12 equiv. of TX-100. In the case of lyophilized and redispersed polymerized liposomes, no significant change in the size was observed, indicating that they have comparable resistance to surfactant action as the original polymerized liposomes. Moreover, the addition of surfactant is another effective method to redisperse the freeze-dried liposomes (Figure 4-3c). The results in Table 4-1 show that after addition of 12 equiv. of TX-100 to freeze-dried liposomes, 100% of liposome redispersion was obtained for all systems studied.

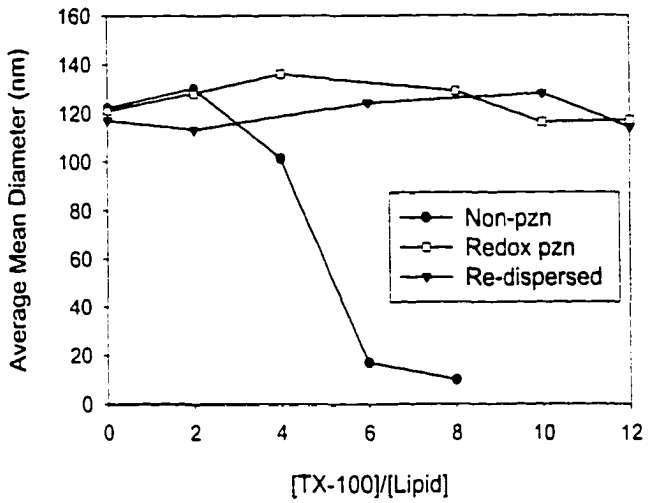

Figure 4-4. Average mean diameter of redispersed liposomes of Sorb/DenPC$_{18:2}$ **3-12c** as a function of added equivalents of TX-100 in comparison with monomeric liposomes and liposomes before redispersion.

These results indicate that appropriately cross-linked liposomes can be successfully lyophilized for storage, then rehydrated to recover the liposomes. The observed stability of the cross-linked liposomes prompted an initial evaluation of their stability towards organic solvents. When cross-linked liposomes in water were diluted with an equal volume of methanol the liposomes remained in suspension. TEM images showed spherical structures similar to the original liposomes in water (Figure 4-3d h l q). There was no precipitate even after the addition of salts (NaCl); therefore, the liposomes were not destroyed by the osmotic shock.

Both QELS and TEM results indicate that cross-linked liposomes from either Acryl/DenPC$_{16:1}$ **3-11c** or Sorb/DenPC$_{18:2}$ **3-12c** or their mixture with PEG / DOPA

lipid exhibit remarkable stability and can be freeze-dried and redispersed in water. Therefore, it was proved that the cross-linked liposomes had higher stability than linearly polymerized polymers. Of course it must be remembered that the water permeability of conventional lipid membranes is very high, nearly ten orders of magnitude greater than that of sodium ion.[103,195] Consequently, we can infer from the present results that the formation of polymer chains in the lipid bilayer does not substantially reduce the passive transport of water across the bilayer membrane of the cross-linked liposomes.

4.3.4 Determination of Liposome Leakage

The leakage was measured with the PTSA/DPX assay. In this assay, the fluorescent dye PTSA and its collisional quencher DPX were incorporated into the liposomes by hydrating the lipid with a PTSA/DPX solution. Excess dye-containing solution outside of the liposomes was exchanged with an isoosmotic non-dye solution by gel chromatography. When the dye escapes the liposomes the dye quenching is diminished by dilution. The leakage of PTSA from liposomes was measured with 30 s scans over the period of several hours. The PTSA leakage was found to be temperature-dependent. The leakage rate is low at room temperature (25 °C), but was much higher at 40 °C for both samples before and after polymerization (Figure 4-5). The phase transition temperature of Acryl/DenPC$_{16,18}$ **2-11c** is 27.8 °C. When the temperature is below its phase transition temperature, the lipid chains are in the solid-like phase and the observed permeability of the liposome is low. When temperature is raised to above the phase transition temperature, the melting of the lipid tails results in an increase in liposome

permeability due to disorder in the bilayer membrane. The monomeric liposome lost 100% of the dye within one hour at 40 °C. However, the polymeric liposome lost only 16% of the dye under the same conditions. At room temperature, unpolymerized liposomes released 43% of entrapped dye after 28 h, whereas less than 10% leakage was measured for polymeric liposomes after the same time period. When the polymerized liposomes were treated with TX-100 (ca. 40 equiv.), the total leakage after polymerization was only 40% of that of monomeric liposomes. Polymerization remarkably reduced the leakage rate both at room temperature and 40 °C due to the restriction of the lipid chain movements. After freeze-drying and rehydration in water, the leakage increased to 35%, close to the total leakage induced by TX-100 after polymerization (40%). These results indicate that the cross-linking structures formed inside the bilayer membrane can only partially contain the contents inside the liposomes upon freeze-drying and surfactant treatment.

It was expected that there should be no difference between the leakage rate at room temperature and 40 °C after polymerization since phase transition of the membrane should be totally suppressed after cross-linking polymerization.[53,124] The relatively high leakage rate at 40 °C (ca. 6 h to reach 40% leakage) may indicate the presence of phase transition inside these cross-linked liposomes and a DSC experiment is going to be performed to test this hyphothesis. Tsuchida et al. measured the CF leakage rate for linear and cross-linked liposomes from bisDenPC **2-10**.[135] Their results also showed a 15 % leakage at 50 °C after 1 h. The linear polymeric liposomes showed a slightly higher leakage (20%). No comparable experiments were performed at room temperature.

Further experiments have been designed to vary the cross-linking density to control the release rate and increase the retention of entrapped compound during freeze-drying. Early studies showed that the freezing rate had a big effect on the leakage rate and the recommended freezing rate is 0.5 °C/h.[193] However, in our case, we used rapid freezing, which may cause distortion of the liposomes and induce the leakage increase. The freezing rate is one of the factors which should be taken into consideration in future experiments.

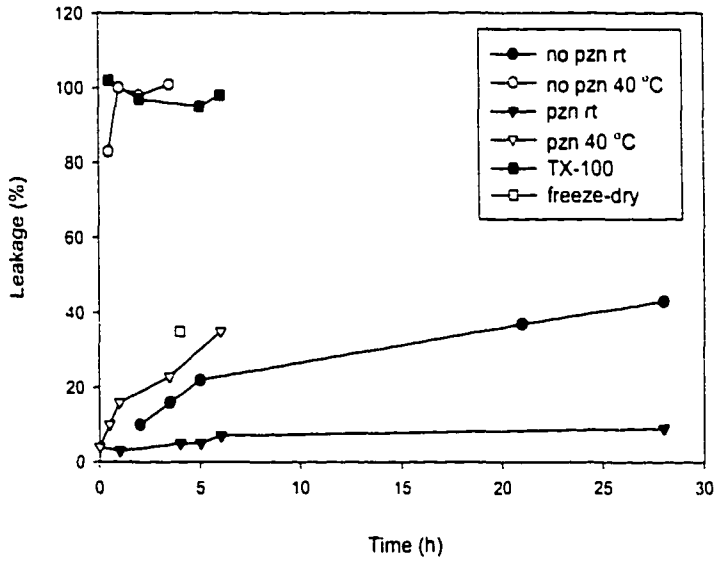

Figure 4-5. Leakage of PTSA from liposomes vs time at 25 and 40 °C.

4.4 Conclusions

In this chapter, we studied the lyophilization and rehydration of cross-linked liposomes from heterobifunctional lipids Acryl/DenPC **3-11c** and Sorb/DenPC **3-12c**. The liposomes were characterized by QELS and TEM. There is no major change in the size and shape of the cross-linked liposomes after lyophilization and rehydration. Moreover, the rehydrated liposomes were resistant to surfactant solubilization. This indicates that there is no difference in stability between polymerized liposomes before and after redispersion. We have prominently emphasized the efficiency of redispersion of lyophilized cross-linked liposomes. The aggregation of liposomes during freeze-drying was found to depend on the liposome surface properties, i.e. the electrostatic or steric effects of incorporated molecules. To increase the redispersion of the freeze-dried liposomes, two surface modifications were introduced, i.e. the incorporation of the negatively charged lipid DOPA and the hydrophilic polymer PEG-lipid. The latter approach was more successful. The strength and flexibility of these hollow polymeric spherical materials suggests they could be considered polymeric nanobubbles.

Appendix A: ^{1}H NMR Spectra

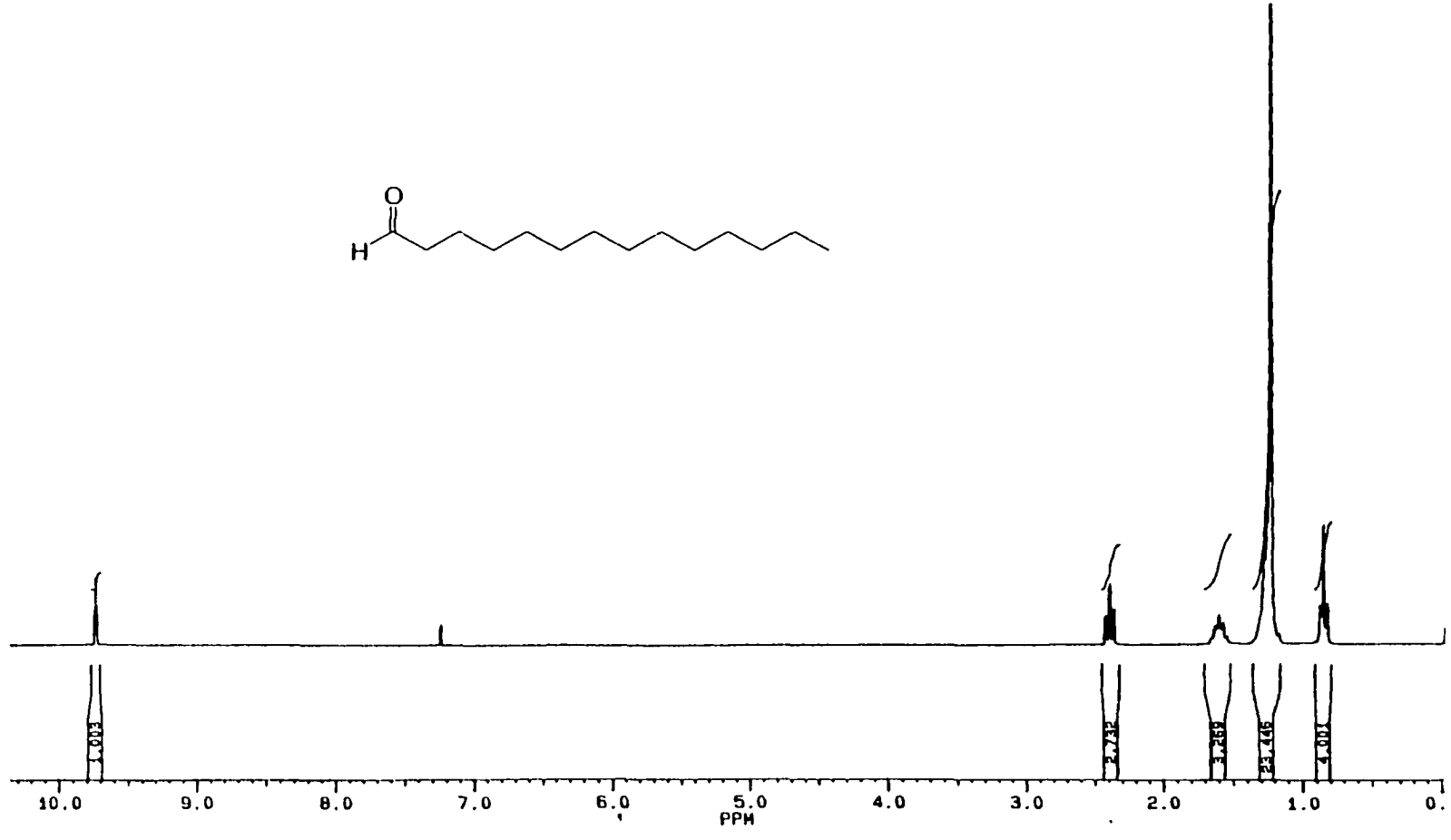

Figure A-1: ^{1}H NMR of Compound **2-18**: tetradecanal

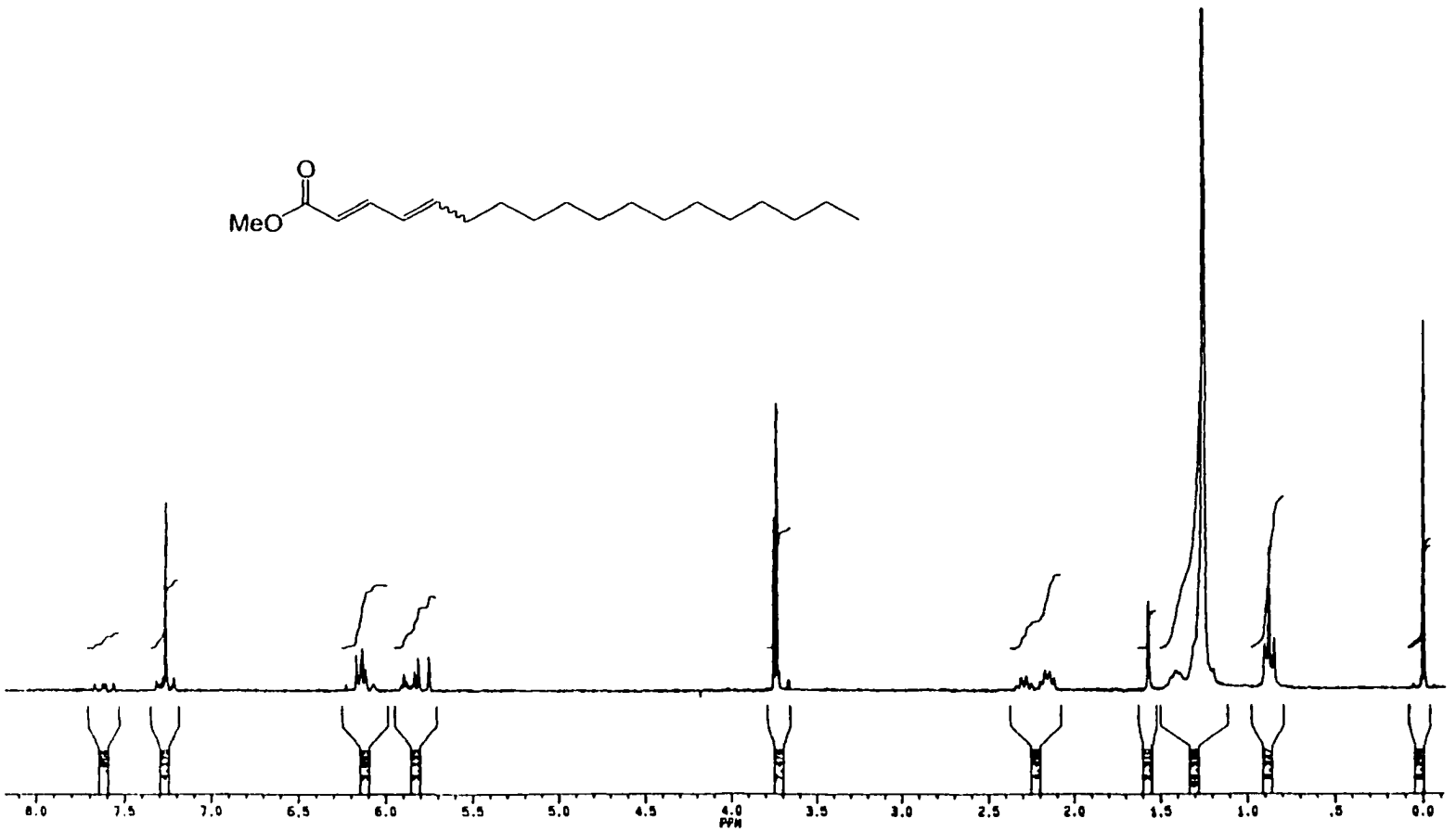

Figure A-2: ^{1}H NMR of Compound **2-19**: methyl 2,4-octadecadienoate

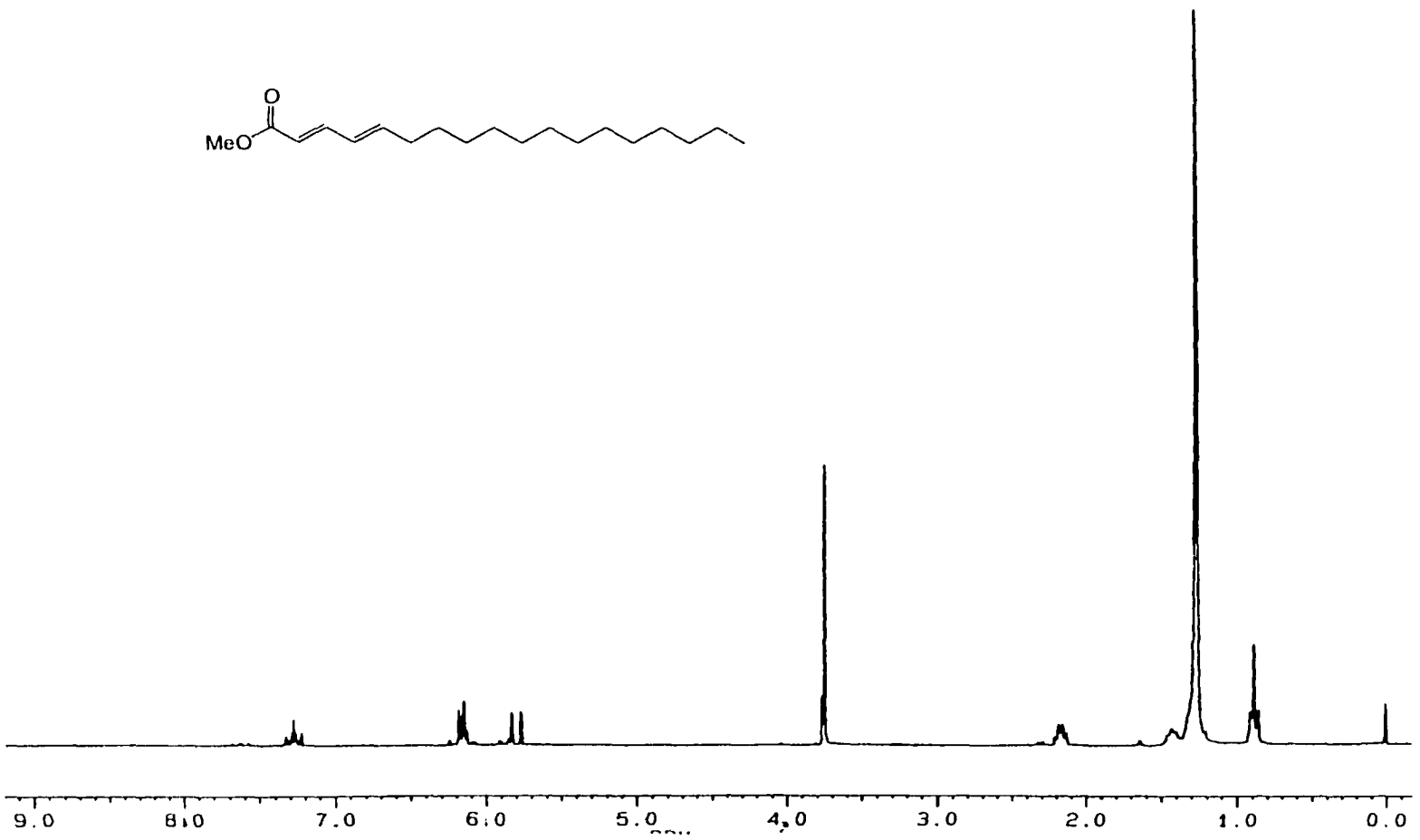

Figure A-3: ^{1}H NMR of Compound **2-20**: methyl (*E,E*)-2,4-octadecadienoate

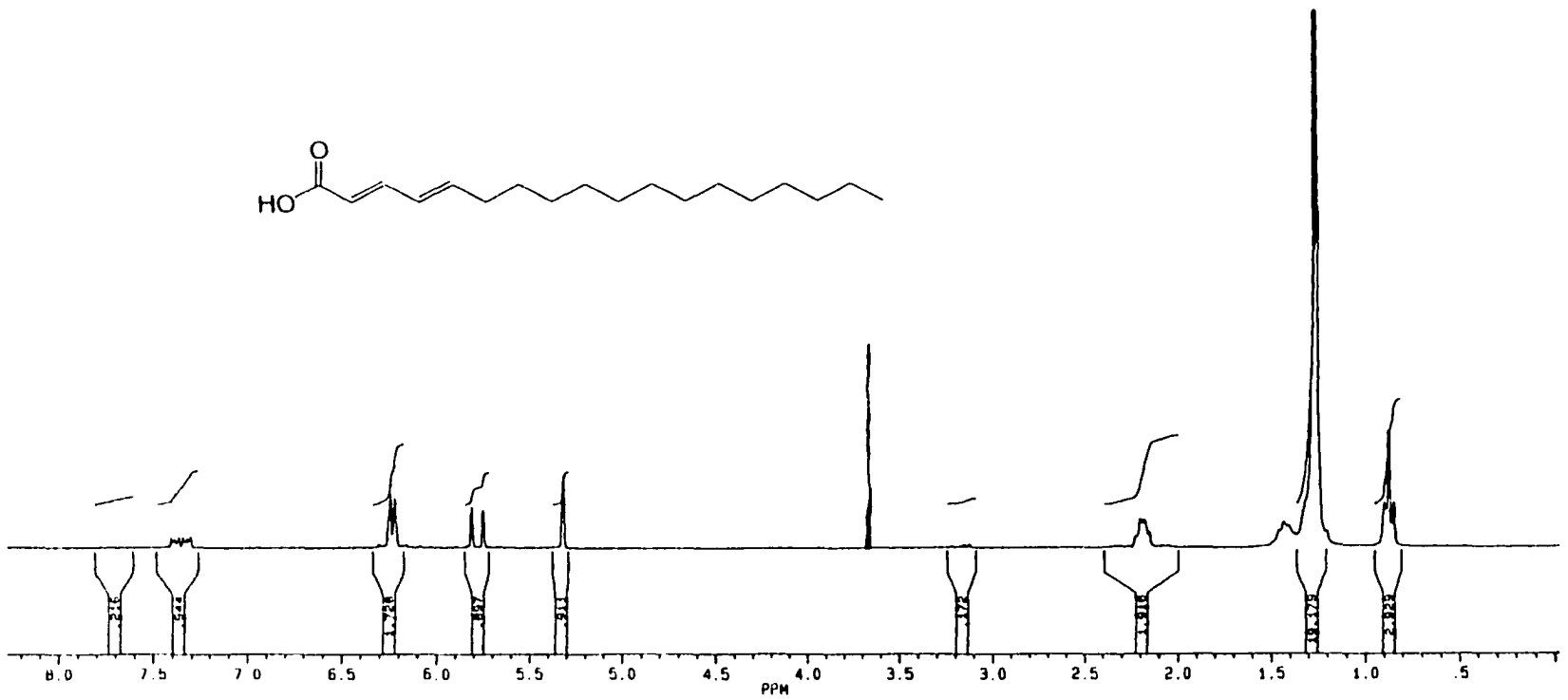

Figure A-4: ^{1}H NMR of Compound **2-21**: 2,4-(*E,E*)-octadecadienoic acid

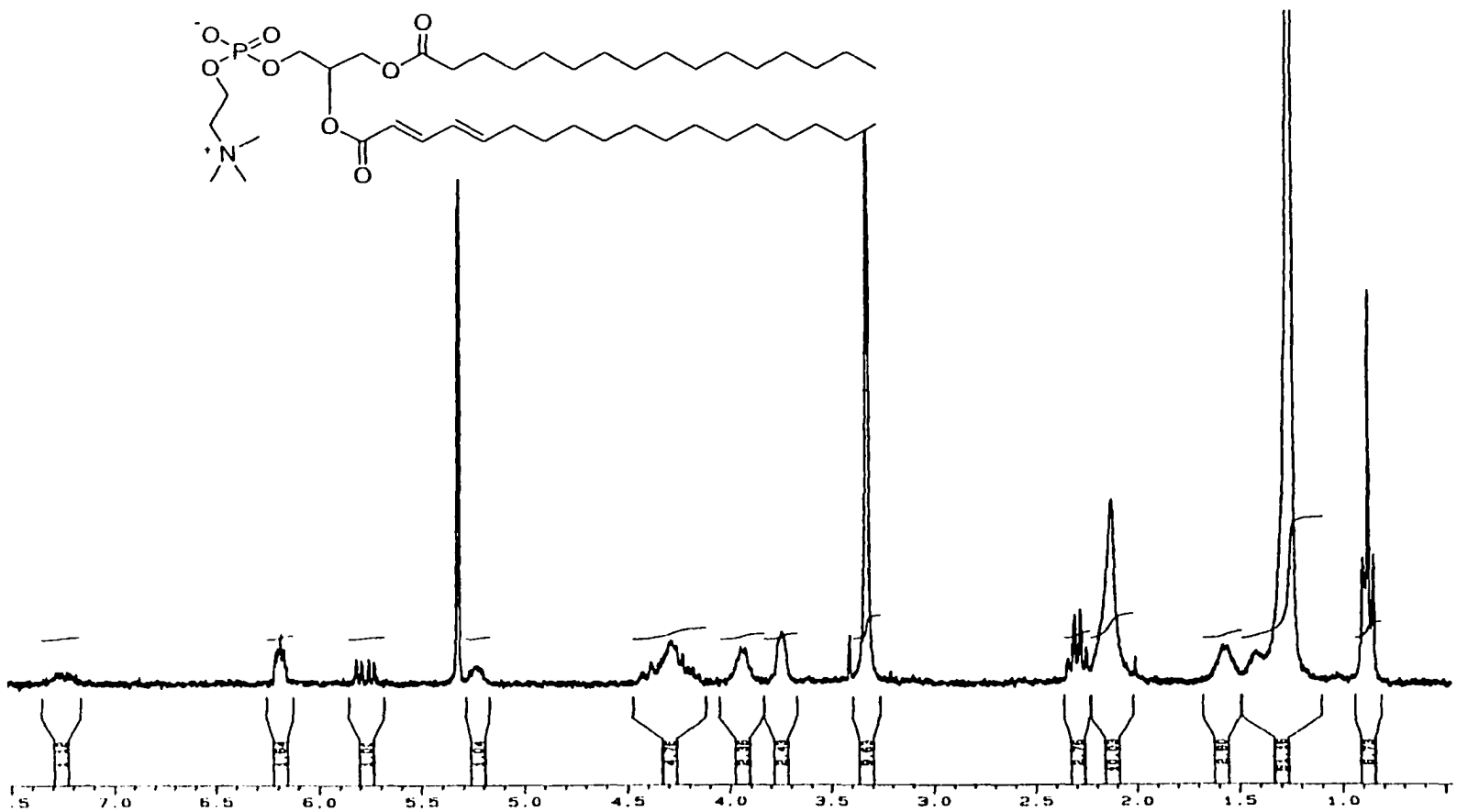

Figure A-5: ^{1}H NMR of Compound **2-11**: 1-palmitoyl-2-(2,4-(*E,E*)-octadecadienoyl)-*sn*-glycero-3-phosphocholine

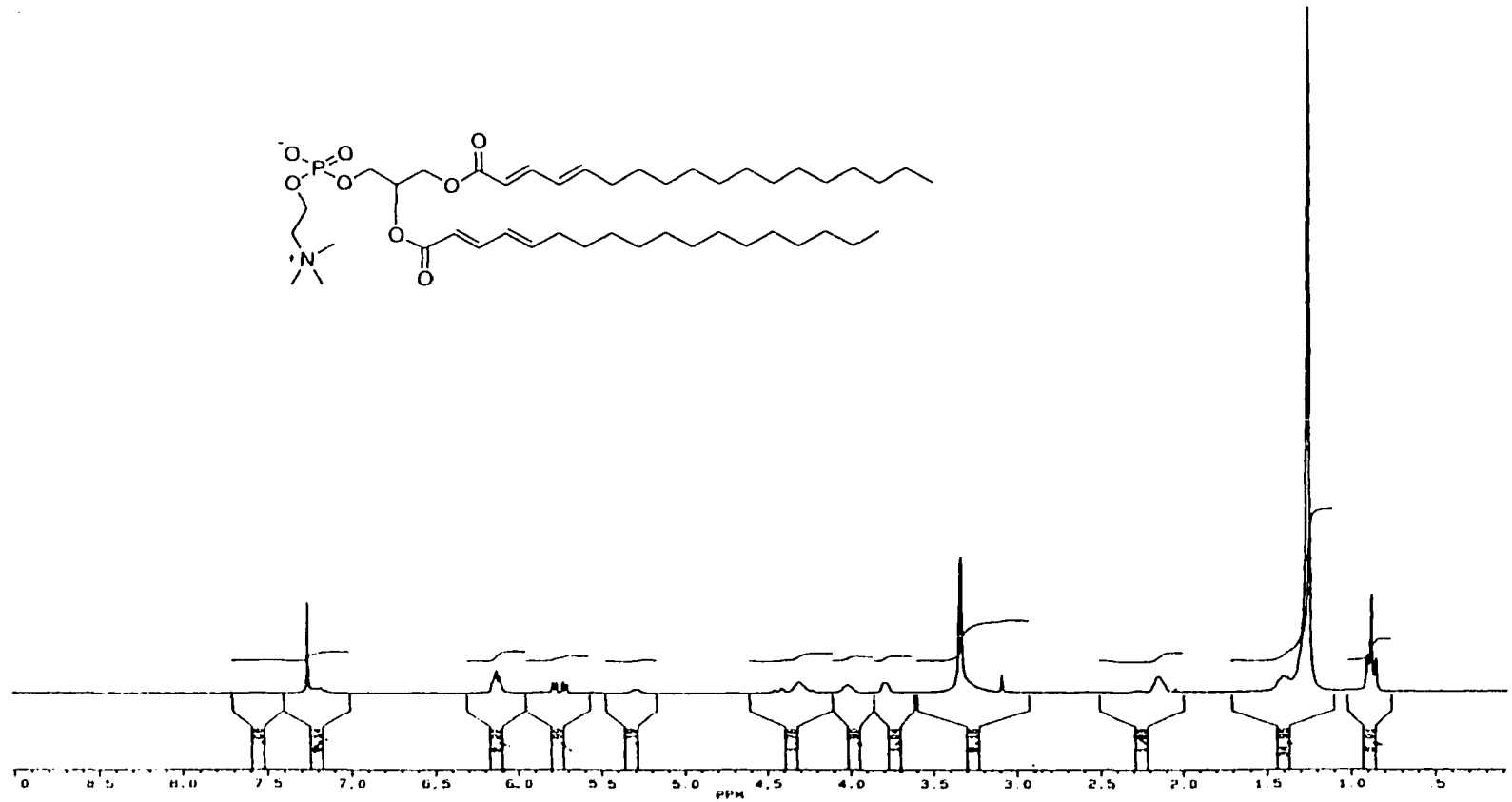

Figure A-6: ^{1}H NMR of Compound **2-12**: 1,2-bis[2,4-(*E,E*)-octadecadienoyl]-*sn*-glycero-3-phosphocholine

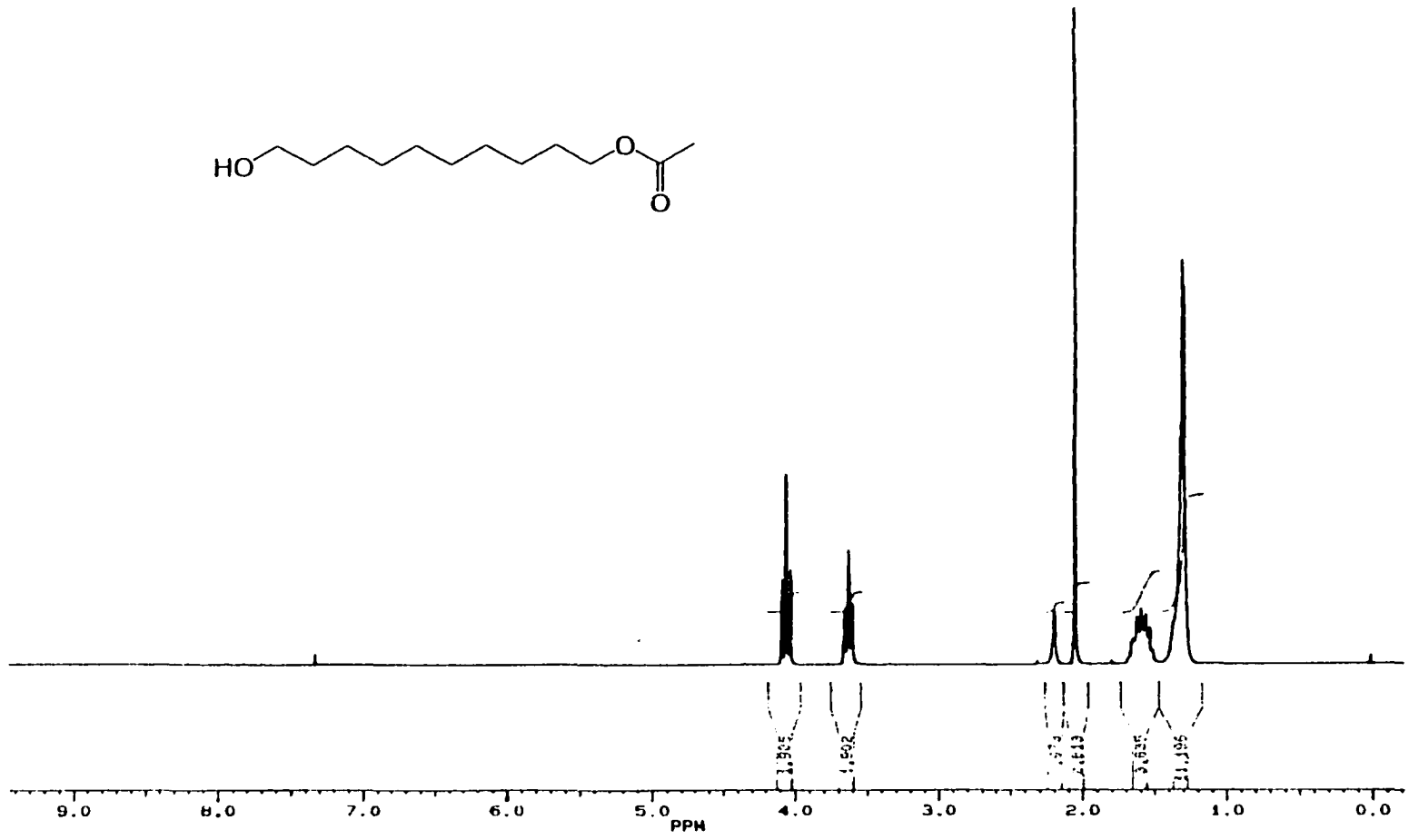

Figure A-7: ^{1}H NMR of Compound **3-13c**: 10-(Acetyloxy)decan-1-ol

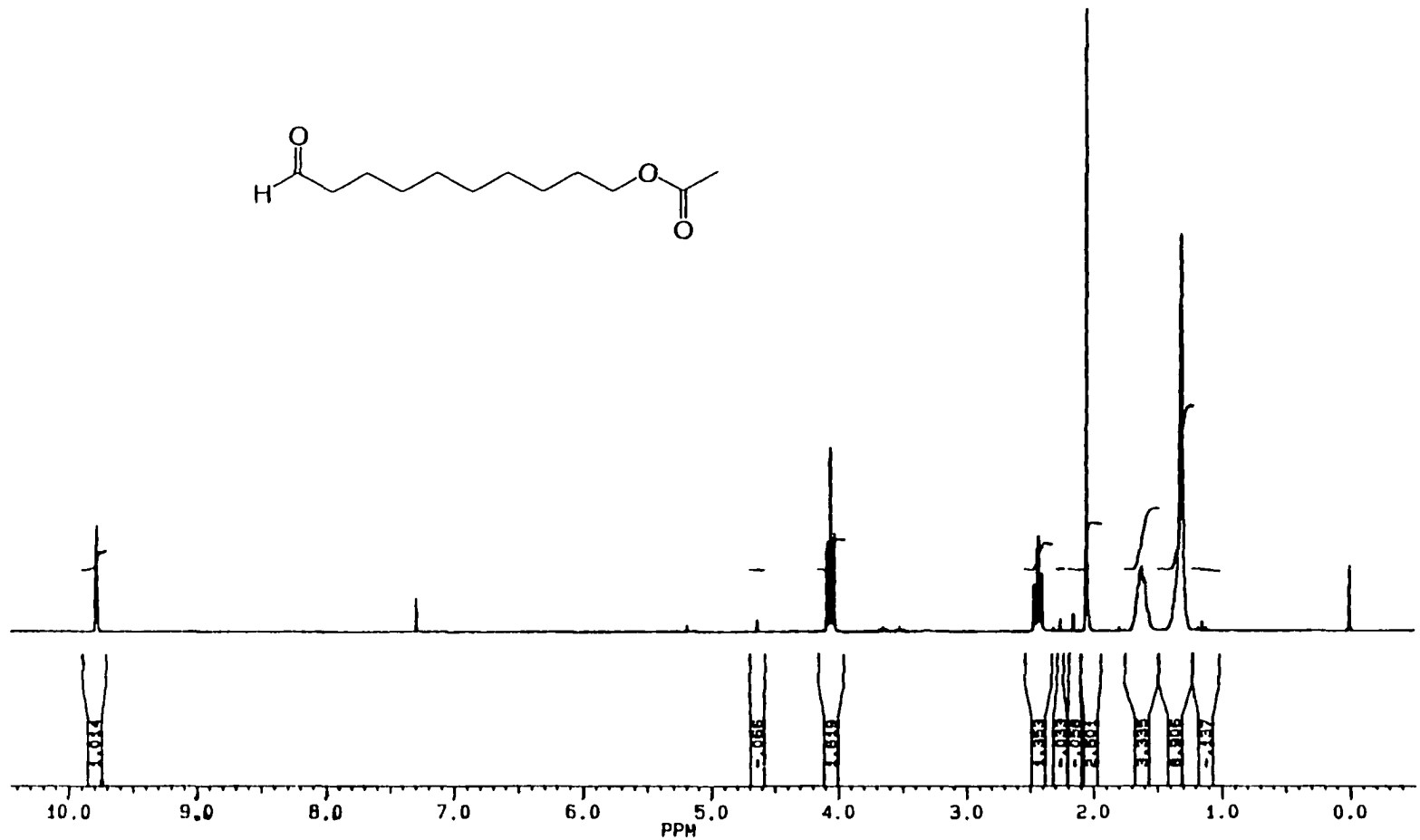

Figure A-8: ^{1}H NMR *of Compound* **3-14c**: 10-(acetyloxy)decan-1-al

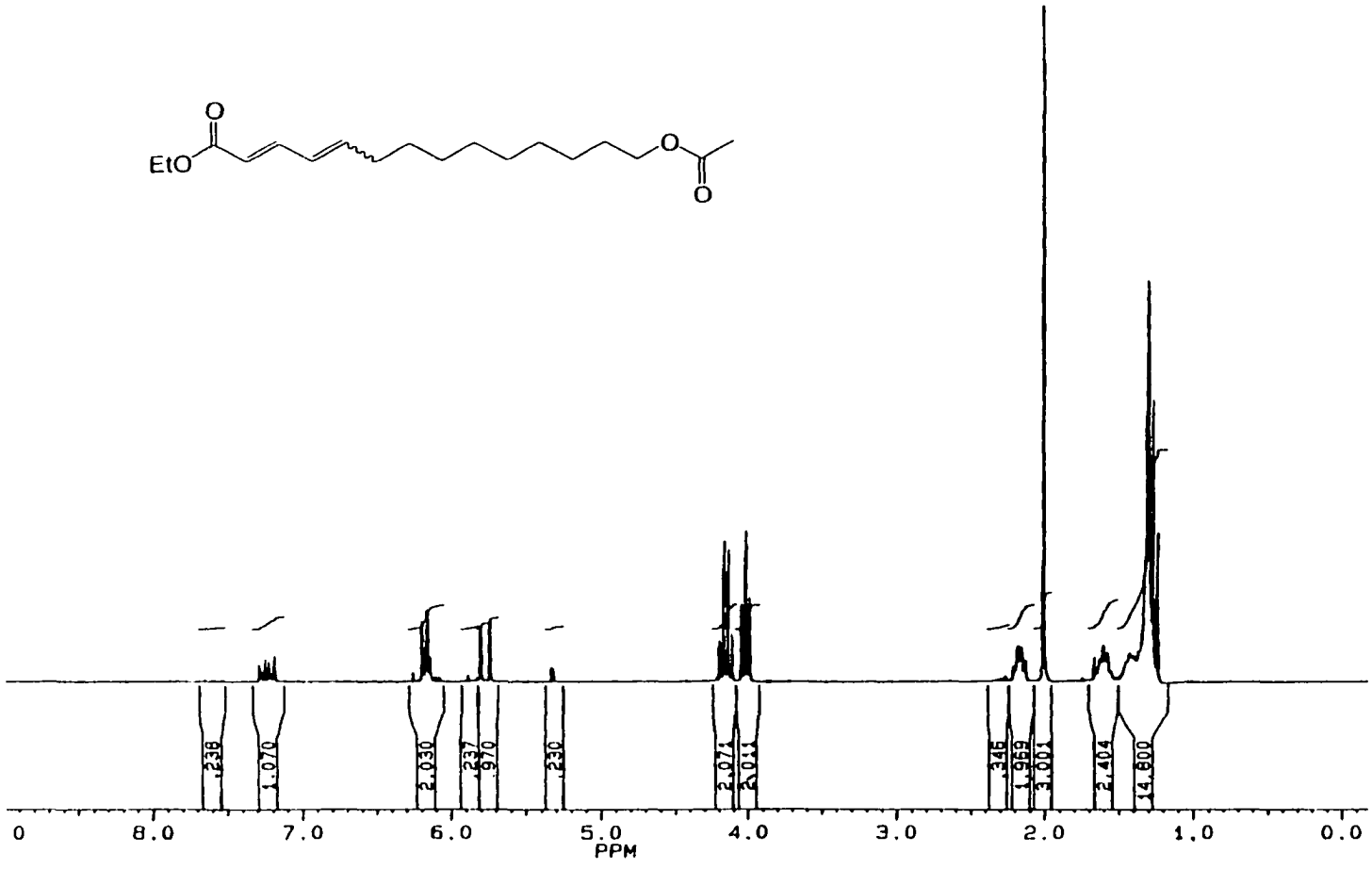

Figure A-9: ^{1}H NMR of Compound **3-15c**: ethyl 10-acetyloxy-2,4-tetradecadienoate

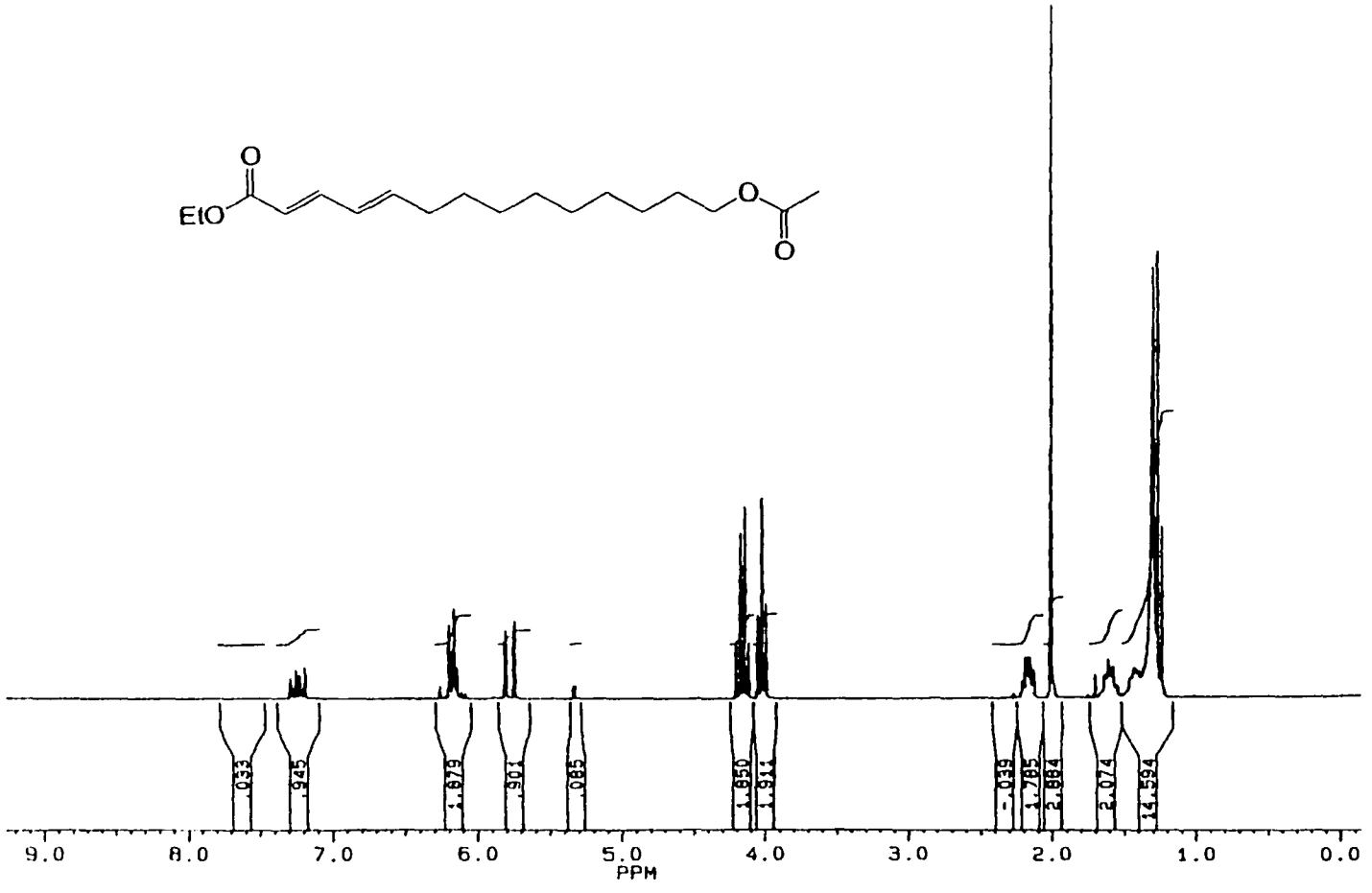

Figure A-10: ^{1}H NMR of Compound **3-16c**: ethyl 10-acetyloxy-(*E*,*E*)-2,4-tetradecadienoate

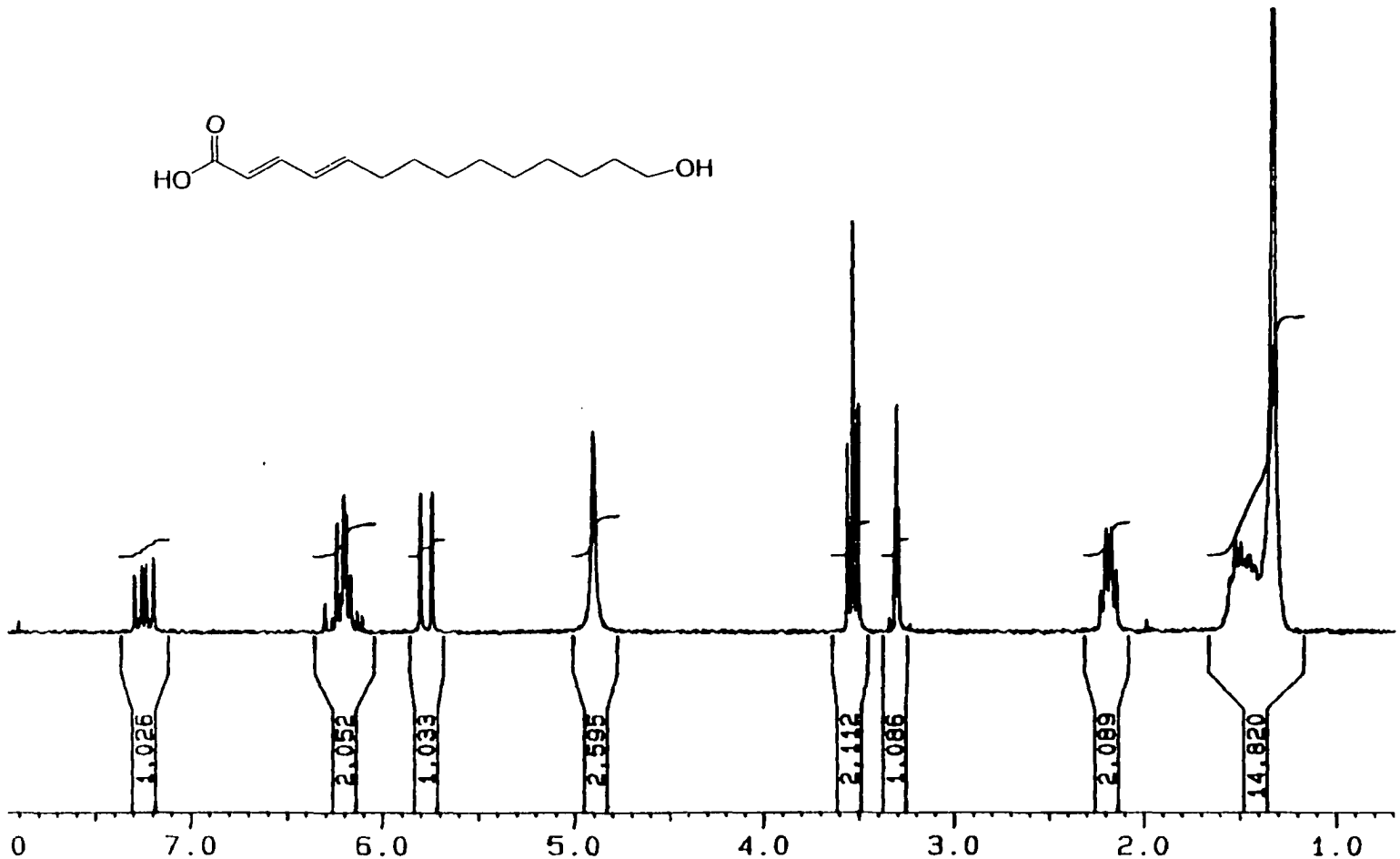

Figure A-11: ^{1}H NMR of Compound **3-17c**: 14-(hydroxy)-2,4-tetradecadienoic acid

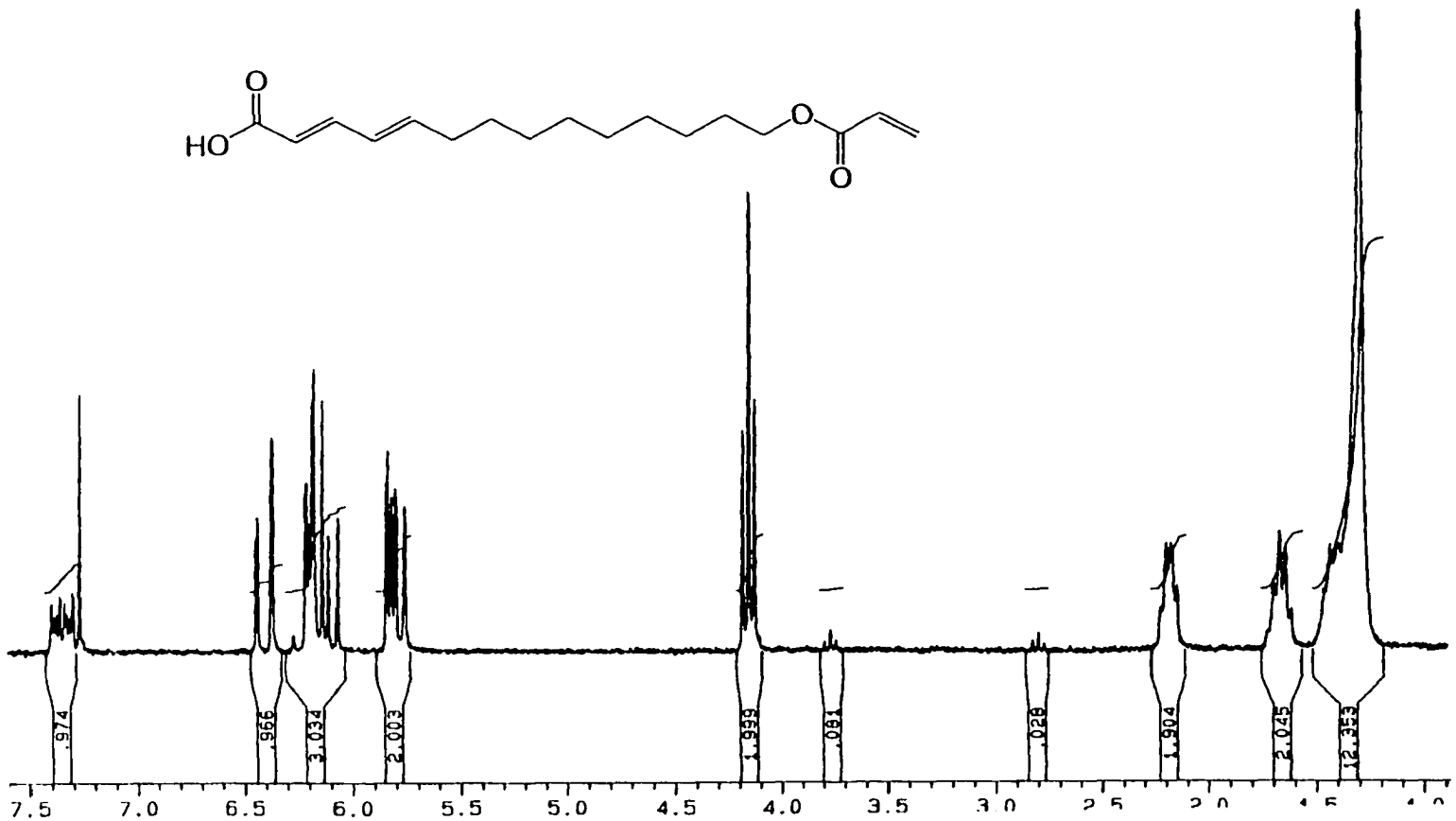

Figure A-12: ^{1}H NMR of Compound **3-18c**: 14-acryloxy-2,4-tetradecadienoic acid (Acryl/Den acid)

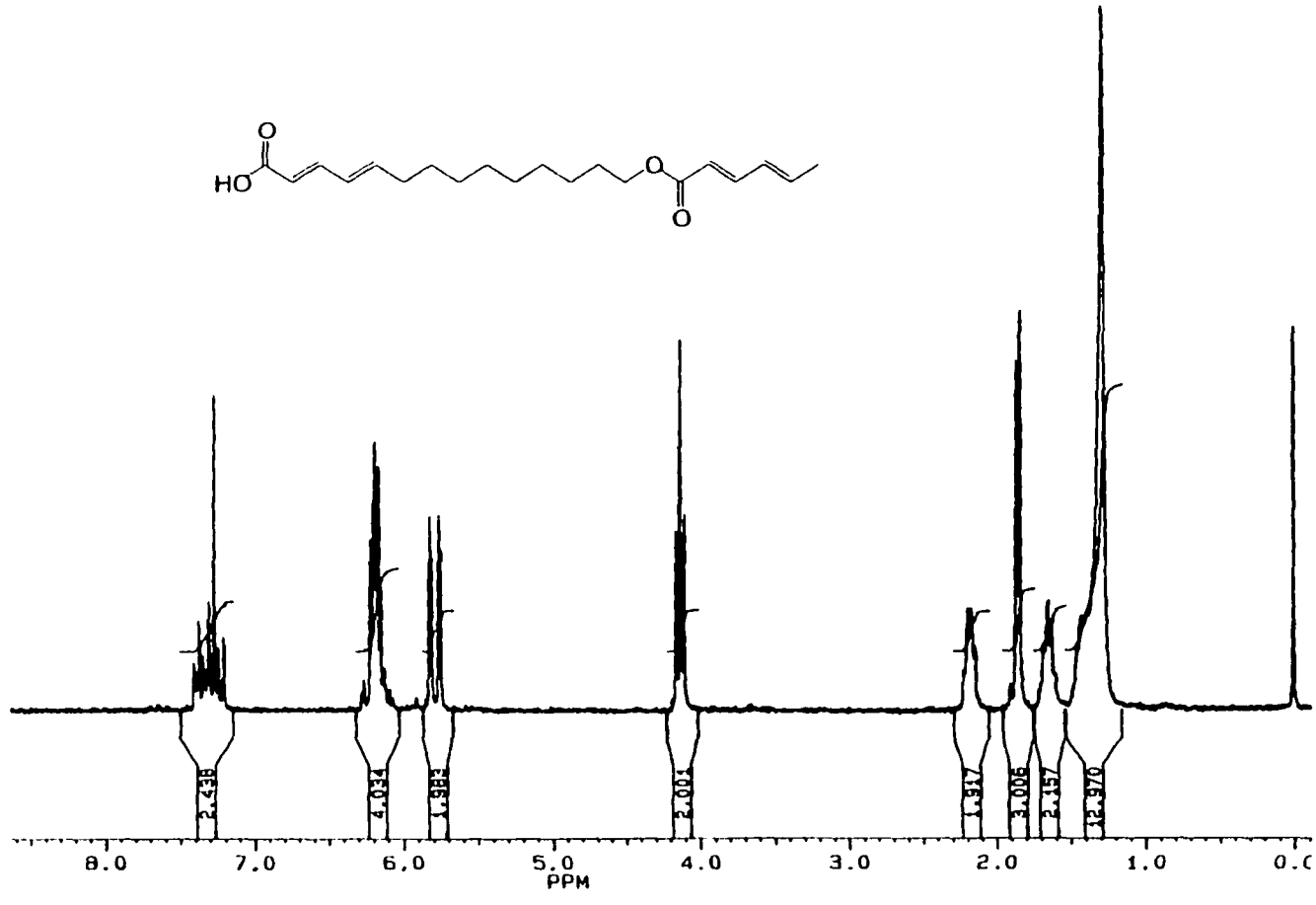

Figure A-13: ^{1}H NMR of Compound **3-19c**: 14-sorbyl-2,4-tetradecadienoic acid (Sorbyl/Den acid)

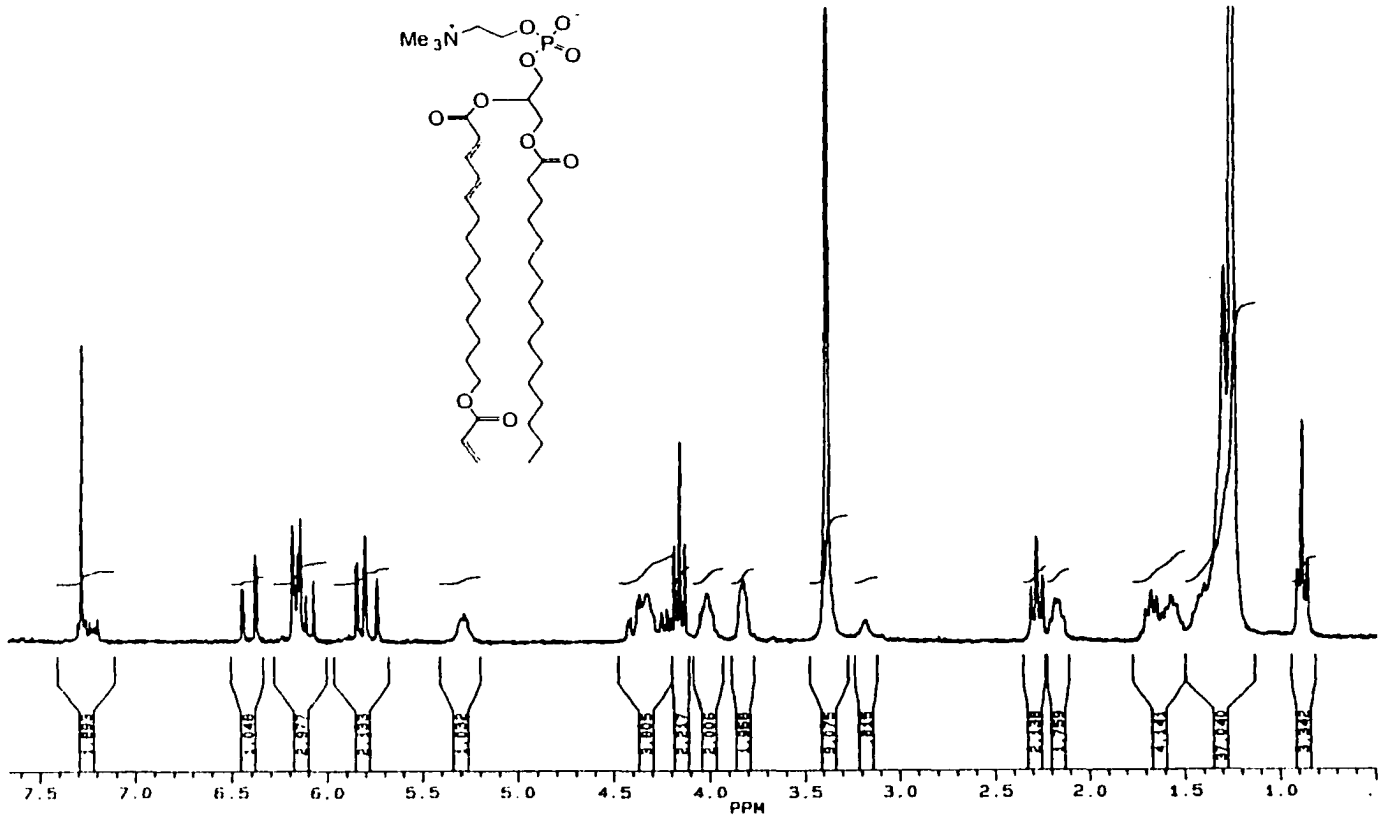

Figure A-14: ^{1}H NMR of Compound **3-11c**: 1-palmitoyl-2-[14-acryloxy-2,4-tetradecadienoic]-*sn*-glycerol-3-phosphocholine (Acryl/Den $PC_{16,18}$)

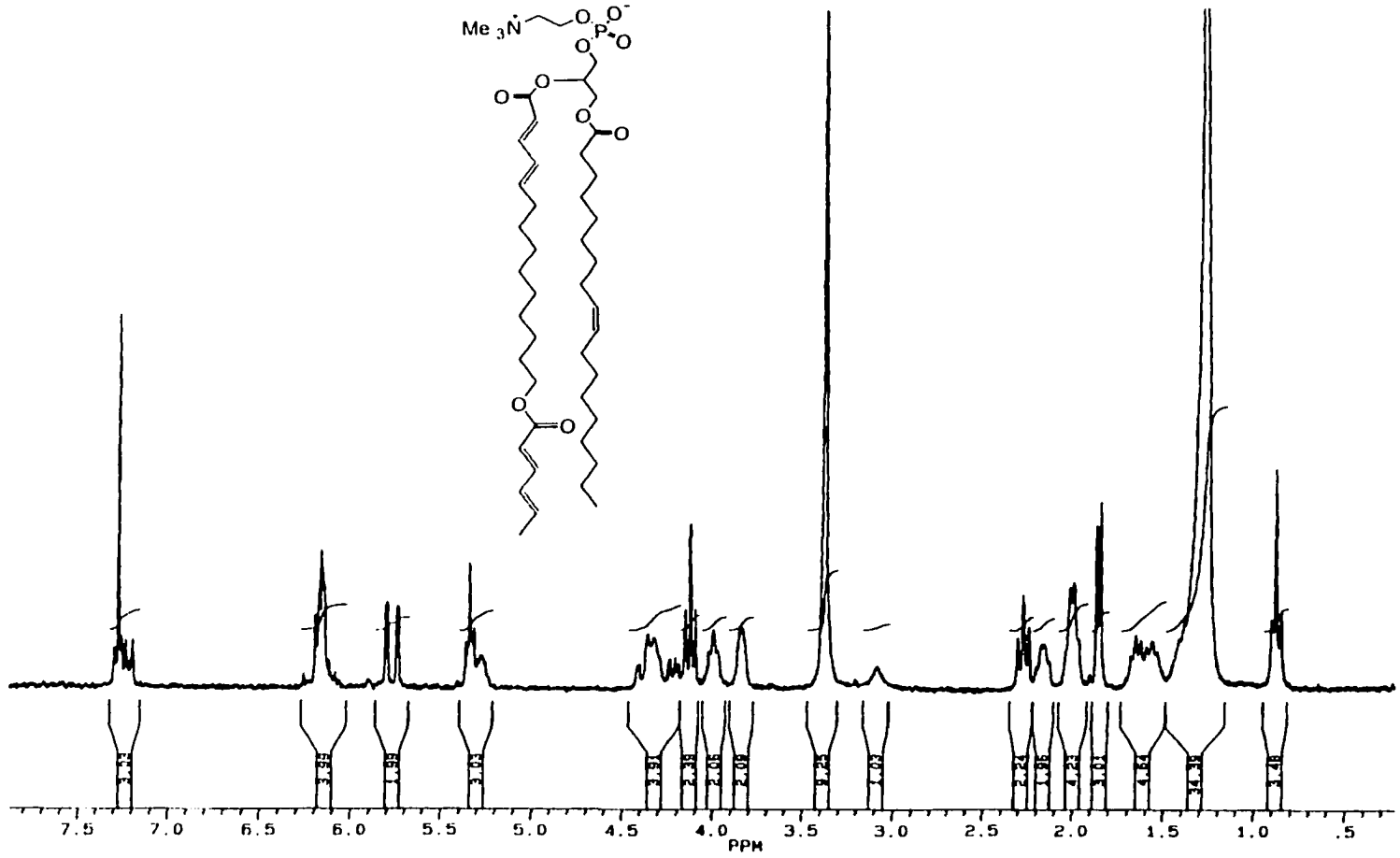

Figure A-15: ^{1}H NMR of Compound **3-12c**: 1-oleoyl-2-[14-sorbyl-2,4-tetradecadienoic]-*sn*-glycero-3-phosphocholine (Sorbyl/Den $PC_{18,21}$)

Appendix B: ^{13}C NMR Spectra

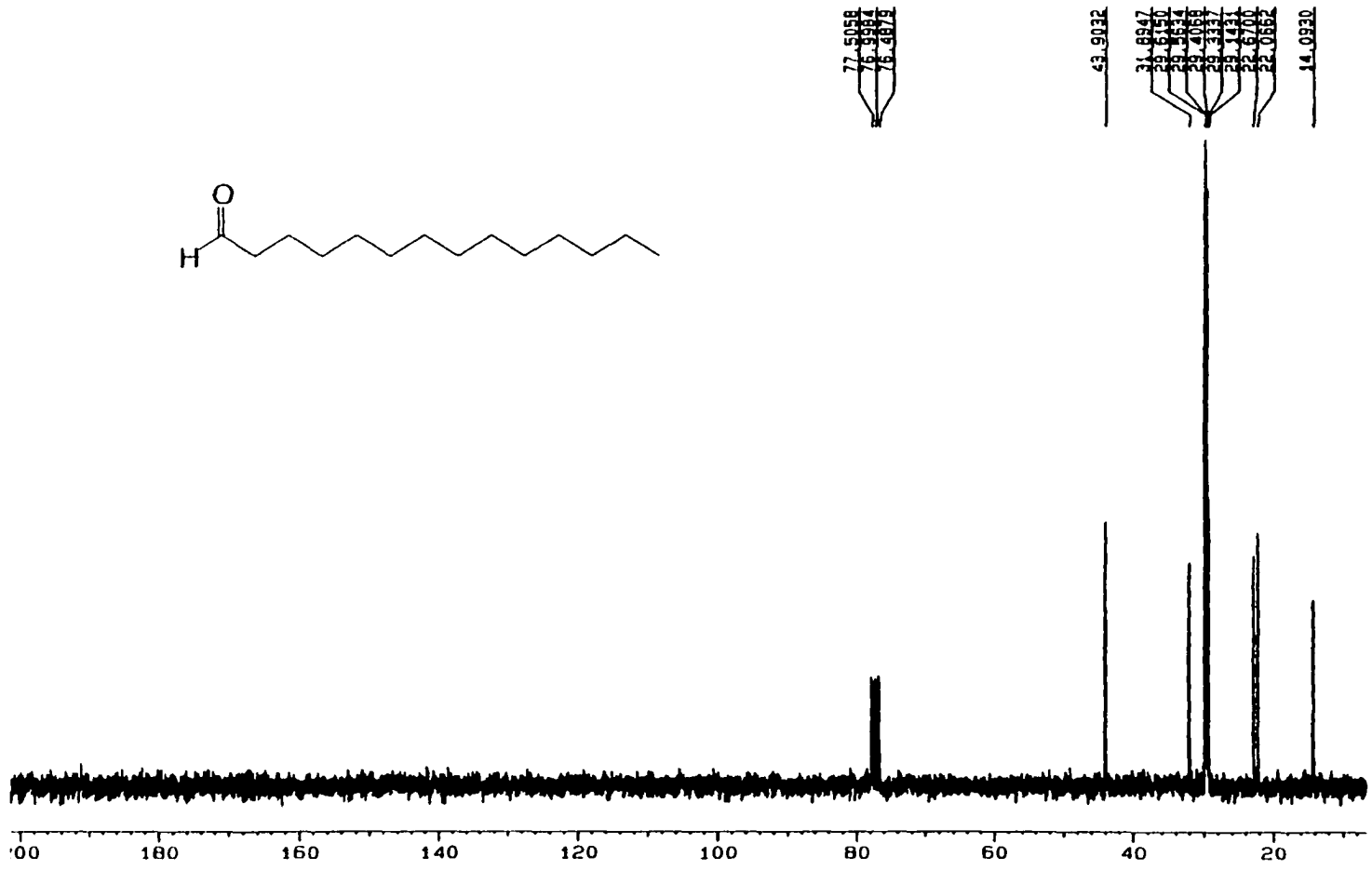

Figure B-1: ^{13}C NMR of Compound **2-18**: tetradecanal

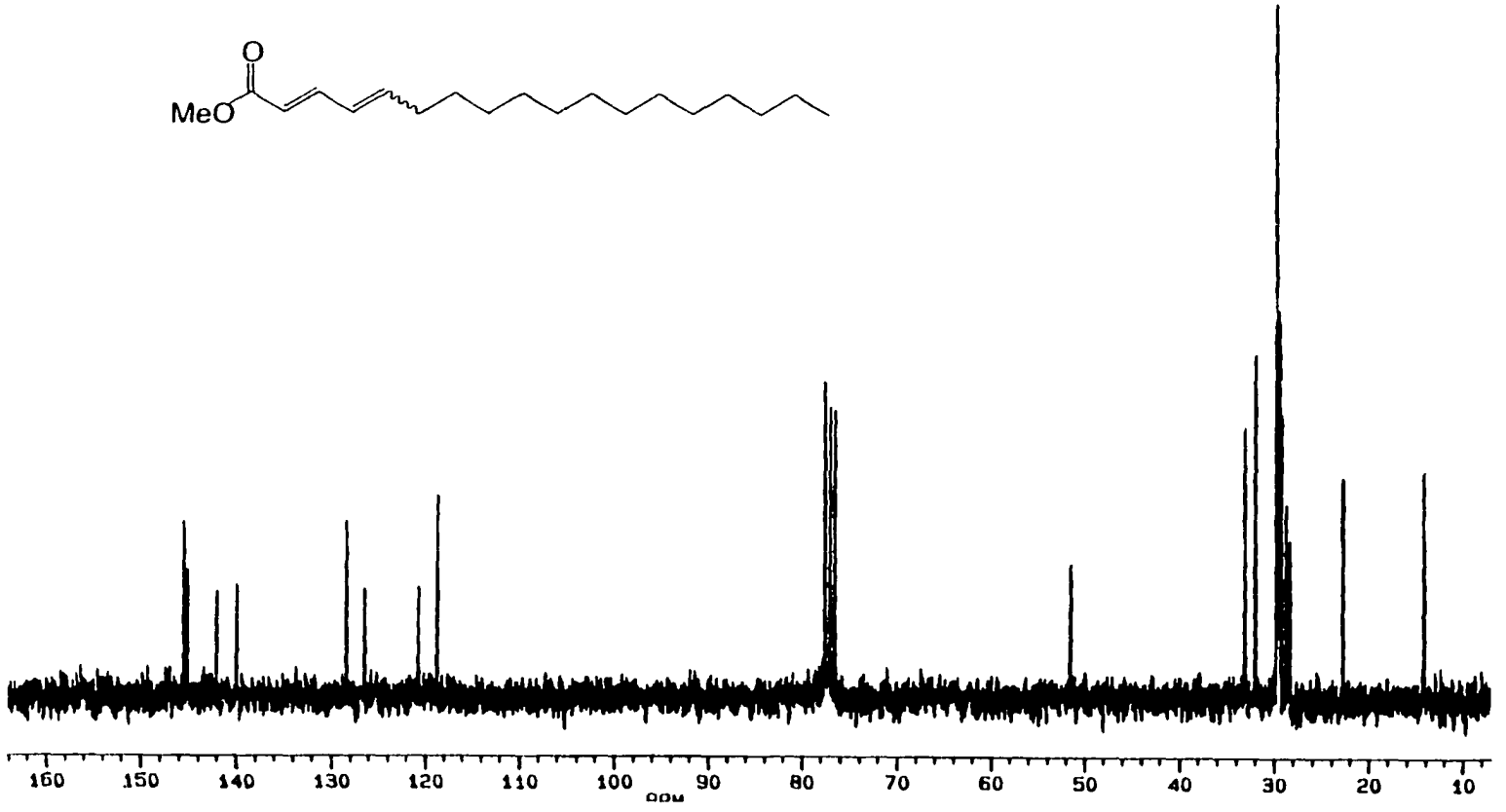

Figure B-2: ^{13}C NMR of Compound **2-19**: methyl 2,4-octadecadienoate

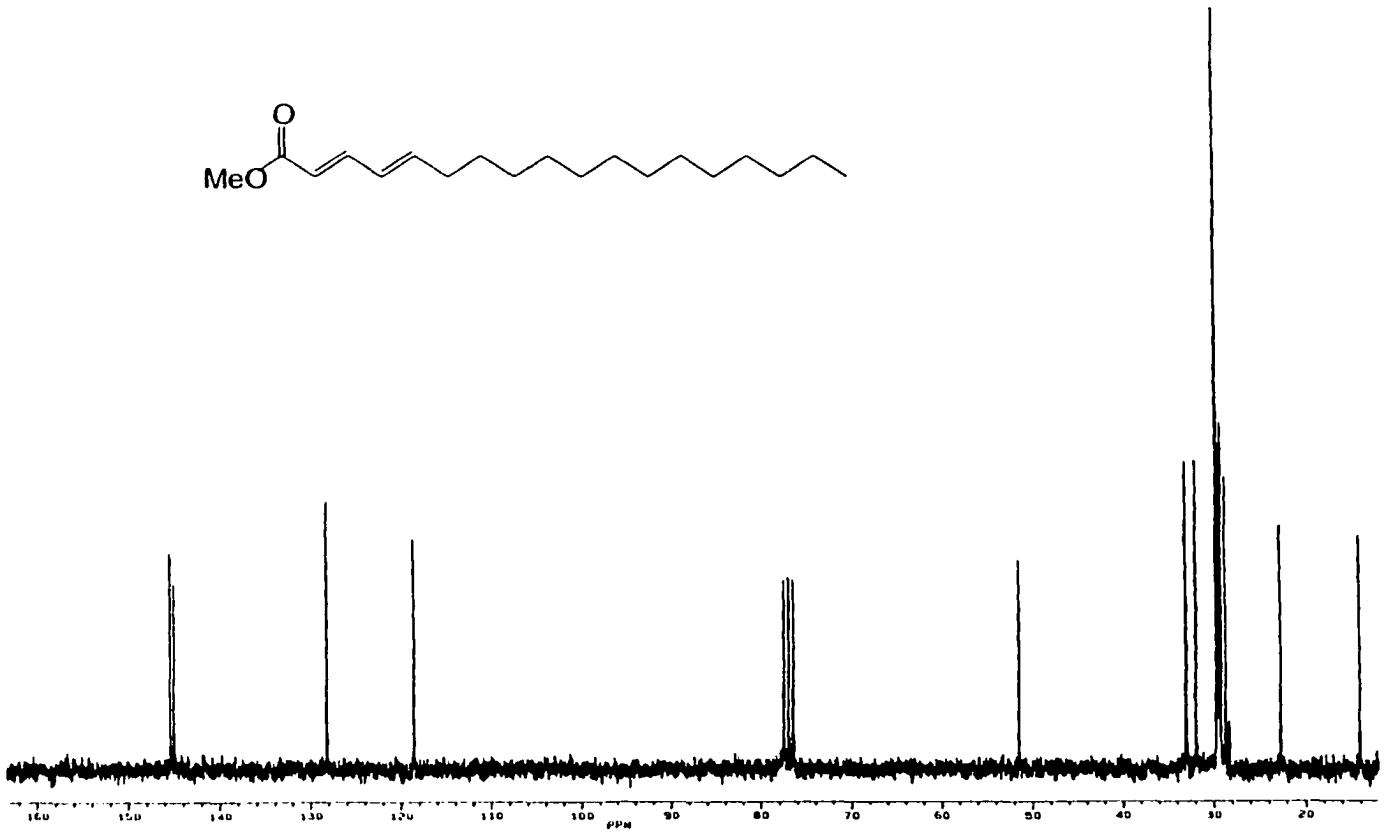

Figure B-3: ^{13}C NMR of Compound **2-20**: methyl (*E,E*)-2,4-octadecadienoate

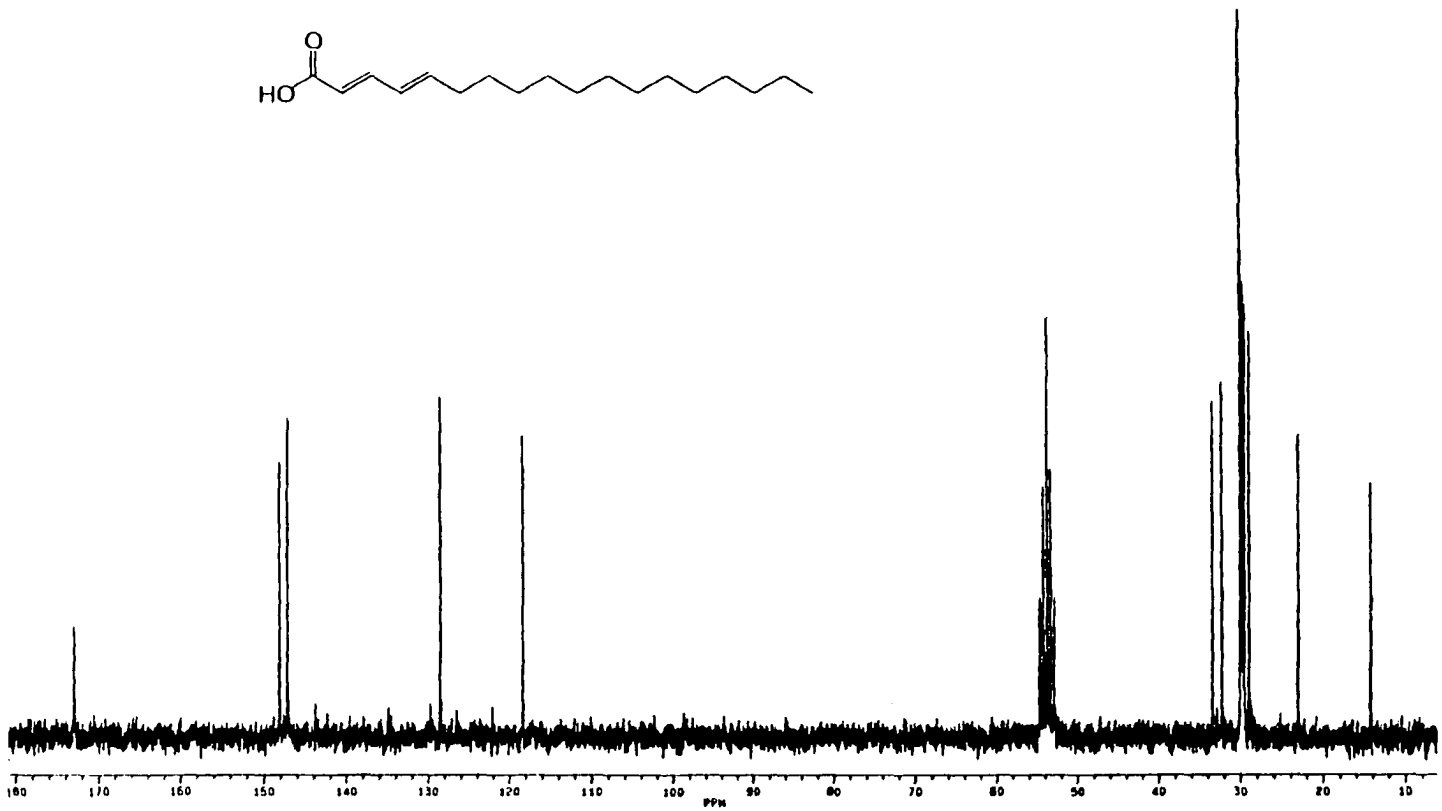

Figure B-4: ^{13}C NMR of Compound **2-21**: 2,4-(*E*,*E*)-octadecadienoic acid

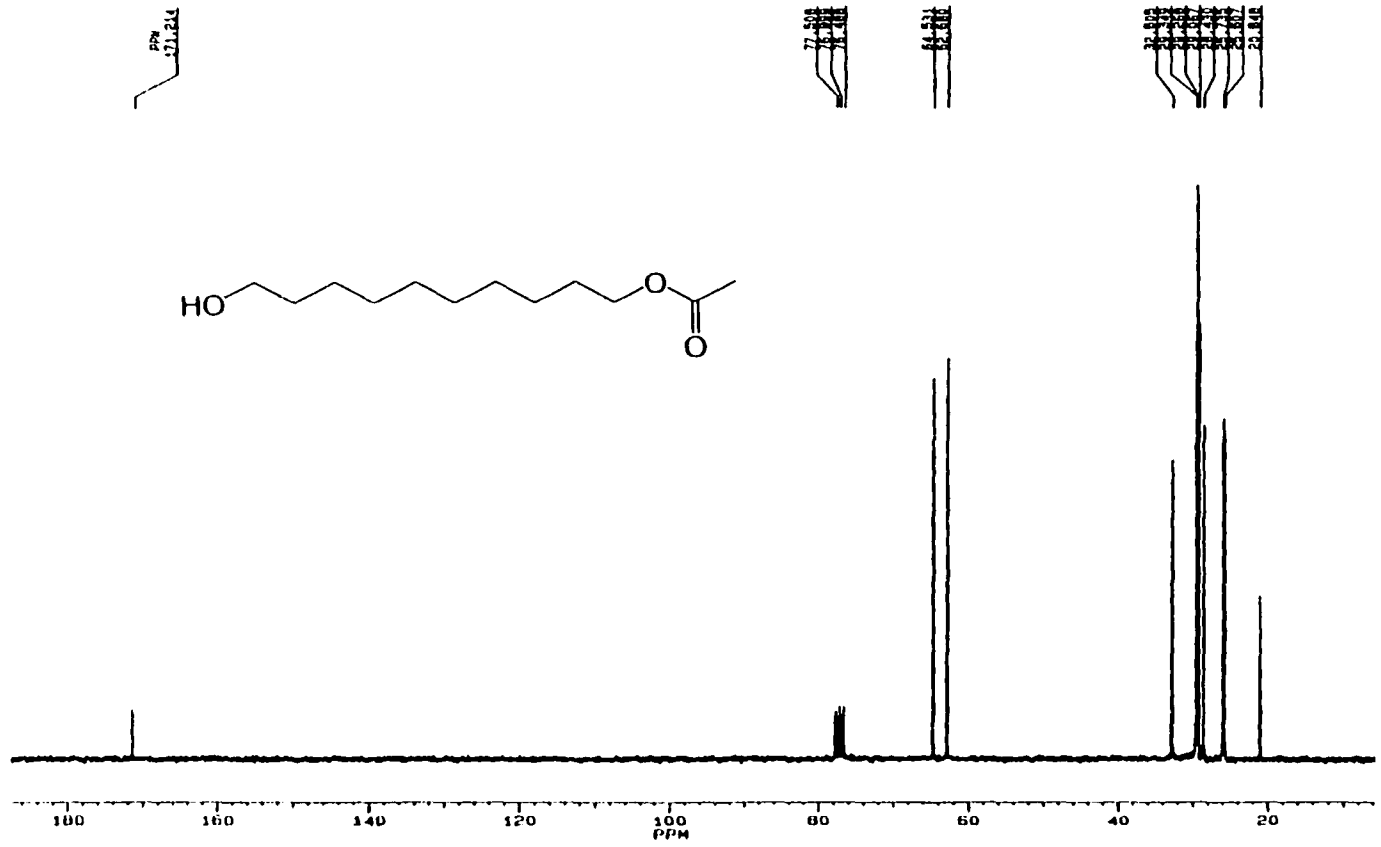

Figure B-5: ^{13}C NMR of Compound **3-13e**: 10-(acetyloxy)decan-1-ol

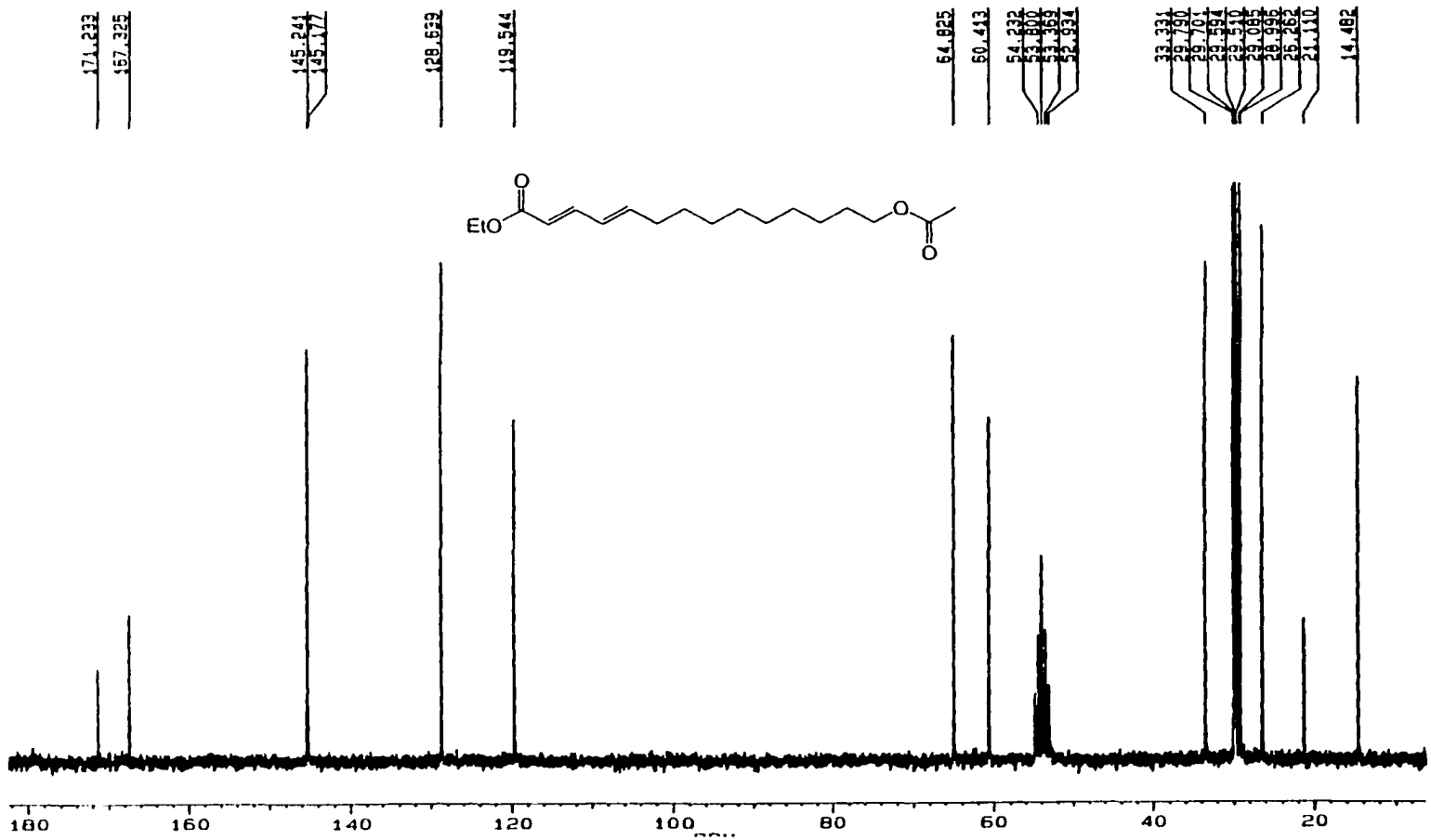

Figure B-6: ^{13}C NMR of Compound **3-16c**: ethyl 14-acetyloxy-(*E*,*E*)-2,4-tetradecadienoate

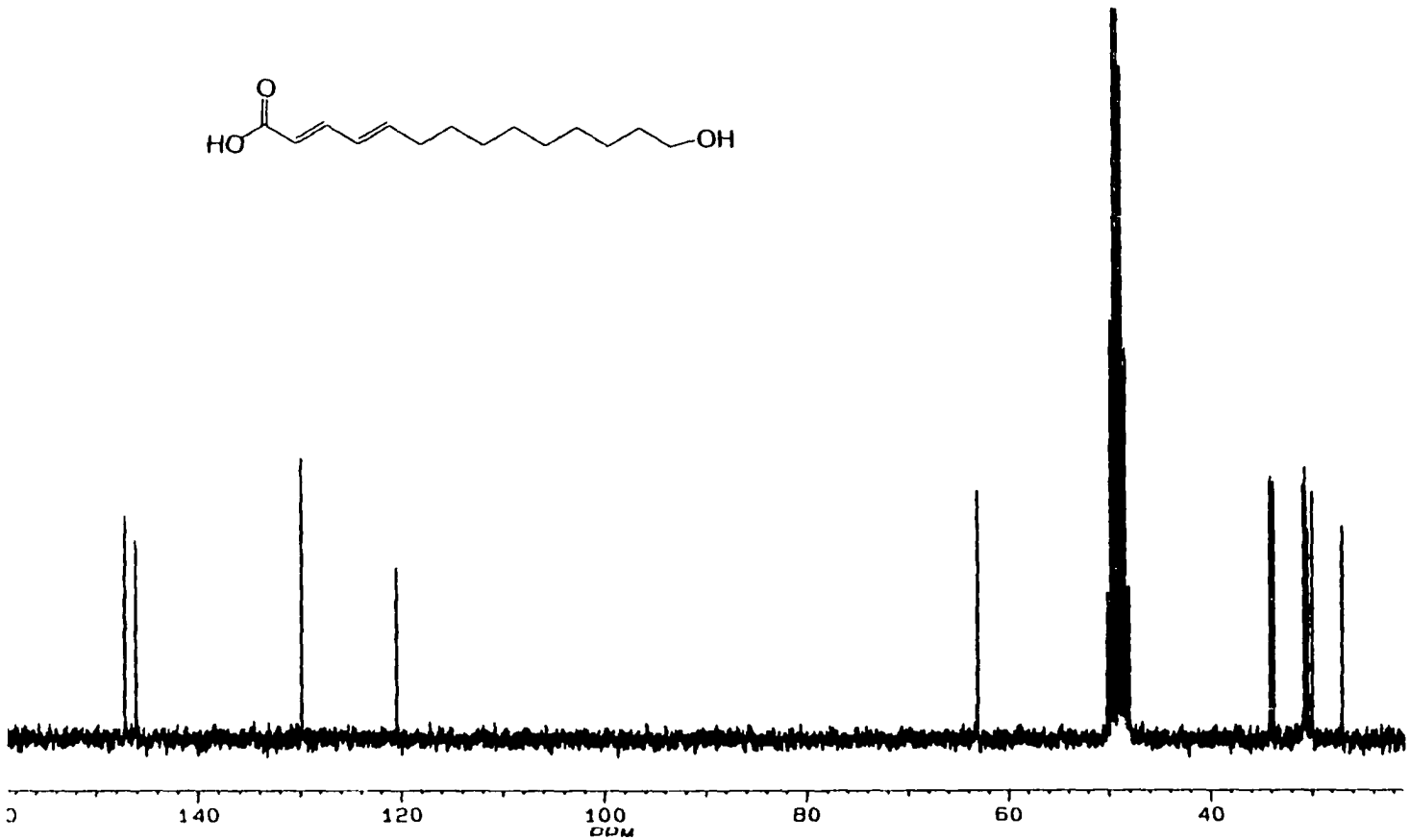

Figure B-7: ^{13}C NMR of Compound **3-17c**: 14-(hydroxy)-2,4-tetradecadienoic acid

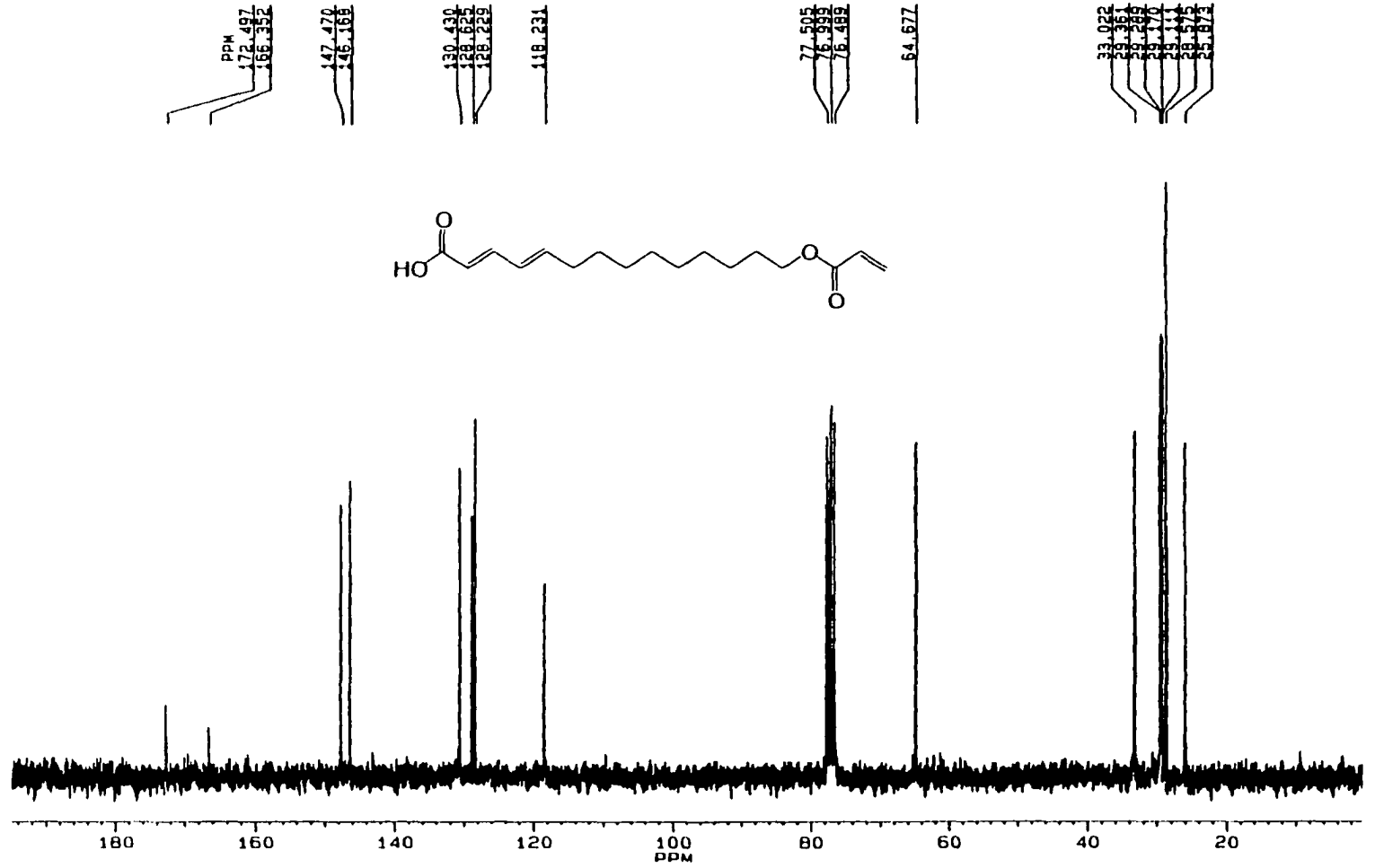

Figure B-8: ^{13}C NMR of Compound **3-18c**: 14-acryloxy-2,4-tetradecadienoic acid (Acryl/Den acid)

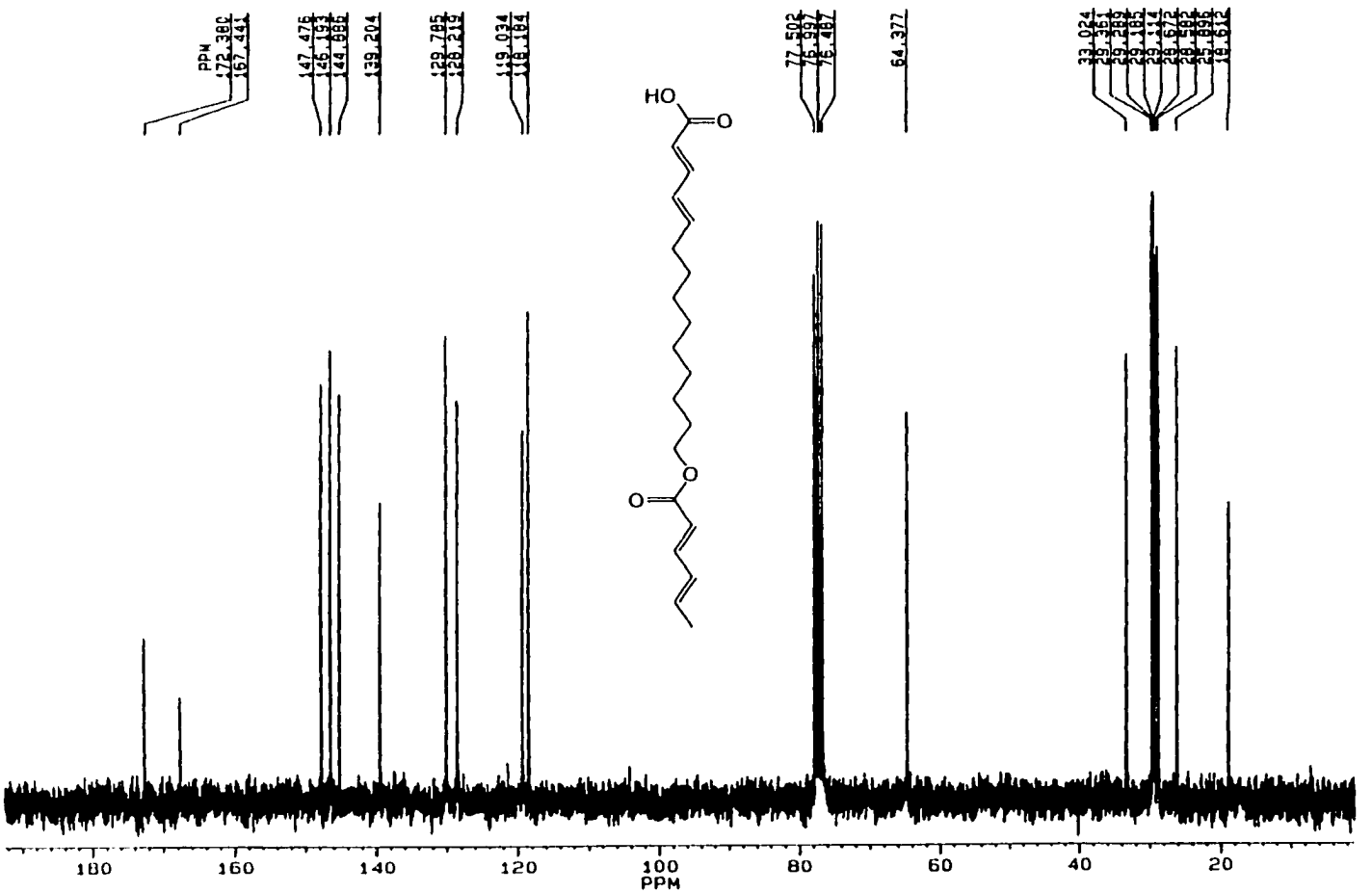

Figure B-9: ^{13}C NMR of Compound **3-19c**: 14-sorbyl-2,4-tetradecadienoic acid (Sorbyl/Den acid)

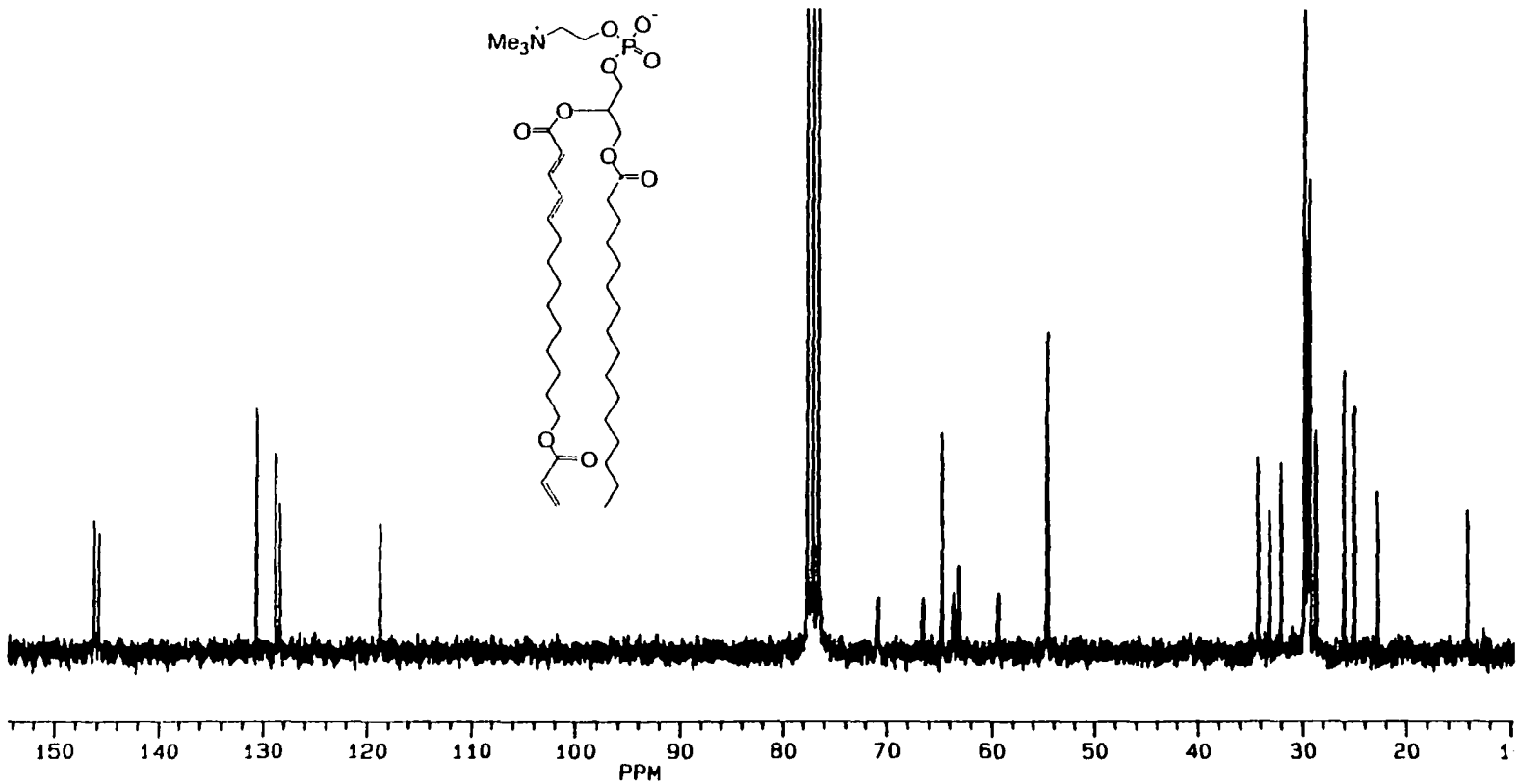

Figure B-10: ^{13}C NMR of Compound **3-11c**: 1-palmitoyl-2-[14-acryloxy-2,4-tetradecadienoic]-*sn*-glycerol-3-phosphocholine (Acryl/Den $PC_{16,18}$)

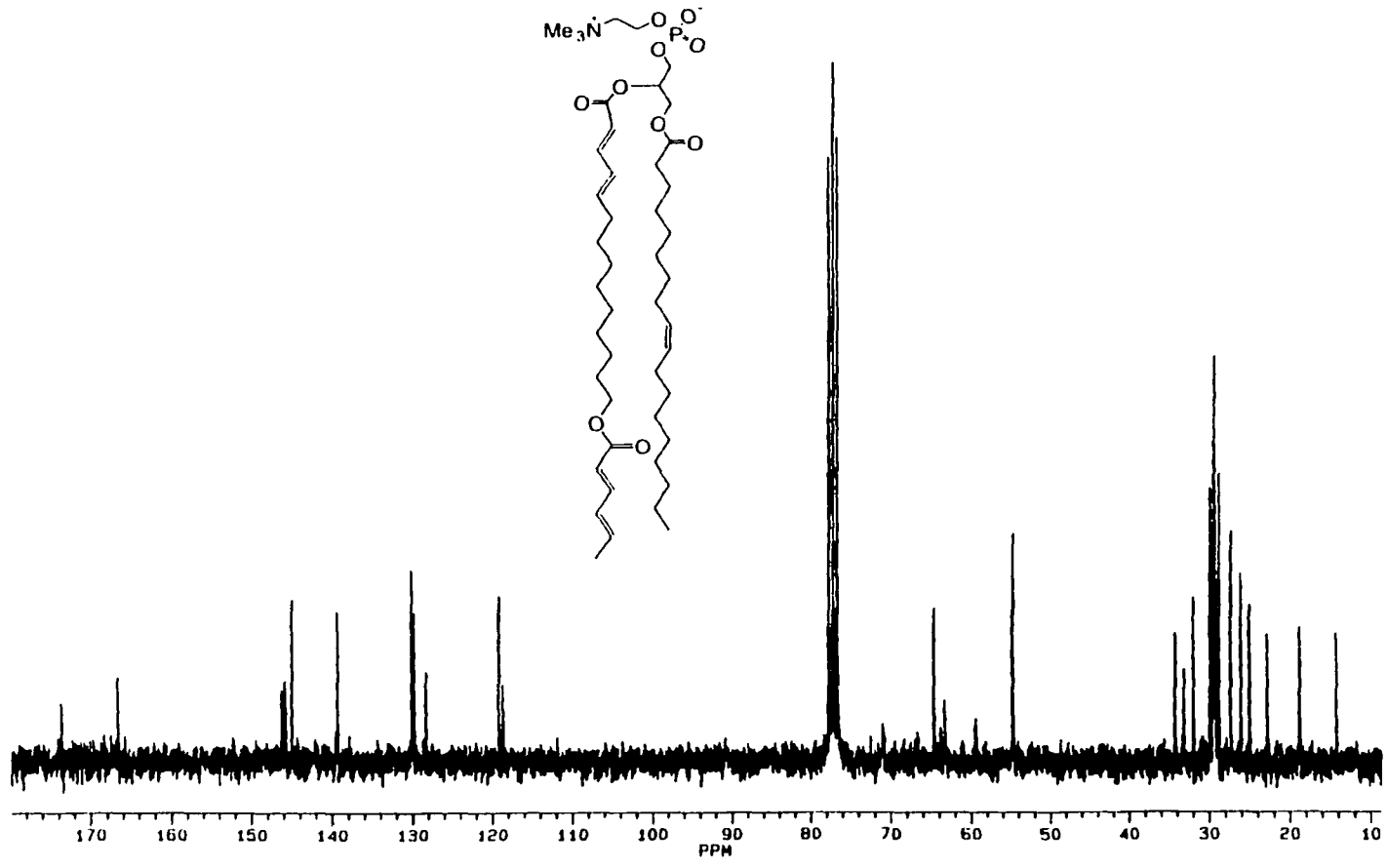

Figure B-11: ^{13}C NMR of Compound **3-12c**: 1-oleoyl-2-[14-sorbyl-2,4-tetradecadienoic]-*sn*-glycero-3-phosphocholine (Sorbyl/Den $PC_{18,21}$)

Appendix C: Mass Spectra

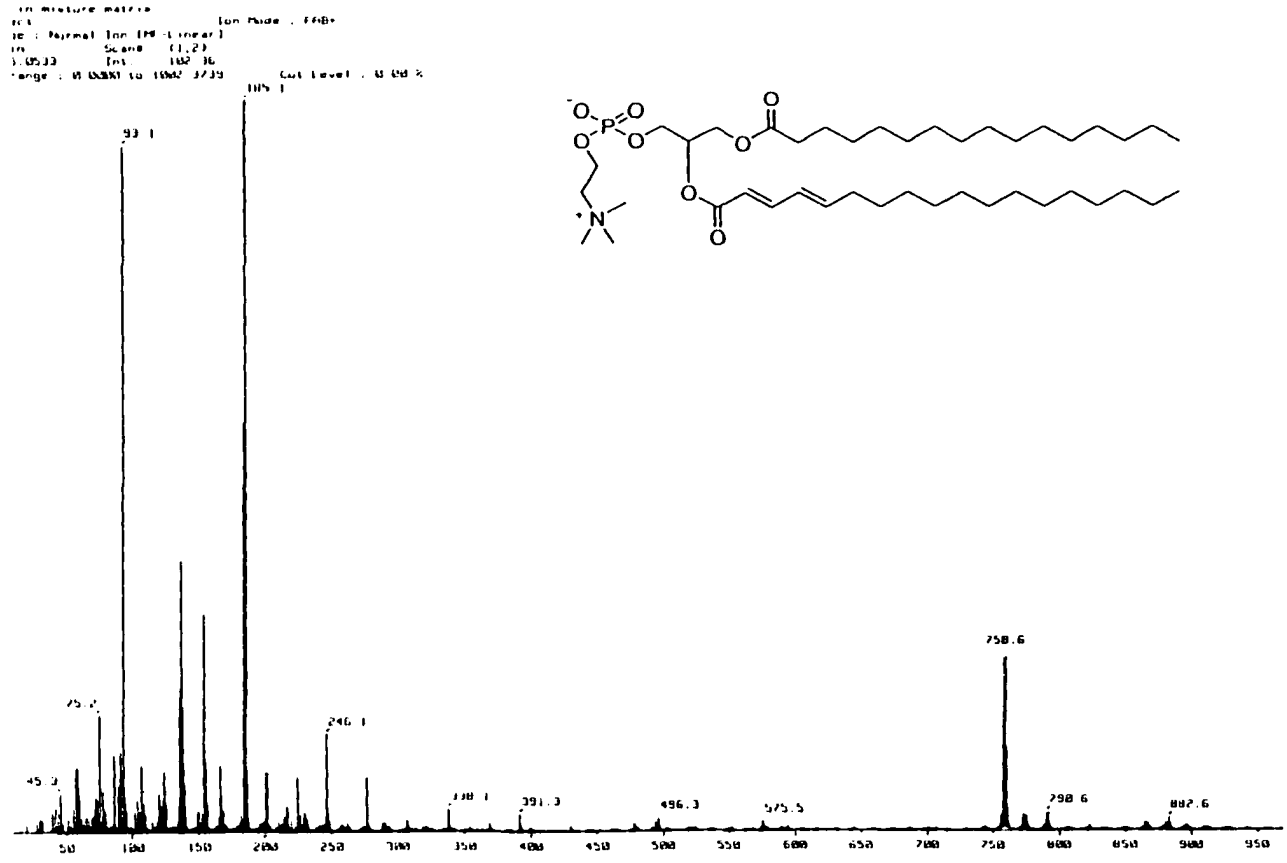

Figure C-1: FAB mass spectrum of Compound **2-11**: 1-palmitoyl-2-(2,4-(*E*,*E*)-octadecadienoyl)-*sn*-glycero-3-phosphocholine

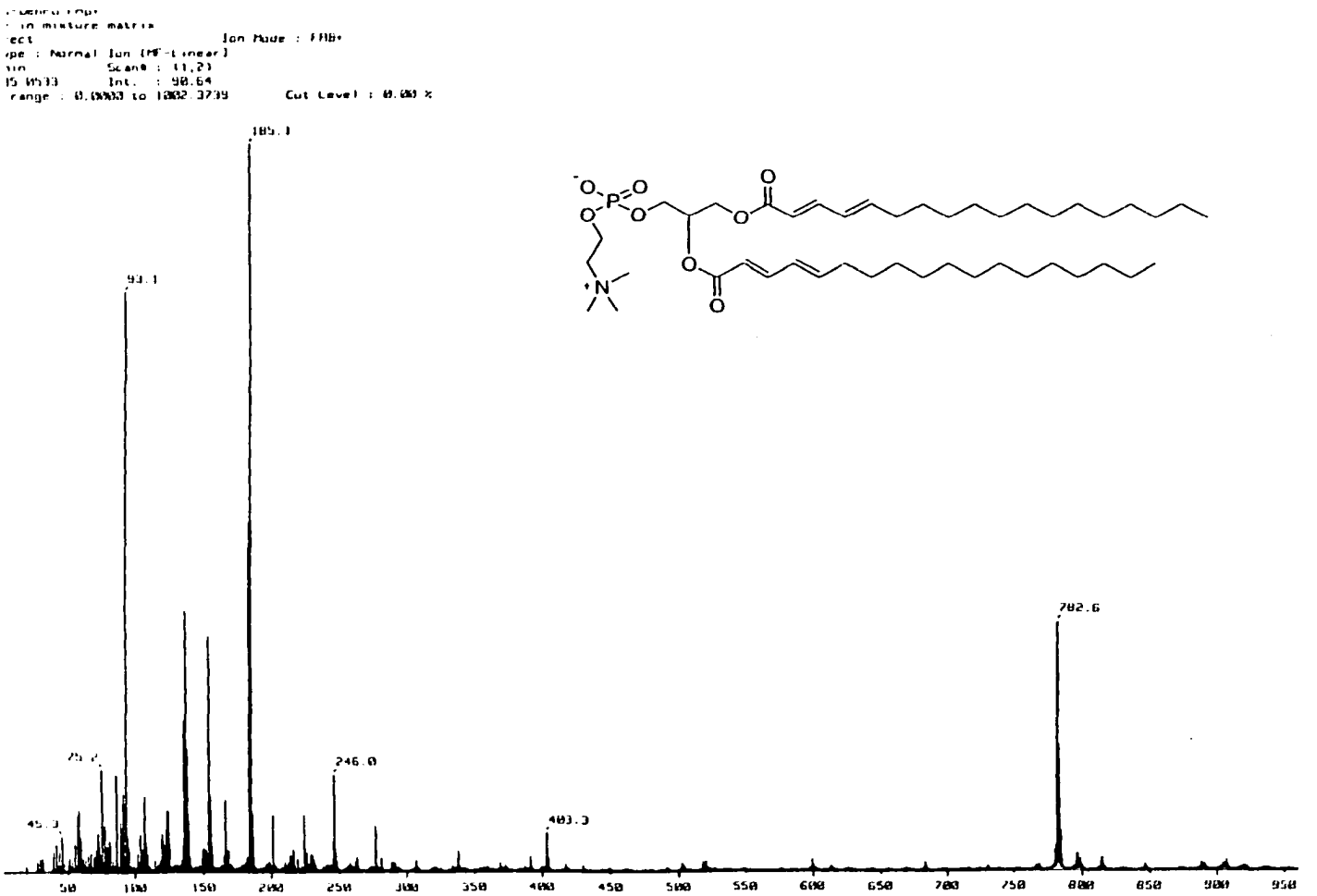

Figure C-2: FAB mass spectrum of Compound **2-12**: 1,2-bis[2,4-(*E,E*)-octadecadienoyl]-*sn*-glycero-3-phosphocholine

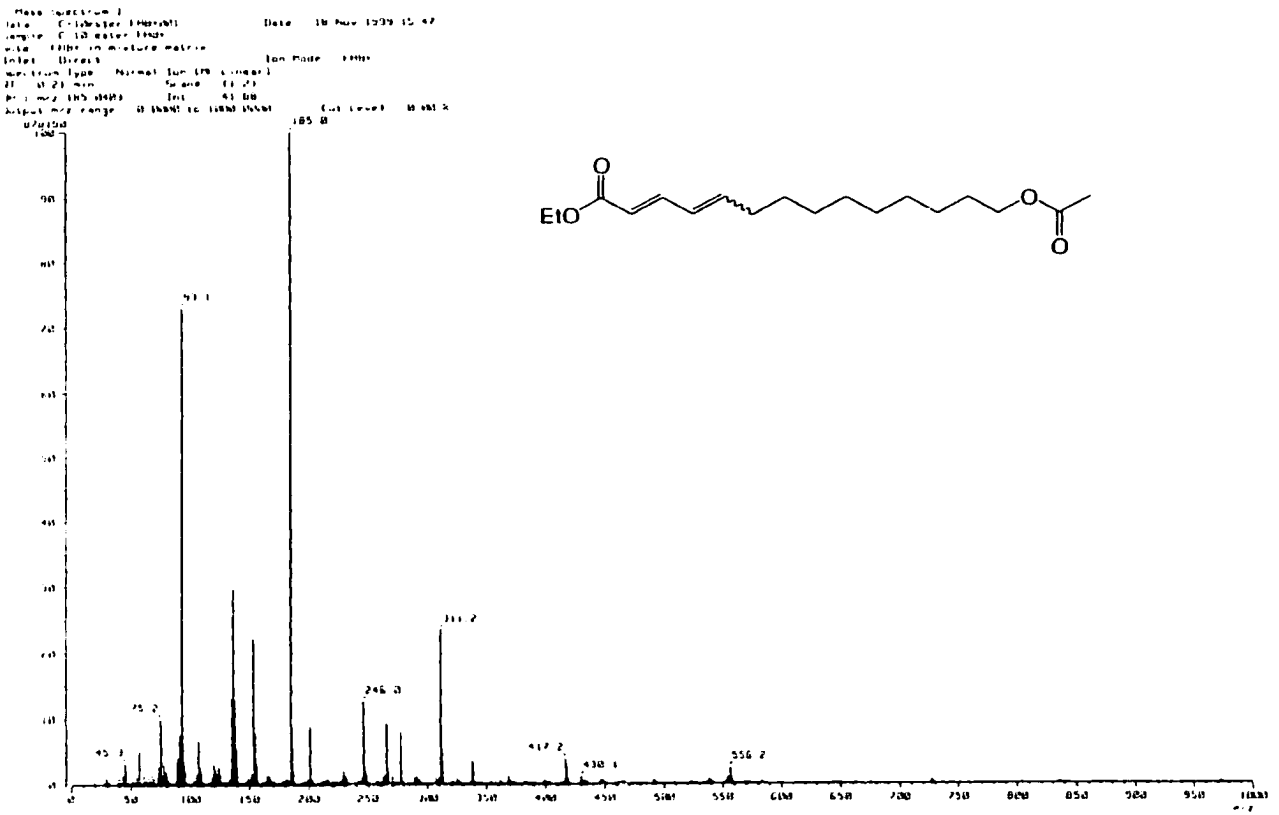

Figure C-3: FAB mass spectrum of Compound **3-15c**: ethyl 14-acetyloxy-2,4-tetradecadienoate

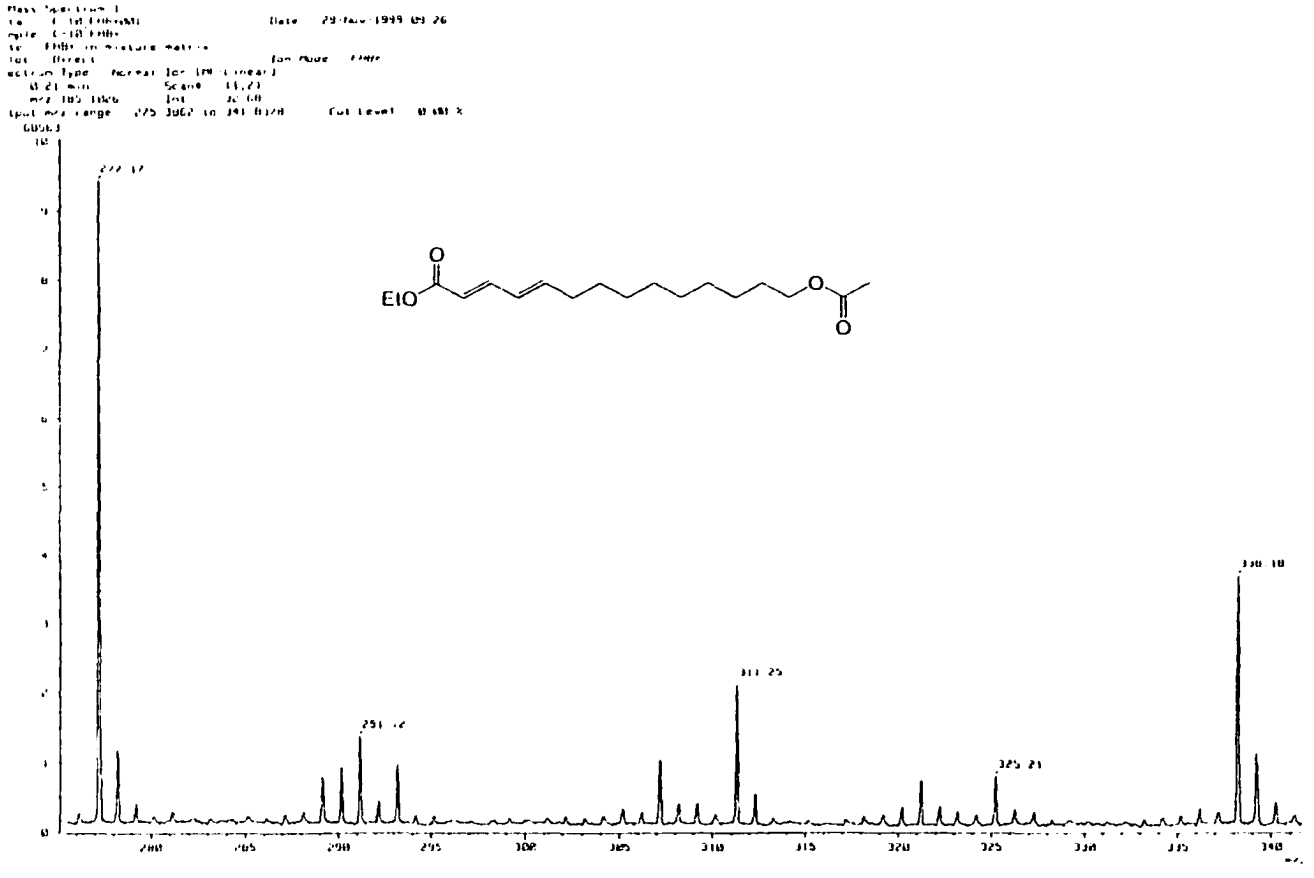

Figure C-4: FAB mass extended spectrum of Compound **3-16c**: ethyl 14-acetyloxy-(*E*,*E*)-2,4-tetradecadienoate

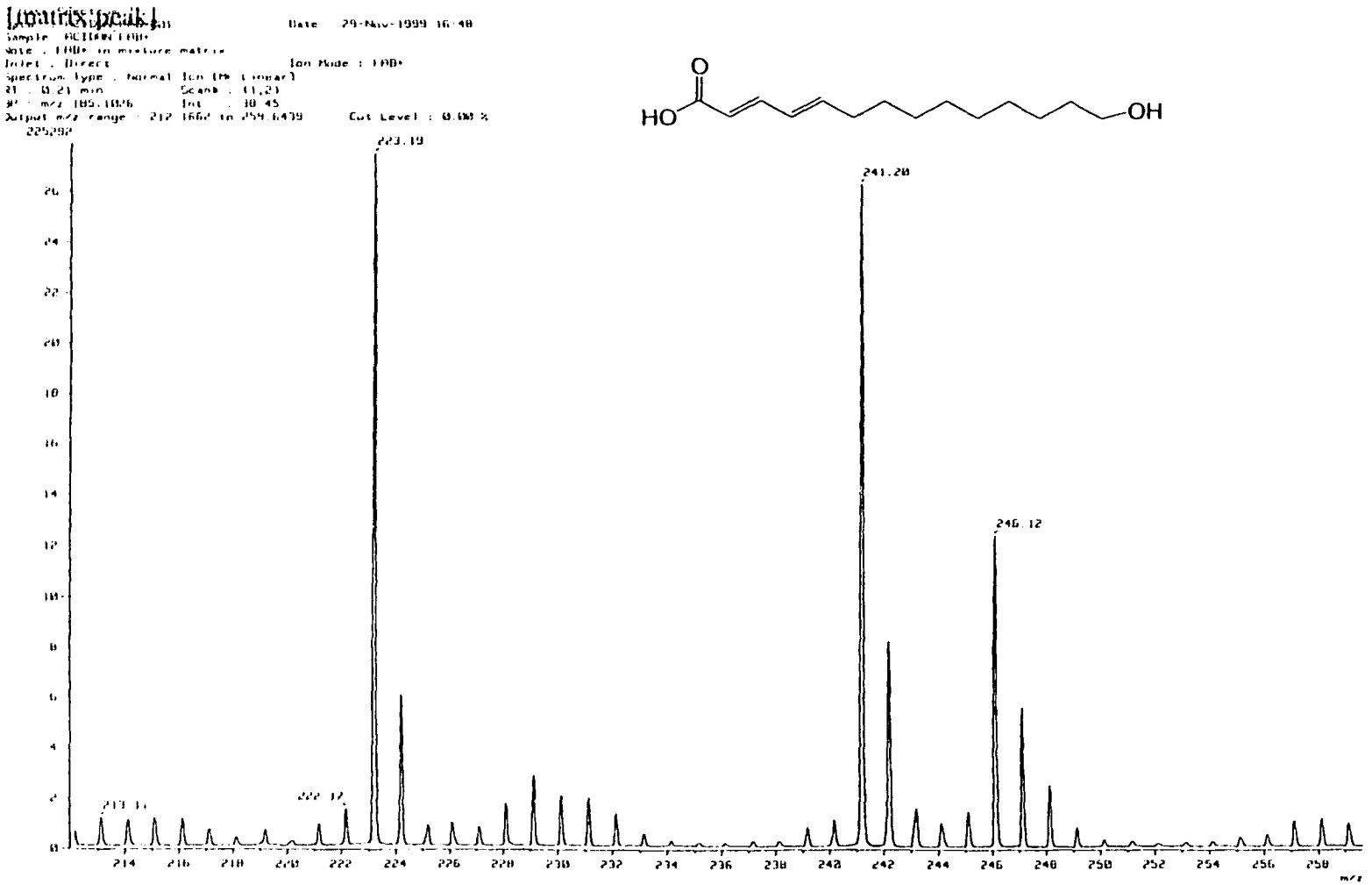

Figure C-5: FAB mass extended spectrum of Compound **3-17c**: 14-hydroxy-2,4-tetradecadienoic acid

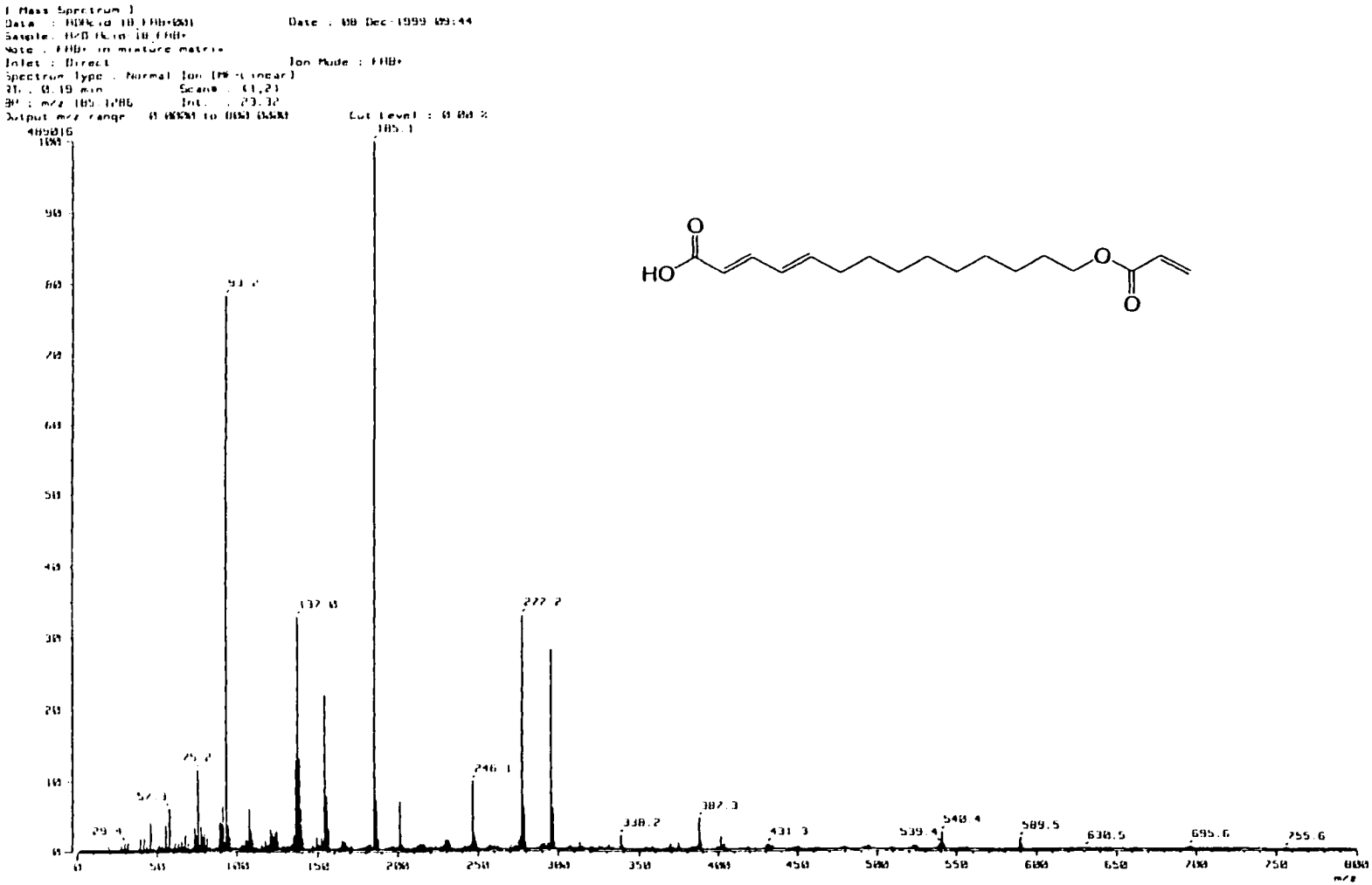

Figure C-6: FAB mass spectrum of Compound **3-18c**: 14-acryloxy-2,4-tetradecadienoic acid (Acryl/Den acid-18)

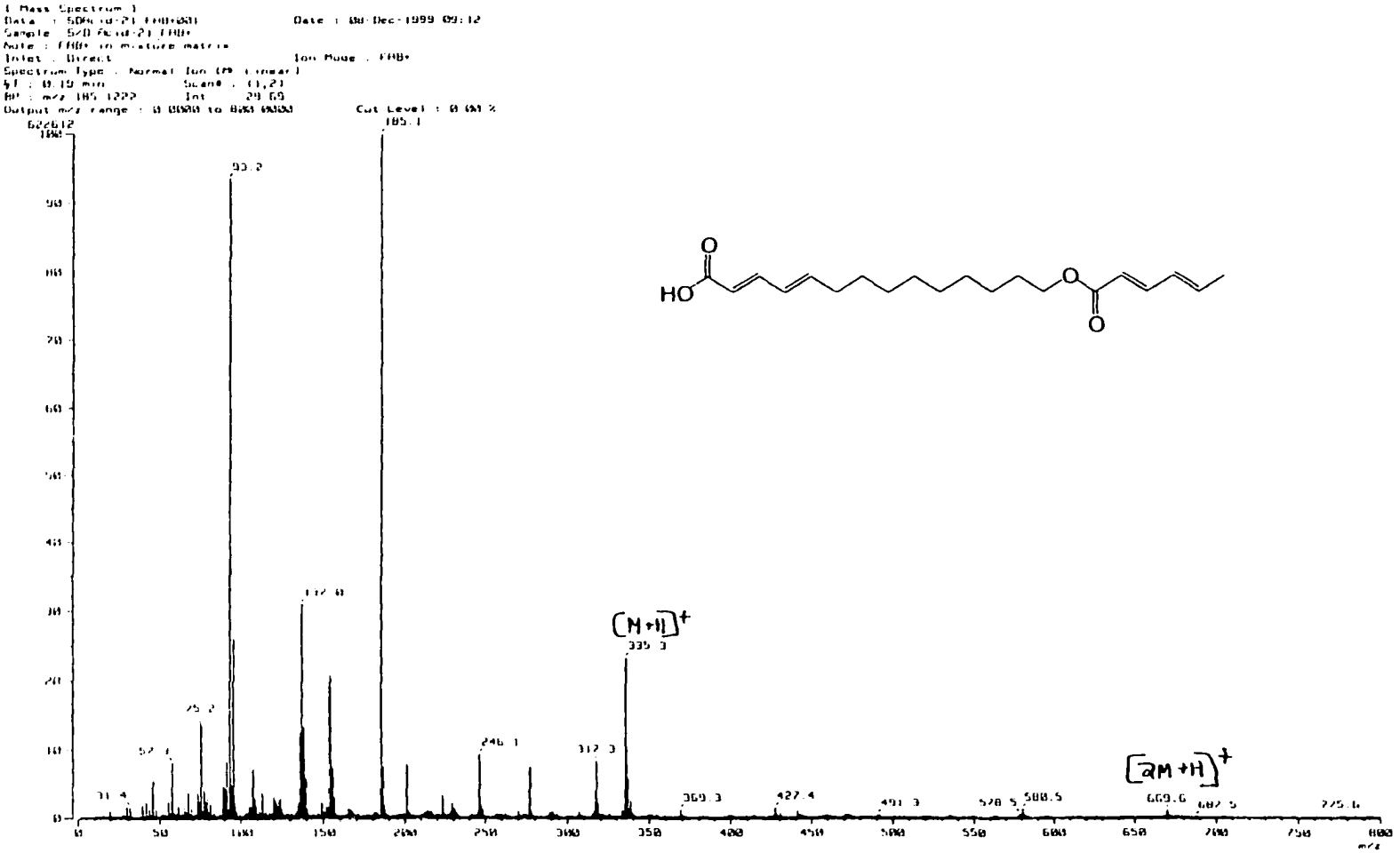

Figure C-7: FAB mass spectrum of Compound **3-19c**: 14-sorbyl-2,4-tetradecadienoic acid (Sorb/Den acid-21)

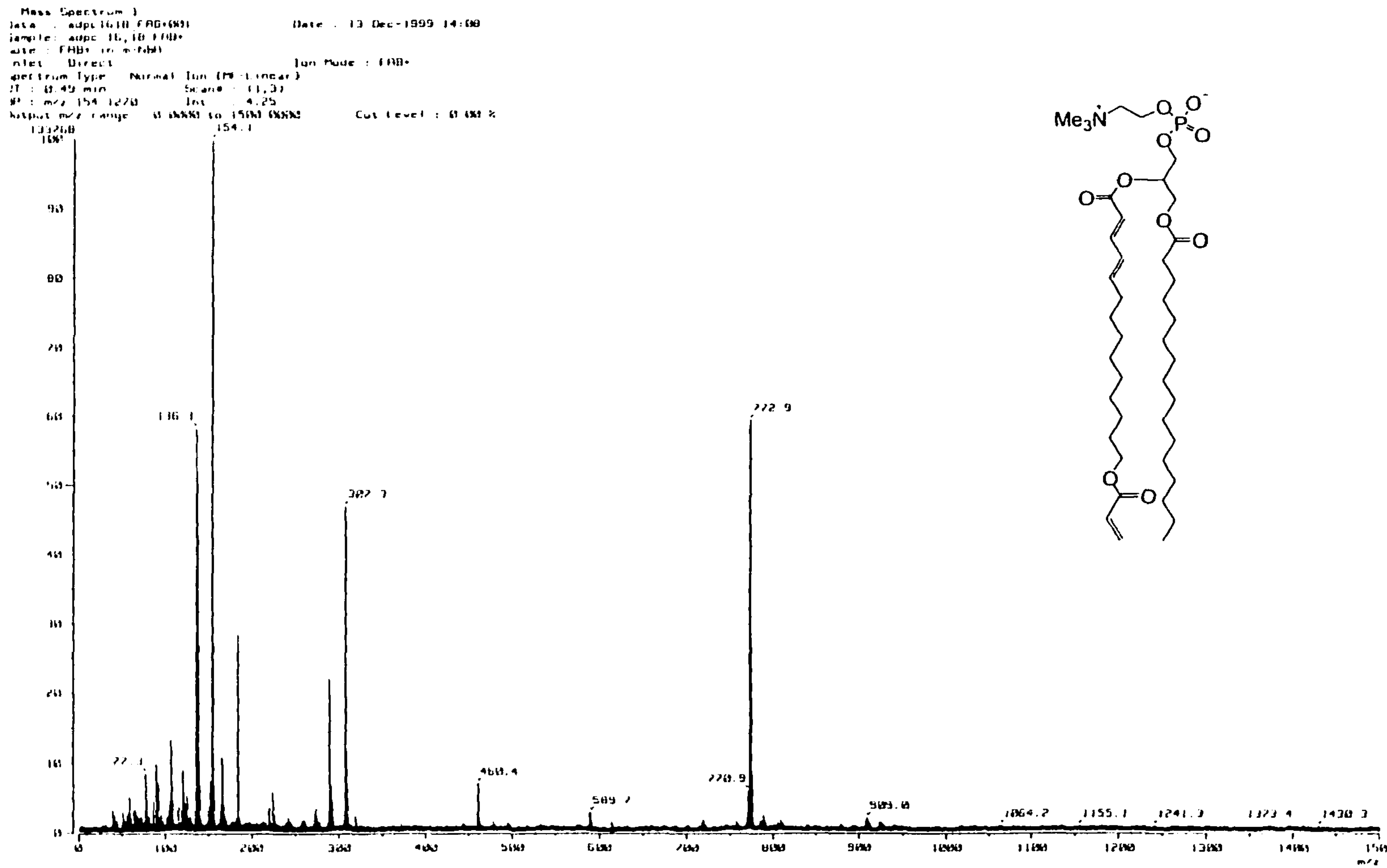

Figure C-8: FAB mass spectrum of Compound **3-11c**: 1-palmitoyl-2-[14-acryloxy-2,4-tetradecadienoic]-*sn*-glycero-3-phosphocholine (Acryl/DenPC$_{16,18}$)

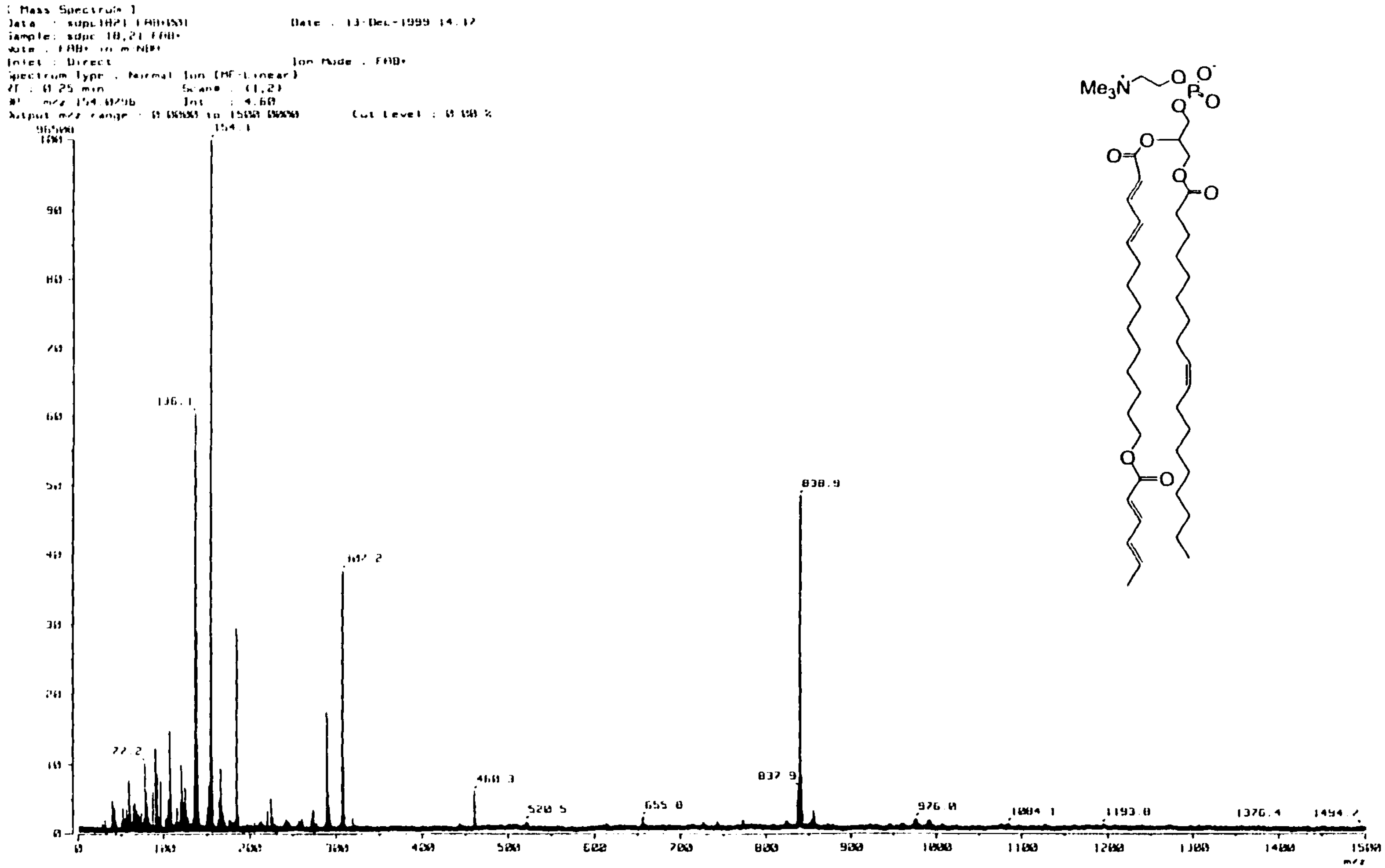

Figure C-9: FAB mass spectrum of Compound **3-12c**: 1-oleoyl-[14-sorbyloxy-2,4-tetradecadienoic]-*sn*-glycero-3-phosphocholine (Sorb/DenPC$_{18,21}$)

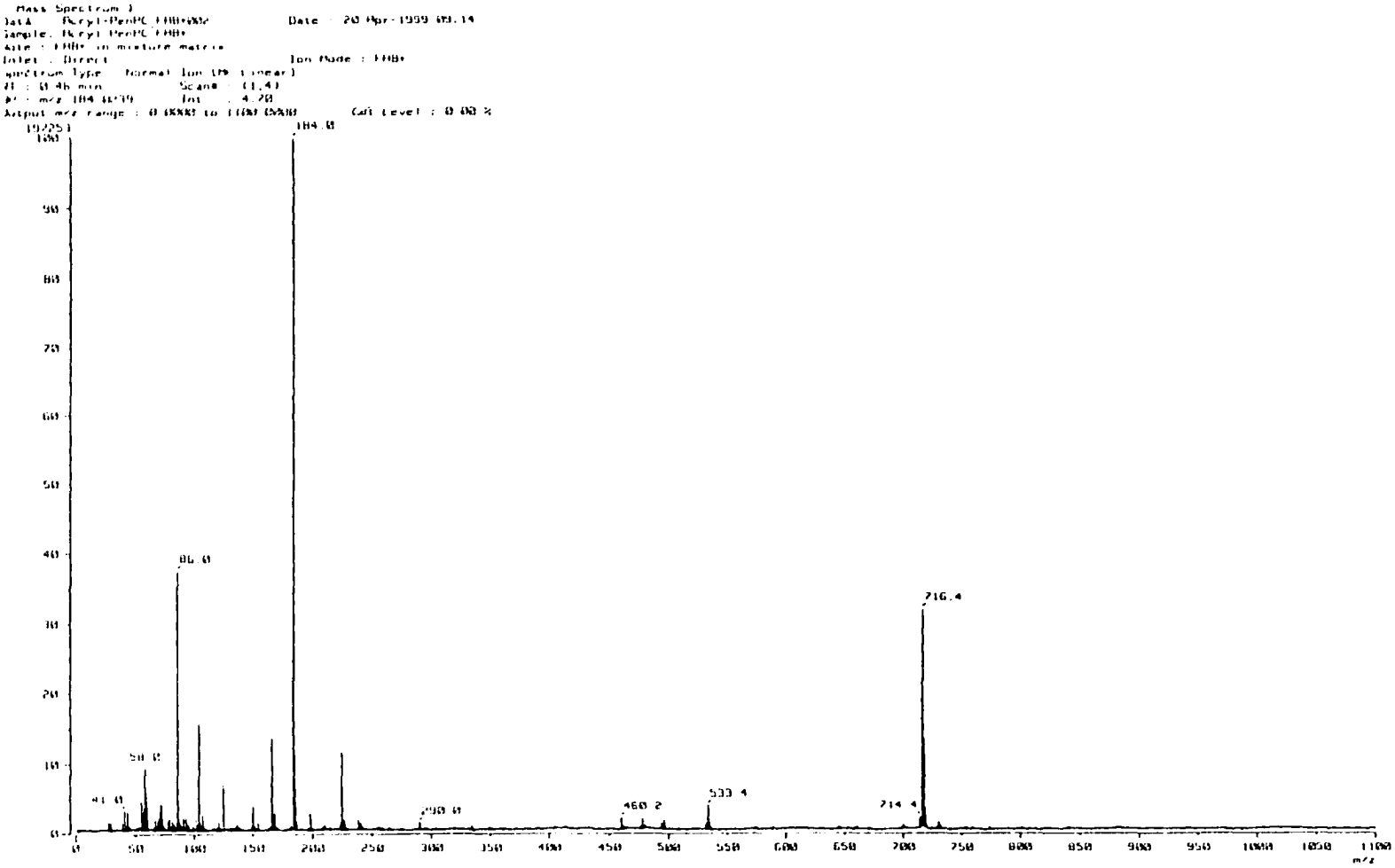

Figure C-10: FAB mass spectrum of Compound **3-11a**: 1-palmitoyl-2-[10-acryloxyl-2,4-decadienoic]-*sn*-glycero-3-phosphocholine (Acryl/DenPC$_{16,14}$)

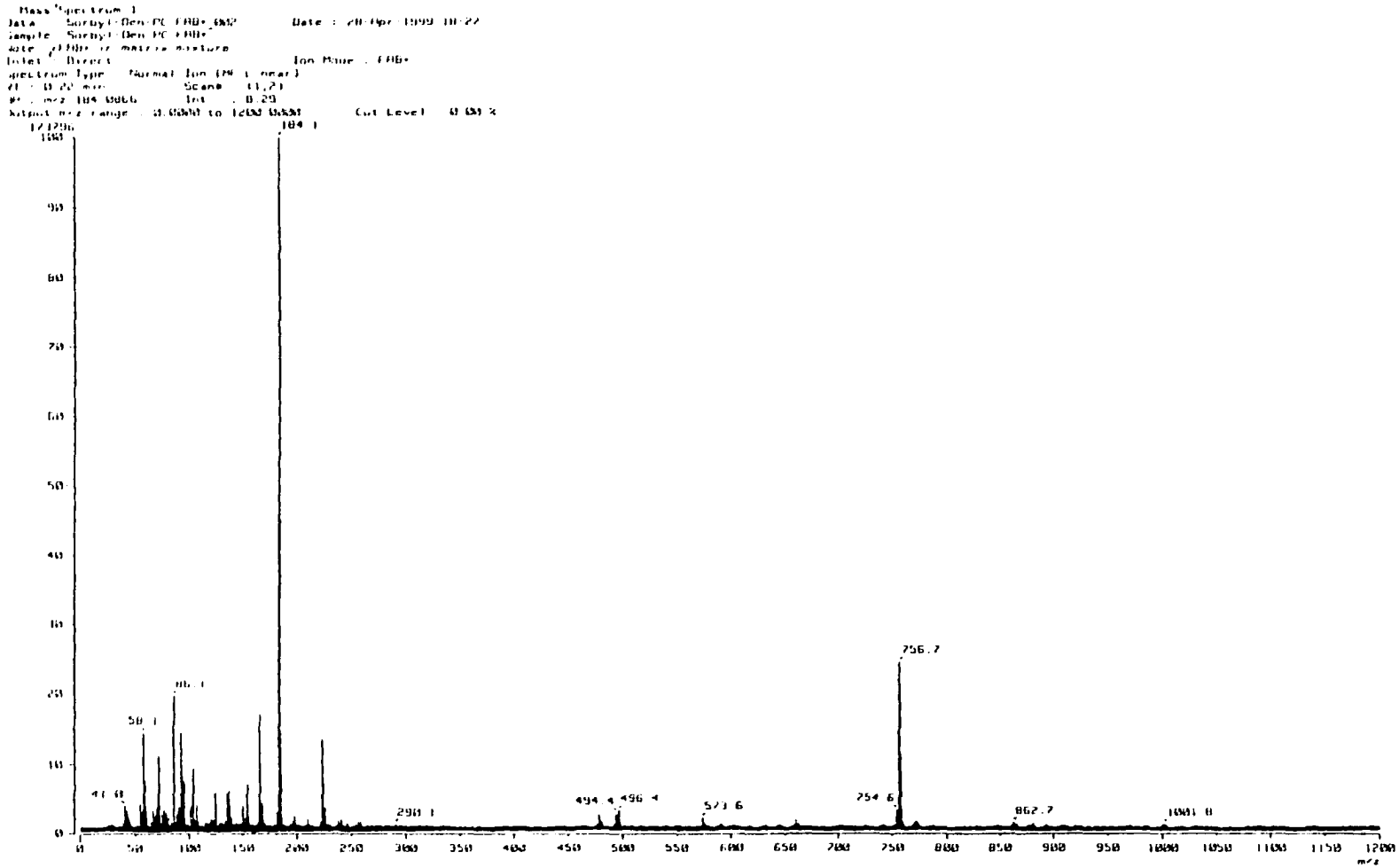

Figure C-11: FAB mass spectrum of Compound **3-12a**, 1-palmitoyl-2-[10-sorbyl-2,4-decadienoic]-*sn*-glycero-3-phosphocholine (Sorb/DenPC$_{16,17}$)

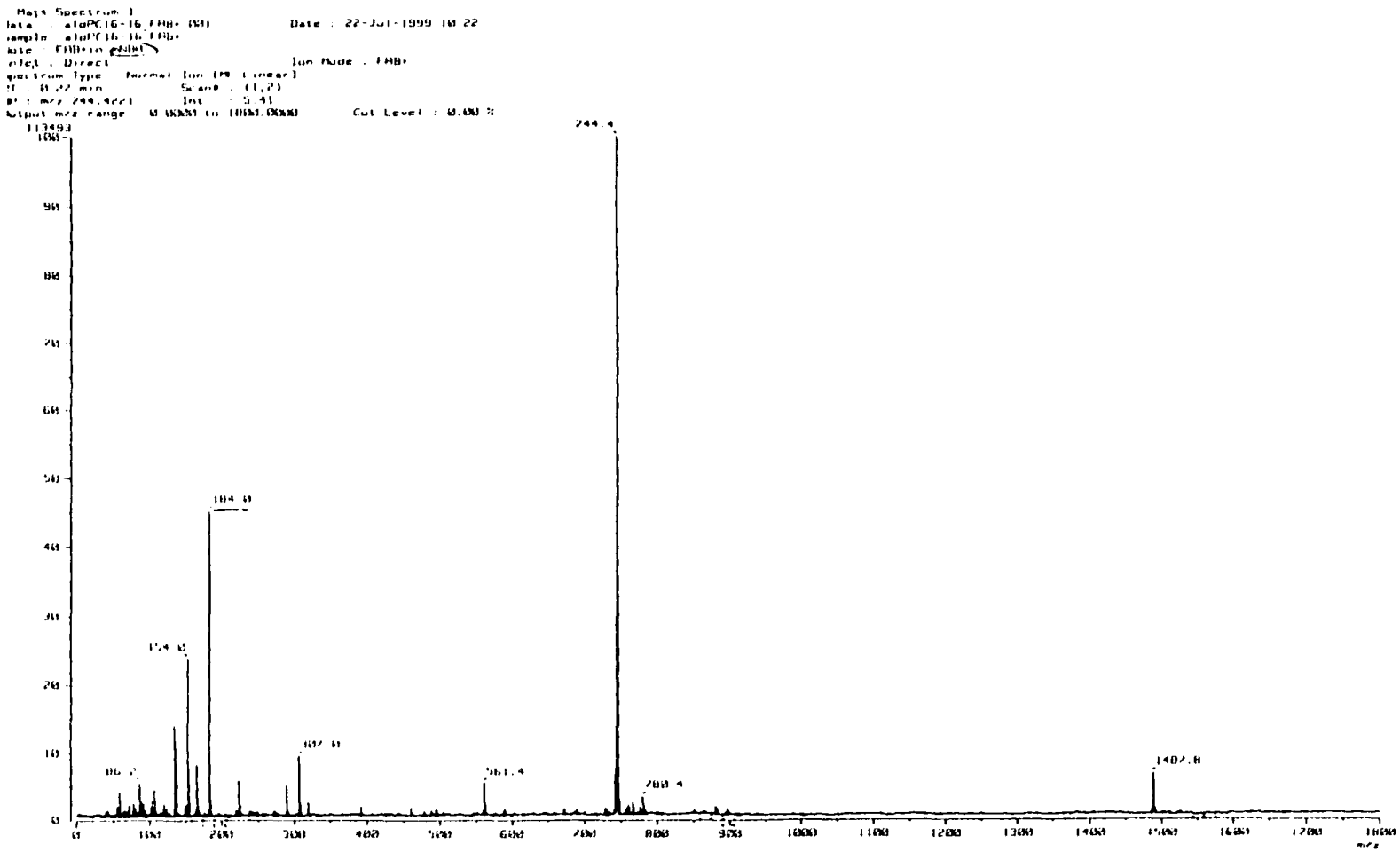

Figure C-12: FAB mass spectrum of Compound **3-11b**: 1-palmitoyl-2-[12-acryloxyl-2,4-dodecadienoic]-*sn*-glycero-3-phosphocholine (Acryl/DenPC$_{16,16}$)

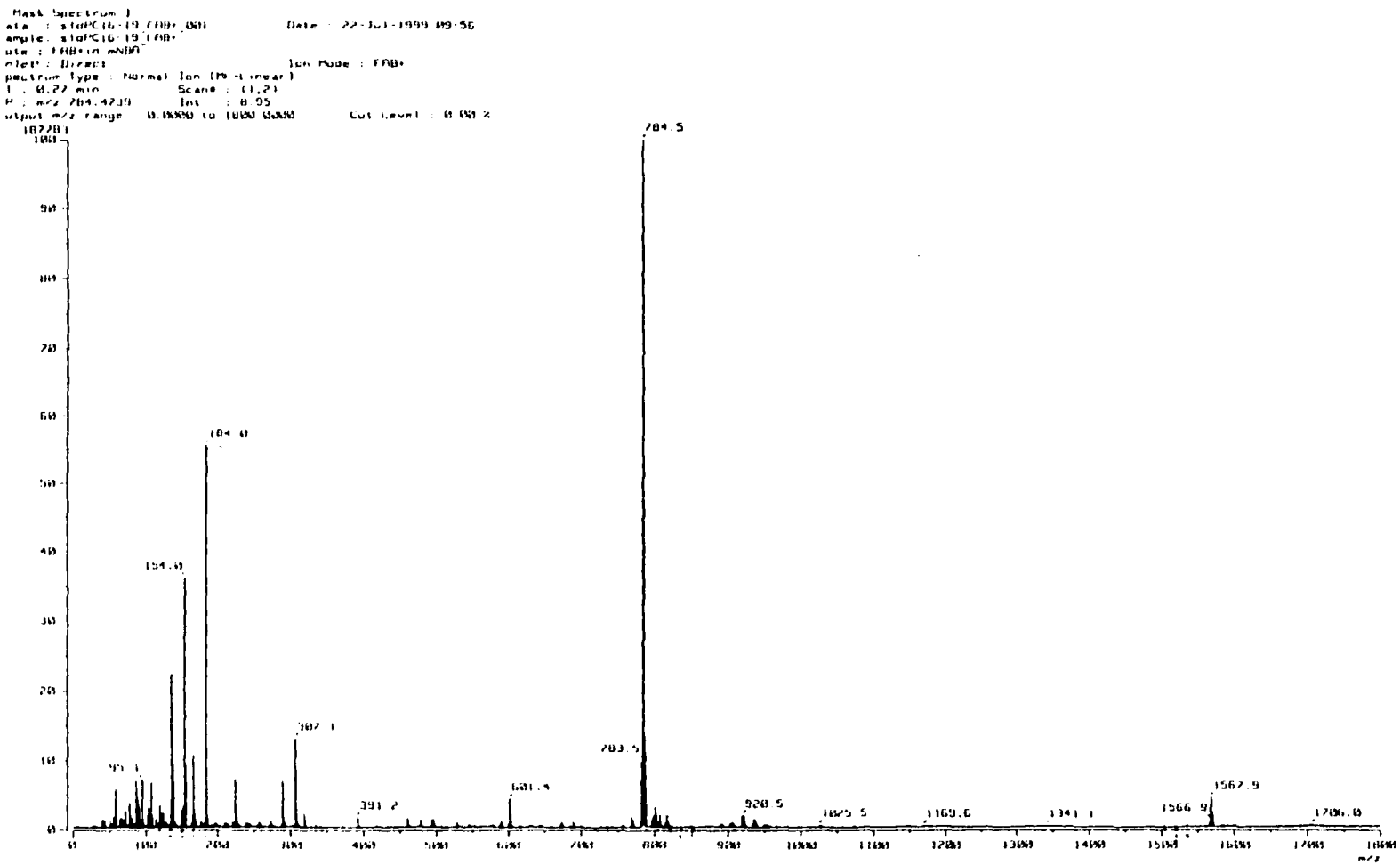

Figure C-13: FAB mass spectrum of Compound **3-12b** 1-palmitoyl-2-[12-sorbyl-2,4-dodecadienoic]-*sn*-glycero-3-phosphocholine (Sorb/DenPC$_{16,19}$)

REFERENCES

1) Fendler, J. H. *Membrane Mimetic Chemistry*; Wiley-Interscience: New York, 1982; Vol. Chap. 6.

2) Tyminski, P. N.; Latimer, L. H.; O'Brien, D. F. *Biochemistry* **1988**, *27*, 2696-705.

3) Deamer, D. W. *Light Transducing Membranes. Structure, Function, and Evolution*; Academic Press: New York, 1978.

4) Moss, R. A.; Fujita, T.; Ganguli, S. *Langmuir* **1990**, *6*, 1197.

5) Xiao, Y.; Gao, X.; Xie, G.; Zhang, Y. *Bioelectrochem. Bioenerg.* **1996**, *39*, 125.

6) Bockris, J. O. M.; Diniz, F. B. *J. Electrochem. Soc.* **1988**, *135*, 1947.

7) Kunitake, T. *New J. Chem.* **1987**, *11*, 141.

8) Ross, E. E.; Bondurant, B.; Spratt, T.; Conboy, J. C.; O'Brien, D. F.; Saavedra, S. S. *Langmuir* **2001**, *17*, 2305-2307.

9) Lee, Y.-S.; Yang, J.-Z.; Sisson, T. M.; Frankel, D. A.; Gleeson, J. T.; Aksay, E.; Keller, S. L.; Gruner, S. M.; O'Brien, D. F. *J. Am. Chem. Soc.* **1995**, *117*, 5573-8.

10) Tanford, C. *Science* **1978**, *200*, 1012-1018.

11) Blokzijl, W.; Engberts, J. B. F. N. *Angew. Chem. Int. Ed. Engl.* **1993**, *32*, 1545-1579.

12) Seddon, J. M. *Biochim. Biophys. Acta* **1990**, *1031*, 1-69.

13) Wennerstrom, H.; Evans, D. F. *The Colloidal Domain: Where Physics, Chemistry, Biology, and Technology Meet*; Wiley-VCH: New York, 1994.

14) Lindblom, G.; Rilfors, L. *Biochem. Biophys. Acta* **1989**, *988*, 221-256.

15) Gros, L.; Ringsdorf, H.; Schupp, H. *Angew. Chem. Int. Ed. Engl.* **1981**, *20*, 305-325.

16) Baillie, A. J.; Florence, A. T.; Hume, L. R.; Muirhead, G. T.; Rogerson, A. *J. Pharm. Pharmacol.* **1985**, *37*, 863.

17) Kiwada, H.; Niimura, H.; Fujisaki, Y.; Yamada, S.; Kato, Y. *Chem. Pharm. Bull.* **1985**, *33*, 753.

18) Hofland, H. E. J.; Bouwstra, J. A.; Gooris, G. S.; Spies, F.; Talsma, H.; Junginger, H. E. *J. Coll. Inter. Sci.* **1993**, *161*, 366-376.

19) Kaler, E. W.; Murthy, A. K.; Rodriquez, B. E.; Zasadzinski, J. A. N. *Science* **1989**, *245*, 1371-1374.

20) Fendler, J. H. *Acc. Chem. Res.* **1980**, *13*, 7-13.

21) Bangham, A. D. *Annu. Rev. Biochem.* **1972**, *41*, 753.

22) Ti Tien, H.; Ottova-Leitmannova, A. *Membrane Biophysics: As Viewed From Experimental Bilayer Lipid Membranes*; Elsevier: New York, 2000.

23) Baker, R. W. *Membrane Technology and Applications*; McGraw-Hill: New York, 2000.

24) Gaber, B. P. S., J. M.; Chapman, D. *Biotechnological Applications of Lipid Microstructures*; Plenum Press: New York, 1988; Vol. 238.

25) Juliano, R. L. *Trends Pharmacol. Sci.* **1981**, *2*, 39-42.

26) Juliano, R. L. *Drug Delivery Systems: Characteristics and Biomedical Applications*; Oxford University Press: New York, 1980.

27) Lasic, D. M., F. *Stealth Liposomes*; CRC Press: Boca Raton, 1995.

28) Janoff, A. S. *Liposomes: Rational Design*; Marcel Dekker Inc.: New York, 1999.

29) Ostro, M. J. *Liposomes*; Marcel Dekker Inc.: New York, 1983.

30) Tirrell, D. A.; Donaruma, L. G.; Turek, A. B. E. *Ann. NY Acad. Sci.* **1985**, *446*.

31) Sunamoto, J.; Sato, T.; Hirota, K.; Fukushima, K.; Hiratani, K.; Hara, K. *Biochim. Biophys. Acta* **1987**, *898*, 323.

32) Bader, H.; Dorn, K.; Hupfer, B.; Ringsdorf, H. *Polymeric Monolayers and Liposomes as Models for Biomembranes*; Springer-Verlag: New York, 1985; Vol. 64.

33) Ringsdorf, H.; Schlarb, B.; Venzmer, J. *Angew. Chem. Int. Ed. Engl.* **1988**, *27*, 113-158.

34) Sackmann, E.; Duwe, H.-P.; Engelhardt, H. *Faraday Discuss. Chem. Soc.* **1986**, *81*, 281.

35) Bangham, A. D.; Standish, M. M.; Watkins, J. C. *J. Mol. Biol.* **1965**, *13*, 238-252.

36) Huang, C. *Biochemistry* **1969**, *8*, 344-352.

37) Deamer, D. W.; Bangham, A. D. *Biochim. Biophys. Acta* **1976**, *443*, 629-634.

38) Schieren, H.; Rudolph, S.; Finkelstein, M.; Coleman, P.; Weissmann, G. *Biochim. Biophys. Acta* **1978**, *542*, 137-153.

39) Szoka, F.; Papahadjopoulos, D. *Proc. Natl. Acad. Sci. USA* **1978**, *75*, 4194-4198.

40) Brunner, J.; Skrabal, P.; Hauser, H. *Biochim. Biophys. Acta* **1976**, *455*, 322-331.

41) Slack, J. R.; Anderton, B. H.; Day, W. A. *Biochim. Biophys. Acta* **1973**, *323*, 547-559.

42) Milsmann, M. H. W.; Schwendener, R. A.; Weder, H. G. *Biochim. Biophys. Acta* **1978**, *512*, 147-155.

43) Rhoden, V.; Goldin, S. M. *Biochemistry* **1979**, *18*, 4173-4176.

44) Hope, M. J.; Bally, M. B.; Webb, G.; Cullis, P. R. *Biochim. Biophys. Acta* **1985**, *812*, 55-65.

45) Brendzel, A. M.; Miller, I. F. *Biochim. Biophys. Acta* **1980**, *596*, 129-136.

46) Fukuda, K.; Shibasaki, Y.; Nakahara, H. *J. Macromol. Sci.-Chem.* **1981**, *15*, 999.

47) Day, D.; Hub, H. H.; Ringsdorf, H. *Isr. J. Chem.* **1979**, *18*, 325-9.

48) Johnston, D. S.; Sanghera, S.; Pons, M.; Chapman, D. *Biochim. Biophys. Acta* **1980**, *602*, 57-69.

49) Hupfer, B.; Ringsdorf, H.; Schupp, H. *Makromol. Chem.* **1981**, *182*, 247-253.

50) Hupfer, B.; Ringsdorf, H. *Chem. Phys. Lipids* **1983**, *33*, 263-82.

51) Johnston, D. S.; Sanghera, S.; Manjon-Rubio, A.; Chapman, D. *Biochim. Biophys. Acta* **1980**, *602*, 213-16.

52) Regen, S. L.; Czech, B.; Singh, A. *J. Am. Chem. Soc.* **1980**, *102*, 6638-6640.

53) O'Brien, D. F.; Whitesides, T. H.; Klingbiel, R. T. *J. Polym. Sci., Polym. Lett. Ed.* **1981**, *19*, 95-101.

54) Lopez, E.; O'Brien, D. F.; Whitesides, T. H. *J. Am. Chem. Soc.* **1982**, *104*, 305-7.

55) Tundo, P.; Kippenberger, D. J.; Klahn, P. L.; Prieto, N. E.; Jao, T. C.; Fendler, J. H. *J. Am. Chem. Soc.* **1982**, *104*, 456-461.

56) Regen, S. L.; Singh, A.; Oehme, G.; Singh, M. *J. Am. Chem. Soc.* **1982**, *104*, 791-5.

57) Higashi, N.; Kajiyama, T.; Kunitake, T.; Prass, W.; Ringsdorf, H.; Takahara, A. *Macromolecules* **1987**, *20*, 29-33.

58) Srisiri, W.; Lee, Y.-S.; Sisson, T. M.; Bondurant, B.; O'Brien, D. F. *Tetrahedron* **1997**, *53*, 15397-15414.

59) Srisiri, W.; Benedicto, A.; O'Brien, D. F.; Trouard, T. P.; Oraedd, G.; Persson, S.; Lindblom, G. *Langmuir* **1998**, *14*, 1921-1926.

60) Singh, A.; Schnur, J. M. *Phospholipids Handbook*; Marcel Dekker: New York, 1993.

61) O'Brien, D. F.; Ramaswami, V. *Vesicles*; John Wiley & Son: New York, 1989; Vol. 17, pp 108-135.

62) Hub, H. H.; Hupfer, B.; Ringsdorf, H. *Springer Ser. Chem. Phys.* **1980**, *11*, 253-8.

63) Fendler, J. H. *Science* **1984**, *223*, 888-894.

64) Paleos, C. M. *Chem. Soc. Rev.* **1985**, *45*, 45-66.

65) Regen, S. L. *NATO ASI Ser., Ser. C* **1987**, *215*, 317-24.

66) O'Brien, D. F.; Armitage, B.; Benedicto, A.; Bennett, D. E.; Lamparski, H. G.; Lee, Y.-S.; Srisiri, W.; Sisson, T. M. *Acc. Chem. Res.* **1998**, *31*, 861-868.

67) Georger, J. H.; Singh, A.; Price, R. R.; Schnur, J. M.; Yager, P.; Schoen, P. E. *J. Am. Chem. Soc.* **1987**, *109*, 6169-6175.

68) Meier, H.; Sprenger, I.; Baermann, M.; Sackmann, E. *Macromolecules* **1994**, *27*, 7581-8.

69) Odian, G. *Principles of Polymerization*; 3rd ed.; John Wiley & Sons, Inc.: New York, 1991.

70) Lamparski, H.; O'Brien, D. F. *Macromolecules* **1995**, *28*, 1786-94.

71) Sells, T. D.; O'Brien, D. F. *Macromolecules* **1991**, *24*, 336-7.

72) Sells, T. D.; O'Brien, D. F. *Macromolecules* **1994**, *27*, 226-33.

73) Lei, J.; O'Brien, D. F. *Macromolecules* **1994**, *27*, 1381-8.

74) Maiti, S.; Palit, S. R. *J. Polym. Sci.* **1971**, *9*, 253-6.

75) Tsuchida, E.; Hatashita, M.; Makino, C.; Hasegawa, E.; Kimura, N. *Macromolecules* **1992**, *25*, 207-12.

76) Liu, S.; O'Brien, D. F. *Macromolecules* **1999**, *32*, 5519-5524.

77) Liu, S.; Sisson, T. M.; O'Brien, D. F. *Macromolecules*, 2001; Vol. 34, pp 465-473.

78) Sadownik, A.; Stefely, J.; Regen, S. L. *J. Am. Chem. Soc.* **1986**, *108*, 7789-91.

79) Sarac, A. S. *Prog. Polym. Sci.* **1999**, *24*, 1149-1204.

80) Dorn, K.; Klingbiel, R. T.; Specht, D. P.; Tyminski, P. N.; Ringsdorf, H.; O'Brien, D. F. *J. Am. Chem. Soc.* **1984**, *106*, 1627-33.

81) Sisson, T. M.; Lamparski, H. G.; Koelchens, S.; Elayadi, A.; O'Brien, D. F. *Macromolecules* **1996**, *29*, 8321-8329.

82) Heckmann, K.; Strobl, C.; Bauer, S. *Thin Solid Films* **1983**, *99*, 256-269.

83) Laschewsky, A.; Ringsdorf, H.; Schmidt, G. *Thin Solid Films* **1985**, *134*, 153-172.

84) Zachariasse, K. A.; Kuhnle, W.; Weller, A. *Chem. Phys. Lett.* **1980**, *73*, 6-11.

85) Georgescauld, D.; Desmasez, J. P.; Lapouyade, R.; Babeau, A.; Richard, H.; Winnik, M. *Photochem. Photobiol.* **1980**, *31*, 539-545.

86) McElhaney, R. N. *Chem. Phys. Lipids* **1982**, *30*, 229-259.

87) Silvius, J. R. *Chem. Phys. Lipids* **1991**, *57*, 241-251.

88) McElhaney, R. N. *Biochim. Biophys. Acta* **1986**, *864*, 361-421.

89) Mabrey, S.; Sturtevant, J. M. *Proc. Nat. Acad. Sci. USA* **1976**, *73*, 3862-3866.

90) Albon, N.; Sturtevant, J. M. *Proc. Nat. Acad. Sci. USA* **1978**, *75*, 2258-2260.

91) Chen, S. C.; Sturtevant, J. M. *Biochemistry* **1981**, *20*, 713-718.

92) Sturtevant, J. M.; Ho, C.; Reimann, A. *Proc. Nat. Acad. Sci. USA* **1979**, *76*, 2239-2243.

93) Nagle, J. F.; Scott, H. L. *Phys. Today* **1978**, *31*, 38-47.

94) Koynova, R.; Caffrey, M. *Biochim. Biophys. Acta* **1998**, *1376*, 91-145.

95) Finegold, L.; Shaw, W.; Singer, M. *Chem. Phys. Lipids* **1990**, *53*, 177-184.

96) Nagle, J.; Wilkinson, D. *Biophys. J.* **1978**, *23*, 159-173.

97) Barton, P.; Gunston, F. J. *Biol. Chem* **1975**, *250*, 4470-4476.

98) Lamparski, H.; Lee, Y. S.; Sells, T. D.; O'Brien, D. F. *J. Am. Chem. Soc.* **1993**, *115*, 8096-102.

99) Johnson, S. M.; Bangham, A. D. *Biochim. Biophys. Acta* **1969**, *193*, 82.

100) Hauser, H. O.; Phillips, M. C.; Stubbs, M. *Nature* **1972**, *239*, 342.

101) Papahadjopoulos, D.; Nir, S.; Ohki, S. *Biochim. Biophys. Acta* **1972**, *266*, 561.

102) Gawrisch, K.; Ruston, D.; Zimmerberg, J.; Parsegian, V. A.; Rand, R. P. F., N. *Biophys. J.* **1992**, *61*, 1213-1223.

103) Fettiplace, R. *Biochim. Biophys. Acta* **1978**, *513*, 1-10.

104) Stein, W. D. *The Movement of Molecules Across Cell Membranes*; Academic Press: New York, 1967.

105) Diamond, J. M.; Wright, E. M. *Annu. Rev. Physiol.* **1969**, *31*, 581-646.

106) Males, R. G.; Phillips, P. S.; Herrig, F. G. *Biophys. Chem.* **1998**, *70*, 65-74.

107) Jain, M. H. *The Bimolecular Lipid Membrane: A System*; Van Nostrand Reinhold Co.: New York, 1972.

108) Tien, H. T. *Bilayer Lipid Membrane (BLM) Theory and Practice*; Marcel Dekker: New York, 1974.

109) Szoka, F.; Papahadjopoulos, D. *Ann. Rev. Biophys. Bioeng.* **1980**, *9*, 467-508.

110) Kanehisa, M. I.; Tsong, T. Y. *J. Am. Chem. Soc.* **1978**, *100*, 424-432.

111) Haxby, J. A.; Kinsky, C. B.; Kinsky, S. C. *Proc. Nat. Acad. Sci.* **1968**, *61*, 300.

112) Bangham, A. D.; De Gier, J.; Greville, G. D. *Chem. Phys. Lipids* **1967**, *1*, 225.

113) De Gier, J.; Mandersloot, J. G.; Van Deenen, L. L. M. *Biochim. Biophys. Acta* **1968**, *150*, 666.

114) De Gier, J.; Haest, C. W. M.; Mandersloot, J. G.; Van Deenen, L. L. M. *Biochim. Biophys. Acta* **1970**, *211*, 373.

115) Klein, R. A.; Moore, M. J.; Smith, M. W. *Biochim. Biophys. Acta* **1971**, *233*, 420.

116) Papahadjopoulos, D.; Jacobson, K.; Nir, S.; Isac, T. *Biochim. Biophys. Acta* **1973**, *311*, 330-348.

117) Corvera, E.; Mouritsen, O. G.; Singer, M. A.; Zuckermann, M. J. *Biochim. Biophys. Acta* **1992**, *1107*, 261-270.

118) Jacobson, K.; Paphadjopoulos, D. *Biochemistry* **1975**, *14*, 152-161.

119) Ramaswami, V.; Haaseth, R. C.; Matsunaga, T. O.; Hruby, V. J.; O'Brien, D. F. *Biochim. Biophys. Acta* **1992**, *1109*, 195-202.

120) Weinstein, J. N.; Yoshikami, S.; Heukart, L.; Blumenthal, R.; Hagins, W. A. *Science* **1977**, *195*, 489.

121) Stefely, J.; Markowitz, M. A.; Regen, S. L. *J. Am. Chem. Soc.* **1988**, *110*, 7463-9.

122) Kolchens, S.; Lamparski, H.; O'Brien, D. F. *Macromolecules* **1993**, *26*, 398-400.

123) Wagner, N.; Dose, K.; Koch, H.; Ringsdorf, H. *FEBS Lett.* **1981**, *132*, 313-18.

124) Hupfer, B.; Ringsdorf, H.; Schupp, H. *Chem. Phys. Lipids* **1983**, *33*, 355-374.

125) Hasegawa, E.; Matsushita, Y.; Eshima, K.; Nishide, H.; Tsuchida, E. *Makromol. Chem., Rapid Commun.* **1984**, *5*, 779-84.

126) Kusumi, A.; Singh, M.; Tirrell, D. A.; Oehme, G.; Singh, A.; Samuel, N. K. P.; Hyde, J. S.; Regen, S. L. *J. Am. Chem. Soc.* **1983**, *105*, 2975-80.

127) Ohno, H.; Takeoka, S.; Iwai, H.; Tsuchida, E. *Macromolecules* **1988**, *21*, 319-22.

128) Pujol-Fortin, M.; Galin, J. C. *Polymer* **1994**, *34*, 1462-1472.

129) Montroy Soto, V. M.; Galin, J. C. *Polymer* **1984**, *25*, 254-262.

130) Hamori, E.; Prusinowski, L. R.; Sparks, P. G.; Hugues, R. E. *J. Phys. Chem.* **1965**, *69*, 1101-1105.

131) Ueda, T.; Oshida, H.; Kurita, K.; Ishihara, K.; Nakabayashi, N. *Polymer J.* **1992**, *24*, 1259-1269.

132) Johnston, D. S.; McLean, L. R.; Whittam, M. A.; Clark, A. D.; Chapman, D. *Biochemistry* **1983**, *22*, 3194-202.

133) Takeoka, S.; Ohgushi, T.; Tsuchida, E. *Macromolecules* **1995**, *28*, 7660-6.

134) Takeoka, S.; Ohno, H.; Iwai, H.; Tsuchida, E. *J. Polym. Sci., Part A: Polym. Chem.* **1990**, *28*, 717-30.

135) Ohno, H.; Ogata, Y.; Tsuchida, E. *Macromolecules* **1987**, *20*, 929-33.

136) Ohno, H.; Takeoka, S.; Iwai, H.; Tsuchida, E. *J. Polym. Sci., Part A: Polym. Chem.* **1987**, *25*, 2737-46.

137) Ohno, H.; Takeoka, S.; Tsuchida, E. *Bull. Chem. Soc. Jpn.* **1987**, *60*, 2945-51.

138) Ohno, H.; Takeoka, S.; Iwai, H.; Tsuchida, E. *Macromolecules* **1989**, *22*, 61-6.

139) Pons, M.; Villaverde, C.; Chapman, D. *Biochim. Biophys. Acta* **1983**, *730*, 306.

140) Anikin, A.; Chupin, V.; Anikin, M.; Serebrennikova, G. *Makromol. Chem.* **1993**, *194*, 2663-2673.

141) Sisson, T. M.; Lamparski, H. G.; Kolchens, S.; Peterson, T.; Elayadi, A.; O'Brien, D. F. *Methodologies and models of crosslinking polymerization in supramolecular assemblies*; Frank, C. W., Ed., 1998; Vol. 695, pp 119-130.

142)Small, D. M. *The Physical Chemistry of Lipids. From Alkanes to Phospholipids*; Plenum Press: New York, 1986; Vol. 4, pp 1-672.

143) O'Brien, D. F. *Photochem. Photobiol.* **1979**, *29*, 679-85.

144) Gaub, H.; Sackmann, E.; Bueschl, R.; Ringsdorf, H. *Biophys. J.* **1984**, *45*, 725-31.

145) Lichtenberg, D.; Robson, R.; Dennis, E. A. *Biochim. Biophys. Acta* **1983**, *737*, 285-304.

146) Kolchens, S.; Ramaswami, V.; Birgenheier, J.; Nett, L.; O'Brien, D. F. *Chem. Phys. Lipids* **1993**, *65*, 1-10.

147) Hauser, H.; Pascher, I.; Pearson, R. H.; Sundell, S. *Biochim. Biophys. Acta* **1981**, *650*, 21-51.

148) Pearson, R. H.; Pascher, I. *Nature (London)* **1979**, *281*, 499-501.

149) Bailey, W. J. *Encyclopedia of Polymer Science and Engineering*; 2nd ed.; John Wiley & Sons, Inc.: New York, 1990.

150) Mullen, K. *Adv. Polym. Sci.* **1995**, *123*, 1.

151) Nezu, S.; Lando, J. B. *J. Polym. Sci., Polym. Chem.* **1995**, *33*, 2455-2461.

152) Stupp, S. I.; Son, S.; Lin, H. C.; Li, L. S. *Science* **1993**, *259*, 59-63.

153) Stupp, S. I.; Son, S.; Li, L. S.; Lin, H. C.; Keser, M. *J. Am. Chem. Soc.* **1995**, *117*, 5212-5227.

154) Huggins, K. E.; Son, S.; Stupp, S. I. *Macromolecules* **1997**, *30*, 5305-5312.

155) Singh, A.; Markowitz, M. A. *New J. Chem.* **1994**, *18*, 377-385.

156) Srisiri, W.; Sisson, T. M.; O'Brien, D. F. *J. Am. Chem. Soc.* **1996**, *118*, 11327-11328.

157) Sisson, T. M.; Srisiri, W.; O'Brien, D. F. *J. Am. Chem. Soc.* **1998**, *120*, 2322-2329.

158) Mancuso, A. J.; Huang, S.-L.; Swern, D. *J. Org. Chem.* **1978**, *43*, 2480-2482.

159) Bonadies, F.; Cardilli, A.; Lattanzi, A.; Orelli, L. R.; Scettri, A. *Tetrahedron Lett.* **1994**, *35*, 3383-3386.

160) Takemoto, K.; Sonoda, N. *Inclusion Compounds of Urea, Thiourea and Selenourea*; Academic Press: Orlando, 1984; Vol. 2.

161) Fieser, L. F. *J. Chem. Ed.* **1963**, *40*, 457.

162) Fieser, L. F.; WIlliamson, K. L. *Oleic Acid from Olive Oil*; 3rd ed., 1979, pp 206-211.

163) Srisiri, W.; Lamparski, H. G.; O'Brien, D. F. *J. Org. Chem.* **1996**, *61*, 5911-5915.

164) Sisson, T. M. *Crosslinking Polymerization in Supramolecular Assemblies*; University of Arizona: Tucson, 1997, pp 1-279.

165) Seelig, A.; Seelig, J. *Biochemistry* **1974**, *13*, 4839.

166) Seelig, A.; Seelig, J. *Biochim. Biophys. Acta* **1975**, *406*, 1.

167) Matsumoto, A.; Ishizu, Y.; Yokoi, K. *Macromol. Chem. Phys.* **1998**, *199*, 2511-2516.

168) Srisiri, W.; Sisson, T. M.; O'Brien, D. F.; McGrath, K. M.; Han, Y.; Gruner, S. M. *J. Am. Chem. Soc.* **1997**, *119*, 4866-4873.

169) Berndl, K.; Kas, J.; Lipowsky, R.; Sackmann, E.; Serfert, U. *Europhysics Lett.* **1990**, *13*, 659.

170) Gregoriadis, G. *Liposomes in Drug Targetting*; Cell Biology:, 1994.

171) Lasic, D. D.; Papahadjopoulos, D. *Medical Applications of Liposomes*; Elsevier Science: Amsterdam, 1998.

172) Rosoff, M. *Vesicles*; Marcel Dekker Inc.: New York, 1996.

173) Tyrell, D. A.; Richardson, V. J.; Ryman, B. E. *Biochim. Biophys. Acta* **1977**, *497*, 469-480.

174) Gregoriadis, G. *Nature* **1977**, *265*, 407-411.

175) Baker, R. *Controlled Release of Bioactive Materials*; Academic Press: New York, 1980.

176) Gerasimov, O. V.; Boomer, J. A.; Qualls, M.; Thompson, D. H. *Adv. Drug Delivery Rev.* **1999**, *38*, 317-338.

177) Mayer, P. R. ; American Chemical Society: Washington, DC, 1997.

178) Armitage, B. A.; Bennett, D. E.; Lamparski, H. G.; O'Brien, D. F. *Adv. Polym. Sci.* **1996**, *126*, 53-84.

179) Lamparski, H.; Liman, U.; Barry, J. A.; Frankel, D. A.; Ramaswami, V.; Brown, M. F.; O'Brien, D. F. *Biochemistry* **1992**, *31*, 685-94.

180) McGee, J. P.; Davis, S. S.; O'Hagan, D. T. *J. Controlled Release* **1994**, *31*, 55.

181) Katayama, N.; Tanaka, R.; Ohno, Y.; Ueda, C.; Houjou, T.; Takada, K. *Int. J. Pharm.* **1995**, *115*, 87.

182) Bogner, J. R.; Goebel, F. D. *Efficacy of DOX-SL (Stealth Liposomal Doxorubicin) in the treatment of Advanced AIDS-Related Kaposi's Sarcoma*; CRC Press: Boca Raton, 1995.

183) Verwey, E. J. W.; Overbeek, J. T. G. *Theory of Stability of Lyophobic Colloids*; Elsevier: Amsterdam, 1948.

184) Napper, D. H. *Polymeric Stabilization of Colloidal Dispersions*; Academic Press: London, 1983.

185) Blume, G.; Cevc, G. *Biochim. Biophys. Atac* **1990**, *1029*, 91.

186) Allen, T. M.; Hansen, C.; Martin, F.; Redemann, C.; Yau-Young, A. *Biochim. Biophys. Acta* **1991**, *1066*, 29.

187) Woodle, M. C.; Matthay, K. K.; Newman, M. S.; Hadiyat, J. E.; Collins, L. R.; Redemann, C.; Martin, F. J.; Papahadjopoulos, D. *Biochim. Biophys. Acta* **1992**, *1105*, 193.

188) Klibanov, A. L.; Maruyama, K.; Beckerleg, A. M.; Torchilin, V. P.; Huang, L. *Biochim. Biophys. Acta* **1991**, *1162*, 142.

189) Litzinger, D. C.; Huang, L. *Biochim. Biophys. Acta* **1992**, *1127*, 249.

190) Bridges, P. A.; Taylor, K. M. G. *J. Pharm. Pharmacol.* **2001**, *53*, 393-398.

191) Tanaka, K.; Takeda, T.; Fujii, K.; Miyajima, K. *Chem. Pharm. Bull.* **1991**, *39*, 2653-2656.

192) van Winden, E. C. A.; Crommelin, D. J. A. *J. Control. Release* **1999**, *58*, 69-86.

193) van Winden, E. C. A.; Zhang, W.; Crommelin, D. J. A. *Pharm. Res.* **1997**, *14*, 1151-1160.

194) Kinsky, S. C. *Methods Enzymol.* **1974**, *32*, 501.

195) Stein, W. D. *Transport and Diffusion across Cell Membranes*: Academic Press: San Diego, 1986.